A Compatible Modulation Strategy for Embedded Digital Data Streams within High Quality Video Signal Transmissions

Gunnar Schmidt

A submission presented in partial fulfilment of the
requirements of the University of Glamorgan/Prifysgol Morgannwg
for the degree of Doctor of Philosophy

This research programme was carried out
in collaboration with the Fachhochschule Braunschweig/Wolfenbuettel

March 1999

Certificate of Research

This is to certify that, except where specific reference is made, the work described in this thesis is the result of the candidate. Neither this thesis, nor any part of it, has been presented, or is currently submitted, in candidature for any degree at any other University.

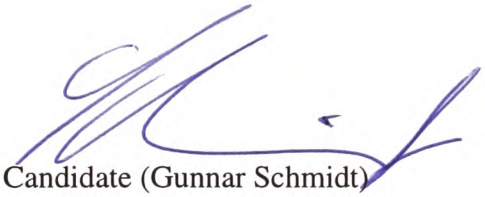

Candidate (Gunnar Schmidt)

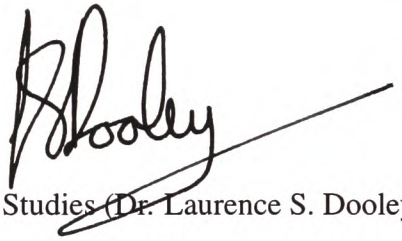

Director of Studies (Dr. Laurence S. Dooley)

20th December 1998.

Date

Acknowledgments

I wish to thank my director of studies, Dr. Laurence S. Dooley for his guidance and support throughout this research and his whole-hearted efforts in providing the necessary resources for the research. With gratitude I would especially like to acknowledge Prof. Dr.-Ing. W. Peter Buchwald from the Fachhochschule Wolfenbuettel, for his many valuable discussions and his supportive input into the theoretical and practical aspects of the project. Further I would like to thank the Communication Department at the Fachhochschule Wolfenbuettel for their assistance throughout the research.

I am especially indebted to Dr.-Ing. habil. Christian Hentchel and Dr.-Ing. Uwe Riemann for their invaluable assistance and fruitful discussions. Also the many students from the Fachhochschule Wolfenbuettel who attended the University of Glamorgan for their Diplom Thesis and thus helping in the development of this research. I would further acknowledge the funding received under the ARC collaboration from British Council and DAAD (Grant No. 443)

Last, but not least I would like to thank my wife Anja, our daughter Linda and son Felix for their constant support and often necessary encouragement.

Summary

Major activity and interest has focused upon High and Enhanced Definition Television systems, for at least the past few decades. From the initial analogue approaches, which concentrated on purely television enhancements, the focus continues to fade more towards fully digital multi-program distribution and ultimately to multimedia solutions. The actual activities throughout Europe and America in launching the Digital Video Broadcasting, DVB and the Advanced Television System Committee, ATSC system, clearly identify that television enhancements are still alive. In parallel, discussions upon data broadcasting, predominantly within the current analogue television systems also have taken place.

The underlying premise of the work presented, is based upon the objective to transmit a compatible enhanced definition television signal within the PALplus standard. A conceptual system is proposed as the framework for this research, containing both a pre-processing and data modulation block, which are coupled via suitable data compression methods. The pre-processing and the additional digital modulation technique has been identified as providing the potential of innovation from which the modulation provides generic digital sub-channels either for multimedia or enhanced resolution extensions.

The originality of the pre-processing techniques is based upon the design of a dual channel sub-band system, which employs two dimensional diagonal filtering together with a Quadrature Mirror Filter bank. From a high definition input, this processing block produces only two sub-bands, rather than the usual four, from which the low pass element represents the compatible component. The high pass element conveys the residual in such a way that full horizontal and vertical resolution can be reconstructed during decoding. The proposed embedded data modulation strategy is based upon a double occupation of the colour sub-carrier. This exploitation is possible due to the inherent phase alternation of the PAL system, so that an additional quadrature modulation of the two colour sub-carriers is feasible.

Both, the pre-processing and modulation blocks introduce crosstalk distortions which compromise the overall efficiency and further encroach on the sensitive issue of compatibility. The thesis provides a complete analysis both theoretical and practical of the implications of these distortions and subsequently proposes solutions which either eliminate or suppress them to a level below a perceptual threshold.

Contents

List of Acronyms

ACTV ..... Advanced Compatible Television

ATSC ..... Advanced Television System Committee

B-Y ..... Blue minus Luminance , PAL colour difference signal

BBC ..... British Broadcasting Corporation

BER ..... Bit Error Rate

BOT ..... Broadcast Online TV

BTCS ..... Broadcast Television System Committee

COFDM ..... Coded Orthogonal Frequency Division Multiplex

CQF ..... Conjugate Quadrature Filter

D2-MAC ..... Half digital audio data rate of MAC

DAB ..... Digital Audio Broadcasting

DCT ..... Discrete Cosine Transformation

DMA ..... Direct Memory Access

DPCM ..... Differencial Pulse Code Modulation

DPSK ..... Differential Phase Shift Keying

DQPSK ..... Differential Quadrature Phase Shift Keying

DSB ..... Digital Satellite Broadcasting

DSNR ..... Display Signal to Noise Ratio

DVB ..... Digital Video Broadcasting

DVC ..... Digital Video Cassette

EBU ..... European Broadcasting Union

EDTV ..... Enhanced Definition Television

EIA ..... Electronic Industry Alliance

EPG ..... Electronic Program Guide

FCC ..... United States Federal Communication Commission

FIR ..... Finite Impulse Response

FM ..... Frequency Modulation

GOP ..... Group of Pictures MPEG sequence arrangement

HD-MAC ..... High Definition Multiplexed Analogue Components

HDTV ..... High Definition Television

HTML ..... Hypertext Markup Language

I ..... In-phase Component

IFA ..... Intra Frame Average

ITC ..... Independent Television Commission

ITU-R ..... International Telecommunication Union - Radiocommunications

JPEG ..... Joint Photographic Expert Group

KLT ..... Karhunen Loeve Transformation

M-JPEG ..... Motion JPEG

MAC ..... Multiplexed Analogue Components

MOU ..... Memorandum Of Understanding

MPEG ..... Motion Picture Expert Group

MQAM ..... Modified Quadrature Amplitude Modulation

MUSE ..... Multiple Sub–Nyquist Sampling Encoding

NAB ..... National Association of Broadcasters

NDBC ..... National Data Broadcasting Committee

NHK ..... Nippon Hoso Kyokai Japanese national TV broadcaster

NICAM-728 ... Near-Instantaneous Companded Audio Multiplex

NRZ ..... Non Return to Zero

NTSC ..... National Television System Committee

OFDM ..... Orthogonal Frequency Division Multiplex

PAL ..... Phase Alternated Line

PALPLUS ..... extended PAL system

PDC ..... Program Delivery Control

PDF ..... Probability Density Function

PSK ..... Phase Shift Keying

Q ..... Quadrature Component

QAM ..... Quadrature Amplitude Modulation

QMF ..... Quadrature Mirror Filter

R-Y ..... Red minus Luminance , PAL colour difference signal

RF ..... Radio Frequency

RMSE ..... Root Mean Square Error

SIS ..... Sound in Sync.

SNR ..... Signal to Noise Ratio

STB ..... Set Top Box

TCI ..... Time Compressed Integration

TDM ..... Time Division Multiplex

TIDE ..... Technology Initiative for Disabled and Elderly people

U ..... scaled B-Y signal for PAL

V ..... scaled R-Y signal for PAL

VBI ..... Vertical Blanking Interval

VHS ..... Video Home System

VPS ..... Video Programming System

VSB ..... vestigial sideband

WST ..... World System Teletext

α	amplitude of the data signal
$A(z)$	alias component (used throughout dual channel subband analysis)
$C(z)$	cross over component (used throughout dual channel subband analysis)

$C_T(z)$	cross over component of the overall transfer function(used throughout dual channel subband analysis)
$C_A(z)$	cross over component of the aliasing component(used throughout dual channel subband analysis)
$C_A(f_y)$	crosstalk attenuation frequency response
ϵ	classification value of different filter combinations (used throughout dual channel subband analysis)
$G_0(z)$	lowpass frequency response of QMF synthesis filter bank
$G_1(z)$	highpass frequency response of QMF synthesis filter bank
f	general frequency
f^*	normalised frequency
f_{Bdata}	bandwidth of the embedded data channels
f_h	reciprocal line duration time
f_s	general sampling frequency
f_{sc}	colour subcarrier frequency
f_x	horizontal frequency of the three dimensional video spectrum
f_x^*	normalised horizontal frequency of the three dimensional video spectrum
f_{sx}	horizontal sampling frequency
f_y	vertical frequency of the three dimensional video spectrum
f_y^*	normalised vertical frequency of the three dimensional video spectrum
f_{sy}	vertical sampling frequency
f_t	time frequency of the three dimensional video spectrum (motion)
f_{st}	time sampling frequency
$h(n)$	general filter impulse response
$H(f)$	general filter frequency response

$h_D(n)$	overall vertical filter impulse response
$H_D(f)$	overall vertical filter frequency response
$H_D(z)$	diagonal filter frequency response
$h_F(n)$	form filter impulse response
$H_F(f)$	form filter frequency response
$h_P(n)$	PAL line delay form filter impulse response
$H_P(f)$	PAL line delay filter frequency response
$H_0(z)$	lowpass frequency response of QMF analysis filter bank
$H_1(z)$	highpass frequency response of QMF analysis filter bank
k	integer count variable, usual used for discrete time
L	interpolation factor
l	integer count variable
n	integer count variable / discrete time
m	integer count variable
N	digital filter order / number of symbols per data channel
p	integer count variable
P_N	noise power of the cross over data signal
r	data rate
ρ	roll off factor
$s(t)$	sampling signal
σ	variance of the data signal
t	time variable
T_B	frame duration time
T_{Bit}	bit duration time
T_s	sampling period

T_z	overall transfer function (used throughout dual channel subband analysis)
$w(n)$	window function
ω	angular frequency
x	horizontal count variable
Δx	horizontal sampling interval
$x(t)$	general input signal
$x(n)$	general discrete input signal
$X(f)$	Fourier transformation of $x(t)$
$X(z)$	Z-transformation of $x(n)$
y	vertical count variable
$y_0(n)$	lowpass signal after QMF bandsplitting
$y_1(n)$	highpass signal after QMF bandsplitting
Δy	vertical sampling interval
z	variable of Z-Transformation

Chapter 1

Introduction

1.1 Background to the research

A considerable amount of research has been undertaken by many scientists and research laboratories to improve today's television systems. This not only relates to a general improvement in picture quality, but also the introduction of additional services to enable multimedia broadcasting.

Major activity and interest has focused upon both HDTV (High Definition Television) and EDTV (Enhanced Definition Television) systems, for at least the past couple of decades [1]. The higher resolution pictures are much better than those afforded by existing television systems, enabling a larger picture format with a wider aspect ratio, as well as home projection systems, so providing a completely different viewing experience, very similar to cinema conditions. In parallel of these activities, further improvements in providing additional services, such as a straightforward multimedia extension to the well known Teletext system have been discussed. The German BOT (Broadcast Online TV) and Intel's "Intercast" system are examples of only two such technical proposals. The benefits which accrue from such systems are manifold, since for instance extra programme information, electronic TV programme guides, multi-lingual high quality sound or special downloading services become possible and therefore very important elements in the discussion of comfort enhancement

within current TV systems. The main stream in this context is currently to combine TV services with the internetwork capability of Personal Computers (PC). This can either be achieved by supplying TV signals to a special PC - card, or vice versa by equipping a TV - set with PC components. The idea of both is to merge their major individual properties, which are namely the advantages of a cheap point to multipoint communication and the high flexibility of a point to point network, to form a new multimedia consumer platform.

These general TV enhancements raise fundamental issues in transmission and storage because of the additional bandwidth requirement. Using modern digital compression and transmission techniques, it is now possible to distribute high resolution signals as well as additional services over standard terrestrial, cable and satellite links. DSB (Digital Satellite Broadcasting), DVB (Digital Video Broadcasting) and DAB (Digital Audio Broadcasting) are only some of the well known keywords for systems either being currently discussed or introduced, though all of these are totally incompatible with today's analogue standards.

There is no doubt that the long term future techniques for multimedia television distribution will be digital, but the existing infrastructure, price and the overall acceptance of the current analogue systems will ensure their existence will be extended for at least a further 20 years.

1.2 Objectives of the research

With the prediction that current analogue television systems will survive for at least the next 20 years and therefore have to coexist with fully digital solutions in the near future, today's systems have to be improved to meet the requirements of a multimedia television broadcasting. In summarising these requirements, multimedia can be defined as an individual mix of general quality (e.g. Audio, Video) together with interactivity. Enhanced image quality, high fidelity and multi-lingual sound, and additional services for deaf or blind people are examples of such quality improvements, where additional information, transmitting in parallel with the actual TV program, known as data casting, provides much more interactivity. This information can be either related to the actual content to provide more background

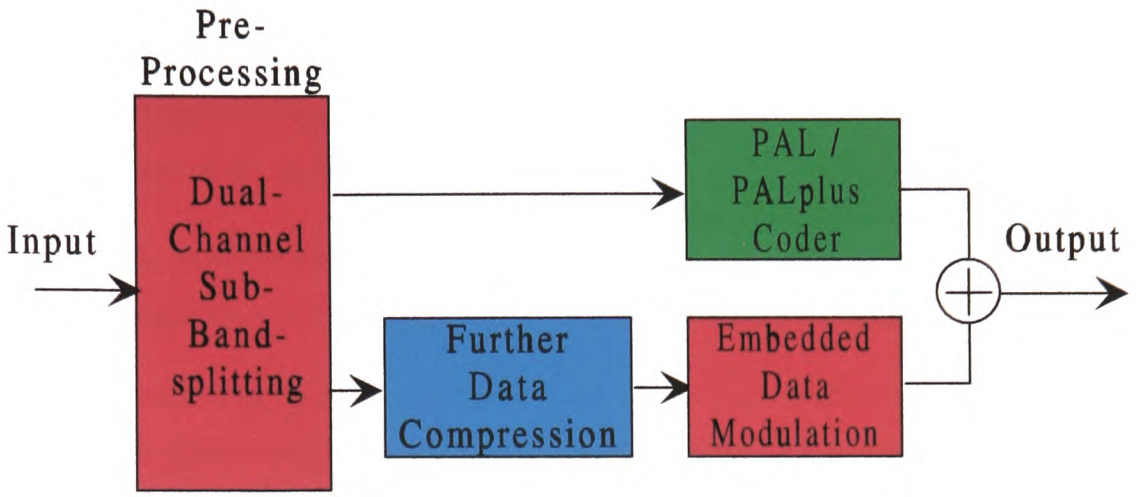

Figure 1.1: Block diagram of the presented system

information during the actual program or more generally, like magazines and downloading functions.

It was expressly to address the problem that any additional service inherently involves the transmission of extra data within a standard television signal, that this research project has its roots. A system was formulated with the clear objective of providing a transparent framework for both PAL (Phase Alternated Line) and PALPLUS (extended PAL system) television standards that would afford such an embedded digital transmission. Figure 1.1 provides an insight into the conceptual system which formed the initial framework for the research. This involves the design of an integrated coding strategy which affords the possibility of a fully compatible EDTV distribution within a standard PAL / PALPLUS television system. To achieve this, a down conversion (decimation) has to be performed to enable the normal resolution TV picture to be received by standard receivers. Also the additional digital signal, which contains the difference between the high resolution picture and the down converted version, has to be transmitted in such a manner that no additional channel capacity is necessary. These primary ideas were presented by Schmidt et. al. in [2] and developed further by Dooley et. al. in [3].

Recently major changes have taken part within the evolution of TV research and development, so that interest in HDTV / EDTV has waned somewhat. This focus will continue

to fade more towards fully digital multi-program distributions and eventually to multimedia solutions. It was with this perspective that two major parts of the initially proposed system were identified as providing potential of innovation, namely

- the pre-processing technique, based on a QMF (Quadrature Mirror Filter) band-splitting in combination with a diagonal filter to enable enhanced resolution transmissions.
- the compatible modulation technique for digital embedded data transmissions from which either multimedia or enhanced resolution extensions are feasible.

The data compression block in Figure 1.1 does not play a major role in this thesis, because many well-proven techniques and solutions are available, a suitable overview of which is provided by Clarke [4]. Furthermore it was readily identified that due to the requisite compression ratio to reach the target data rate, that is the capacity provided by the embedded data transmission, the overall achievable subjective image quality enhancement would certainly be inferior in the context of providing EDTV quality. It is much more reasonable to exploit the additional transmission capacity therefore for new multimedia services. A comparison however, of several well known and also some special compression algorithms are reviewed in the context of the results obtained and for completeness in order to fulfil the original aims of the project.

The main objectives within this research thesis are listed below:-

- Development of the principles of the "Dual-Channel Sub-Band" technique as a variant of the more general four band implementation [5][6];
- Establishing a theoretical framework in which the problem of aliasing and cross-over components can be formulated and further the resultant distortions analysed and evaluated;
- Considering methods of finding solutions to integrate this approach within interlaced scanned video signals;
- Investigating the feasibility of compatible additional embedded data modulation within a PAL / PALPLUS television signal [7];

- Proposing a novel solution, that neither uses the blanking intervals nor inserts additional carriers for compatible embedded data modulation within the video signal. In order to provide a higher data rate this proposal is based on a double occupation of the colour sub-carrier in a PAL/PALPLUS television system;
- Development of design methodologies for horizontal and vertical form filtering to avoid cross-talk components and therefore keeping overall compatibility;
- Establishing a theoretical framework for a subjective orientated evaluation of the visual degradations raised by cross-talk distortions [8];
- Development and realisation of a real time video simulation system.

In conclusion, the objectives of this thesis recognise the novel details of the previously identified innovative blocks within the original proposed system framework. It is clear that the importance of compatibility is inherent in both sections and consequently a major focus is given to distortions, aliasing and cross-talk effects upon the PAL / PALPLUS signals. With the theoretical analysis, various optimisations are highlighted and specific methods of quality evaluation are presented. The verification of the proposed principles is performed by simulation, for which a real time system was developed.

1.3 Outline of the thesis

Chapter 1: Introduces the background and goals of this research

Chapter 2: This chapter sets the basis in the area which is addressed within this thesis by introducing the fundamental theory and thus forming a base especially for Chapter 4.

Chapter 3: Summarises the results of literature surveys and previous work together with highlighting the motivations of the research to justify the project in comparison with other activities and research already undertaken

Chapter 4: Within this major part of the thesis, the theoretical analysis of the aforementioned system is given. The chapter is divided into four sections of which the first three are related to the main processing blocks, but the focus is set on the two major, previously introduced parts.

Chapter 5: Discusses the practical results supported by simulation with the focus on compatibility and subjective performance.

Chapter 6: Conclusions and further work

Appendix A: Gives a straightforward extension of a standard QMF approach to analyse the two dimensional dual band version introduced in Chapter 4

Appendix B: Comparison of vertical form filters used within Chapters 4 and 5

Appendix C: Overview of the developed real time video simulation system

Appendix D: Selected papers published during this research

Chapter 2

Basics of video signal processing

This chapter introduces the fundamental principles which underpin the research presented in this thesis. A fundamental role is given to the basics of one and two dimensional sampling, together with the family of QMF (Quadrature Mirror Filter)s which are explored for band-splitting applications. An introduction to PAL and PALPLUS provides the necessary background for the later analysis. This basic Chapter is divided into three Sections:-

Section 2.1: This section reviews the basic principles of sampling. Starting from the common one dimensional theory, this model is extended into two and further three dimensions providing the basis for a 3-D spectrum view of a video signal.

Section 2.2: This section introduces the fundamental issues dealing with QMF principles necessary for the theoretical analysis used throughout Section 4.1.

Section 2.3: This section expands the sampling basics presented in Section 2.1 to include interlaced scanning and the derivation of the corresponding three dimensional video signal spectrum. Subsequently an introduction to the PAL TV standard is given with the focus upon various colour sub-carrier issues forming the basis for Section 4.2. Finally, a brief overview of PALPLUS is given.

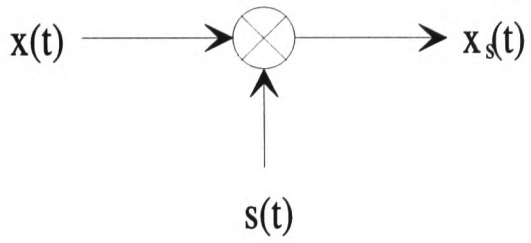

Figure 2.1: A model for the sampling process

2.1 Fundamental sampling

2.1.1 One dimensional sampling

The simplest model for the sampling process is the multiplication of a continuous waveform and a special sampling signal, as shown in Figure 2.1

The sampling signal $s(t)$ is a set of periodic Dirac functions, known as an impulse train, where one Dirac function is defined as:-

$$\delta(t-T) = 0 \text{ for } t \neq T \tag{2.1}$$

$$\int_{-\infty}^{+\infty} \delta(t)dt = 1 \tag{2.2}$$

With a period T_s, $T_s = 1/f_s$ where f_s is the sampling frequency, the sampling signal becomes:-

$$s(t) = T_s \sum_n \delta(t - nT_s) \qquad n = -\infty, \ldots, -2, -1, 0, 1, 2, \ldots, +\infty \tag{2.3}$$

The multiplication $x_s(t) = x(t)s(t)$ results in the discrete signal $x_s(t)$, so that $x_s(t)$ differs from zero only for the instants where

$$t = nT_s \tag{2.4}$$

To analyse a sampled signal it is necessary to look at its properties in the frequency domain. The Fourier transformation defines the relationship between the time and frequency. It is defined as

$$X(f) = \int_{-\infty}^{+\infty} x(t)e^{-j2\pi ft}dt \tag{2.5}$$

and the inverse transformation:-

$$x(t) = \int_{-\infty}^{+\infty} X(f) e^{j2\pi ft} df \tag{2.6}$$

With Equation (2.4), t is substituted by nT_s and to simplify the expressions, the normalised frequency is introduced as:-

$$f^* = \frac{f}{f_s} = fT_s \tag{2.7}$$

With such substitutions, the discrete versions of Equation (2.5) and (2.6) can be derived as [9, Section 2.1]:-

$$X(f^*) = \int_{-\infty}^{+\infty} x_s(n) e^{-j2\pi f^* n} dn \tag{2.8}$$

$$x_s(n) = \int_{-\infty}^{+\infty} X(f^*) e^{j2\pi f^* n} df^* \tag{2.9}$$

This Fourier transformation is used for a further analysis of a sampled signal by applying their correspondences listed for example in [9, Table 2.1 / 2.2] or [10, Table 1.1]. With this assistance the Fourier transformation of the sample signal $s(t)$ (Equation (2.3)) is given as

$$s(t) = T_s \sum_n \delta(t - nT_s) \Longrightarrow S(f^*) = \sum_k \delta(f^* - k) \tag{2.10}$$

for $k = -\infty, \ldots, -2, -1, 0, 1, 2, \ldots, +\infty$, that is an infinite spectrum containing discrete frequency components a distant f_s apart.

The multiplication of $x(t)s(t)$ in the time domain is equivalent to a convolution in the frequency domain so that a sampled signal spectrum becomes:-

$$X_s(f^*) = X(f^*) * \sum_k \delta(f^* - k) = \sum_k X(f^* - k) \tag{2.11}$$

Equation (2.11) shows that the signal spectrum is repeated at every discrete component of a sampling signal spectrum $S(f^*)$, so that it is an infinite periodic repetition of the baseband $X(f)$, at distance f_s. The relationship between signal bandwidth and sampling frequency is also defined with Equation (2.11). The sampling frequency must be twice the maximum bandwidth, otherwise spectral band overlapping occurs, which leads to the non reversible effect known as aliasing. The maximum baseband frequency occurring without aliasing is commonly referred as Nyquist frequency.

2.1.2 Multidimensional sampling

To develop the above explanation formally in a multidimensional manner, a comfortable approach is given in [11, Section 1.4] by defining Equation (2.8) and (2.9) in matrix notation. However, a more straightforward approach from the previous section is used within this thesis [9, Section 2.2].

The signal $x(t_x, t_y)$ has a two dimensional nature and is sampled by an orthogonal, equidistant sampling function $s(t_x, t_y)$, which is a two dimensional Dirac lattice.

$$\begin{gathered} s(t_x, t_y) = \Delta x \Delta y \sum_x \sum_y \delta(t_x - x\Delta x, t_y - y\Delta y) \\ x, y = -\infty, \ldots, -2, -1, 0, 1, 2, \ldots, +\infty \end{gathered} \tag{2.12}$$

Δx and Δy define the sampling period in the x and y dimension respectively, so that

$$f_{sx} = \frac{1}{\Delta x} \qquad f_{sy} = \frac{1}{\Delta y} \tag{2.13}$$

and the normalised sampling frequencies are respectively given by

$$f_x^* = \frac{f_x}{f_{sx}} \qquad f_y^* = \frac{f_y}{f_{sy}} \tag{2.14}$$

With the two dimensional extension of the Fourier transformation

$$X(f_x^*, f_y^*) = \int_{-\infty}^{+\infty} \int_{-\infty}^{+\infty} x_s(x, y) e^{-j2\pi(f_x^* x + f_y^* y)} dx dy \tag{2.15}$$

$$x_s(x, y) = \int_{-\infty}^{+\infty} \int_{-\infty}^{+\infty} X(f_x^*, f_y^*) e^{j2\pi(f_x^* x + f_y^* y} df_x^* df_y^* \tag{2.16}$$

and using similar correspondences to those in the previous section, the spectrum of a two dimensional sampling signal is given as:-

$$S(f_x^*, f_y^*) = \sum_k \sum_l \delta(f_x^* - k, f_y^* - l) \tag{2.17}$$

Finally, the sampled signal spectrum can be derived as:-

$$X_s(f_x^*, f_y^*) = X(f_x^*, f_y^*) * \sum_k \sum_l \delta(f_x^* - k, f_y^* - l) = \sum_k \sum_l X(f_x^* - k, f_y^* - l) \tag{2.18}$$

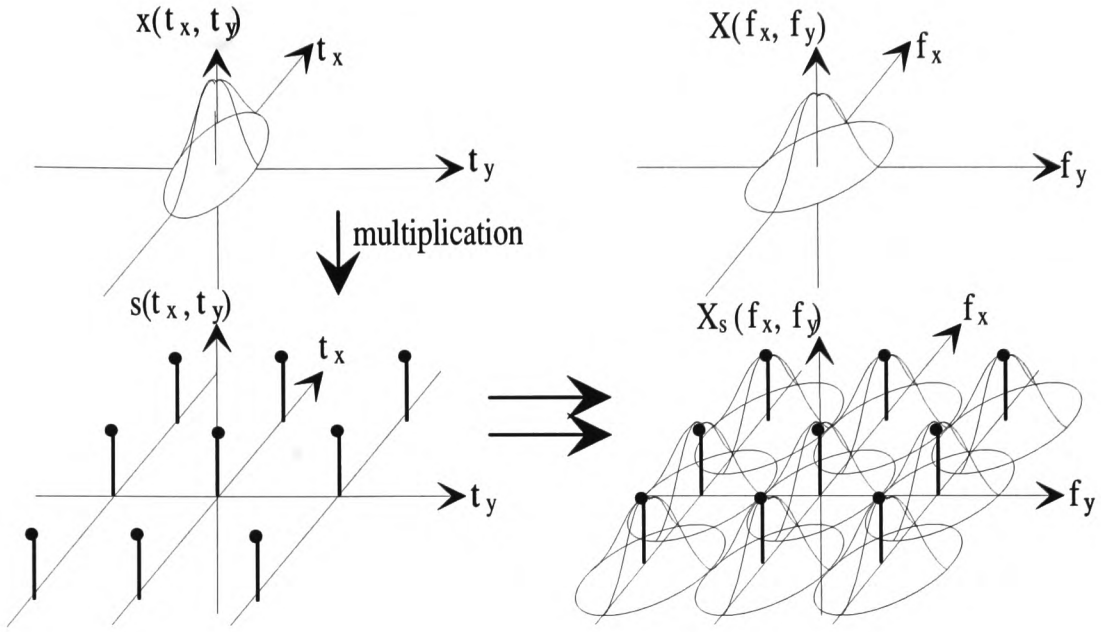

Figure 2.2: Example of a two dimensional sampling

As in one dimensional analysis, the spectrum of a two dimensional signal, that is sampled in each of its dimension, consists of the baseband and an infinite number of periodic replicas. Figure 2.2 graphically shows this for a 2D case.

The development of a three dimensional sampling model can be performed in the same way and similar to the one and two dimensional analysis, the resulting spectrum contains infinite periodical replicas [9, Section 2.2][12, Section 2.3.3]. The three dimensional sampling model is used when analysing the spectral properties of a video signal and extensively within the field of video signal processing. However, normally only two dimensions are discussed at a time, so that the principles of the two dimensional model are sufficient.

2.2 Quadrature Mirror Filter Design

A maximally decimated filter bank, that is a subband system where the new sampling frequency is exactly twice the bandwidth of each subband, implies aliasing distortions within each subband due to the non-zero transition bandwidths of the filters. To avoid this, the anal-

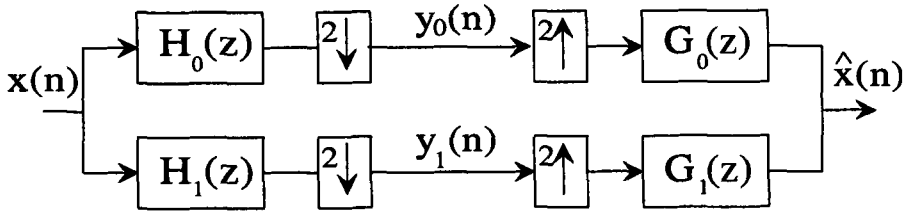

Figure 2.3: Simple one dimensional QMF bank

ysis filter must have sufficient stopband attenuation and a guard space between each subband, but in practice some alias components will remain. During reconstruction in the synthesis section, such a non overlapping filter strategy provides a sub-optimal overall frequency response in that there are clearly visible amplitude distortions. The QMF solution however, proposes overlapping responses of the filter characteristics and thus permits aliasing. These effect can be cancelled by a special choice of the analysis and synthesis filter combination.

Figure 2.3 reviews the standard two band analysis/synthesis filter bank for one dimensional signal processing [13, Section 5.1.1]. The input signal $x(n)$ is initially passed through the two analysis filters $H_0(z)$ and $H_1(z)$, which divides the input into two subbands, before being subsequently subsampled by a factor of two to form $y_0(n)$ and $y_1(n)$ respectively. In the synthesis section, each band is interpolated by a factor of two and further filtered by applying the synthesis filters $G_0(z)$ and $G_1(z)$, before combining their outputs to $\hat{x}(n)$.

In the z - domain the overall system can be expressed as,

$$\hat{X}(z) = \frac{1}{2}[H_0(z)G_0(z) + H_1(z)G_1(z)]X(z) + \frac{1}{2}[H_0(-z)G_0(z) + H_1(-z)G_1(z)]X(-z) \quad (2.19)$$

where the second term covers the aliasing components. From Equation (2.19) it is obvious that if $H_0(-z)G_0(z) + H_1(-z)G_1(z) = 0$ aliasing is cancelled. This is fulfilled if the filters are chosen to be:-

$$G_1(z) = -H_0(-z) \qquad H_1(z) = G_0(-z) \quad (2.20)$$

With this substitution Equation (2.19) reduces to:-

$$\hat{X}(z) = \frac{1}{2}[H_0(z)G_0(z) - H_0(-z)G_0(-z)]X(z) = T(z)X(z) \quad (2.21)$$

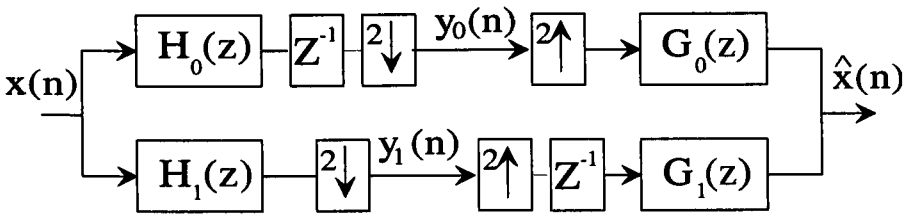

Figure 2.4: Simple one dimensional QMF bank for even filter orders

where $T(z)$ is referred as the overall transfer function. To ensure no phase distortion within the system, it is clear that if the filters are selected to be symmetric FIR (Finite Impulse Response) filters, the overall system has a constant group delay. $H(z)$ can then be written as $e^{-j\omega\frac{N}{2}}|H(z)|$, where N is the filter order, so that the transfer function:-

$$T(z) = \frac{1}{2}e^{-j\omega N}[|H_0(z)||G_0(z)| - (-1)^N|H_0(-z)||G_0(-z)|] \tag{2.22}$$

Equation (2.22) shows that the system is only usable by applying odd filter orders, otherwise $T(e^{j\omega})$ will have a notch at $\omega = \frac{\pi}{2}$. For using even filter orders, the system has to be slightly changed by placing an additional delay in the lowpass analysis and in the highpass synthesis path (Figure 2.4). This system can be expressed as

$$\hat{X}(z) = \frac{1}{2}[z^{-1}H_0(z)G_0(z) + H_1(z)z^{-1}G_1(z)]X(z) + \frac{1}{2}[-z^{-1}H_0(-z)G_0(z) + H_1(-z)z^{-1}G_1(z)]X(-z) \tag{2.23}$$

and further by choosing the filters as

$$G_1(z) = H_0(-z) \qquad H_1(z) = G_0(-z) \tag{2.24}$$

the transfer function becomes:-

$$T(z) = \frac{1}{2}e^{-j\omega N}[|H_0(z)||G_0(z)| + (-1)^N z^{-1}|H_0(-z)||G_0(-z)|] \tag{2.25}$$

To avoid amplitude distortions $T(z)$ must be an all-pass response (an amplitude value equal to one for all values of ω), which is only possible by using trivial cosine filters [14]. Several design techniques have been developed, e.g. [14] [15] [16], to approximate this constraint by applying filters with superior transition bandwidth and passband-stopband characteristics. Other design methods like [17] guarantee amplitude and phase distortion-free reconstituted

signal, but not necessarily for the individual subband signals. More detailed information upon QMF theory and applications are given in [13].

The extension of these basics into two dimensions is straightforward and can be taken as a separable product of identical 1-D QMF pairs [18][19]. This means a 2-D input is initially processed in one dimension generating two subbands, which are then processed in the other direction, so giving a total of four subbands, LP/LP, LP/HP, HP/LP and HP/HP, for the horizontal and vertical directions respectively. For reconstruction, the resulting four bands are processed in an inverse order [4, Section 5.5]. More universal solutions including non separable multidimensional filters are given in, for example [13, Section 12] [20] [21] [22].

2.3 Principles of television

2.3.1 The three dimensional video signal spectrum

It is advantageous to employ the principles of three dimensional signal processing theory in analysing the video signal spectrum, because of the two dimensional nature of pictorial information taken together with the extra temporal dimension. For TV transmissions, this information is converted into a one dimensional signal by the scanning process, usually at the camera and reconstructed at the television tube, so the real scene is first sampled into a number of pictures per second and then in lines per picture. In digital video signal processing, this resulting data flow is further sampled during analogue-to-digital conversion. Regarding this fact, the digital video signal undergoes a three dimensional sampling process, so the resulting spectrum can be derived by applying the principles introduced in Section 2.1.

When considering only the two dimensional horizontal/vertical spatial part of the spectrum , the situation is identical to that shown in Figure 2.2, but in the vertical/temporal plane however, it is different due to the interlaced sampling structure. This structure divides one frame into two fields aiming to enhance the temporal resolution, so that consecutive scan lines are no longer part of the same field (Figure 2.5). To analyse the resulting spectrum,

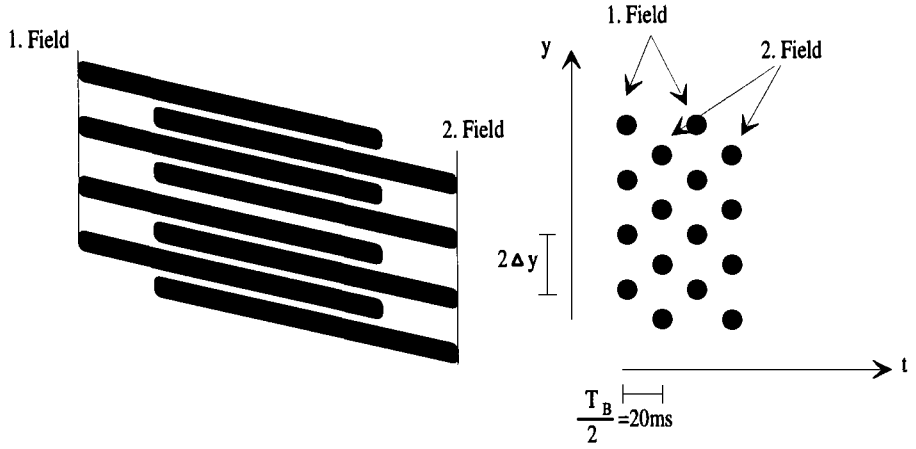

Figure 2.5: Interlace sampling in the vertical / temporal plane

the offset lattice in Figure 2.5 is split into two orthogonal sub-grids as shown in Figure 2.6. Both are considered separately with respect to the time shift inherent in the second sub-grid, so that the superposition results in the final spectrum [12, Section 2.3].

The first sub-grid is given as

$$s_1(t_y, t_t) = \frac{1}{2}\Delta y T_B \sum_y \sum_p \delta(t_y - y2\Delta y, t_t - pT_B) \qquad y, p = -\infty, \ldots, -2, -1, 0, 1, 2, \ldots, +\infty \tag{2.26}$$

where the second includes additionally the aforementioned time shift:-

$$s_2(t_y, t_t) = \frac{1}{2}\Delta y T_B \sum_y \sum_p \delta(t_y - y2\Delta y - \Delta y, t_t - pT_B - \tfrac{T_B}{2}) \tag{2.27}$$

The Fourier transformation of Equation (2.26) can be derived similar as for Equation (2.17)

$$S_1(f_y^*, f_t^*) = \frac{1}{2}\sum_l \sum_m \delta(f_y^* - \frac{l}{2}, f_t^* - m) \tag{2.28}$$

and also for Equation (2.27) with respect to the time shift [10, Table 1.2]

$$S_2(f_y^*, f_t^*) = \frac{1}{2}\sum_l \sum_m \delta(f_y^* - \frac{l}{2}, f_t^* - m) e^{-j\pi(l+m)} \tag{2.29}$$

so that finally the superposition of Equation (2.28) and Equation (2.29) results in:-

$$S(f_y^*, f_t^*) = S_1(f_y^*, f_t^*) + S_2(f_y^*, f_t^*) = \sum_l \sum_m \delta(f_y^* - \frac{l}{2}, f_t^* - m)(\frac{1}{2} + (-\frac{1}{2})^{l+m} \tag{2.30}$$

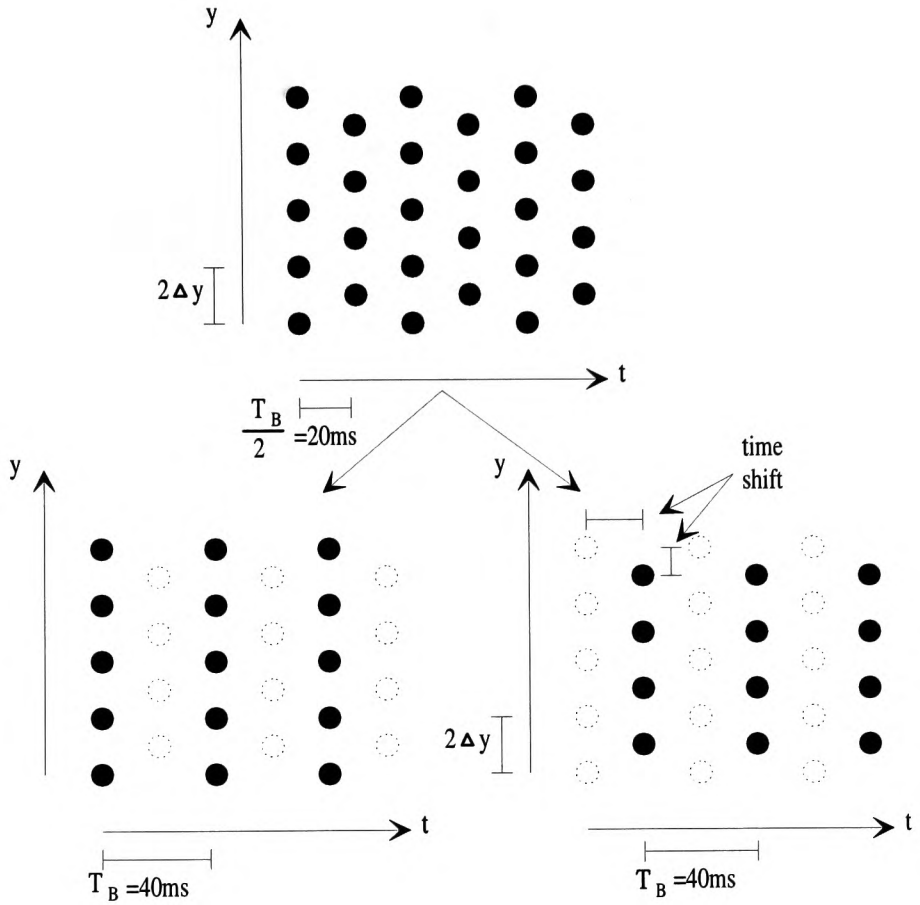

Figure 2.6: Offset sampling grid splitting into two orthogonal sub-grids

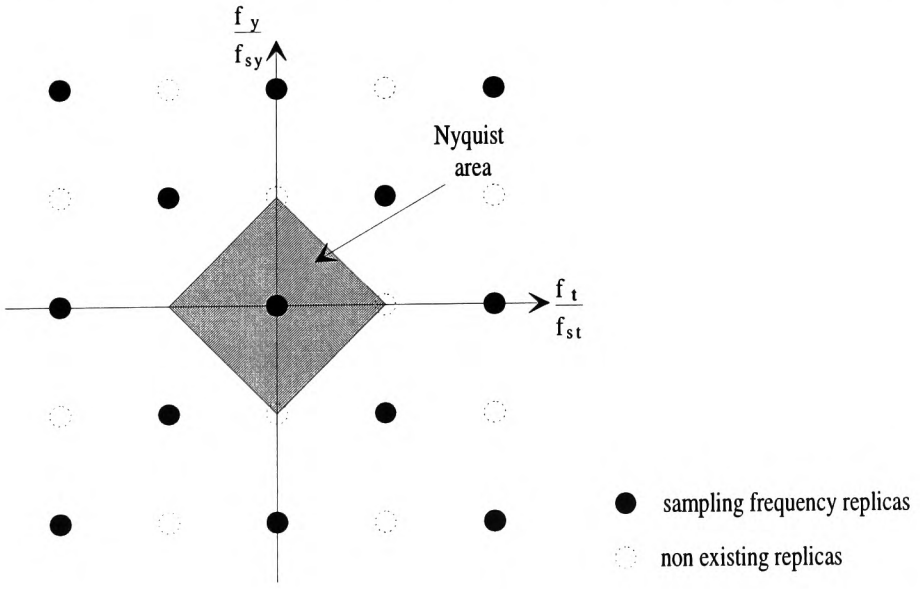

Figure 2.7: Spectrum and Nyquist area of an interlaced sampled signal

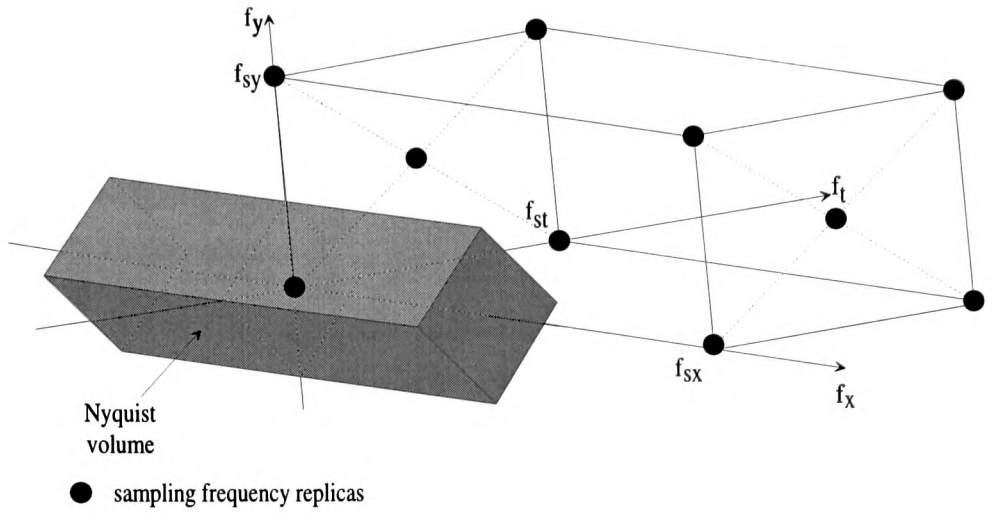

Figure 2.8: Three dimensional Nyquist volume of an interlaced sampled video signal [12, Section 2.3.6]

Equation (2.30) shows that for $l + m$ =odd all replicas are cancelled and thus provides the diamond shaped Nyquist area in the vertical/temporal plane, as shown in Figure 2.7.

The two dimensional horizontal/vertical and vertical/temporal spectra can be combined into a three dimensional view. This is performed in Figure 2.8, by outlining the Nyquist volume, which covers those frequencies where there is no aliasing. The Nyquist volume repeats periodically in each dimension at the corresponding sampling frequency replicas indicated in Figure 2.8 for the positive frequencies. More detailed information related to different sampling structures is given in [23].

Any arbitrary single signal frequency can be split into its three dimensional components. The frequency therefore must be first divided by the vertical sampling rate, that is the reciprocal scan line duration, to derive the horizontal frequency part indicated by cycles per picture width ($\frac{c}{pw}$). If this value is an integer all other components are zero, meaning a stationary horizontal sinusoidal pattern. If not, the fractional part indicates the phase shift from line to line, so consequently multiplying by the number of lines per frame results in cycles per picture height ($\frac{c}{ph}$). Due to the fact that a picture is scanned from top to bottom, the actual mathematical order is inverted, so the derived vertical frequency component must also be inverted. Further more, a fraction greater than 0.5 implies a frequency component beyond

the Nyquist volume, so that it is an alias component. The temporal component is derived similar by multiplying the vertical frequency fraction with the temporal sampling frequency, which is either the number of frames or fields for progressive and interlaced scan respectively. Every such identified position has a symmetry part which can be simply derived by inverting each single component.

The outlined frequency separation is an initial step in video signal analysis and forms the basis for multidimensional signal processing. It provides the possibility to estimate the appearance of additional frequencies within the video signal, as for example a supplementary carrier. Throughout the next section these principles will used to analyse the components and the visibility of the colour subcarrier implemented in both the NTSC (National Television System Committee) and PAL (Phase Alternated Line) TV standards.

2.3.2 Introduction to PAL

The explanation presented of the PAL system in this thesis is been restricted to those parts which are specifically of interest within the context of this research hence this section will concentrate on the principles of QAM (Quadrature Amplitude Modulation) and further the special techniques applied to the PAL colour modulation.

The PAL colour system is based on the NTSC (National Television System Committee) system which was introduced in 1952 in the USA. Both systems had to be compatible to the ubiquitous black and white televisions available at the time. The novelty of NTSC was to find a colour subcarrier which fitted into the TV spectrum with nearly no disturbances to the luminance signal. Due to the scanning process, the spectrum of the luminance is discrete and consists simply multiples of the line frequency (vertical sampling). Choosing the colour subcarrier frequency to be an odd multiple of half the line frequency, means the colour carrier will fits exactly into the gaps between the spectral luminance components [24]. For NTSC the colour carrier is given as

$$f_{SC} = (2n+1)\frac{f_H}{2} \tag{2.31}$$

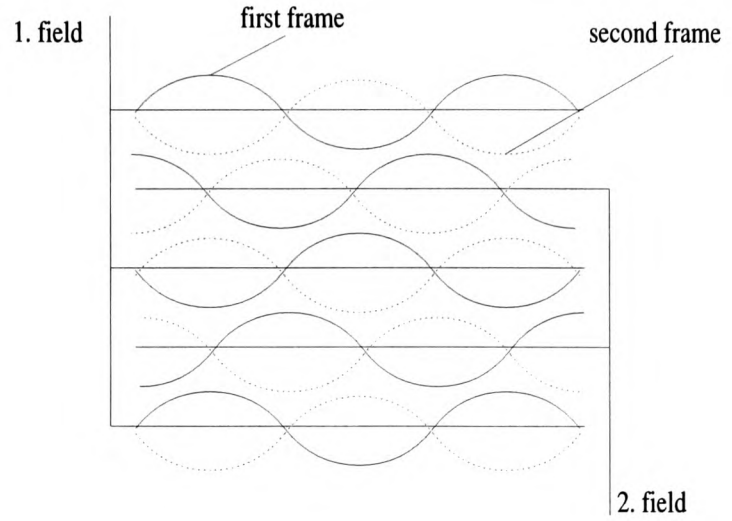

Figure 2.9: Colour carrier phase over one frame

where n is an integer chosen to be as high as possible, also to reduce visibility [1]. The half line offset guarantees that the carrier is anti phase on consecutive lines and also, due to the odd number of line within a frame, in consecutive frames. An integration over that period insures that the carrier disappears (Figure 2.9). With the principles given in the previous section, the position of this colour carrier can be identified within the three dimensional Nyquist volume of a video spectrum. In NTSC the colour subcarrier is standardised to be $f_{SC} = 3.579541875MHz$ (Equation (2.31)).

$$f_{SC(x)} = \frac{f_{SC}}{f_h} = \frac{3.579541875MHz}{15.73425kHz} = 227.5\frac{c}{pw} \tag{2.32}$$

$$f_{SC(y)} = -\frac{0.5cycles}{2\Delta y}525\frac{\Delta y}{ph} = -131.25\frac{c}{ph} \tag{2.33}$$

As mentioned in the previous section, the sign minus considers the different vertical counting orders. With respect to the interlaced scanning the phase shift of 0.5 cycles take place over two lines. Finally the temporal component is:-

$$f_{SC(t)} = -\frac{0.25cycles}{field}59.94\frac{field}{s} \approx 15\frac{c}{s} = 15Hz \tag{2.34}$$

The following table summarises the components and Figure 2.10 displays the colour carrier positions in the three dimensional frequency plot of the video spectrum.

[1] $n = 227$ and $f_H = 15734.25Hz$ for NTSC

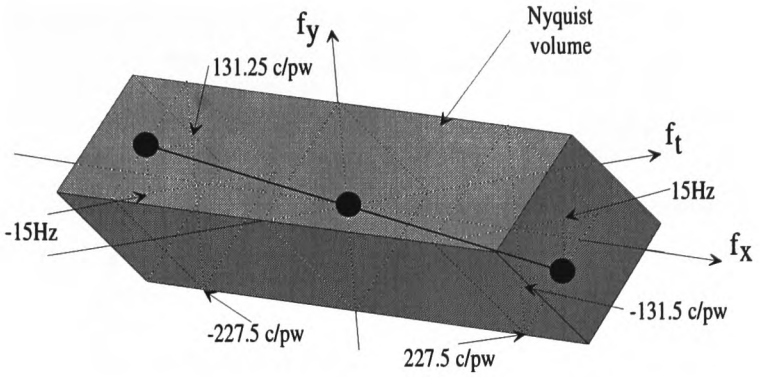

Figure 2.10: Three dimensional frequency plot of the NTSC video spectrum

$f_{SC(x)}, f_{SC(y)}, f_{SC(t)}$	$\frac{c}{pw}$	$\frac{c}{ph}$	Hz	$\frac{c}{pw}$	$\frac{c}{ph}$	Hz
f_{SC}	227.5	-131.25	15	-227.5	131.25	-15

The visual pattern of the introduced subcarrier is diagonal, oriented from the top right to the lower left hand side. Further, it moves upwards, so that the pattern will be in anti phase during consecutive frames. For the human eye however, this integration period is to long for a total cancellation, so that some perceptual interference will be inevitable.

The colour subcarrier is modulated with the two colour difference signals I (In-phase Component) and Q (Quadrature Component), which are derived from R-Y (Red minus Luminance) and B-Y (Blue minus Luminance), respectively, using a Quadrature Amplitude Modulation, QAM, with suppressed carrier. The overall bandwidth limitation of $5MHz$ of the luminance signal reduces the upper sideband of the modulation product to the range between $4.43MHz$, which is the carrier and $5MHz$, so the bandwidth of the colour signals is limited to approximately $0.5MHz$. To enhance the colour resolution the I component is modulated with $1.5MHz$ bandwidth, resulting in single side band modulation for frequencies above $0.5MHz$. Figure 2.11a shows an example of such a composite signal over one scan line. The colour burst at the beginning of the active line period provides the colour carrier phase information for correct demodulation at the receiver. Figure 2.11b gives an insight to the frequency multiplexing which embeds colour signals within the luminance spectrum.

The inherent problem of the NTSC system is the colour distortions due to phase shifts

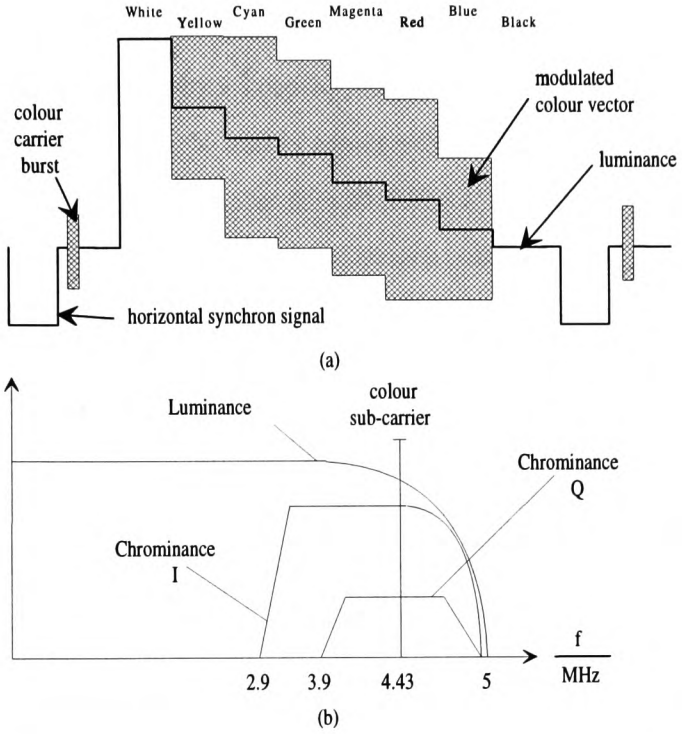

Figure 2.11: (a) NTSC video scan line and (b) frequency multiplex for colour signal integration

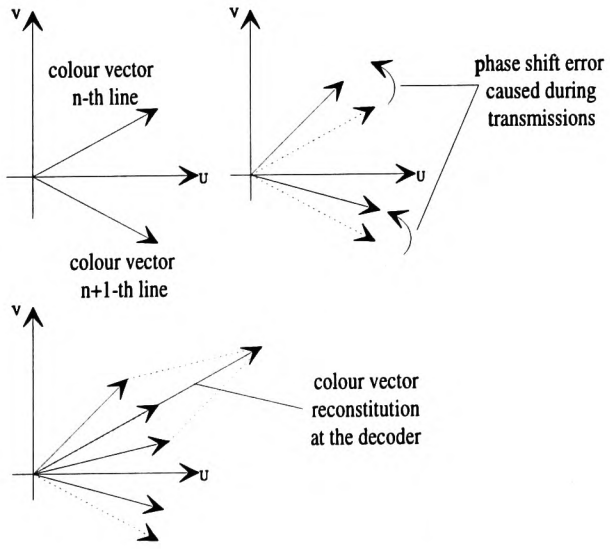

Figure 2.12: Phase error compensation in PAL systems

which occur during transmission. The PAL system overcomes this problem by alternating the colour carrier phase between 90 and 270 degrees for the V (scaled R-Y signal for PAL)-Component from line to line, while keeping the phase for the U (scaled B-Y signal for PAL)-component constant at 0^o. V and U represents the colour difference signals derived from R-Y and B-Y respectively, similar as with I and Q for NTSC. The alternating phase, together with an averaging at the receiver transforms a colour phase shift during transmission into a much more acceptable colour saturation error. Figure 2.12 displays this effect.

Due to the phase alternation, the colour subcarrier becomes totally different from that of NTSC. The phase switching between 90^o and 270^o can be modelled as an additional phase modulation with a square wave of half the line frequency. This results into the suppression of the original subcarrier position for the V-Component and also into subsequent frequency components of $f_{SC}\pm$ multiples of $\frac{f_H}{2}$. The frequency shift of $\frac{f_H}{2}$ further implies that the half line offset used for the colour carrier frequency of NTSC cannot be chosen for PAL. Therefore a quarter offset is used. Together with an additional $25Hz$ offset the visibility of the PAL subcarrier is similar to that of NTSC [24, Section 3.3.4.3]. The carrier frequency for PAL is given as:-

$$f_{SC(U)} = (4n-1)\frac{f_H}{4} + 25Hz = 1135\frac{15625Hz}{4} + 25Hz = 4.43361875MHz \quad (2.35)$$

Similar to NTSC the frequency components within the three dimensional spectrum can be derived as:-

$$f_{SC(Ux)} = \frac{f_{SC}}{f_h} = \frac{4.43361875MHz}{15.625kHz} = 283.7516\frac{c}{pw} \quad (2.36)$$

$$f_{SC(Uy)} = -\frac{0.7516cycles}{2\Delta y}625\frac{\Delta y}{ph} = -234.875\frac{c}{ph} \quad (2.37)$$

$$f_{SC(Ut)} = -\frac{0.875cycles}{field}50\frac{field}{s}43.75\frac{c}{s} = 43.75Hz \quad (2.38)$$

It is clear that the temporal frequency is beyond the Nyquist volume, so that the actual components must be taken from those which are aliased into the Nyquist volume as indicated by Figure 2.13a for the U carrier. The V-carrier frequency is different due to the already

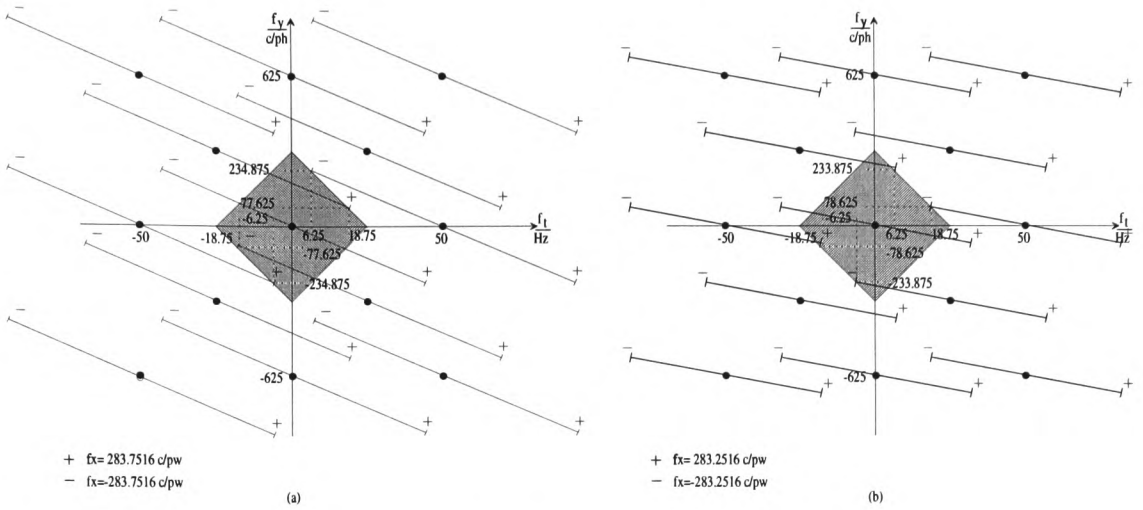

Figure 2.13: Colour carrier positions of the (a) U and (b) V component within a PAL video vertical temporal spectrum

mentioned phase switching:-

$$f_{SC(V)} = f_{SC(V)} \pm \frac{f_H}{2} = 4.43361875MHz \pm \frac{15625}{2} \tag{2.39}$$

Only the difference will be analysed here; the addition changes only the horizontal component by one cycle per picture width, the overall spectral situation will remain exactly the same.

$$f_{SC(Vx)} = \frac{f_{SC}}{f_h} = \frac{4.42580625MHz}{15.625kHz} = 283.2516\frac{c}{pw} \tag{2.40}$$

$$f_{SC(Vy)} = -\frac{0.2516cycles}{2\Delta y}625\frac{\Delta y}{ph} = -78.625\frac{c}{ph} \tag{2.41}$$

$$f_{SC(Vt)} = -\frac{0.625cycles}{field}50\frac{field}{s}31.25\frac{c}{s} = 31.25Hz \tag{2.42}$$

The V temporal frequency component is also outside the Nyquist volume. Figure 2.13b shows this graphically. The following table summarises the components, which are further outlined in Figure 2.14

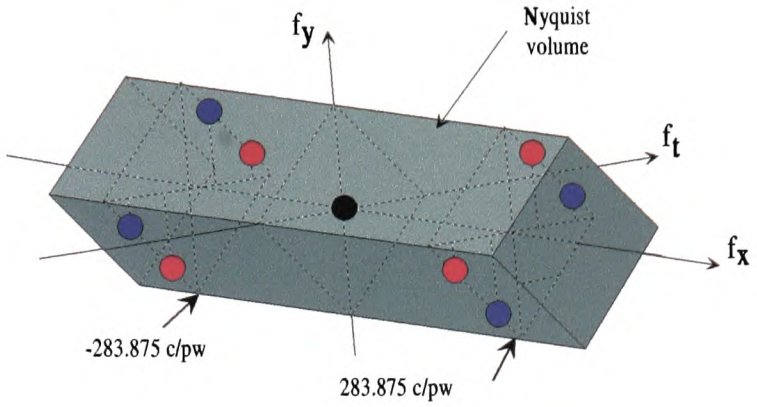

Figure 2.14: Three dimensional frequency plot of the PAL video spectrum

$f_{SC(x)}, f_{SC(y)}, f_{SC(t)}$	$\frac{c}{pw}$	$\frac{c}{ph}$	Hz	$\frac{c}{pw}$	$\frac{c}{ph}$	Hz
$f_{SC(U1)}$	283.7516	77.625	18.75	−283.7516	−77.625	−18.75
$f_{SC(U2)}$	283.7516	−234.875	−6.25	−283.7516	234.875	6.25
$f_{SC(V1)}$	283.2516	233.875	6.25	−283.2516	−233.875	−6.25
$f_{SC(V2)}$	283.2516	−78.625	−18.75	−283.2516	78.625	18.75

As explained above the colour modulation used within PAL is not a QAM as in NTSC, furthermore, it is a normal amplitude modulation with one carrier for the U-component and due to the alteration a second carrier for the V-component. Therefore a higher colour resolution as in NTSC for both difference signals is possible. So PAL standardised $1.3MHz$ bandwidth for each, which implies a single side band above $0.5MHz$, similar to the Q-component of NTSC.

For the decoding process, the PAL-line-delay plays an important role. It provides a simple splitting property of the two colour components together with the line averaging necessary to compensate phase distortions (Figure 2.15). The key element is the line delay, which stores continuously one video line, so that the actual line n, and the previous line $n-1$, are both available. The subtraction and summation of both simultaneously ensures the averaging as well as the separation, because of the vertical lowpass / highpass combination implemented by the summation and subtraction, respectively.

The integration of the colour signal into the existing luminance is not totally free from

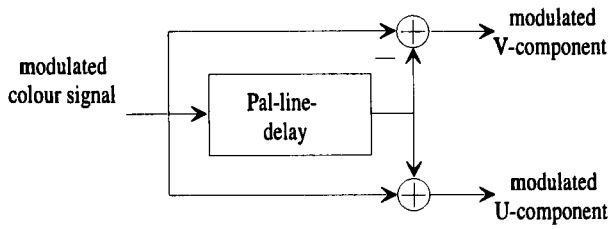

Figure 2.15: PAL-line-delay decoder

interference. Due to the frequency multiplex, cross-effects disturb both the colour and the luminance signal, referred to as cross colour and cross luminance, respectively. To avoid cross luminance the frequency range of the colour signal, which is approximately from $3MHz$ to $5MHz$, is suppressed within the luminance signal path of the receiver. Cross colour is more critical, because high detailed luminance cross over to appear as colour which is well known for example as the colour flicker which occurs on striped clothing. Several research activities have focused on this area to improve picture quality by reducing the cross distortions [25].

More detailed information either on NTSC or PAL is given in [24] [26].

2.3.3 PALplus technique

In 1989, a European initiative was established to improve the viewing experience of the standard colour PAL TV system. The resulting system, called PALPLUS, embraces a number of significant enhancements. The most obvious is a wider 16 : 9 picture format, which is better suited to the human field of vision. This enlargement of a factor 4/3 follows a horizontal resolution enhancement of the same value to keep the overall spatial resolution provided by PAL. Within PALPLUS this is done by suppressing the cross distortions which afflict ordinary PAL pictures [27]. A major aim of PALPLUS is that it should be fully compatible with the standard PAL system. The issue of compatibility therefore requires that PALPLUS has to support two different picture geometries, namely 16 : 9 and 4 : 3. To avoid visual distortion in standard TV receivers, the coder performs a vertical decimation from 576 active lines down to 432, referred as the centre signal, so providing the correct aspect ratio on all 4 : 3 tubes, but with black bars appearing at the top and bottom of the screen, in the well known

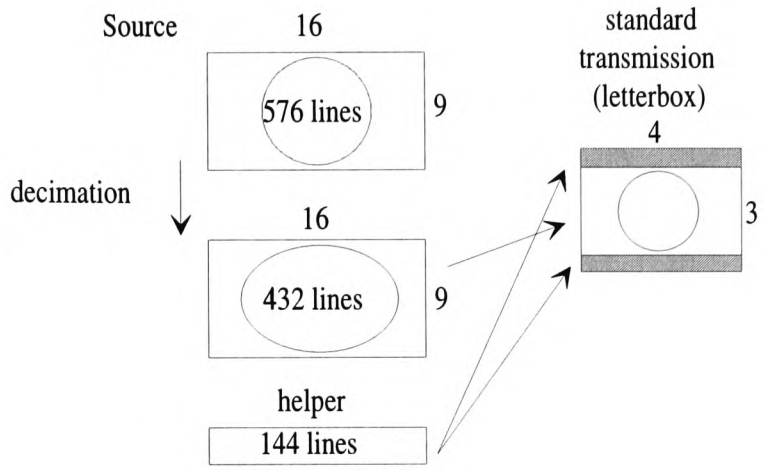

Figure 2.16: PALplus compatible 16:9 transmission using the "Letterbox" format

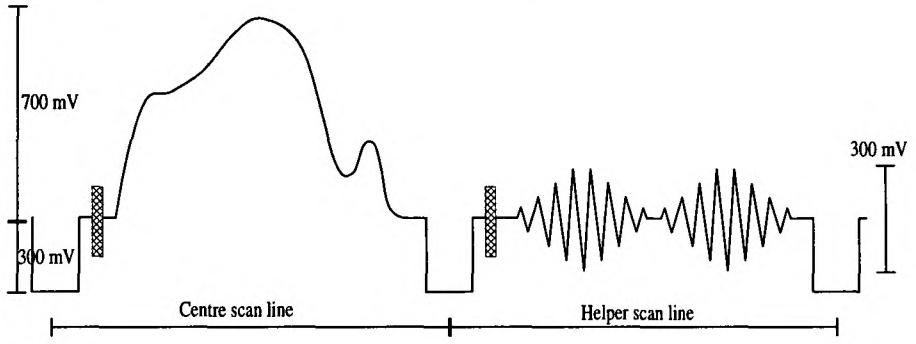

Figure 2.17: Scan line of an PALplus centre and helper signal

"Letterbox" format, as given in figure 2.16.

The additional vertical information necessary for reconstruction in the PALPLUS decoder, is referred to as the "vertical helper", and is transmitted in the 144 lines which comprise the unused black bars. To ensure that this information is not visible, it is modulated with the U-phase of the colour sub-carrier and attenuated in amplitude into a range of $\pm 150mV$. Figure 2.17 gives an example of a centre signal and one helper scan line. Depending on the picture source, either film or camera, the bandsplitting works in either inter- or intra field processing mode. A signalling protocol provides the receiver with the necessary information. To ensure a distortion free recombination of the whole picture at the decoder side, the principles of Quadrature Mirror Filtering theory are used for both bandsplitting and synthesis. A treatise upon this with a focus on PALPLUS is given in [28] and [29].

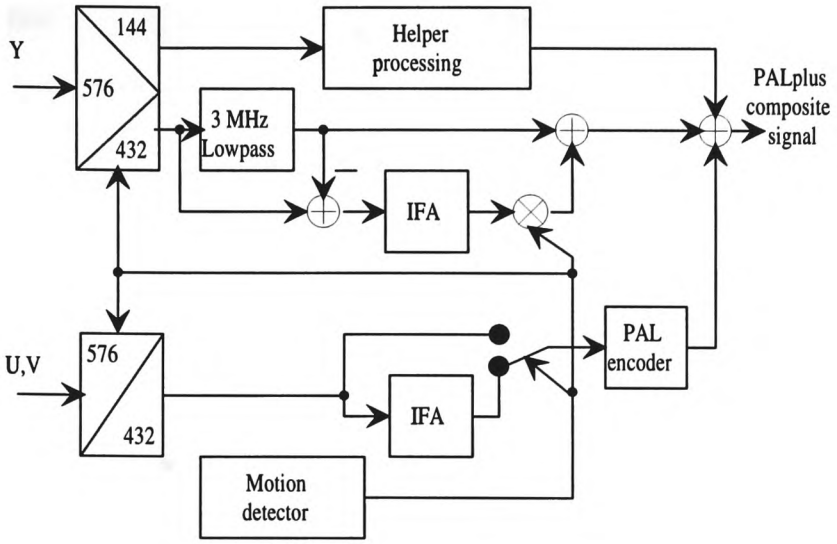

Figure 2.18: Block diagram of an PALplus encoder and decoder including IFA (Intra Frame Average)

Figure 2.18 shows the simplified block diagram of the PALPLUS processing. The incoming luminance and chrominance is initially bandsplit to form the centre and, for the luminance, the helper signal using the aforementioned QMF technique. No helper is generated for the colour signal. To reduce the effect of both, cross luminance and cross colour distortions and thus provide maximum luminance resolution, the centre signal subsequently undergoes the Colour plus technique before being integrated to form the composite output. At the decoder the signal is processed in the reverse order.

The Colour plus technique benefits from the fact that the colour subcarrier has a 180^o phase shift between two consecutive lines within a frame (see previous section). Deriving either the sum or the difference of these the colour carrier or the luminance is eliminated and thus the luminance or chrominance remains, respectively. This however, works only perfectly if the processed lines have identical content. The encoder provides the by calculating the average of two neighbouring lines as illustrated in Figure 2.19. For the luminance this processing is performed only within frequencies above $3MHz$, because only in this spectral area are disturbances caused by cross distortions. As with the bandsplitting, the Colour plus technique distinguishes between film and camera mode. This is necessary because of the inter field processing during camera mode. For film sources no motion is possible within

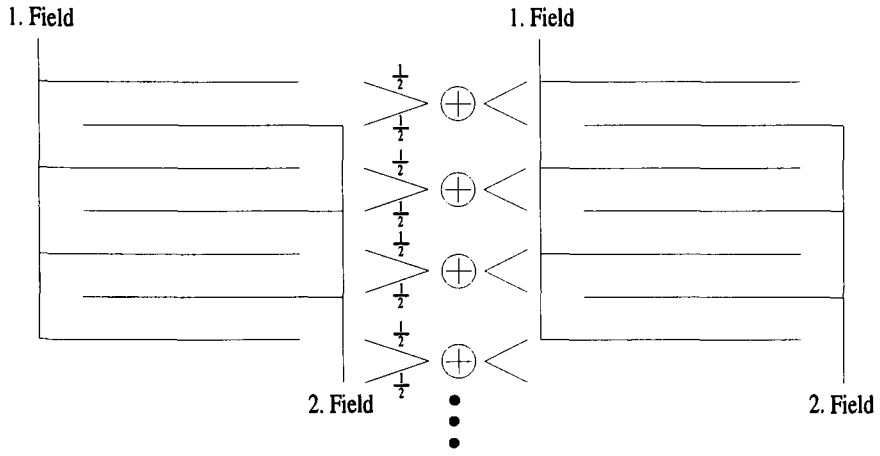

Figure 2.19: IFA example of a PALPLUS encoder

the fields of one frame so nothing additional is needed, but in contrast, for camera sources a motion adaptation must be included. This is achieved by including a motion detector, which switches the Colour plus processing off, if motion exceeds a threshold, so that the colour is processed as usual and no luminance is transmitted above $3MHz$.

The helper processing is also a crucial part of the PALPLUS technique. Due to the amplitude attenuation, the helper is more prone to noise distortions than the centre signal. This results in a noisy line structure after reconstitution at the decoder [30]. Suppressing these effects, a companding technique together with a coring part is defined with PALPLUS [31]. The whole processing in both encoder and decoder is performed digitally with a source sampling rate of $13.5MHz$ conforming the ITU-R (International Telecommunication Union - Radiocommunications) 601 standard [32]. More detailed information are given in [27] [31] [33] [34].

Chapter 3

Discussion upon related activities and literature survey

Since the introduction of home television in Europe in 1951, the standard for black and white transmission has not been changed. In 1967, TV pictures became coloured, using mostly the PAL-system[1], but without losing compatibility to the existing black and white standard. Another milestone was the introduction of Teletext in 1984 [2], which was the first data service within a Television signal. The system was based on the WST (World System Teletext) standardised in 1974 and is still the actual system currently in use.

In the middle of 1995, the PAL system was updated to PALPLUS with major improvements of the colour processing and perhaps more obviously, an update to a wider 16 : 9 aspect ratio, all under the constraint of compatibility. Thus, since TV first became available, the basic system parameters have changed only very little.

July 1996 was the official start for a new fully digital television service in Germany. The commercial content provider "DF1" began its program distribution via satellite based on the digital video broadcasting (DVB) standard. To receive the wide offering of channels on different subjects, the viewer must be in possession of a special decoder, the so called STB (Set

[1] Only two European countries use SECAM

[2] in Germany

Top Box), and even more be a subscriber of the service. New features like "Near Video on Demand" or "Pay-per-View" are also included. One year later DF1 had financial problems. In parallel, the MMBG, which was a joint partnership for public and commercial TV broadcasters was founded to push digital television into the market. Their proposed system, also based on DVB, used a different conditional access, the system that enables program access and that regulates charging, compared with DF1, so that different decoders were necessary for the consumers. The MMBG also had problems and finished their activities before completion. This brief review however illustrates the difficulties with launching new incompatible systems and reinforces the fact that the coexistence of digital and analogue systems will be around for some considerable time to come.

The following sections will explore the investigations made to overcome the limitations of todays analogue television systems. Starting by highlighting the limitations, the motivation of developing an EDTV, multimedia system will be outlined, followed by an overview of various fields within these activities to describe the major motivations for this work. The survey is divided into four sections related to the objectives of this thesis recognised in Section 1.2:-

Section 3.1: This section concentrates upon the issue of enhanced definition TV transmissions. A brief review of the motivation on developing such an extension is given before discussing digital and compatible approaches.

Section 3.2: This section covers those parts dealing with embedded data transmission. Highlighting the limitations inherent with current teletext systems, other proposals are reviewed with the focus to provide multimedia capabilities.

Section 3.3: This section reviews data compression techniques in general

Section 3.4: This section reviews the technology changes which have taken place over the duration of this project, with the focus shifting the interest from pure enhanced definition TV developments to more general multimedia activities.

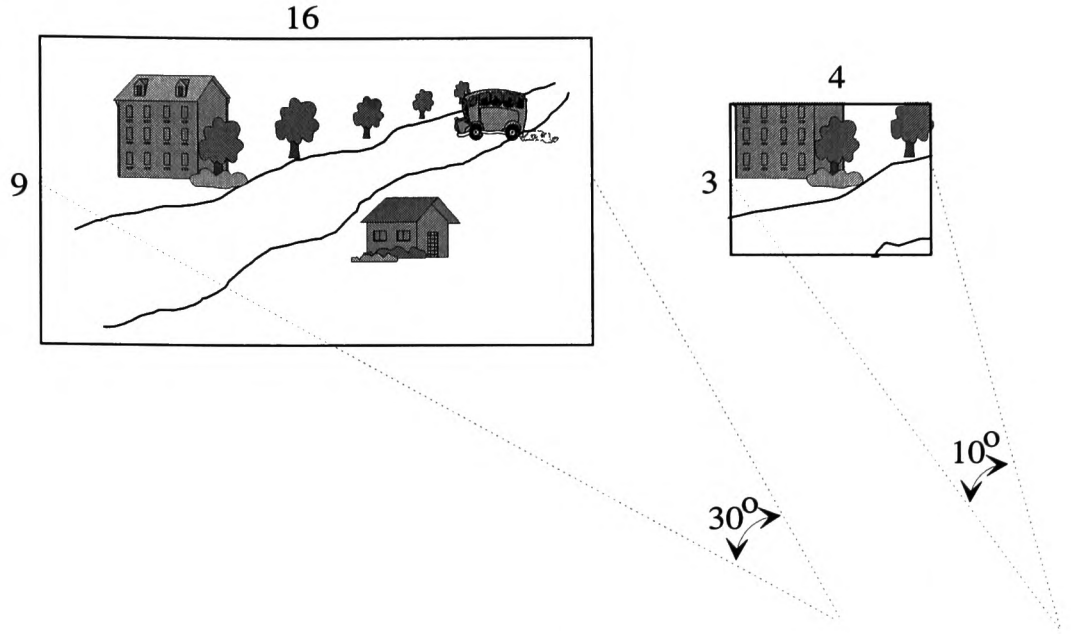

Figure 3.1: Screen size and viewing angle for HDTV

3.1 Enhanced definition Television

The aim of HDTV development was to construct a television system that can exhibit pictures with sensational reality [35]. With the experience taken from movies shown at cinema conditions it is obvious that to achieve more reality the usual viewing distance must be reduced. Experiments clarified that a horizontal viewing angle of at least 30^o together with a wider aspect ratio is necessary [35] (Figure 3.1). This however implies, that the overall resolution must be increased. With the basic theory given in [24, Section 1.3.1.2] it is straight forward to calculate that the line number must be at least doubled to make sure that the eye is not able to perceive the line structure.

Apart from the psycho-optical demands, basic inherent limitations are present within the standard video systems due to the scanning process. This process is inadequate in that neither a prefilter nor postfilter is used and thus clearly implies alias distortions, which were first mentioned by Kell [36]. In subjective tests he found that the vertical resolution is less than the number of lines provided. At the receiver, the missing postfilter introduces distortions (post aliasing), because the spectral images of the video signal are not suppressed. Figure 3.2

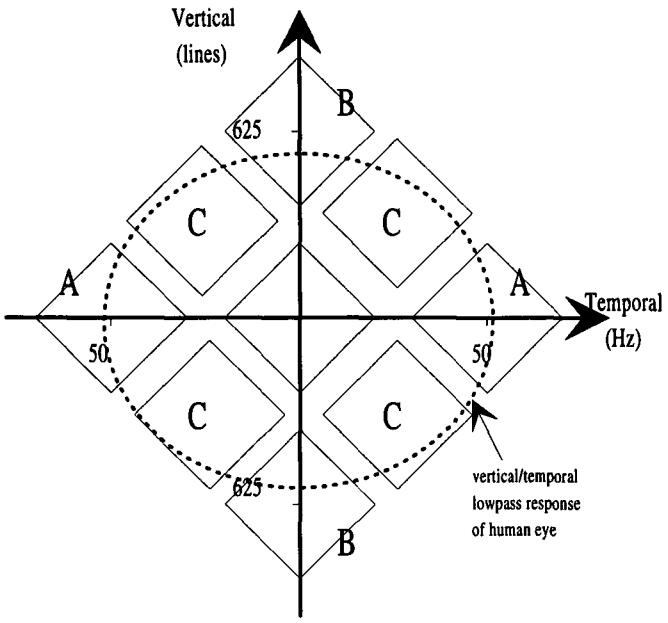

Figure 3.2: Vertical / temporal frequency spectra of an interlace video signal

displays the vertical / temporal frequency spectrum of an interlaced video signal, to provide an insight into the fundamental sources of error [37], which are namely:

- large–area flicker (A)
- line structure (B)
- interline flicker and line crawl (C)

The dashed line in Figure 3.2 shows the vertical / temporal lowpass response of the human eye [38]. The eye however is a postfilter, which cannot suppress the surrounding images (A,B and C) of the signal spectra, which are responsible for the aforementioned errors.

By summarizing the above limitations, the definitions for an HDTV system can be found as follows [39]:

- the spatial resolution has to be at least doubled in horizontal and vertical directions
- the aspect ratio has to be extended from 4 : 3 to at least 5 : 3 [3]

[3] the aspect ratio currently being implemented is 16 : 9

Parameter	Value
Aspect ratio	16 : 9
Sample per active line	1920
Sampling lattice	Orthogonal
Sampling frequency R, G, B, Y	Sampling frequency is an integer multiple of $2.25MHz$
Sampling frequency C_1, C_2	Colour-difference sampling frequency to be 1/2 luminance sampling frequency
Interlace	2 : 1
Frame rate	30 / 25
Lines/Frame	1125 / 1250

Table 3.1: Parameters of an HDTV studio signal

- increase of temporal sampling frequency, at least in the receiver (e.g. $100Hz$ technique)
- improvements to colour cross distortions

From these basic requirements the important parameters for an HDTV signal representation proceeded mainly by extending the values of ITU-R 601 [32], which is the digital standard for the conventional TV format. Table 3.1 summarises these parameters of an HDTV studio signal [35]. It should be mentioned that the number of samples per active line are more than doubled, because of the wider aspect ratio. These basic parameters have been standardised by ITU-R 709 [40] with the objective to form an international unique studio production basis for global program exchange.

The wish to have an international standard for HDTV production and further for distribution was mainly pushed by the Japanese, because their national broadcaster NHK (Nippon Hoso Kyokai) has been working on developing HDTV studio equipment and the HDTV transmission system MUSE (Multiple Sub–Nyquist Sampling Encoding) [41] since 1968, so they were in a far more advanced stage compared to other countries. In Europe, an initiative started in 1986, with the launch of the Eureka 95 project [42] which was an attempt at

defining a European HDTV standard. Based on this, studio and consumer facilities were built as well as a transmission system, HD-MAC (High Definition Multiplexed Analogue Components). This was a compatible high definition extension to the existing D2-MAC (Half digital audio data rate of MAC) system, which should have been introduced as the future satellite television broadcasting system. The failure of MAC (Multiplexed Analogue Components) to be universally accepted [43] lead to the stopping of the Eureka 95 project before its official completion date. In 1987, the FCC (United States Federal Communication Commission) founded the Advisory Committee to advise the FCC on facts and circumstances regarding advanced television systems. From 1987 to 1991, many technical system proposals were made to the Committee. Between 1991 and 1992 five HDTV systems (four digital, one analogue) were completely reviewed and tested with the main result that no consideration should be given to analogue based proposals and that the proponents of the four digital systems should combine their efforts into the "Grand Alliance" [44][45][46]. In December 1996 the FCC adopted the Grand Alliance System as the new ATSC (Advanced Television System Committee) standard to be the digital television transmission system for terrestrial broadcasting in the United States [47]. In 1989, another European initiative commenced to try and improve the viewing experience of the standard colour PAL TV system. The resulting proposal, called PALPLUS, embraces a number of significant enhancements, including a wider 16:9 picture format, which is better suited to the human field of vision, together with a decrease in the cross distortions which afflict ordinary PAL pictures [27], but with however, no overall improvement in picture resolution. The other major aim of PALPLUS was that it was fully compatible with the standard PAL system (see Section 2.3). The European DVB – Project was founded in 1993, after one year of initial studies of the European Launching Group for DVB, by signing a DVB-MOU (Memorandum Of Understanding) that established fully the needed infrastructure to develop a unique set of specifications for satellite, cable, terrestrial and multipoint television delivery [48]. Since beginning with only 18 members, this collaborative group now involves over 200 organisations from around the world [48]. The major developments took place during 1994 and 1995 by concentrating upon the standardisation of satellite and cable delivery systems before focusing on the more complex terrestrial part. First field trails were performed during 1995.

It is obvious that eventually two systems would remain, namely the European DVB and the American ATSC. Both are fully digital and concentrate more upon multiple program and new service delivery than on HDTV. They were developed however to support a diverse set of picture resolutions within the range from VHS (Video Home System) quality up to high end HDTV transmissions. Currently they compete with each other to be adopted as national standards around the world, in a similar manner to what happened approximately 30 years ago during the colour TV introduction with PAL and NTSC. Compared to that situation, DVB and ATSC are technologically much more closer, because both use MPEG (Motion Picture Expert Group) video compression as a core mechanism [47], which actually makes interoperability possible [49] in principle.

3.1.1 HD-MAC versus MUSE

HD-MAC and MUSE were the two early systems considered to be introduced as the national standard for HDTV program delivery. As previously mentioned HD-MAC did not succeed, whereas in Japan HDTV programmes are transmitted for several hours a day using the MUSE transmission system. Both techniques are analogue which means applying the principles of analogue modulation strategies, although the signal processing is performed in the digital domain. MUSE is totally incompatible to any previous existing TV standard. In contrast HD-MAC was developed to be the high resolution representative of the MAC family so compatibility was given to the D2-MAC system. D2-MAC was introduced for direct satellite television broadcasting providing perfect luminance / chrominance separation by using a TDM (Time Division Multiplex) scheme and further high-fidelity, four-channel digital audio together with some improved data services. Figure 3.3 shows the main differences between PAL and MAC by comparing one scan line of each video signal. In the MAC scan line the chrominance and luminance components are time compressed before being time sequentially multiplexed, where as for the PAL system a frequency multiplex is used (see Section 2.3). The two colour difference signals within MAC are transmitted line sequentially [50]. HD-MAC works similarly and also MUSE applies these principles, using the TCI (Time Compressed Integration) system, of signal component multiplexing [51,

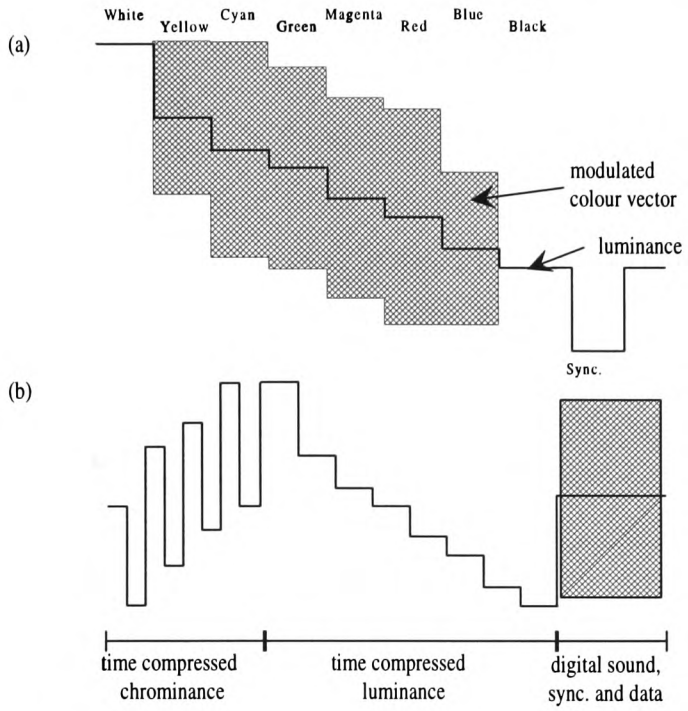

Figure 3.3: Comparison of (a) PAL and (b) MAC scan line

Section 3.1.2].

The video bandwidth of HD-MAC and MUSE is approximately $20MHz$, from which a corresponding sampling frequency of $54MHz$ and $48.6MHz$ is mandatory, fulfilling the Nyquist's sampling theory [52]. The alluded time compression of luminance and chrominace components leads to overall bandwidth expansion, so that a bandwidth compression technique must be employed to enable satellite transmission within an $8MHz$ channel [53, Section 4.4]. The necessary compression ratio of four is achieved by implementing the basic technique of three dimensional subsampling, similar for both systems [54][55]. A simplified block diagram of the encoder and decoder structure is given in Figure 3.4. There are two different processing paths, one for stationary and one for moving portions of the image, where additionally HD-MAC implements a third, intermediate path. Each path accomplishes a different subsampling scheme to take care of the different psycho optical requirements, which are basically high resolution in stationary scenes and lower resolution in motion areas. A motion detector switches between these signal paths.

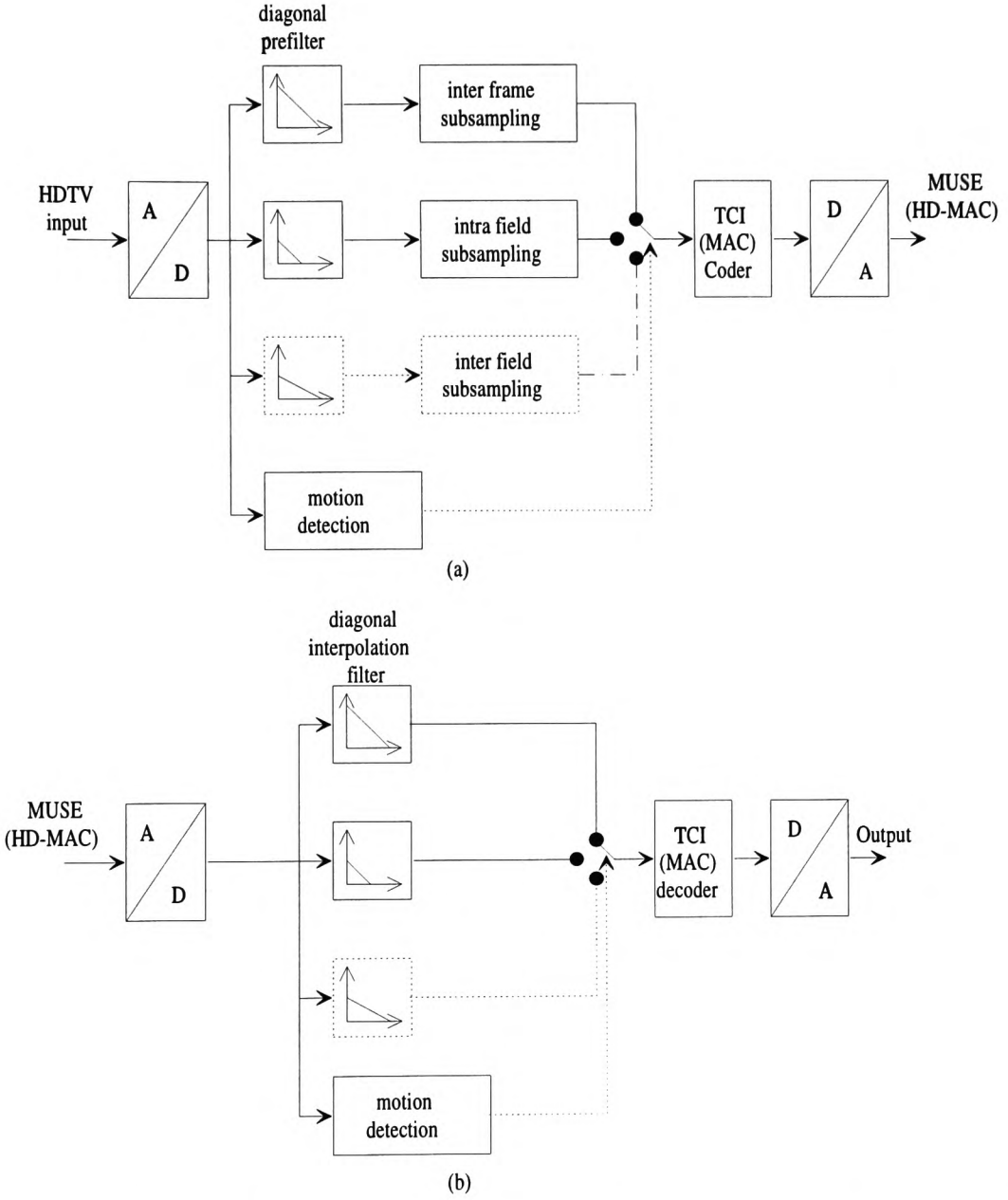

Figure 3.4: Principal block structure of HD-MAC/MUSE (a) encoder and (b) decoder

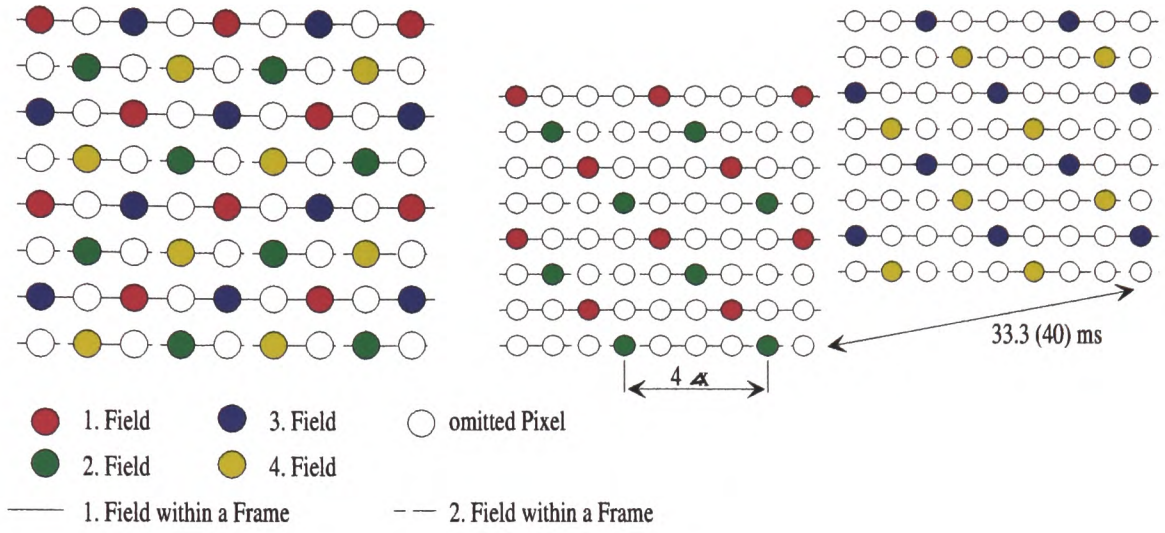

Figure 3.5: Subsampling lattice of MUSE and HD-MAC for the stationary path

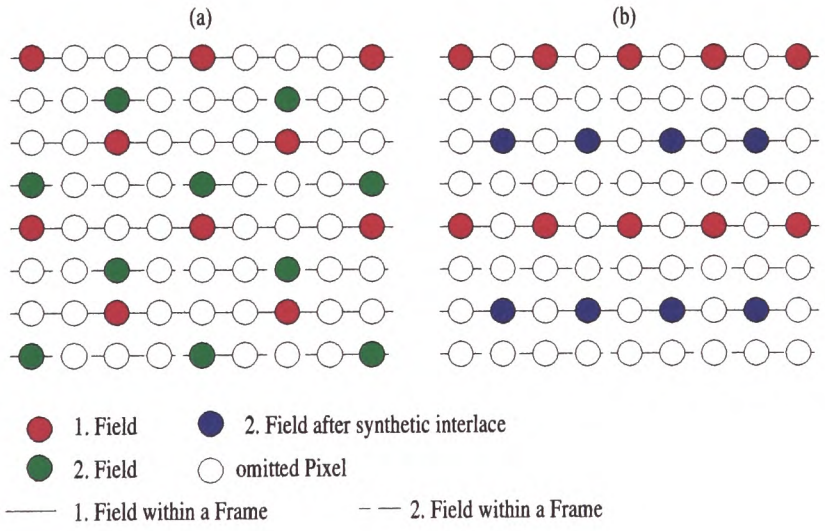

Figure 3.6: Subsampling lattice of MUSE and HD-MAC for the (a) motion path and (b) the intermediate path for HD-MAC

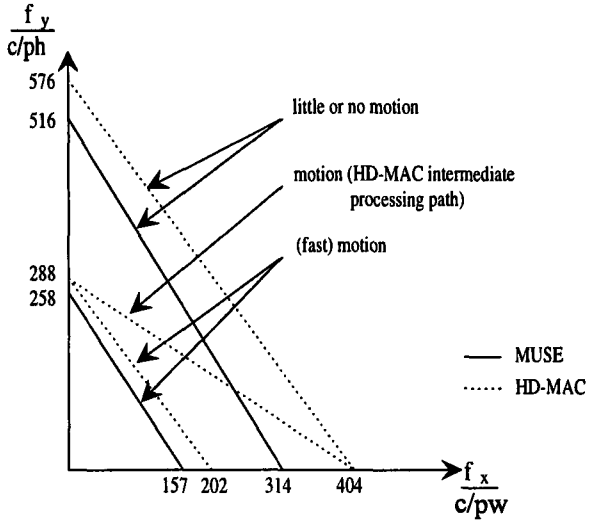

Figure 3.7: Diagonal spatial resolution of MUSE and HD-MAC for their motion paths [55]

To provide the necessary bandwidth compression of four implies that only every fourth pixel of a scan line has to be transmitted. Figure 3.5 shows the spatial / temporal subsampling lattice for the stationary, that means no-or-little motion, path. The offset between the consecutive pixel is chosen such that after four fields only a spatial diagonal subsampling lattice remains. Figure 3.6a shows the offset scheme for the fast motion path. The intra-field processing performs no temporal processing, so each field undergoes the same subsampling. Figure 3.6b gives an insight to the intermediate processing of HD-MAC. It is an offset subsampling within the first field of a frame, the second field is totally omitted [55]. Only for D2-MAC compatible reasons is a synthetic interlace subsequently introduced.

From this brief technical description, it is obvious that both systems use the principles of diagonal offset subsampling within each of their different processing paths, so the input signal initially undergoes a diagonal pre-filtering (Figure 3.4). Figure 3.7 compares the different responses between HD-MAC and MUSE within their processing paths. Generally, both systems provide similar resolution, however due to the intermediate motion path, HD-MAC supplies full horizontal for most of the time resolution. Furthermore HD-MAC uses vector based motion detection allowing a more accurate selection of the processing method and also a motion vector assisted signal reconstitution at the decoder. Summarising this brief comparison, the subjective picture quality provided by HD-MAC is superior to the MUSE

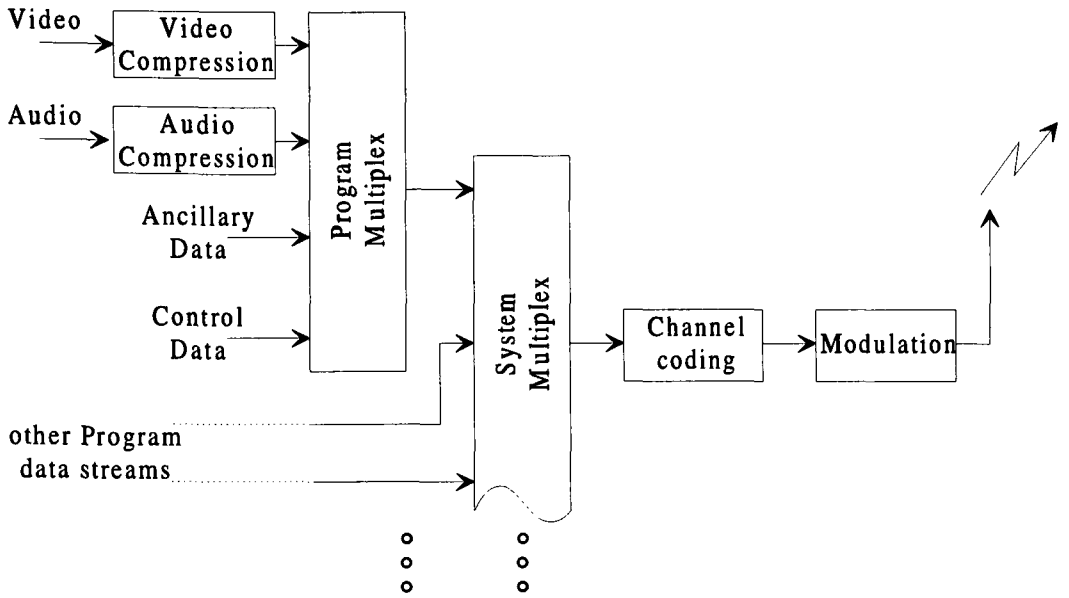

Figure 3.8: Generalised block diagram for DVB and ATSC systems

system; however, this is only achieved at the expense of greater coder complexity.

3.1.2 DVB versus ATSC

As previous alluded, current activities upon new television distribution systems involve fully digital solutions, that means both digital processing within encoder and decoder and further applying the principles of digital transmission techniques. The two main systems, DVB and ATSC, use similar technologies for data compression and modulation, but they are developed under the premise of different philosophies. Where as ATSC focuses upon HDTV terrestrial distribution, the DVB emphasis is upon multi-program delivery via satellite and cable containing standard resolution pictures. Both systems however are developed to support different resolutions and further their standards include derivatives for satellite, cable and terrestrial transmission.

Figure 3.8 shows a generalised block diagram of a digital television system like DVB and ATSC developed from [56] and [57]. The initial video and audio signal undergo digital compression before subsequently being multiplexed with supplementary and control data to form a single program data stream, which is further combined with other similar streams

providing multi-program facilities. The following channel coding introduces the error coding before the signal is subsequently modulated. The reason for the similarity of DVB and ATSC within this simplified block diagram is that the core technology of both systems are based upon MPEG strategies. They are applying MPEG-II video coding [58], which is discussed more detailed in Section 3.3 and MPEG-II multiplexing [59]. DVB also uses MPEG-II audio coding [60], where ATSC employs Dolby Digital AC-3 [61] multichannel surround sound. The channel coding and clearly the modulation technique differ totally.

The ATSC system supports two video formats. A 1280 by 720 pixel and a 1920 by 1080 pixel scan format, both with frame rates of $25Hz$ matching cinema projection standards and of $60Hz$-field / $30Hz$-frame as for NTSC. Provision is made for progressive scan displays of 60 full resolution pictures, instead of 60 interlace fields [62]. As mentioned the video compression, as well as the output data stream multiplex is accomplished in accordance with the MPEG–2 standards to form an overall symbol rate of 10.76 MSymbols/s. The transmission system provides two modes, one for terrestrial broadcasting and one for high data rate cable transmission. The terrestrial mode uses 3 bits/symbol while using 4 bits/symbol in cable environments. Several modulation techniques were investigated by the Grand Alliance to exhibit the best overall performance with the result that the vestigial sideband modulation (VSB) is superior to quadrature amplitude modulation (QAM). The overall bandwidth requirement for transmission is $6MHz$.

Compared to $6MHz$ transmission bandwidth allocated for ATSC, European's broadcaster have the luxury of $8MHz$ [62] for DVB delivery. Different modulation techniques together with different output bit rates are applied by DVB-S, DVB-C or DVB-T depending upon the transmission technology, namely satellite, cable or terrestrial, respectively. Within DVB-S and DVB-C an output data stream of $38MBit/s$ is delivered containing four to eight simultaneous standard resolution television programs, where within DVB-T a stream of $24MBit/s$ can carry up to six such programs. The modulation technique is based on quadrature phase-shift keying and on quadrature amplitude modulation for satellite and cable, respectively. For terrestrial transmission an OFDM (Orthogonal Frequency Division Multiplex), well known from DAB, where the COFDM (Coded Orthogonal Frequency Di-

vision Multiplex) variant is employed. With this technology the high bit-rate signal is spread over several thousand narrow channels, with each channel operating at a much lower data rate [62].

Although DVB is focused on multi standard resolution TV distribution, it also supports an optional high-definition mode, where the number of lines and pixels are doubled. This mode however, provides no backward compatibility to standard resolution, so high definition pictures are to be simulcast alongside standard pictures [62].

3.1.3 Compatible Systems

Since HDTV is under discussion many ideas and solutions have been presented to distribute high quality TV pictures compatible with standard systems. Compatibility in this sense means to retain the utility of the available receivers with the new system however, some impairments in the performance of the old TV-sets usually occur because the new system is designed to meet different objectives [1, Section 6.1]. So the issue of compatibility implies the protection of existing systems, but also some compromises while the new service is established. From this definition Hopkins suggested five levels of compatibility [4] [63][1, Section 6.5]:

- Level 0: Incompatible,
- Level 1: The HDTV signal can be converted to provide the standard signal to conventional receiver,
- Level 2: Same as level 1 but only simple techniques are required,
- Level 3: The HDTV image can be received and displayed by conventional TV-sets, but impairments are inherent,
- Level 4: Same as level 3, except the conventional receiver provides its highest quality,
- Level 5:The conventional receiver has all the quality of the HDTV image.

[4]Level 0 means total incompatibility

From a practical viewpoint the definition of compatibility is covered by level 1 to level 3. Level 4 is only applicable when the conventional signal and transmission channel is left unvaried, e.g. as for two channel (see further on) or simulcast approaches.

At this point it is worth defining the terminology of forward and backward compatibility. Forward means the new services are accessible from conventional systems while backward refers to conventional services being accessible by new systems. Usually forward compatibility is meant within this context, because this directly covers the issue of impairments upon conventional receivers. This does not mean in any way that backward compatibility is less important, but it is generally less technically complex, because new receivers are designed to address these issues.

Similar to the mentioned level approach, but from a more practical background G.J. Tonge postulates three compatible categories for pictures quality enhancements [64]:

- Techniques applicable only to the receiver processing
- Techniques applicable to both receiver and signal source, but a standard transmission channel
- Techniques using MAC

It is obvious that the two first categories can be mapped to level 1 and level 2 where the third matches the definition of level 3. Tonges postulation could be easily developed further to more detailed categories providing a better skeleton to the variety of compatible system proposals. The following list is used throughout this survey:

1. Techniques applicable only to the receiver processing
2. Techniques applicable to both, receiver and signal source, but a standard transmission channel without any residual information
3. Same as 2 but with residual information transmission outside the same transmission channel

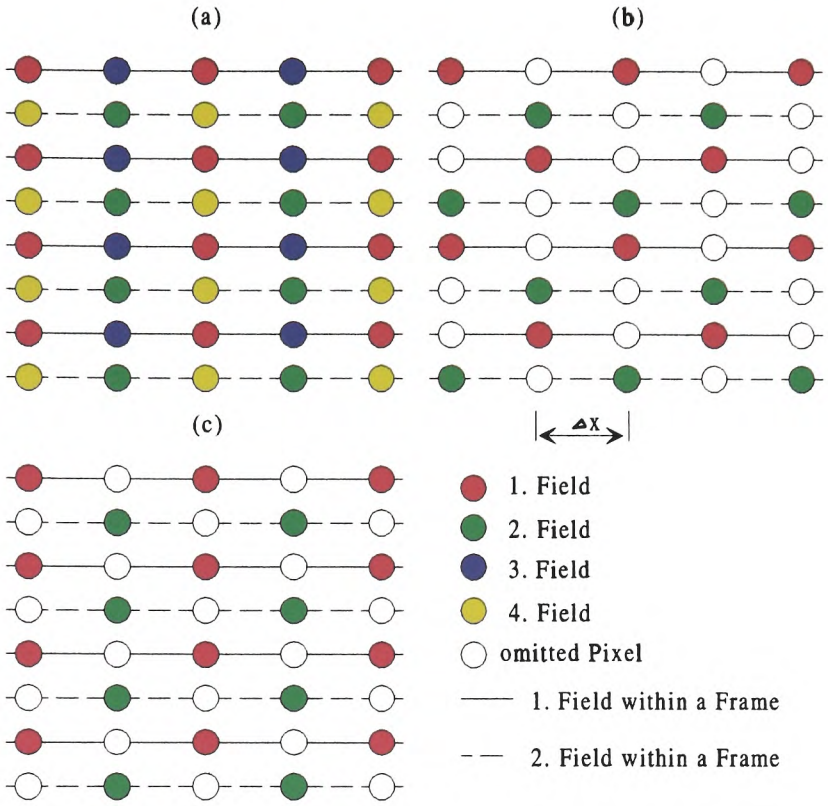

Figure 3.9: Different offset lattices (a) inter frame line offset (b) modified line offset (c) inter field line offset

4. Same as 3 also with residual information transmission, but within the same transmission channel

5. Techniques using MAC

The first category covers mainly those techniques related to flicker and line crawl reduction [65]. The variety of solutions proposed in this area focus predominantly upon conversion to higher frame rates and interlaced - progressive scan transformation [24, Section 5.3.2]. An optimum is accomplished by applying both principles [66].

Techniques related to the second category usually involve applying pre- and post-filtering to avoid aliasing artefacts due to the scanning process of the camera and distortions caused by post aliasing (insufficient image suppression) at the receiver, so consequently providing a Kell–factor of one [67].

The following categories deliver additional information providing real resolution enhancements at the receiver. The purpose of compatibility implies however, the necessity of a standard component transmitted in a standard channel and an additional part, further referred as residual signal, carrying the remaining resolution. These enhancements do not only relate to proposals for HDTV distribution, meaning a doubling of horizontal and vertical resolution (a lot of techniques presented supply only the standard number of lines), but an increased horizontal resolution due to the wider aspect ratio of for example 16 : 9 or non interlaced scanning. These systems mainly use the term "Enhanced" instead of "High", such as EDTV. The implementation of pre-processing aiming to split the input signal into both components, is generally required. Filter implementations related to this subject are given in [68][69]. Bandsplitting techniques related to provide a wider aspect ratio are proposed for example by Hentschel [28] and Herfet [29] applying Quadrature Mirror Filters (see Section 2.2). For HDTV signals the principles of two dimensional sub-band decomposition are also often proposed [70, Section 13.2] decomposing the input signal into the required standard and residual components.

A number of suggestions are made to transmit the residual in a second standard channel. This implies for HDTV resolution, which is twice the horizontal and vertical of that of the standard TV signal, the bandwidth requirement for transmission is four times higher, so for the aforementioned two channel approach, pre and post processing is used to perform an overall compression of two. A number of proposals are based on subsampling to form an offset sampling lattice in the spatial domain [71] or a multidimensional extension of these [72] [73] [74]. Figure 3.9 summarises possible offset lattices derived from an interlaced HDTV input. The inter-frame line offset (Figure 3.9a) provides the full resolution after integration within four fields. The trade-off is however, the necessity of a complex three dimensional prefilter. The lattice given in Figure 3.9b is the commonly used offset, because each field is processed independently and thus only intra field prefiltering is required. It is clearly visible that a paired line structure is inherent with this technique, which implies a reduced vertical resolution [12, Section 5.4.2]. Figure 3.9c is the inter-field version of Figure 3.9b which incurs no vertical resolution loss. It should be mentioned that for all three strategies a diagonal prefilter is mandatory.

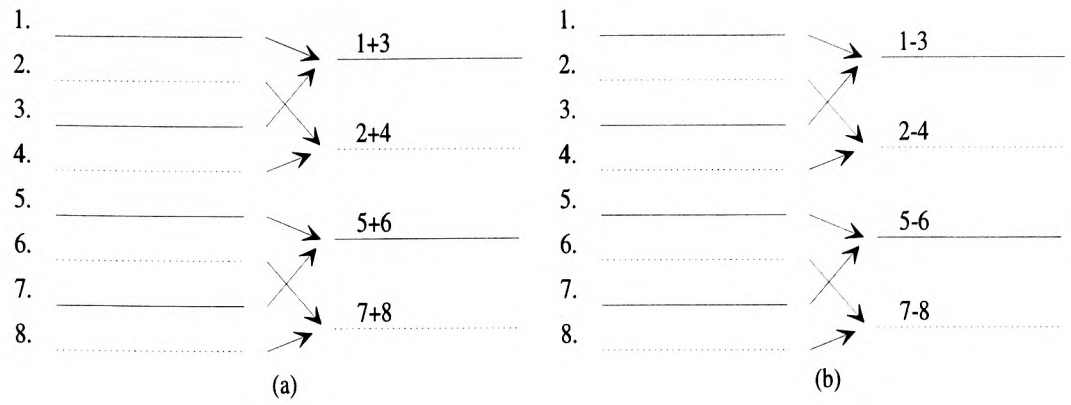

Figure 3.10: Simple signal splitting example into (a) standard component and (b) residual component

Following a bandwidth compression of two, the signal must be subsequently split into the aforementioned standard and residual component. This is not trivial, because of the interlaced and further offset sampling arrangement. A simple, commonly used strategy is given in Figure 3.10. This procedure combines a vertical two-tap cosine prefilter and a subsequent subsampling by two. The advantage of this simple approach is the possibility of perfect signal reconstitution at the receiver. The standard signal however is very much affected, because of processing non vertical adjacent pixel due to aforementioned spatial offset structure. Similar techniques, but focussing more towards non interlaced inputs, are presented by Sauerburger and Stenger in a case study fashion [71].

A possible solution for residual transmission within a two channel approach, is presented in [71] using the so called taboo channels, which are the unused gaps in the spectrum introduced to avoid inter channel crosstalk. Another suggestion is to allocate two satellite channels that conform to the E–MAC specification [75], but generally these strategies conflict with the availability of transmission channels and further imply technical problems for example different delays between the two components [1, Section 2.13].

B. G. Haskell proposes an interesting alternative [76]. Starting from a composite HDTV signal (Figure 3.11a), which is developed straightforwardly with the principles as used in NTSC, a so called semicompatible counterpart is derived performing line stretching in time by a factor of two, thus reducing all frequencies by half. Two stretched lines are then trans-

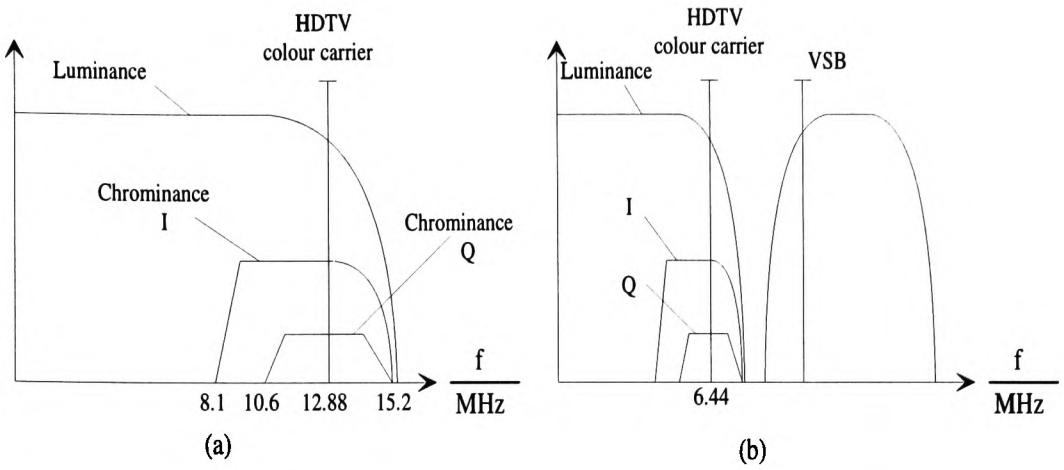

Figure 3.11: (a)Composite HDTV signal (b) semicompatible HDTV signal [76]

mitted in parallel, one line is sent as it is, while the other is sent as a line differential signal, similar as given in Figure 3.10b, on the VSB (vestigial sideband) carrier (Figure 3.11b). An enhanced version of this proposal is presented in [77] using a field differential approach to derive the residual signal, which is further transmitted within the semicompatible signal spectrum rather than using VSB techniques. For this embedded residual, quadrature amplitude modulation on the picture carrier is suggested, as principally shown in Figure 3.12. The main philosophy delivering a semicompatible signal is the property of easy conversion either to standard NTSC or HDTV-NTSC format. With the same formalism it is possible to define a PAL-type semicompatible signal [76][77].

The residual delivery within a standard video signal was initially presented by Fukinuki [78] [79]. He proposes the so called "Fukinuki-Hole", which recognises a frequency area within the Nyquist volume of a luminance video signal, similar as for the colour sub-carrier insertion. From Section 2.3 it is shown that a carrier frequency is chosen to be the odd multiple of half the line rate introducing a nearly invisible slow upwardly moving checkerboard pattern. If the phase of this carrier is inverted on alternate fields, a new, additional carrier is introduced and appears similar as the colour subcarrier, but its checkerboard pattern is slowly moving in the opposite direction. Figure 3.13 gives an insight of the two locations within the vertical / temporal frequency plot. For signal separation at the decoder, temporal filter methods must be employed to distinguish between the information delivered within this

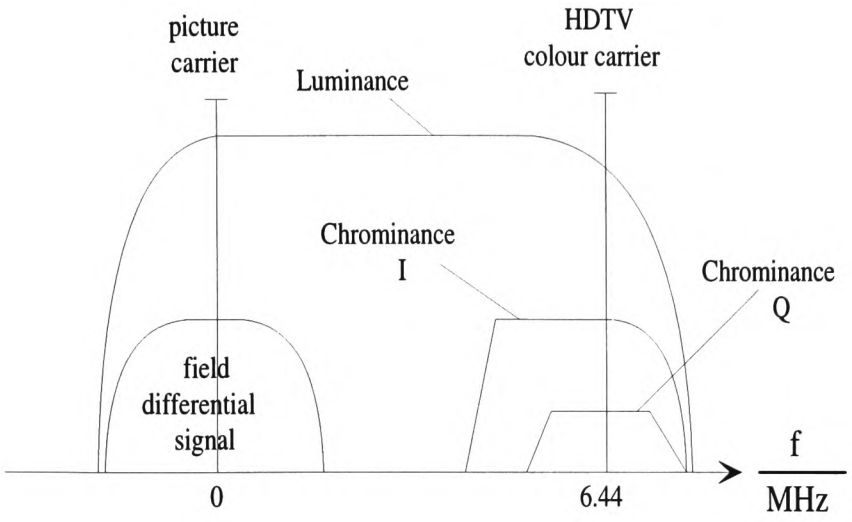

Figure 3.12: Semicompatible HDTV signal employing embedded residual modulation [77]

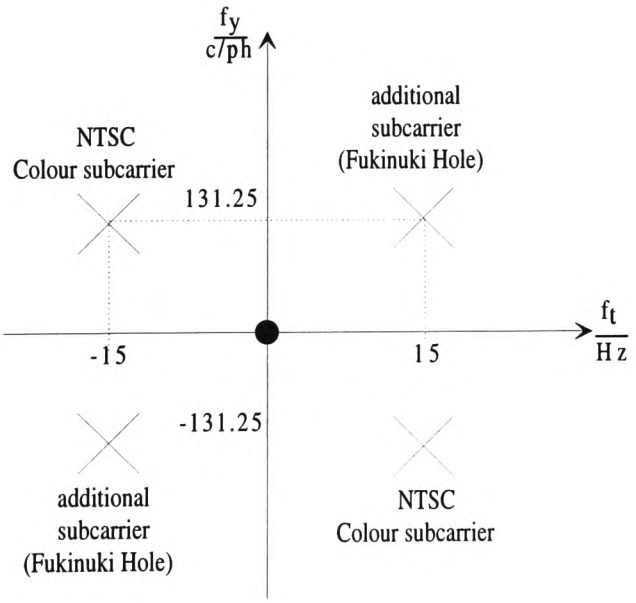

Figure 3.13: Colour and additional carrier positions within NTSC

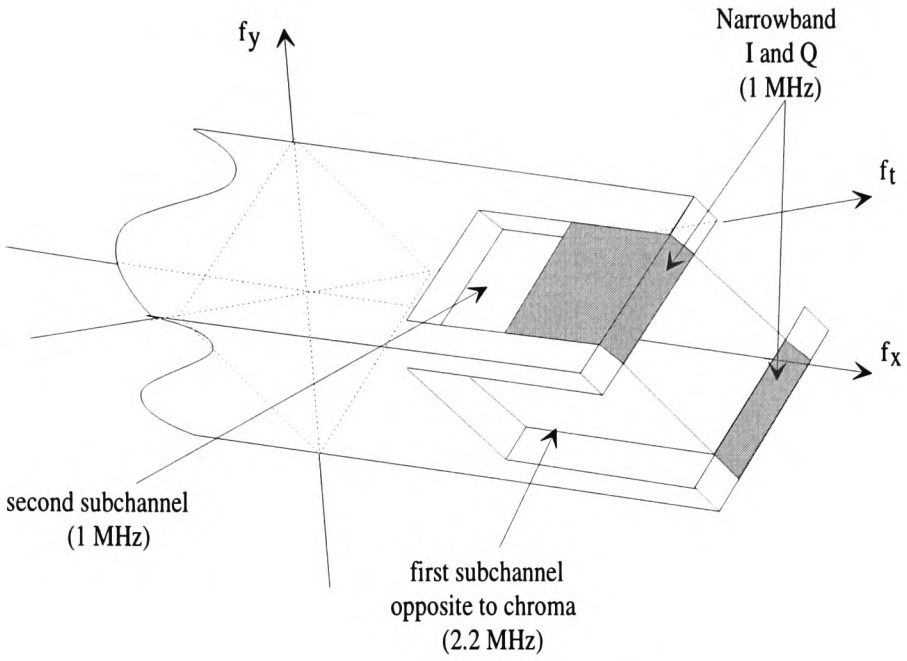

Figure 3.14: NTSC Nyquist volume identifying sub-channels using narrowband chroma [80]

approach.

The initial activities of Fukinuki are further developed by Isnardi [80]. His analysis of the three dimensional NTSC spectrum is aimed at enabling two embedded sub-channels to be available for ancillary information transmission. The three dimensional frequency volume in Figure 3.14 shows that the first sub-channel occupies the same location as in Fukinuki's scheme. The second benefits from a narrowband chroma approach, suggesting the two colour different signals, I and Q, to be transmitted with identical bandwidth (compare Section 2.3). Three dimensional filtering is employed at both the encoder and decoder to limit the Nyquist volume of the chroma and ancillary signals to their specific range and further providing definite spectral location for each component to keep the main luminance signal free from crosstalk.

In [81] and [82] an ACTV (Advanced Compatible Television) system is proposed using the aforementioned sub-channels. Starting from a widescreen HDTV input, the signal is initially split into four components, namely the main NTSC, a side panel, a horizontal luminance detail and a vertical / temporal luminance helper signal. The side panels and the

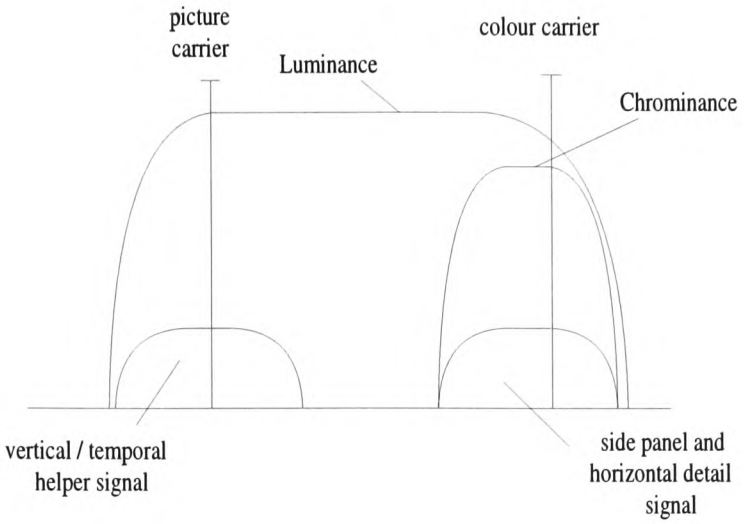

Figure 3.15: ACTV signal spectrum

horizontal detail signals are transmitted using QAM within the previous outlined first sub-channel, where as the helper is quadrature modulated with the picture carrier. Figure 3.15 shows the resulting signal spectrum of the composite NTSC signal.

Several similar suggestions either for one or two channel transmissions have been made, e.g. in [81] [83] [84] [85]. They differ mainly upon which input format they support, interlace, progressive, number of lines, aspect ratio and in which way the residual is delivered for signal reconstitution. Most of the compatible approaches relate to NTSC compatibility, because along the way in standardising a new enhanced TV system in the United States, initially compatibility was required. A comprehensive system comparison is given in [1].

Europe concentrated for a long time upon the fifth level, like the previous alluded Eureka 95 project (Section 3.1.1) or the extended definition MAC (E-MAC) system [86]. The reason behind this was the vision that future TV delivery will taken place via direct satellite transmissions, for which MAC was developed, but since MAC has been cancelled the motivation has been lost. Instead a wide-screen PAL compatible system, PALPLUS, was introduced (see Section 2.3).

3.2 Embedded data modulation

Additional information delivery within a television signal has been seen to be a very attractive facility ever since television services have become widely available. The benefits which accrue from such a facility are manifold, because for a given infrastructure additional services such as extra program information, electronic TV programme guide, multi-lingual high quality sound or special down loading services are feasible. Early systems occupied parts of the VBI (Vertical Blanking Interval), which is a generally unused space between the vertical synchronisation and the actual active video picture. Other activities have explored the use of sub-channels within a television signal, predominantly focused upon HDTV and EDTV compatibility approaches as presented in Section 3.1.3, where the additional resolution is analogue modulated. These approaches however, can be further developed to allow digital ancillary data transmission. The crucial compatibility issue when attempting to integrate digital data within a TV signal, is to ensure that no visible distortions appear on the picture, which normally tends to be a trade-off between subjective quality and achievable data rate.

There are currently several on going activities and lots of discussions on data broadcasting predominantly focusing within the NTSC signal. The "Intercast Industry Group" for example is a non-profit alliance of computer, television, cable and online companies creating a medium which combines television and the Internet on the PC [87]. Intercast (Internet + Broadcast) means the transmission of HTML (Hypertext Markup Language) pages over broadcast television signals, which can be either related to the traditional TV program or totally independent. The technology used by the Intercast group is adopted from WavePhore, which is a small company that proposes the use of different parts of the analogue NTSC signal. A similar group, named "Datacast Partners", concentrate in the same direction, but uses "DegiDeck" technology [87].

Since 1994, the NDBC (National Data Broadcasting Committee), which is a joint initiative between the NAB (National Association of Broadcasters) and EIA (Electronic Industry Alliance), to develop national technical standards for high-speed data broadcasting systems using the NTSC signal as a delivery medium [88]. Originally, five companies submitted

proposals for consideration, but only two advanced to extensive further testing, namely the "DigiDeck" and the "WavePhore" system. After completion in 1996 the NDBC concluded that DigiDeck's technology is a viable system for a data broadcasting service [88].

AUDETEL is a system for transmitting a spoken AUdio DEscription of the TELevision picture and is an example for services for visually impaired people. AUDETEL has been developed by a consortium which is supported by the European TIDE (Technology Initiative for Disabled and Elderly people) however, it has so far not been successfully introduced in Europe, where in North America the BTCS (Broadcast Television System Committee) system already has allocated a suitable sound carrier and transmits audio described programmes several hours per week [89].

Three generally distinct possibilities can be identified for additional information delivery. Firstly, data insertion in the blanking period, either vertical or horizontal, which is the most common technique for a variety of services. Secondly, data insertion outside the active video signal, which actually means that the video signal is left unchanged, while the additional signal is introduced similar to the principles of audio transmission. Finally, the third category points to data insertion strategies within the active video signal. In the sense of compatibility these methods are the most crucial, because data is modulated together with the displayed picture information.

3.2.1 Data insertion in the blanking period

A practical example of TV data transmission in the vertical blanking period is the well-known Teletext system, that was developed in the late '70 to deliver public information to television viewers in the comfort of their home [90]. This service was initially aimed to deliver simple text pages, containing for example news, program or weather information, at low overall cost to the consumer however, since its creation, Teletext has undergone several enhancements. Four levels are currently distinguished related to the support of different character sets and further new extensions were added to handle independent data services as for example sub-titling, PDC (Program Delivery Control) [91], EPG (Electronic Program

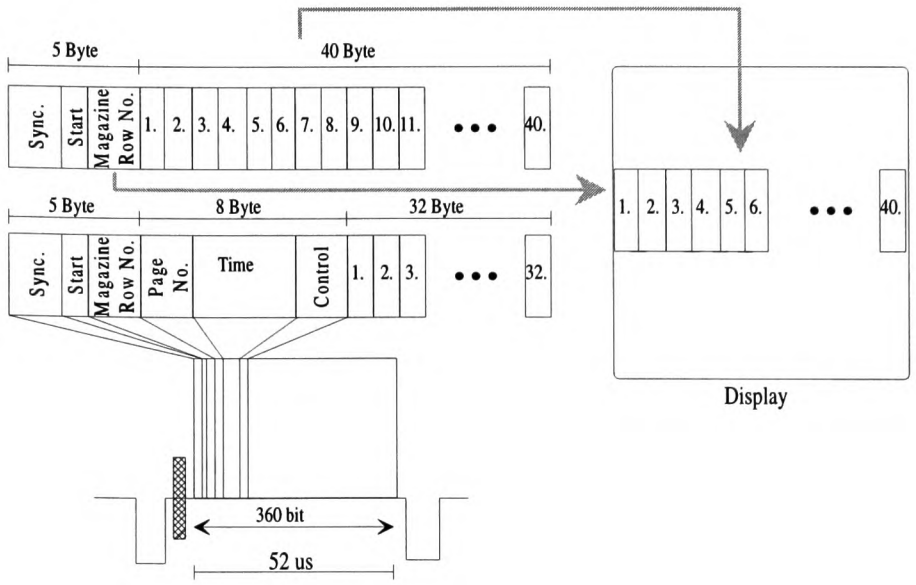

Figure 3.16: Scan line carrying Teletext data [93]

Guide) or transparent downloading. An indication that Teletext is well accepted can be seen in the allocated lines for transmission, which have been grown from an initial only four to the current ten [92].

Figure 3.16 gives an insight into a scan line carrying Teletext data. It is obvious that no modulation is employed. The data are NRZ (Non Return to Zero) coded followed by pulse shaping using Gaussian low-pass filtering resulting in a roll-off factor of approximately one. Due to the video bandwidth restrictions of $5MHz$, 360 bits organised in 45 Bytes, are delivered within one scan line. The leading five bytes are used for synchronisation and control information, with the payload (user data) delivered within the following 40 bytes. The header line of each Teletext page occupies an additional eight control bytes, so only 32 bytes remain for user data. Each byte of the user data carries one character of the Teletext page where the horizontal position on which it appears on the screen, directly correlate to the transmission order, so one Teletext scan line delivers one horizontal line of the visual page. The whole page consists of 20 plus one header line, so that if assuming an allocation of four VBI lines per frame a full Teletext page is delivered within 0.24 second [93] (blank lines are not transmitted).

The Teletext system is unidirectional, which implies that the entire information content

	ITC recommendation	BBC	ARD / ZDF		ITC recommendation	BBC	ARD / ZDF
6		Local Noise		318			
7	Commercial Data	Network Noise		319		Local Noise	
8		Datacast		320	Commercial Data	Network Noise	
9				321		Datacast	
10	Teletext			322			
11			Teletext	323	Teletext		Teletext
12		Ceefax		324		Ceefax	
13				325			
14				326			
15				327			
16			Data (VPS)	328			Data
17			Test Signals	329	Ancillary		Test Signals
18	Ancillary			330			
19	Test Signals	Test		331	Test Signals	Test	
20		Subtitles	Teletext	332		Subtitles	Teletext
21	Broadcast-Data	ITS		333	Broadcast-Data	ITS	
22	Quiet	Test		334	Subtitles	Test	
23				335			

Table 3.2: VBI line allocation

must be transmitted periodically, so if users requests a specific page, they have to wait until it is transmitted.

Another service, named data broadcast or Datacast, implemented within the VBI is aimed to deliver messages to a closed group of users (e.g. for news agencies). The Datacast line structure is different from the ordinary teletext line. It also differs in that the information can be interpreted without reference to other lines, so it is not page based [94].

Since October 1985, the VPS (Video Programming System) transmits data in Germany within the VBI line 16. The data provides mainly television program information focussing on video recording in the way that the recorder is synchronised with the program transmission, so if a specific TV distribution is delayed or cancelled the video recorder will take this into account. The modulation is similar to that of the general data services [24, Section 3.4.5], using a bi-phase coding to transmit 108 bits within the scan line.

Another, new service is the so called "Line 23 signalling". It is introduced together with PALPLUS and provides four signalling features, namely transmitted aspect ratio, subtitle conditions, enhanced TV services and extensions [95].

Table 3.2 summarises the services which are currently been using together with their allocation of the provided 36 VBI lines. Not all broadcasters follow the ITC (Independent

Television Commission) recommendation however, all expend the most capacity on Teletext. It is also clear that the VBI is nearly completely occupied, so that any additional expansion of Teletext or even new multimedia service provision is nearly impossible.

The achievable data rate however, provided by the Teletext systems, is far too low for multimedia applications. A more efficient approach to use the capacity the VBI actually provided, is to combine the raw data rate of all available lines to one transparent data channel. Thus a maximal data rate of

$$35\frac{line}{frame}360\frac{bit}{line}25\frac{frames}{s} = 315K\frac{bit}{s} \tag{3.1}$$

should be possible. A suggestion for the American NTSC television system, called VBI [96] was made by WavePhore, USA, following this philosopy. This system occupies the first ten lines of each field and thus also provides a $150kBit/s$ data rate.

Not only the vertical blanking is usable for additional information delivery, also the horizontal blanking interval provides potential for data services. The available capacity over one frame is similar to that provided by VBI techniques [24, Section 3.4.3]. A system called SIS (Sound in Sync.), developed by the BBC (British Broadcasting Corporation), is an example of inserting data in the horizontal blanking period for digital audio transmission. A trade-off of this system is, that it caused synchronisation problems at the receiver however, though it is currently used for high quality audio within the Eurovision-Network.

Another fully compatible system using the horizontal blanking interval is proposed by Finger et.al. [97]. Avoiding the problems inherent with the SIS technique, this system uses a data signal amplitude of less than $20mV$. To ensure nevertheless a sufficient error rate, the data stream is modulated using spread spectrum technology before being added to the blanking interval. At the decoder a correlation receiver ensures the data reconstitution. Figure 3.17 provides a block diagram giving an insight to this principle. The system is designed to provide a datarate of $150Kbits/s$ with error rates less than 10^{-4}. It should be mentioned that the German Telekom adopted this system for their new BOT service. First trails were demonstrated during the Berlin fair (IFA'95).

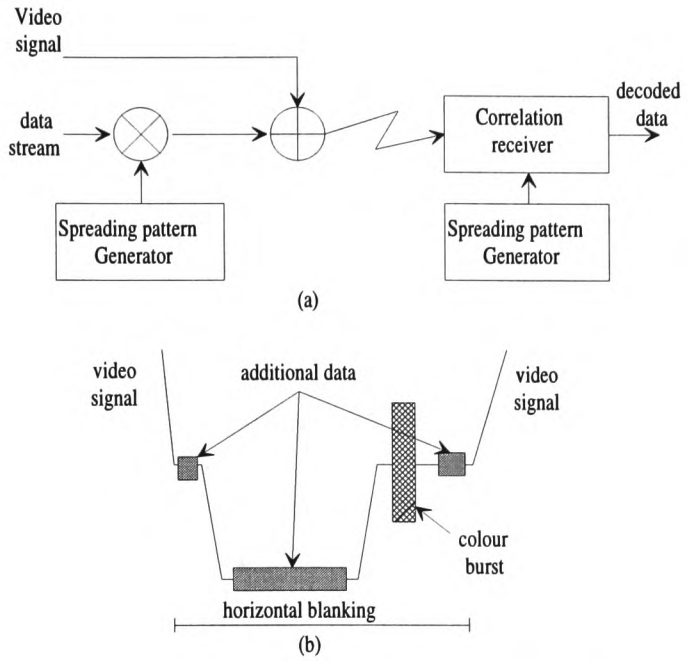

Figure 3.17: Principal block diagram for embedded data delivery within the horizontal blanking period using spread spectrum technology [97]

3.2.2 Data insertion outside the active video

The overall transmitted television signal is a frequency multiplex of video and audio signals. Therefore the audio is modulated, mostly using FM (Frequency Modulation) on a carrier located above the video baseband before both parts are subsequently amplitude modulated by the picture carrier. New services can exploit this approach by inserting supplementary sub-carrier modulated by data signals. This was actually performed by introducing a second audio channel in Germany in 1975 enabling both stereo and twin-mono sound.

In the mid 1980's the BBC developed a fully digital solution for stereo and twin-mono sound called NICAM-728 (Near-Instantaneous Companded Audio Multiplex). It provides $728 Kbit/s$ raw data transmission capacity usable either for two audio or two data channels or further in a mixed mode. The data stream is modulated employing DQPSK (Differential Quadrature Phase Shift Keying) on a sub-carrier above the ordinary audio carrier (Figure 3.18). The packet structure of NICAM-728, laying on top of the raw data stream, provides additionally a parallel ancillary data service of $11 Kbit/s$ data-rate [98].

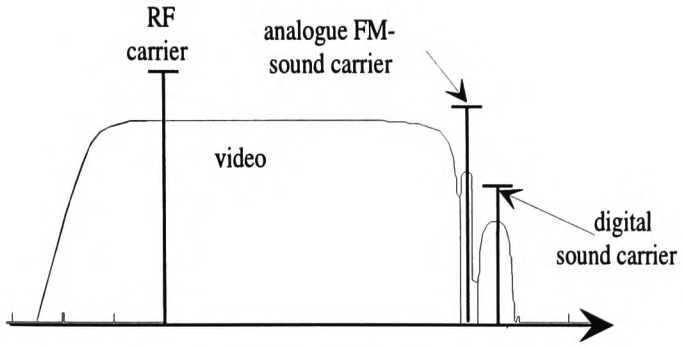

Figure 3.18: TV signal spectrum with integrated NICAM carrier [98]

Similar to the NICAM-728 system, another WavePhore system, called TVT1 includes an additional carrier between the colour- and sound carriers subsequently PSK (Phase Shift Keying) modulated. To limit interference, the video base-band must be attenuated at high frequencies however, the remaining distortions are masked by other NTSC effects [96]. This system provides a data-rate of $384 Kbit/s$

Another solution is proposed by Dinsel [99], involving an additional carrier, modulated by a 16 QAM, which is subsequently modulated by the original FM sound carrier. The system was originally proposed for enhanced digital audio for PALPLUS together with the MUSICAM data compression technique (MPEG-II Audio Layer2), called "MUSICAM-on FM" however, it has not been implemented, because of the decoder complexity. The carrier frequency needs to be chosen to be a multiple of half the line frequency to reduce visible interference and also has to be high enough so that the whole additional spectrum can be placed outside all audible frequencies. Figure 3.19 shows the proposed solution. This technique enables a typical throughput of between 128 and 196 kbit/s.

3.2.3 Data insertion inside the active video

The previous two sections identified, that the available capacity for new supplementary services is limited really to the aforementioned techniques, mainly due to the allocation of already established services. In considering more sophisticated data applications than those currently available, new channels which are embedded within the active video signal need to

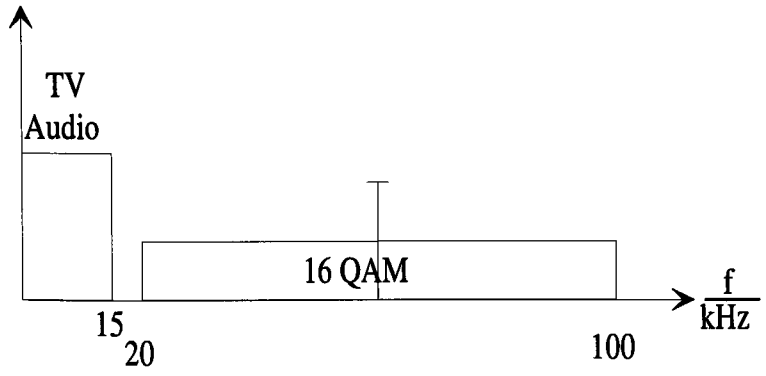

Figure 3.19: Modulation scheme proposed by Dinsel [99]

be examined to provide potential for exploration.

The insertion of additional data within the active video signal implies that such methods will inevitably encroach upon the sensitive issue of compatibility. Early research in this field [100][101] used the principles of spread spectrum technology, while concentrating upon the optimisation of the spreading sequences to supply a reasonable compromise concerning subjective visibility. The modulated data signal is added to the video with very low amplitude. A correlation decoder at the receiver demodulates the data signal and although the presented results gave a reasonably good subjective impression, the achievable data rate is however rather low.

Another novel approach was suggested by Ruppel [102] [103], who employed QAM of the picture carrier closed to the ACTV-I proposal by Insardi (refer Section 3.1.3) however, Rupel developed a MQAM (Modified Quadrature Amplitude Modulation) technique providing enhanced cross-talk properties. This is accomplished by taking care of the different RF (Radio Frequency) demodulation techniques usually used at the receiver, namely envelope and synchron demodulation. The envelope technique principally performs demodulation by deriving the absolute value of the complex input, so is insensitive to phase changes, where as the synchron method derives the real component and thus recognises any phase variation. A straightforward QAM implementation provides perfect signal separation at the receiver if synchron demodulation is employed however if not, unacceptable cross-talk effects will occur. Conversely, an implementation of pure additional RF phase modulation will

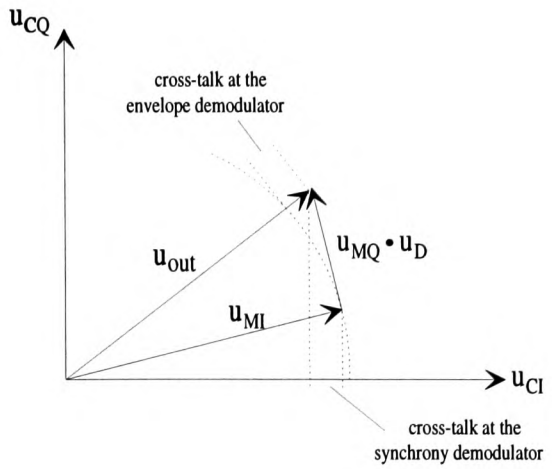

Figure 3.20: Principle phase relationship for MQAM technology [102]

ensure optimal results for envelope based receivers, but fails for all others. Ruppel's MQAM suggestion is a combination of phase and quadrature modulation aimed at providing an optimum for both demodulation types. The principles are given in Figure 3.20. The input signal u_{TV} is initially modulated with the in-phase and quadrature component of the RF carrier, u_{CI} and u_{CQ}, respectively. The quadrature part u_{MQ} undergoes further modulation with the data signal stream u_D, before being subsequently added with the in phase component u_{MI} to form the final output signal u_{out}. Figure 3.20 indicates the remaining cross-talk for both demodulation techniques. Ruppel pointed out that his proposal allows a $4dB$ higher data signal power compared to the worst case scenario utilising QAM [103] and achieved a $500KBit/s$ data rate.

The enterprise "DigiDeck" proposes a different solution, inserting an additional carrier at the lower end of the Nyquist slope, which is subsequently DPSK (Differential Phase Shift Keying) modulated to provide $500KBit/s$ data rate [96]. The DigiDeck system was one of the submissions evaluated by the NDBC for a data cast technique within NTSC.

As mentioned previously, the modulation techniques suitable for additional data transmission, benefits from earlier research undertaken during HDTV and EDTV development.

In [104][105][106] during the development of the PALPLUS, a strategy was proposed for modulating the additional analogue widescreen information together with the colour carrier, however this was never implemented.

3.3 Data compression techniques

Data compression plays a vital role in digital signal processing, especially in digital audio, image or video processing. The raw data rate, for example of a digital TV signals following ITU-R601 is $216MBit/s$, but with modern compression techniques like MPEG-II the bit rate can be compressed to less than $5Mbit/s$ providing acceptable subjective quality.

This section reviews the principles of image and video compression techniques. The survey is closely related to the basics on which the standardised compression schemes, e.g. JPEG (Joint Photographic Expert Group) and MPEG are built and will further be used to evaluate their suitability, so fulfilling the original objectives of this research project.

There are many suggestions available for classifying the various compression principles [4, Section 1.5] [70, Section 1.3] [107, Section 5] however, the layout used in this thesis distinguishes in principle three categories. The first refers to lossless coding techniques, where lossless is defined as an information transmission without any loss, but also without any overheads. The second focuses upon lossy principles, which means transmissions with some information loss, but in such a way that whatever is omitted is unusable at the information sink. The third section reviews the various algorithms by highlighting their application within the most important compression standards currently available. A brief review of all three classifications now follows.

3.3.1 Lossless coding principles

Any digital signal data stream can be considered from the view point of information theory, with definitions and laws describing and characterising basic properties of this specific source. Within this theory a principal communication model is defined, containing infor-

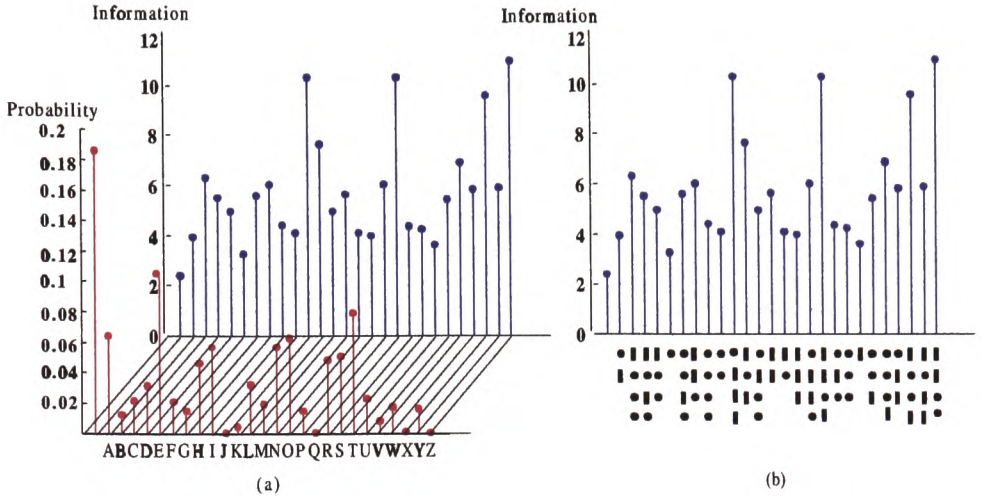

Figure 3.21: (a) example of probability and information content (b) historical Morse alphabet as an example of variable length coding

mation source and destination linked via a transmission channel. During communication the source transmits sequentially symbols, which are selected from a finite set, called an alphabet. This selection process defines the information carried by each symbol and can be further measured with their probability. Figure 3.21a shows as an example the probability distribution of the English letters. It is obvious that certain letters are used more often than others and thus they are carrying less information. A simple approach to make use from this inherent property is to transmit the symbols with different code lengths, such that those symbols occurs more often are mapped to short code words and vice versa. This principle was directly applied with the Morse-Alphabet (Figure 3.21a).

From a more theoretical definition, a source is characterised by its entropy, which is a measure of the information carried with each symbol of the source alphabet, or in other words the mean information transmitted by this source. A further characterisation is the maximal decision possibility of an information source, which is identical to the entropy for a uniform probability distribution of their symbols. The difference of both is defined as the redundancy and identifies the compression ratio accomplished with variable length coding algorithms. Figure 3.22a gives a practical example. The picture of Lena is usually 8 Bit coded, but the grey-level occurrences are different, so from the probability distribution an entropy can be

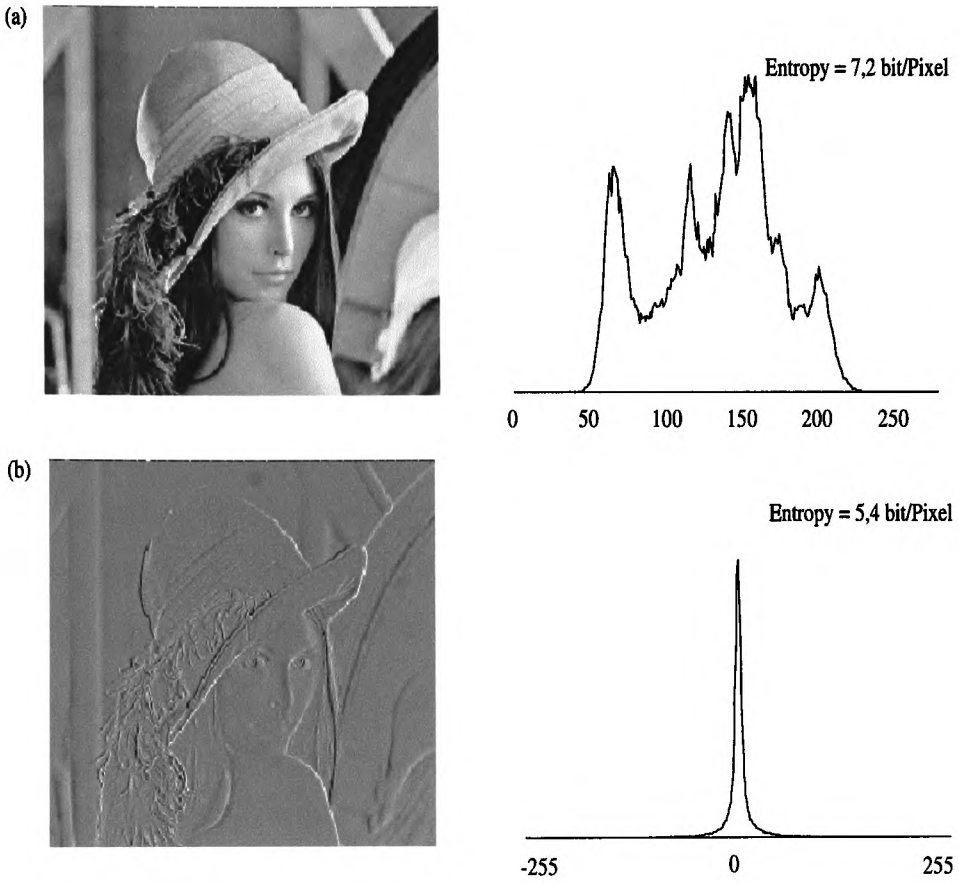

Figure 3.22: (a) "Lena" and grey-level probability distribution (b) differential picture and grey-level probability distribution

derived which is less than 8 Bit. The knowledge of these level probabilities provides an overall compression potential by applying variable length rather than fixed codewords of each grey-level. Two main algorithms are applied to derive variable wordlength codes from a given source statistic, namely Huffman and Arithmetic coding. The Huffman-code ensures an optimal efficiency [107, Section 3.1.1], but the mean code-wordlength equals the source entropy only if the symbol probabilities are negative powers of two, e.g. $\frac{1}{2}$, $\frac{1}{4}$, etc. The arithmetic coding principles overcome this limitation [4, Appendix 1][70, Section 3.4].

It is clear that with such a simple statistical model only a small amount of the redundancy is exploited and removed. More potential can be achieved by including the relationship of consecutive symbols. This is performed with either block- or conditional coding [107,

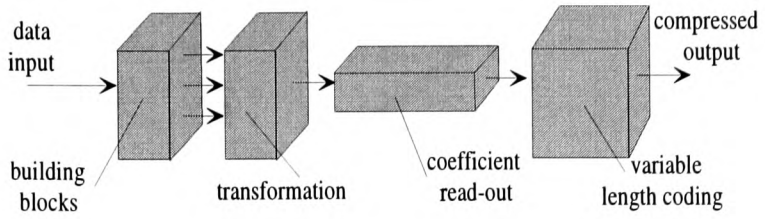

Figure 3.23: Principal block diagram of a transformation encoder

Section 3.1.2/3.1.3]. Block-coding combines a finite number of linked symbols to form blocks, which further undergo variable length coding, where conditional coding derives the codeword for the actual coded symbol from the statistical relation of the previous symbols. Both techniques raises fundamental problems coursed by the number of variable word-length code sets that must be generated and available during coding and decoding.

For image and video data compression the major redundancy is found between the neighbouring samples, because of unique areas usually inherent with natural pictures. To use this compression potential and further to overcome the problems of large codeword sets, the difference between consecutive samples is initially derived before employing variable length coding. Figure 3.22b shows such a difference image of Lena, processed by subtracting the horizontal neighbouring samples, together with the difference grey-level statistics. It is obvious that the entropy decreases significantly with this source model. This differential is not limited to the horizontal direction however, also vertical, diagonal and temporal neighbourhoods or combinations of all can be employed. Generally these strategies are known as predictive coding, whose basis is to predict the upcoming sample and further derive a prediction error by subtraction. With such a two dimensional prediction, followed by a variable length coding, a compression ratio of two can be achieved [70, Section 7.2]. This realistically is the maximum attainable for all lossless algorithms.

Another pre-processing technique to exploit neighbouring redundancy is transform coding. Figure 3.23 shows the principal processing steps. The input data samples are initially combined into usually fixed length blocks before applying the transformation algorithm to derive a set of coefficients representing each block. The purpose of transformation is to concentrate the energy, originally carrying by each data sample within the blocks, to only a few

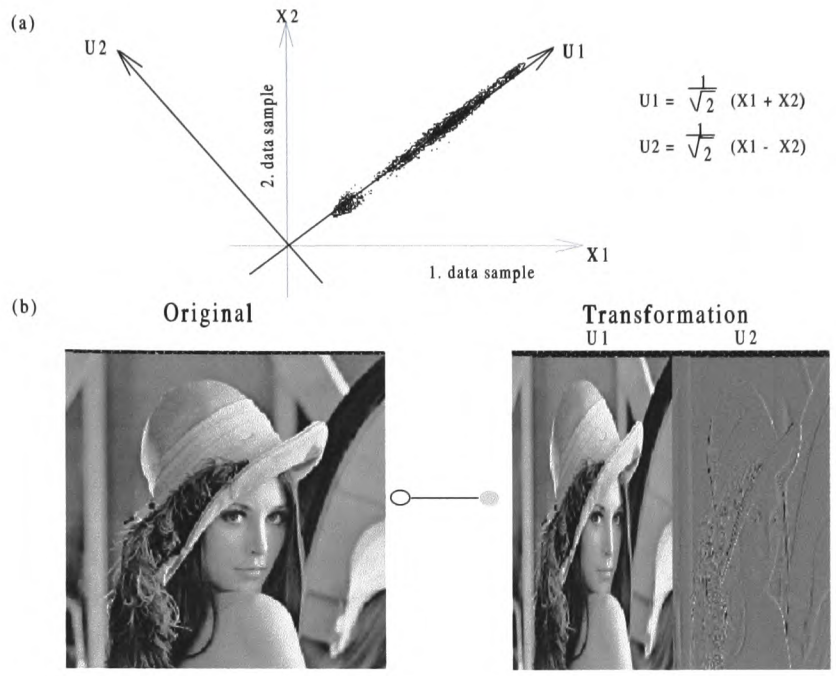

Figure 3.24: (a) Coordinate rotation as a simple transformation example and (b) the application upon "Lena"

coefficients and thus providing excellent condition for further variable length coding. For decoding, the inverse transformation must be employed. Figure 3.24a gives an insight to this principle by applying a simple transformation within a block of two horizontal neighboured samples of the input image "Lena". Both, X_1 and X_2 contain values over their whole range, but due to the fact of consecutive similarities, concentrated along the diagonal direction. Performing a coordinate rotation of 45 degrees, it is obvious that only the coefficient U_1 captures the whole range of gray-levels while the variance of U_2 is reduced. Figure 3.24b shows the result of this transformation. From the coding perspective, there are no clear benefits for the first coefficient, but it is also apparent that there is much merit with the second coefficient.

The block size is clearly not restricted to two data samples. For image and video coding the picture is commonly segmented into non overlapping two dimensional blocks, usually 8 by 8 pixels in size [108, Section 4.1.5] [109, Section 3.3]. A straightforward expansion of the previous simple example to larger and further two dimensional blocks leads to the "Walsh-Hadamard" transformation [4, Section 3.3.1][107, Section 5.3.1b] while there are

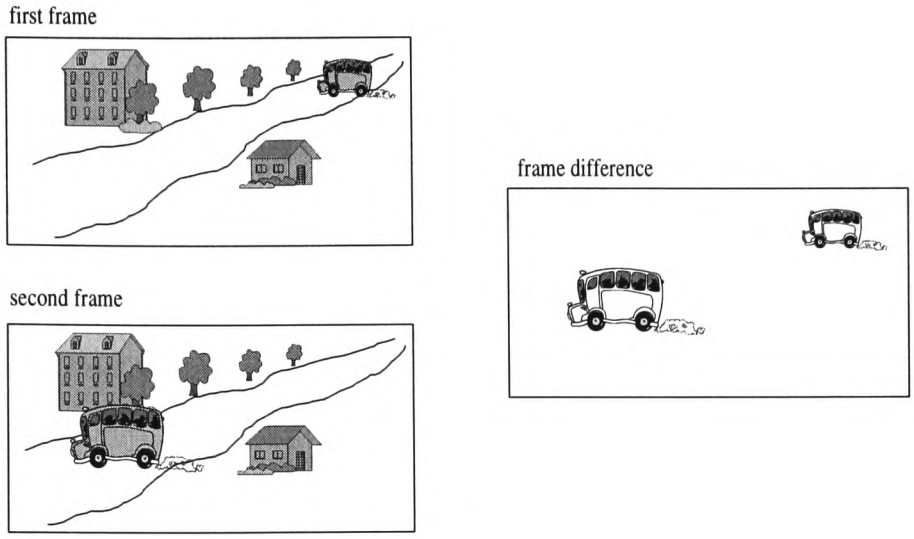

Figure 3.25: Example of redundancy between consecutive frames

many other transformation algorithms available [107, Section 5.3.1e] of which the DCT (Discrete Cosine Transformation) has been the most widely enforced. The advantages of the DCT against the others are the relatively good de-correlation properties together with decomposing the data into their underlying spatial frequencies [109, Section 3.4] without the inherent problems associated with discontinuities (spectral leakage) at the ends of a data block, which are well known from classical Fourier transform theory [4, Section 3.3.2]. It should be mentioned that the KLT (Karhunen Loeve Transformation) is optimal in the sense of de-correlation properties however, from a real-time implementation point of view the DCT is much more superior.

The compression principles analysed so far relate only to intra-frame processing, however major redundancy can be exploited by employing inter-frame techniques. Figure 3.25 gives an example by simply deriving the difference of consecutive frames within a video sequence, so that in the difference picture only the moving parts remain. This technique is usually applied in hybrid implementations together with, for example DCT, coding.

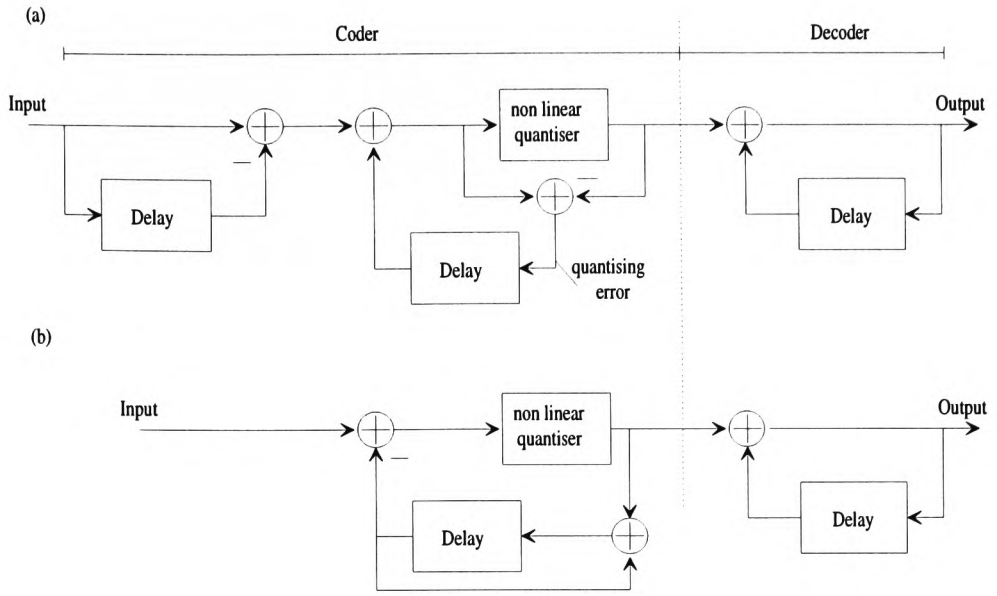

Figure 3.26: (a) Block diagram of basic DPCM technique and (b) the transformation into the commonly used structure

3.3.2 Lossy coding principles

The data compression ratio achievable with lossless algorithms is limited, as outlined in the previous section to a maximum of two. To provide higher rates, lossy techniques must be employed. Lossy means to omit unusable information from the communication process, which will not be processed at the receiver. For image and video applications the destination is clearly the human eye, so psycho-visual considerations are generally important [4, Section 1.2][107, Section 4.3], however mainly two properties of the human eye are utilised from the common principles, namely the masking effect and the eye's spatial bandpass response. Masking means that the eye is less sensitive to low contrast details in the surrounding of a highly modulated signal portion as for example an edge. The eye's spatial characteristics amongst others includes the oblique effect, which is a property that the human vision focuses predominantly upon horizontal and vertical structures, so that a loss on diagonal parts can be tolerated [110].

The DPCM (Differencial Pulse Code Modulation) technique was an early approach in making use of the masking effect. It is a combination of differential coding followed by

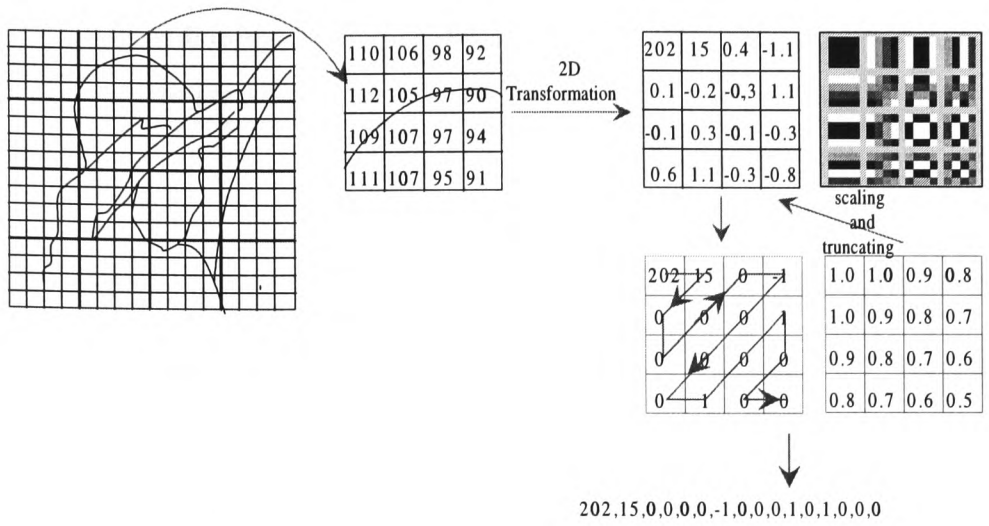

Figure 3.27: Processing steps for DCT coding

non linear quantisation, providing an accurate representation for small and a much coarse representation for large differences. The inevitable introduction of quantising noise at large differences is hidden in part due to the mask effect mentioned above. Figure 3.26a shows a block diagram of the principle behind a DPCM strategy. The subtraction at the encoder implies an integration at the decoder. This involves a quantiser with error feedback to avoid an accumulation of quantising errors. The given hybrid block structure can be transformed in the more compact, commonly used version [24, Section 4.4.4] (Figure 3.26b).

The principles of transform coding, as alluded to in the previous section, are generally lossless however, they provide the possibility to adapt the eye's frequency characteristics by the coding process. Figure 3.27 gives an example of a two dimensional DCT coding, employing a 4 by 4 block size and shows the block pattern represented by the corresponding coefficients. To fit the coding to the human eye's spatial frequency response the coefficients are scaled according their visual perception and further truncated to the nearest integer value. This is similar to quantising each coefficient independently, so high frequencies are represented coarsely with a fewer number of bits, than those representing low frequency components, so again exploiting the mask effect. Finally, the coefficients are read, usually by applying the so called "Zig-Zag scan". The advantage of this method is that the coefficients are ordered according their importance, so that due to the scaling process, most parts of the

still image compression	intra frame video compression	inter frame video compression
JPEG	M-JPEG	MPEG-I / MPEG-II
	DV(C)	H.261 / H.263

Table 3.3: Examples of common standards in the area of digital image and video compression

sequence contain zeros, which provides further compression potential (e.g. variable length or run length coding).

3.3.3 Standardised compression techniques

There are many different industrial interests in employing digital image and video compression techniques, e.g. in consumer-, computer-, television- or telecommunication areas. The convergence of these interests into a resulting standardisation provides the potential for a large volume of sales which ultimately lowers the cost of integrated circuits for all. Furthermore, a standardised technology lowers the barriers that are usually present to its deployment and therefore reduces the risk factor [109, Section 1.2].

Table 3.3 compares the most common standards, which are already established together with their application fields. The scope of JPEG is the coding of continuous-tone-greyscale or colour digital still image data [111]. It specifies the encoder, decoder and the interchange format. JPEG distinguishes between four modes of operation, namely a sequential DCT-based, a progressive DCT-based, a lossless and a hierarchical mode. The lossless mode directly applies the two dimensional differential coding technique introduced in Section 3.3.1 followed by a Huffman or Arithmetic variable length coding. The implementation of the two DCT-based modes are specified similar as shown in Figure 3.27, but with a further processing of the compressed data stream such that the DC-coefficient is differential coded with that of the following block and the AC-coefficients in a run length fashion. The final Huffman- or Arithmetic coding provides a further compression ratio enhancement (Figure 3.28). The key difference between the two DCT modes is that the input picture is encoded in multiple rather than in a single scan for the progressive and sequential mode, respectively.

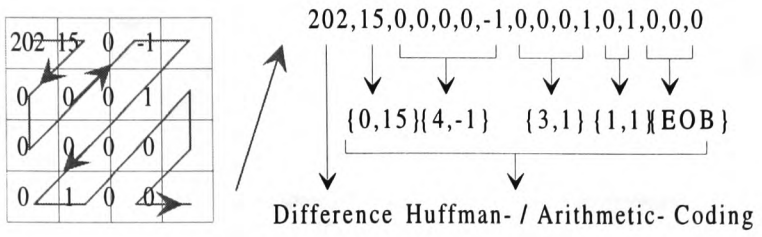

Figure 3.28: Further compressed data stream processing standardised by JPEG

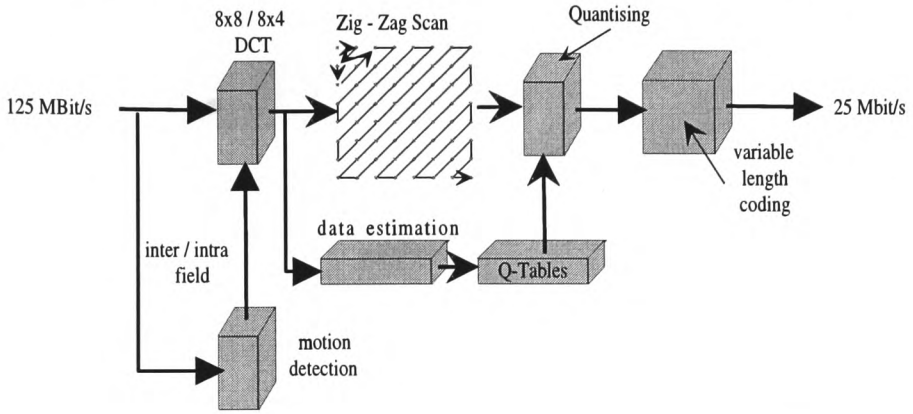

Figure 3.29: Block diagram of the DVC pseudo standard

This allows a quick rough vision however at the cost of implementation complexity. The hierarchical operation mode provides encoding of an image at multiple resolutions, which can be either lossy or lossless. A compact overview of the JPEG standard is given by Wallace in [112].

The JPEG standard is originally developed for still pictures, however, there is no reason not to apply these coding principles for moving sequences. This is what is actually addressed by the M-JPEG (Motion JPEG). The M-JPEG is not a separate standard, it simply employs the JPEG within each frame of a video sequence. This simple strategy implies two major disadvantages, firstly it cannot provide the optimal coding efficiency, because inter frame redundancy is not incorporated and secondly a continuous output data stream is not possible.

Figure 3.29 shows the block diagram used with the DVC (Digital Video Cassette) consortium pseudo standard for consumer and semi-professional video recording. The main coding principles are similar to those specified by JPEG, but additionally a forward data estimation

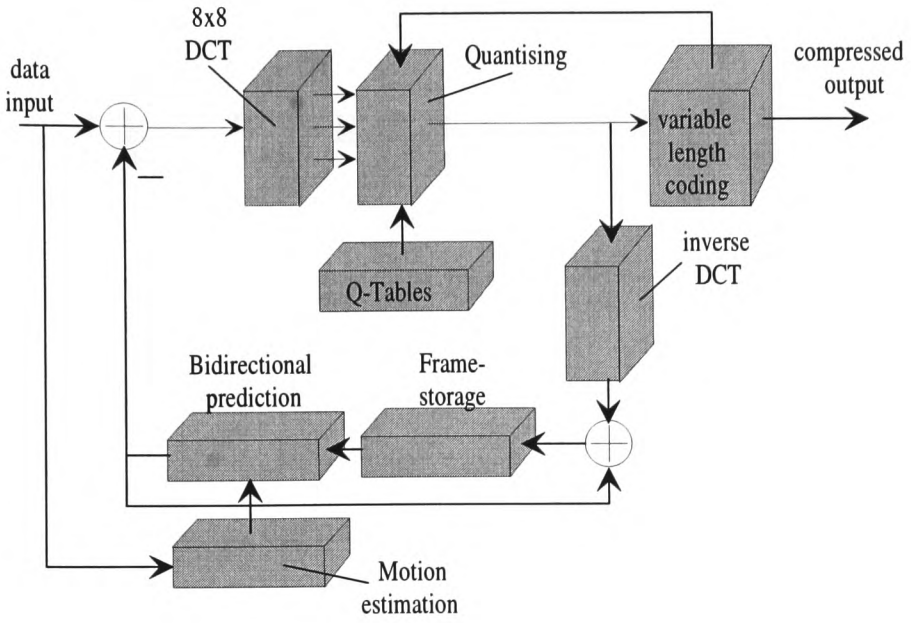

Figure 3.30: Block diagram showing MPEG coding principles

is employed to provide a dynamic adaptation of the quantising tables and thus the possibility of a continual output data stream. Furthermore, a motion detector switches between an intra- and inter- field DCT mode for the processing of an interlaced input. The DVC compression technique however, makes no use of inter frame redundancy, thus the compression ratio is limited to five [113] [109, Section 19.1.5].

In contrast to the previous explained standards, MPEG-I/II and also H.261/H.263 makes use of the redundancy inherent with consecutive frames. The underlying principles are identical for both compression families and are similar to those introduced in Section 3.3.1. Figure 3.30 gives an insight to the basic block diagram used with MPEG. It is a temporal DPCM structure with a DCT instead of a non linear quantiser. Further, the DPCM loop derives the difference of the actual frame and a predicted version of it, provided by motion estimation. MPEG first implements the concept of bidirectional prediction, that is a technique utilising information from the preceding and upcoming pictures. Therefore three different coding categories are distinguished, namely I-, P-, and B-pictures. Intra frame coded or I-pictures are processed without any correlation to neighbouring frames (similar to JPEG). Predicted or P-pictures are coded with respect to the closest I- or P-picture in a for-

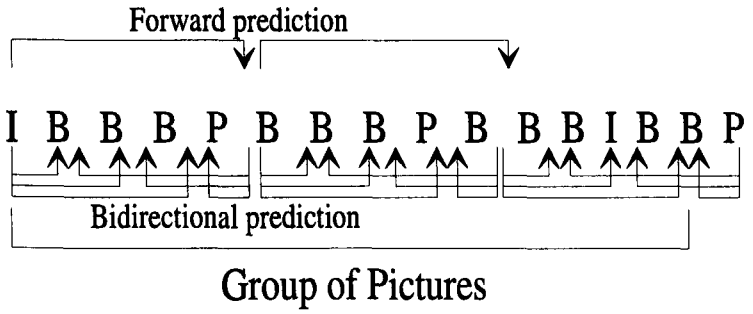

Figure 3.31: Example I-, P- and B-picture outline within a GOP

ward direction and bidirectional or B-pictures are interspersed between the I- and P-pictures and are coded with respect to the immediately adjacent I- and P-pictures either proceeding, preceding, or both [109, Section 5.4.1]. The decision which coding category is applied to which frame, is arranged by the GOP (Group of Pictures). Figure 3.31 shows such an example arrangement. The GOP starts with an I-picture and ends before the next I, so that only one inter-frame coded picture exists within each GOP. Both the choice of the length and number of P- and B- pictures between consecutive I-frames is totally flexible, though the potential for accumulative errors due to large number of P-frames needs to be continually kept in mind.

The underlying technique in deriving motion estimated pictures is based upon motion vectors, which are commonly obtained by applying block matching algorithms. The image is segmented into blocks, where for each block the displacement to the position in the following picture is derived utilising correlation techniques or more faster versions thereof [114].

In comparison to MPEG-I, which was initially aimed for computer applications, MPEG-II is a straightforward development focussing towards television operation. Thus different picture resolutions and different colour schemes are supported as well as frame / field based motion vector calculations. The flexibility of MPEG-II found attention in a profile / level approach to take care of the different needs of various applications, e.g. TV broadcasting, consumer video recording or professional applications [115, Section 3.4.6]. It should be mentioned that both MPEG standards contain three parts, covering audio, video and systems aspects [116] [59] [58] [60]. Concerning telecommunication coding standards H.26x, their

coding principles are generally identical to those of MPEG however, the complex asymmetry of MPEG encoder and decoder structure is not acceptable for telecommunication applications, so that some loss in compression performance is inevitable to keep the delay between encoder and decoder low [109, Section 19.2].

3.4 Contemporary review and interim conclusion

This chapter has reviewed the areas of enhanced television, data broadcasting and also the main activities within the field of data compression. It was shown in Section 3.1 that the motivation of enhancing contemporary television is still very much alive. The initial efforts in standardising an either enhanced or high definition system has produced different solutions such as MUSE, HD-MAC together with others whose focus was for a NTSC compatible system. All these analogue systems however, failed to become universally accepted. Much more success is promised by the current fully digital solutions. Two systems dominate currently, the European DVB and the American ATSC system and both are actively lobbying to be accepted in many countries around the world. Both solutions are highly flexible and are no longer only focused upon HDTV alone, but on multi-program and multimedia distribution. This promise is tempered somewhat by the total lack of compatibility with conventional TV systems.

There is no doubt that future television will be digital, but this issue of compatibility raises several problems as seen during the launch of such a new service in Germany. In contrast the PALPLUS initiative shows that if compatibility is the basis, a much easier introduction and therefore an increased acceptance is possible. Such systems cannot hope to provide the same level of service, but as clearly outlined throughout the review of compatible strategies, there is much potential in enhancing current analogue system for distributing supplementary services.

Section 3.2 reviewed current available techniques enabling such supplementary services. It was outlined that there is a need for more sophisticated techniques than those currently available which exploit only the vertical and horizontal blanking periods. These parts of

the video signal are fully occupied. Other strategies, for example additional digital modulated carriers outside the video signal cannot be universally proposed, because such services as NICAM-728 have already been allocated these spectral regions. So realistically only the active video signal provides additional potential for enhanced supplementary services. Throughout the review, additional picture- and colour sub-carrier modulation was identified to be suitable for this purpose from which the colour sub-carrier approach is the more attractive in terms of providing an acceptable data rate for such services.

The main focus of this work was to transmit an enhanced television signal compatible with a PALPLUS signal. The PALplus system offers a much broader opportunity and potential to reach the goal of a compact encoded HDTV input for transmission in standard channels, because the standard implicitly embraces aspect ratio conversion. The major difference in comparison with other activities is the deriving of a digital residual which undergoes further digital compression before being digitally modulated. It must be highlighted as mentioned throughout this chapter that the interest in pure HDTV systems will continue to fade more towards multimedia solutions, so that the proposed compatible modulation strategy to enable digital sub-channels will become an important issue.

To complete the original idea of this work, Section 3.3 reviews the main activities in the area of digital data compression. After an initial introduction of lossless and lossy principles, the main standardised techniques are presented to provide an estimate of feasible compression ratios, with current technology.

Chapter 4

Compatible embedded digital data modulation for high quality TV

The block diagram of the proposed system is shown in Figure 4.1 and is analysed in detail in this chapter. As mentioned in Section 1.2 this chapter will concentrate predominantly on a system based around the PAL / PALPLUS analogue transmission technique. The input HDTV signal initially undergoes preprocessing where it is decomposed into two main components using the "Dual-Channel Subband Technique" proposed by Schmidt at al [6] and which is further discussed later. Firstly, the down-conversion (decimation) section generates the standard resolution TV element which is to be subsequently PALPLUS coded to form the compatible signal. The second component is a digital residual signal, which undergoes further digital compression before being integrated together with the analogue PALPLUS signal to form a composite EDTV signal. This integration provides a fully compatible modulation framework, which enables digital embedded subchannels within a PAL / PALPLUS television signal. In this context the capacity is utilised for the residual signal, but more generally this is a transparent technique and therefore available for many other sorts of new television and multimedia services.

This chapter will concentrate upon the three processing blocks and hence is separated into three sections:-

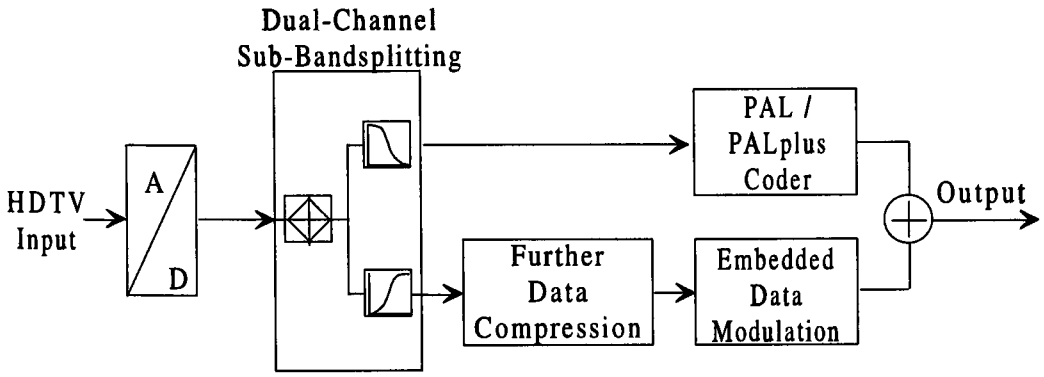

Figure 4.1: Block diagram of the presented system

Section 4.1: The section will concentrate upon the "Dual Channel Subband" processing. It will discuss the use of QMF techniques, in order to eliminate aliased artefacts, in combination with diagonal filtering methods. This will be analysed as the initial stage in deriving a compressed residual signal. The effect of subsampling an interlaced signal is also considered together with the necessary modifications required when applying this technique within this environment.

Section 4.2: A description of the proposed modulation techniques for a compatible embedded data transmission is given in this section. After a brief review of the possibilities for additional data integration within a PALPLUS signal, the section concentrates upon the additional colour carrier modulation strategy.

Section 4.3: The analysis and evaluation of suitable data reduction techniques are identified in this section, to compress the residual data rate. An overview of achievable data rates is provided and a rationale presented as to the implications of these rates upon the system performance and overall research objectives.

Section 4.4: A summary of the results obtained are given in this Section.

4.1 Dual channel sub-band coding

4.1.1 Principles

The overall encoder design is based closely upon the principles of sub-band coding, with the crucial difference being that a 2-D diagonal prefilter is employed, together with a lowpass - highpass band-splitting filter combination, which conforms to a Quadrature Mirror Filter (QMF) approximation. This results in only two sub-bands being generated instead of four, so improving throughput. This implementation is particularly useful, where a low resolution version of the input signal is required such as for example, in compatible applications [2][3]. The drawback however, is that a straightforward hierarchical expansion of the sub-band signals is no longer feasible.

The typical HDTV spectrum shown in Figure 4.2, illustrates that the signal can be sub-band coded into four-channels of equal bandwidth, prior to being decimated and transmitted. At the decoder, all four signals are interpolated to facilitate full signal reconstruction. For this particular application however, only two sub-bands are required. To reduce the number of sub-bands from the usual four to two, two-dimensional diagonal filtering is initially performed to suppress all oblique frequencies in the spatial plane. Subjectively the loss of such information is acceptable, since the probability of diagonal components occurring is generally much less than for either horizontal or vertical frequencies [117]. The spectral effect of diagonal filtering is illustrated in Figure 4.3. It can be seen that the input signal bandwidth is halved without compromising either horizontal or vertical resolution. The standard resolution signal is obtained, with the residual spectrum consisting of only the two wedge-shaped high frequency components shown in Figure 4.3a. Following decimation by a factor of two, these spectral wedges fold back into the same frequency range as the lowpass band, so the requisite bandwidth of the sub-bands for the residual signal becomes equivalent to that of the normal resolution signal (see Figure 4.3b).

The block diagram in Figure 4.4 shows the analysis / synthesis filter bank arrangement for processing only two bands. After the initial diagonal filtering $H_D(z_1, z_2)$, $x(n_1, n_2)$ is

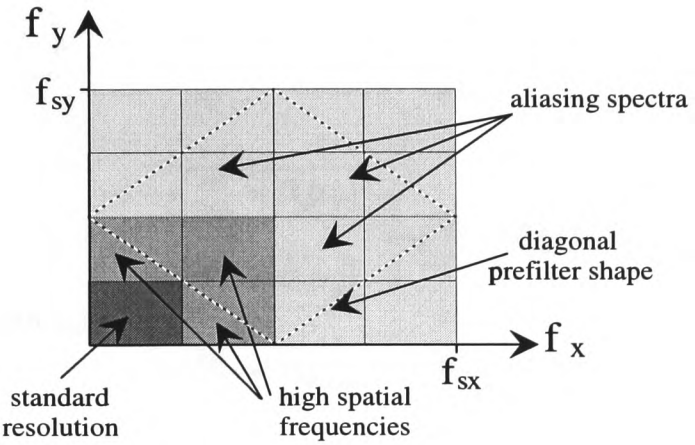

Figure 4.2: Input spectrum with respect to four sub-bands

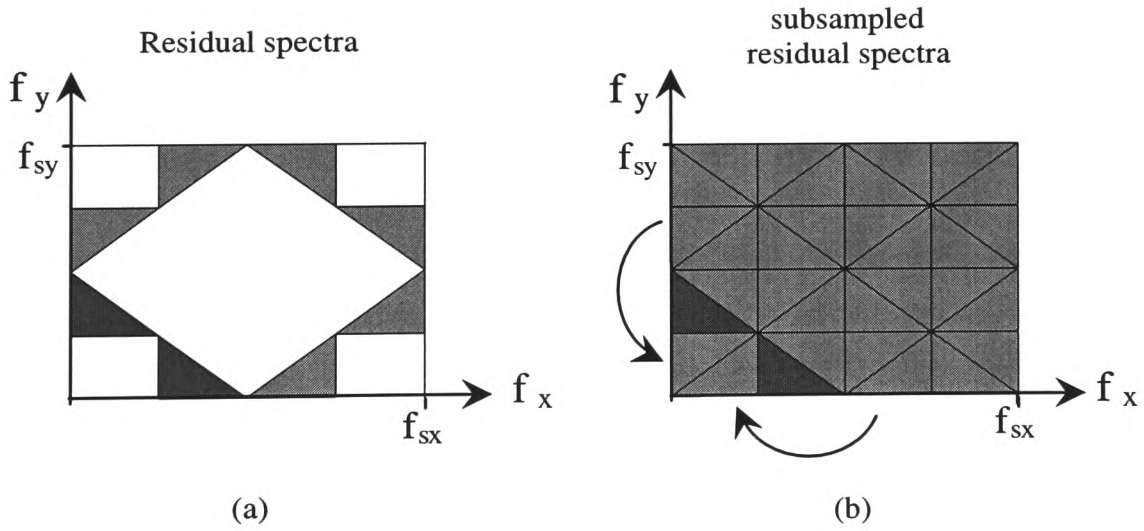

Figure 4.3: (a) Highpass bands with diagonal pre-filter (b) decimated highpass signal

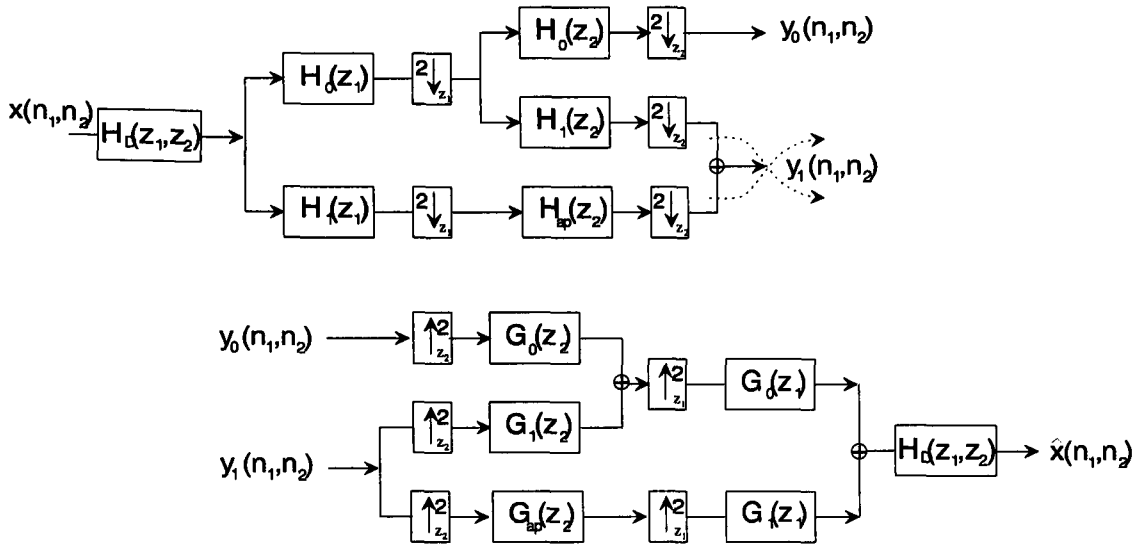

Figure 4.4: Block diagram of the dual channel QMF bank approach

subsequently band-split for horizontal frequencies by a low- / highpass filter combination before each band is processed in the vertical direction. Generally, the ordering of horizontal and vertical filtering is interchangeable, so reversing the order makes no difference for this implementation. In the four band case however, there is significant merit in undertaking the vertical processing first, because of implementation complexity. In the low-frequency branch in Figure 4.4 a further vertical band-splitting produces a lowpass band, which is $y_0(n_1, n_2)$ after subsampling, and a highpass band containing the vertical wedge-shaped frequency region. Due to the diagonal filtering only a group delay equalization, $H_{ap}(z_1, z_2)$, which is an all-pass filter, is necessary for the horizontal high frequency branch so after adding the two high pass signals, only one high frequency band is derived, $y_1(n_1, n_2)$. For signal reconstitution y_0 and y_1 are processed in reverse order to form the output $\hat{x}(n_1, n_2)$. The non-ideal diagonal filter response leads to aliased distortion, because both the high resolution horizontal and vertical wedges are folded back after subsampling (see Figure 4.3b), so that an overlapping occurs along the diagonal frequency components. The effect of this error upon the residual spectrum is indicated by the dark oblique criss-cross pattern in Figure 4.5, and leads to crosstalk. It is proven in Appendix A, that the reconstituted signal can be written

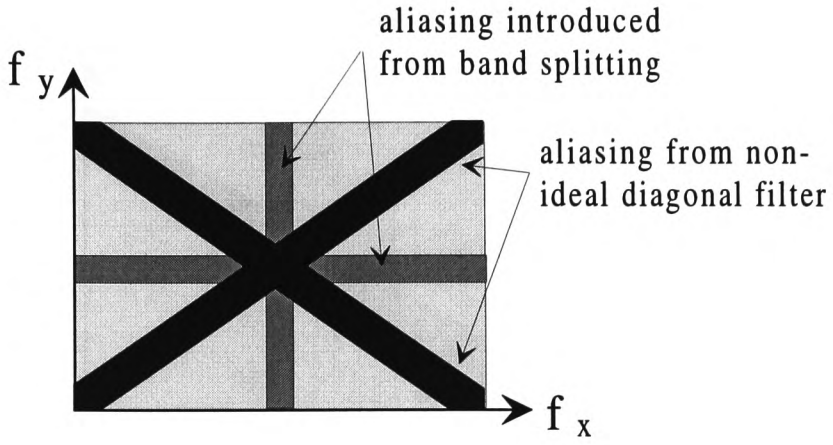

Figure 4.5: Frequency overlap following the subsampling of the residual signal

as:-

$$\begin{aligned}\hat{X}(z_1,z_2) =& \frac{1}{4}[T(z_1,z_2)+C_T(z_1,z_2)]X_D(z_1,z_2)+\\ & \frac{1}{4}[A_1(z_1,z_2)+C_{A1}(z_1,z_2)]X_D(-z_1,z_2)+\\ & \frac{1}{4}[A_2(z_1,z_2)+C_{A2}(z_1,z_2)]X_D(z_1,-z_2)+\\ & \frac{1}{4}[A_3(z_1,z_2)+C_{A3}(z_1,z_2)]X_D(-z_1,-z_2)\end{aligned} \tag{4.1}$$

where $T(z_1,z_2)$ and $A_1(z_1,z_2)\ldots A_3(z_1,z_2)$ denote what is commonly referred as the transfer function and the alias components respectively. $C_T(z_1,z_2)$, $C_{A1}(z_1,z2)\ldots C_{A3}(z_1,z_2)$ highlight the signal components which occur due to the addition of the two sub-bands to form $y_1(n_1,n_2)$ and consist of vertical high frequency crosstalk terms, which because of the subsampling appear as horizontal frequencies and vice versa. The dotted arrows in Figure 4.4 illustrate this phenomenon. Choosing the horizontal and vertical QMF-pairs as given in Appendix A.1, the alias terms of Equation (4.1) are significantly reduced due to alias cancellation, but it is clear that no overall cancellation can occur, so that apart from the addition of the two sub-bands, the system is close to a standard four-band implementation, where the fourth band (the high diagonal frequency components) has been removed. If ideal diagonal pre- and post-filtering is assumed, the frequencies responsible for this aliasing are suppressed and so these terms are no longer taken into account as shown in Figure 4.6. The crosstalk signal component $C_T(z_1,z_2)$ of the transfer function can lead to additional amplitude distortions depending on the analysis / synthesis filter shape. Figure 4.7a provides an example by

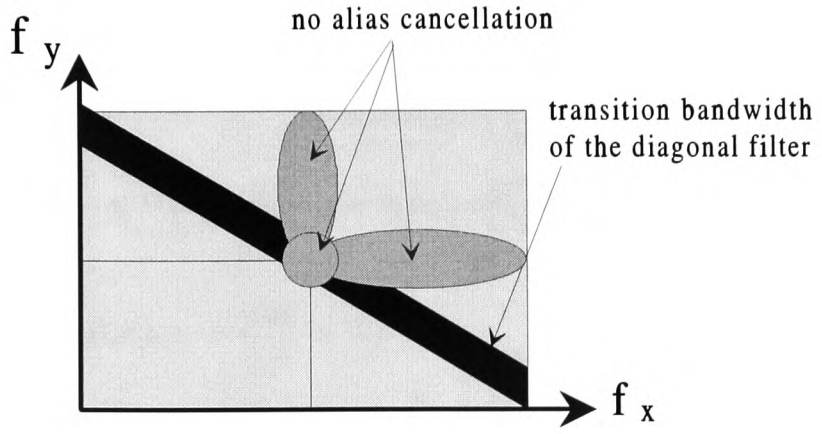

Figure 4.6: Two dimensional frequency region where no alias cancellation is possible

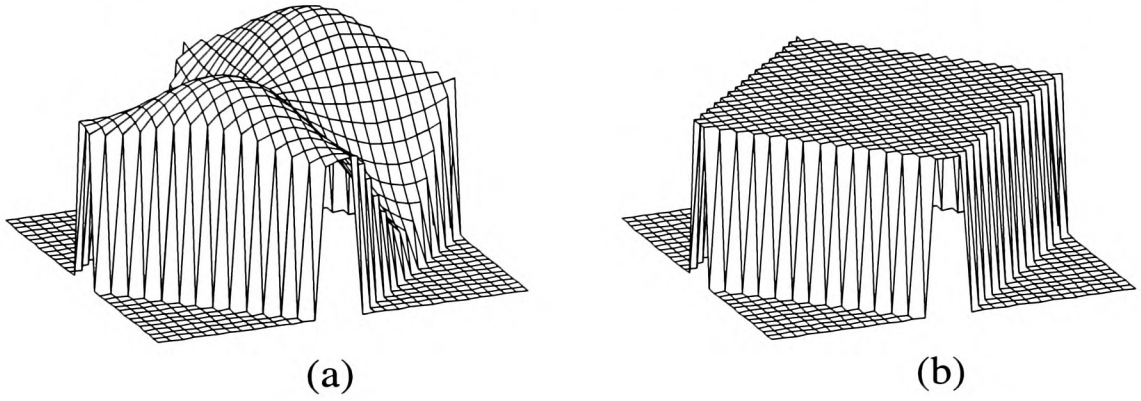

Figure 4.7: Transfer function $T(z_1, z_2)$ (a) without crosstalk and (b) with crosstalk cancellation

using a cosine filter for $H(z)$ and an ideal diagonal filter response.

The analysis of $C_T(z_1, z_2)$ as given in Equation (A.14) shows that if it is possible to invert one item, $C_T(z_1, z_2)$ will be cancelled and thus this additional distortion in $T(z_1, z_2)$ will be eliminated. One possibility to achieve this is to consider the vertical band-splitting to be even-filter order as introduced in Equation (2.23) in Section 2.2, rather than odd orders for the horizontal and vertical dimensions. Figure 4.8 gives the modified block diagram. As derived in Appendix A.2 the crosstalk term $C_T(z_1, z_2)$ will be cancelled and $T(z_1, z_2)$

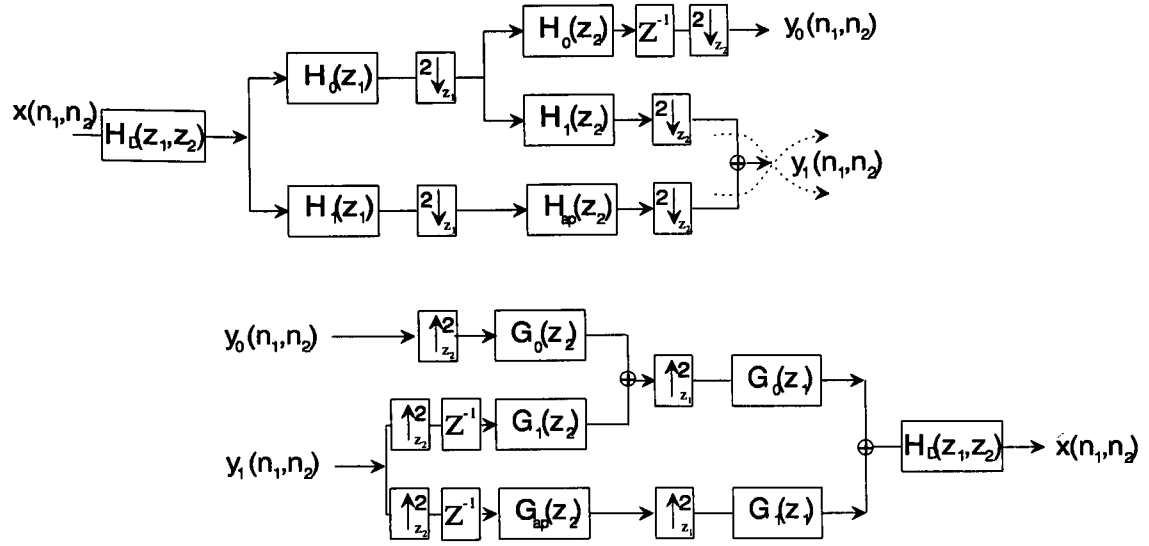

Figure 4.8: Modified block diagram using even-order filter order for vertical band splitting

reduces to

$$T(z_1, z_2) = e^{-j(\omega_1 N_1 + \omega_2 N_2)}[z_2^{-1}|H(z_1)|^2|H(z_2)|^2 + z_2^{-1}(-1)^{N_2}|H(z_1)|^2|H(-z_2)|^2 - z_2^{-1}(-1)^{N_1}|H(-z_1)|^2|H(z_2)|^2] \quad (4.2)$$

Figure 4.7 compares the two resulting transfer functions for $T(z_1, z_2)$.

Some additional comments are beneficial on the role of the all-pass filters $H_{ap}(z_2)$ and $G_{ap}(z_2)$ in the analysis and synthesis filter banks respectively. During analysis within Appendix A, these filters are set to be vertical lowpass as it would be the case in the usual four band arrangement. This is done for simplification, so that it is straightforward to see which components are cancelled due to alias compensation. In the proposed system, from a spectral viewpoint the initial diagonal filter makes this lowpass filtering redundant, so that only a delay has to be included to ensure the correct phase relationship. Using all-pass filters gives several advantages for this implementation. Firstly, considering even filter orders for vertical band splitting, an all-pass is a simple delay which reduces overall design complexity. Another advantage is given in the transfer function, Equation (4.2). The all-pass filters avoid the $6dB$ attenuation that will usually occur at diagonal frequency location where all four bands converge, if the fourth band is omitted. A drawback however, is that a leakage in aliasing compensation at this point occurs. By designing the diagonal filter so that the frequencies

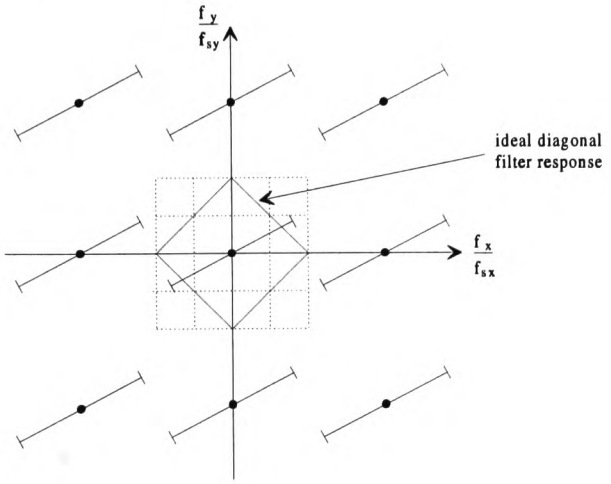

Figure 4.9: 2-D frequency plot of a diagonal image pattern used as the input signal

responsible for this aliasing are sufficiently suppressed, the effect of this particular distortion can be reduced.

4.1.2 Distortion analysis

As previously mentioned, there are alias and crossover components inherent within the dual channel sub-band design that lead to additional distortions. These distortions can be balanced with both the diagonal and the band-splitting filters. To analyse which alias or crossover terms are responsible for what distortion, a diagonal sinewave pattern is processed by investigating each subsampling component separately. Figure 4.9 shows the frequency components of the input signal. It is obvious that there must be distortion, because they clearly exist beyond the pass band of the ideal diagonal filter indicated in the diagram. To simulate the worst case scenario for this arrangement, the diagonal pre filter is omitted.

Figure 4.10 shows the outcome after processing the input from Figure 4.9 within each dimension separately and finally their superposition. The grey shaded regions will highlight the passbands of the crossover and alias terms taken from Equation (A.20) to (A.26). Figure 4.10a shows the situation caused due to horizontal alias components $X_D(-z_1, z_2)$. These components are covered by the transition bandwidth of $C_{A1}(z_1, z_2)$ and are therefore not suppressed. A similar case occurs in Figure 4.10b for the vertical alias components

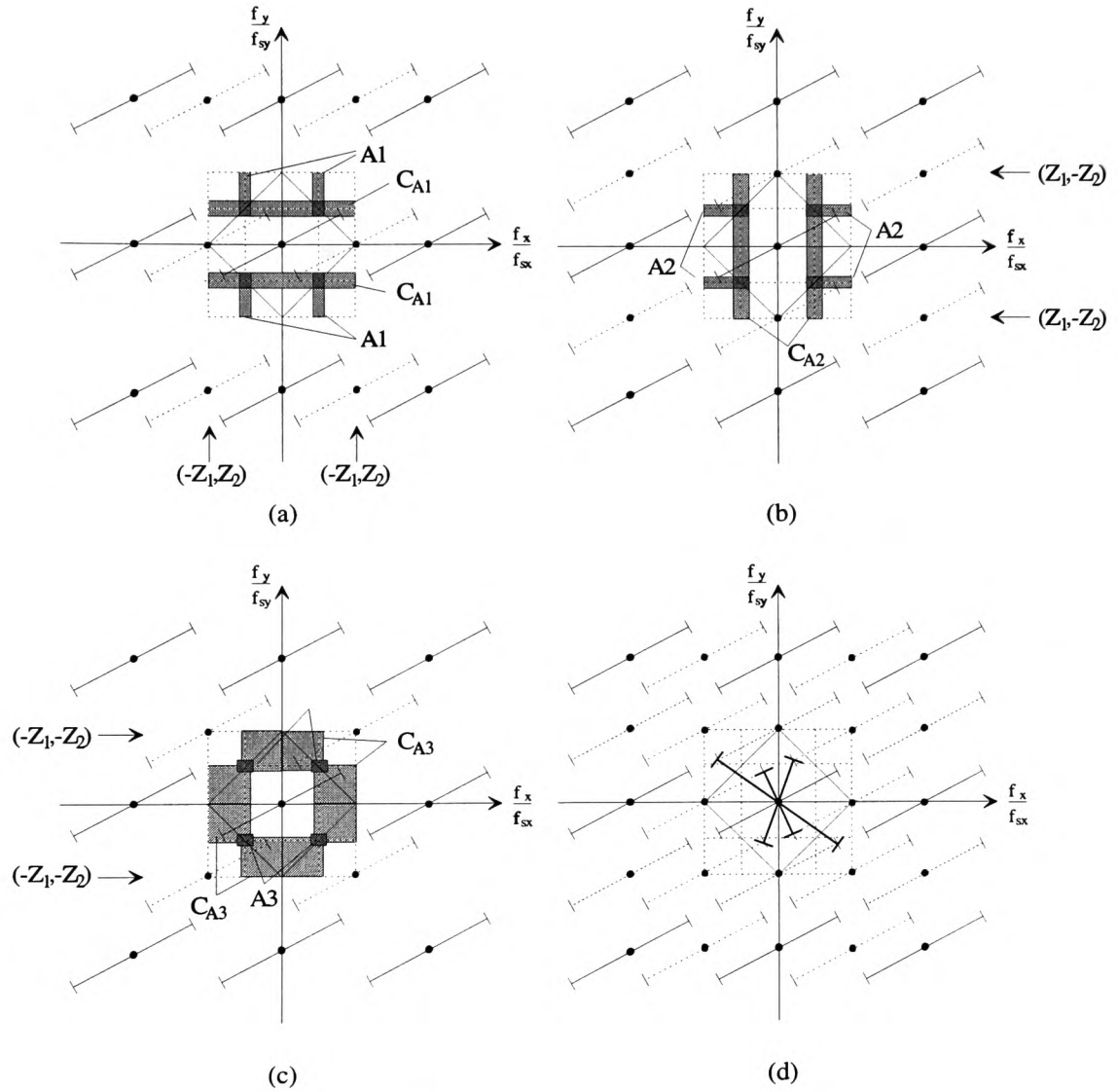

Figure 4.10: 2-D frequency plot of the input signal from Figure 4.9 after (a) horizontal subsampling, (b) vertical subsampling, (c) diagonal subsampling and (d) superposition of (a), (b) and (c)

$X_D(z_1, -z_2)$, where the alias term $A_1(z_1, z_2)$ is responsible for insufficient attenuation. The diagonal alias parts $X_D(-z_1, -z_2)$, also introduce additional frequencies as shown in Figure 4.10c. The superposition of all these components is illustrated in Figure 4.10d. The new frequencies introduced due to the previous mentioned aliasing and frequency crossover are marked by a bold line, combining the corresponding positive and negative frequency parts. Four diagonal sinewave pattern are visible including the one which was originally processed. Assuming diagonal post filtering to avoid post aliasing (distortion caused by insufficient suppression of imaging which occurred due to sampling) and thus recover the baseband for this sampling arrangement, only two diagonal patterns remain and these are totally different from the original input signal.

Figure 4.10 gives a clear view how each component compromises the overall performance of this sub-band design. The major effect is introduced by $C_{A3}(z_1, z_2)$ and the diagonal aliasing $X_D(-z_1, -z_2)$, due to the overlapping after the fold back of the high frequency wedges (Figure 4.3b). The influence of $C_{A3}(z_1, z_2)$ can only be reduced by the diagonal pre filter, so this filter must be carefully designed. At certain frequencies additional distortions also occur due to the other cross over and aliasing components. Generally the narrower the transition of the band-splitting filter the narrower the passband of the aliasing and crossover terms, however, the peak will be at 6dB due to the overlapping of transition bandwidth of the analysis and synthesis filters (both have $3dB$ attenuation at half the Nyquist frequency). Considering a wider passband, cross over can occur also for frequencies within the baseband of the diagonal filter. This effect is not so critical, because the attenuation reduces the visibility of this additional components.

4.1.3 Filter Design Considerations

Diagonal filter:- As previous outlined the diagonal filter as an initial processing stage plays an important role and thus has a major impact upon overall performance.

The method used for diagonal filter design is based on a two dimensional sinc function rotated by 45 degrees before subsequent windowing. The 2-D sinc function is expanded

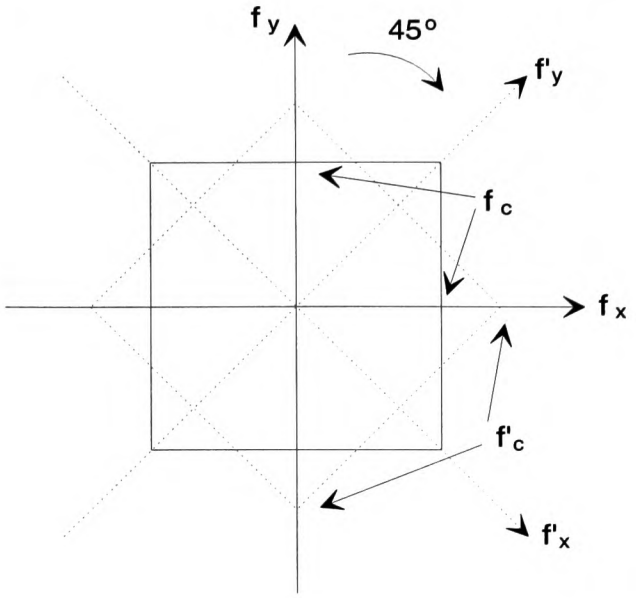

Figure 4.11: Diagonal filter transformation in the 2-D frequency domain

from the one dimensional case as given in Equation (4.3)[118]

$$h(n_1, n_2) = sinc(2\pi \frac{f_c}{f_s} n_1) sinc(2\pi \frac{f_c}{f_s} n_2) \tag{4.3}$$

With the knowledge that a rotation in the frequency domain results in an identical rotation in the spatial domain, the spatial coordinates n_1 and n_2, are transformed to n_1' and n_2', due to the rotation, principally illustrated in Figure 4.11.

$$n_1' = n_1 cos(\Theta) + n_2 sin(\Theta) \qquad n_2' = -n_1 sin(\Theta) + n_2 cos(\Theta) \tag{4.4}$$

Setting $\Theta = 45^o$ Equation (4.4) becomes

$$n_1' = n_1 \sqrt{\frac{1}{2}} + n_2 \sqrt{\frac{1}{2}} \qquad n_2' = -n_1 \sqrt{\frac{1}{2}} + \sqrt{\frac{1}{2}} \tag{4.5}$$

and further merging Equations (4.3) and (4.5)

$$h(n_1, n_2) = sinc(2\pi \frac{f_c}{f_s} (n_1 \sqrt{\frac{1}{2}} + n_2 \sqrt{\frac{1}{2}})) sinc(2\pi \frac{f_c}{f_s} (-n_1 \sqrt{\frac{1}{2}} + \sqrt{\frac{1}{2}})) \tag{4.6}$$

Care must be taken upon the definition of the cut-off frequency f_c. It is commonly defined as shown in Figure 4.11 at the crossing of the axes, so this point must also be transformed:-

$$f_c' = f_c \sqrt{\frac{1}{2}} \tag{4.7}$$

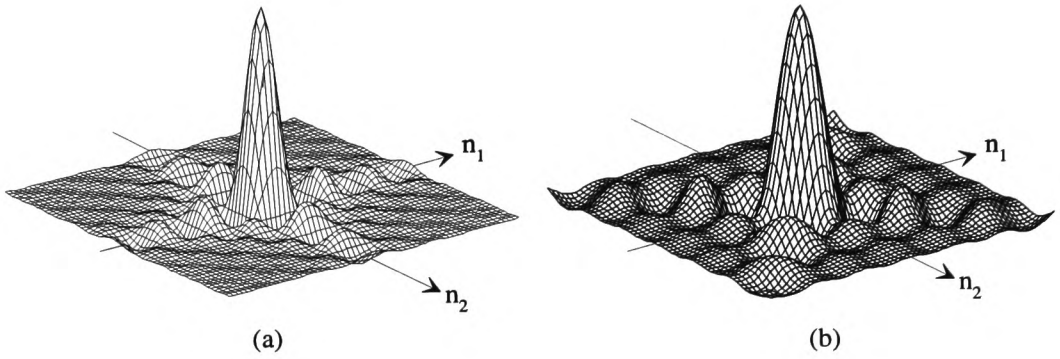

Figure 4.12: Diagonal filter transformation in the 2-D frequency domain (a) 2-D expansion from Equation (4.3) and (b) the 45 degree rotated version

Equation (4.7) assumes that the horizontal and vertical cut-off frequencies are identical. Figure 4.12 provides an insight to this rotation.

The two dimensional window functions used to fulfill the filter design are also expanded from their one dimensional versions, similar to those given in Appendix B.2. One method is identical to that given in Equation (4.3) for the 2-D sinc function, so for the window:-

$$w(n_1, n_2) = w(n_1)w(n_2) \tag{4.8}$$

This approach results in windows which cover a rectangular region of support. In Section 3.3.2 of Dudgeon [11] a method is shown to support a circular region:-

$$w(n_1, n_2) = w(\sqrt{n_1 + n_2}) \tag{4.9}$$

A rotated version of Equation (4.8) is also possible. However the analysis from [119] clearly shows, that no major differences are related to the selection of one of these methods, so for further simulations a rectangular region of support is sufficient.

QMF filter:- The finite transition bandwidth of band-splitting filters introduces aliased components into each sub-band due to the subsequent decimation. As shown with the QMF theory in Section 2.2 such aliasing can be cancelled from the reconstituted signal at the receiver under a specific set of design criteria. These rules apply to both the analysis and synthesis filters and may be summarised as:-

- the lowpass / highpass analysis filters must be mirror images of each other.
- the lowpass interpolation filter should have the same transfer function as the lowpass analysis filter.
- the highpass interpolation filter should also have the same transfer function as its analysis counterpart, but with a phase delay of $\pi \frac{rads}{sec}$.

As well as the alias cancellation properties of QMF theory, consideration has also to be given to eliminating both amplitude and phase distortion from the resultant output. The only linear-phase FIR filter which is totally free of amplitude distortion, confirming these previous rules, is a two-tap cosine filter [14], although the corresponding frequency separation within each sub-band is very poor. In order to achieve an output which is approximately free from amplitude errors while implementing higher order filters by providing superior separation capabilities, an important property is that each filter must have an attenuation of $3db$ at half of the Nyquist frequency. A simple design method which guarantees this uses a windowed sinc-function to calculate the filter coefficients. The design then continues recursively by changing the zero-crossing points of the sinc-function until the desired goal is reached. The stopband and passband ripples also have to be balanced by the design parameters of the selected window.

Several other design methods have also been developed. Johnston [16] presented a recursive method by using the Hooke and Jeaves search algorithm to minimise the ripples of the overall transfer function. A comparison of the Johnston examples given in [16] with filters designed by the previous method shows, that Johnston's method is slightly superior, especially due to the fact that the ripples are symmetric around $0dB$. This cannot be guaranteed by the recursive windowing method. Smith and Barnwell [17] presented an alternative procedure called CQF (Conjugate Quadrature Filter). Starting from a designed product filter, which is anti-symmetrical around half of the Nyquist frequency and further provides equi-ripples in pass- and stop-band, the analysis and synthesis lowpass filters can be decomposed. A consequence of this decomposition is that the linear phase of the sub-filters is lost though the overall phase linearity of the system still exists if the product filter has linear

phase. Some other interesting alternatives for QMF designs can be taken from Wavelet theory [13][120]. The so called "biorthogonal filter banks" do not necessarily require that the lowpass interpolation filter must be identical to its analysis counterpart, so that the complexity for band-splitting can be shifted to the encoder, which is attractive for some applications. Furthermore these filters provide ideal signal reconstitution in terms of the fact that the output is totally free of all alias-, amplitude- and phase distortions. This leads to the property of perfect reconstruction which Vaidyanathan proved in a maximally decimated case is directly equivalent to biorthogonality. This is also closely related to the property of paraunitariness in respect of polyphase components of analysis and synthesis filter banks [13, Chapter 6]. An overview of such biorthogonal filter banks is given in [121].

The windowing design and the CQF method is extensively analysed by Meissner [122]. Due to the fact that the lowpass sub-band component should represent the compatible part of the dual channel sub-band scheme, the CQFs are not applicable because of their sub-filters have non linear phase. For the simulations the band-splitting filters are designed using the windowing method, because they are only slightly inferior compared to Johnston's filters and the design implementation is much easier as proven by Meissner. The analysis of biorthogonal filter banks has not been explicitly considered within this application, because the focus has been upon the overall system principles. There are however no reasons at all for not directly replacing the above traditional filters with such wavelet-based structures in the dual channel system.

4.1.4 Motion adaptive decimation

This section focused upon the modifications within the dual channel sub-band strategy necessary to process interlaced video signals, rather than progressive scanned images as previously discussed. Starting with a review of the problems inherent with sub-sampling and filtering an interlaced input, a motion adaptive proposal is developed to show three different scenarios of how a set of diagonal and band-splitting filters must be arranged to work within this context. The actual method implemented for motion detection is not the basis of this analysis, because there are many available solutions which can be readily chosen for implementation.

A brief overview of these is given towards the end of the section.

In contrast to decimation in the horizontal plane which is straightforward, down-sampling in the vertical plane raises a number of problems because of the interlaced nature of the input signal. Figure 4.13a shows the vertical/time sampling lattice of such an input signal, while Figure 4.13b evinces the equivalent half resolution. Figure 4.14 illustrates the respective spectra corresponding to the line positions given in Figure 4.13 [11]. The line positions of the second field in the equivalent half resolution image (Figure 4.13a) are clearly not a subset of those of the input. If this anomaly, caused by the decimation process is ignored, a non-uniform line structure will result as shown in Figure 4.13c and d. This leads to additional aliased components being generated (see Figure 4.14c and d), which reduces the resolution to only a quarter, instead of half the input signal.

To obviate this non-uniform line structure, the two fields have to be processed separately. Two distinct prefilters derived from the same prototype function, are designed within the vertical dimension to have an identical amplitude response, but different group delays. Switching synchronously with each field between the two filter coefficient sets, will interpolate the lines in every second field to their correct position.

When using intrafield filtering, the phase relationship between the two consecutive fields within a frame is not taken into account, so that frequencies greater than half the Nyquist frequency of the input signal are not suppressed and are clearly visible as aliased components. To prevent this unacceptable distortion, an interfield prefilter has to be used. This approach achieves for the down-converted signal, the maximum vertical resolution without any aliasing artefacts, however a feature of interfield filtering, is that it introduces motion blur in moving (non-stationary) scenes. To combine the advantages of the two prefiltering techniques that is, no motion artefacts in intrafield and maximum vertical resolution in interfield processing, a motion adaptive algorithm is employed in the design. Figure 4.15 graphically explains the situation. For the case where little-or-no motion is detected (low value of k), interfield prefiltering is used, whereas if high motion is detected (high value of k), intrafield processing is performed.

The discussion so far relates only to problems within vertical band-splitting for inter-

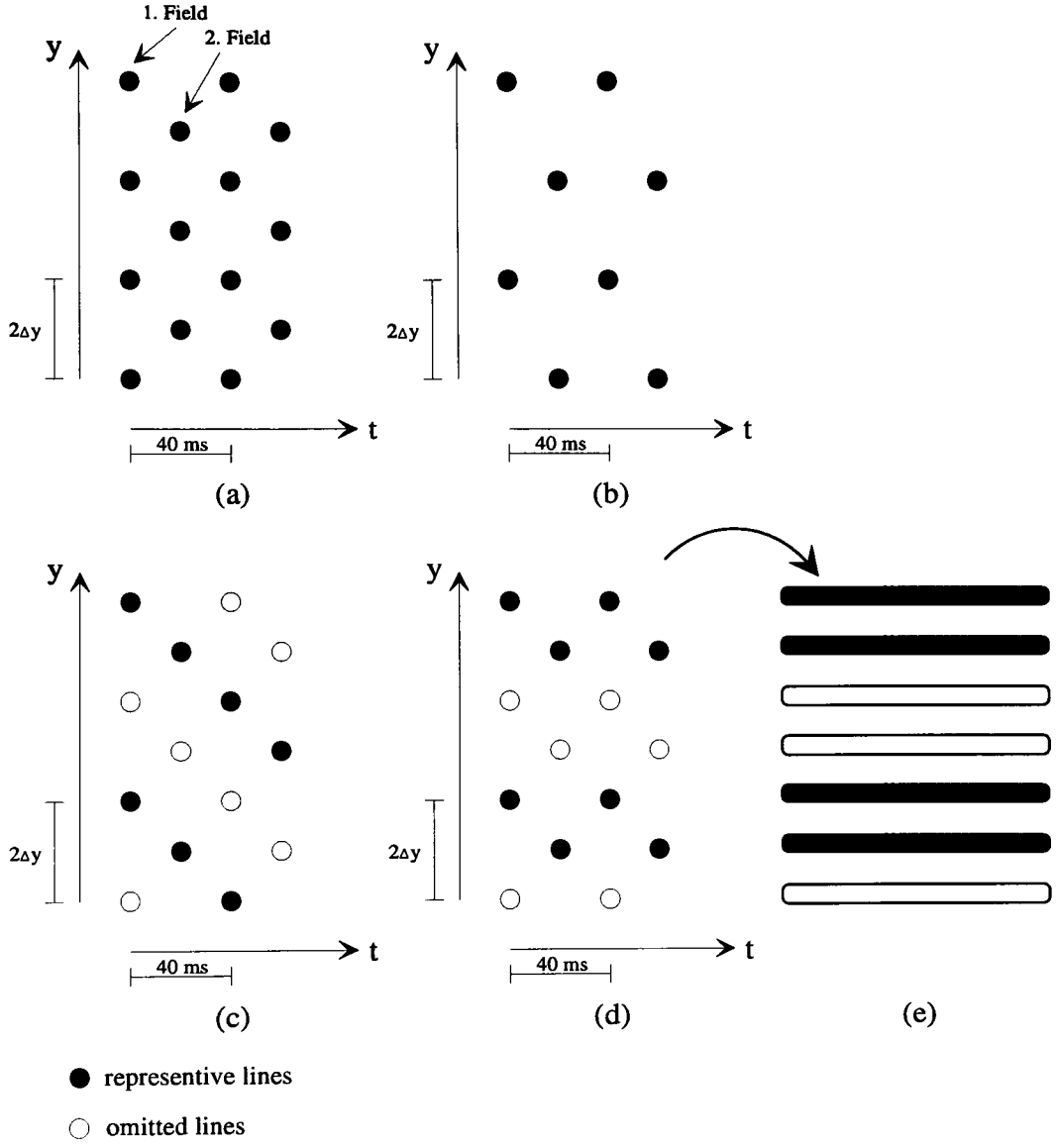

Figure 4.13: vertical/temporal sampling lattice of (a) an interlaced input signal and (b) the equivalent half resolution signal. (c) The vertically decimated signal without respect to the field and (d) with respect to the field.

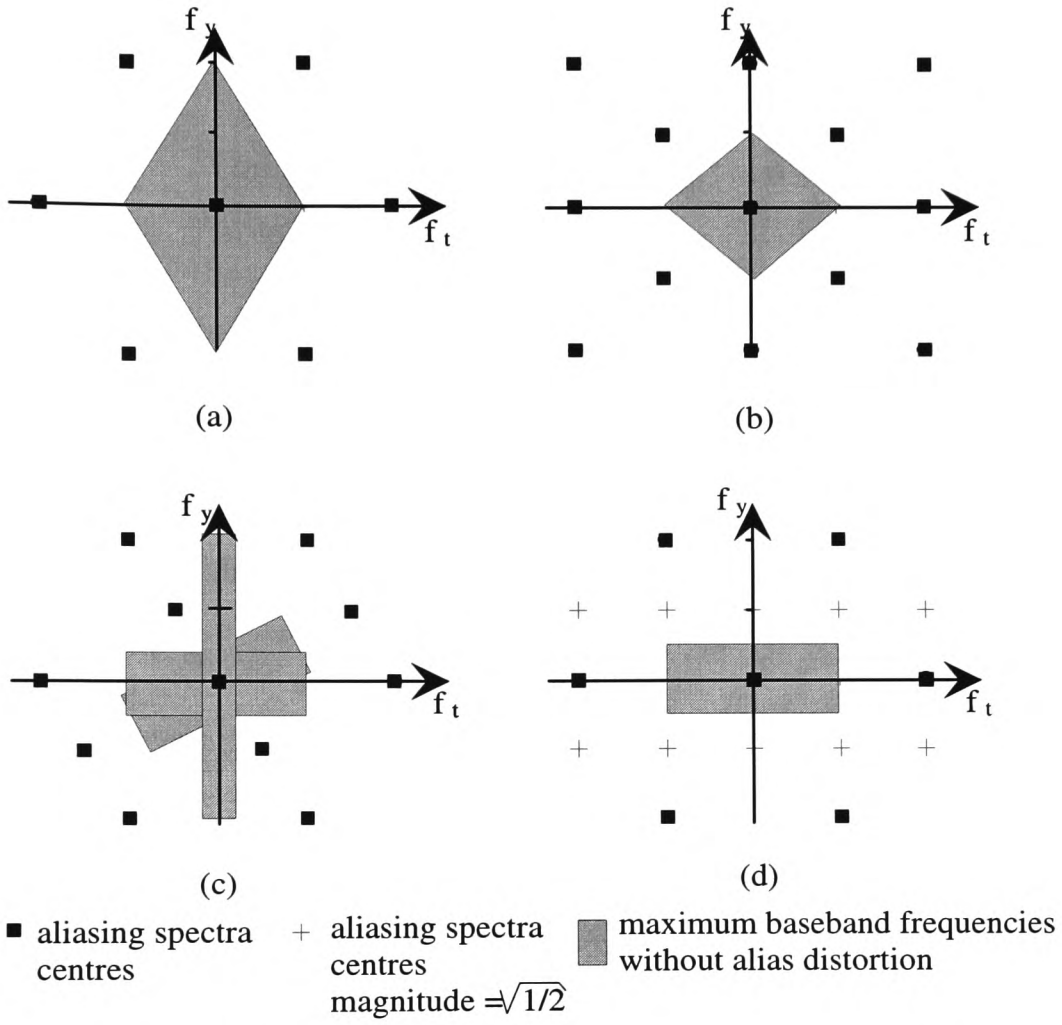

Figure 4.14: Corresponding spectra for Figure 4.13

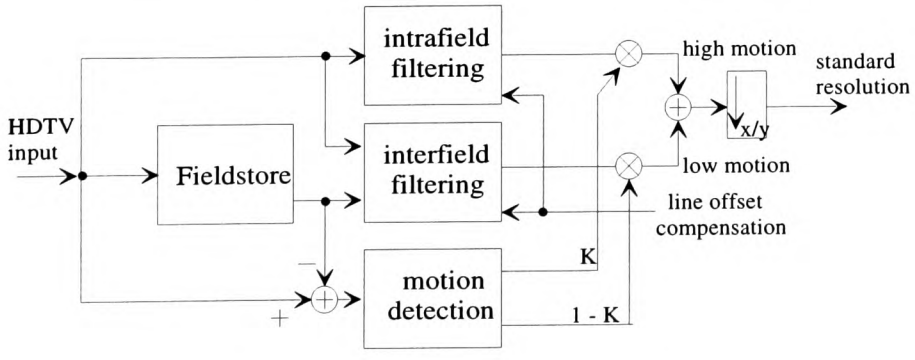

Figure 4.15: Block diagram of the motion adaptive down-converter used for this application

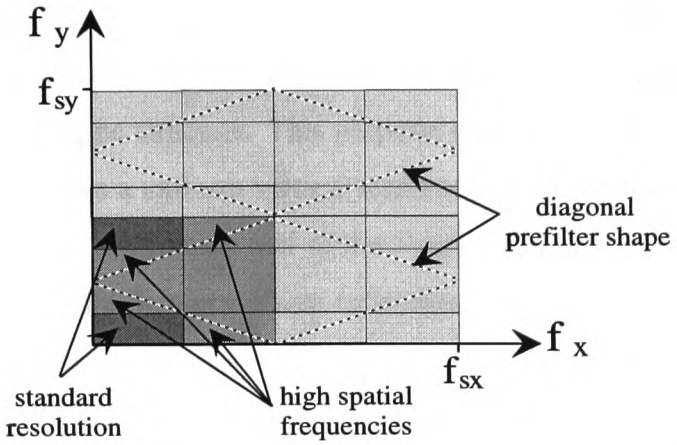

Figure 4.16: Spectral situation with respect to intra field processing

laced input signals. The specific dual channel sub-band implementation requires, as outlined earlier, a diagonal pre- and post-filter. These filters also introduce blur for moving scenes if only inter field processing is employed.

A straightforward adoption of the dual channel sub-band strategy is to process the interlaced input within a field for moving scenes, where for no-or-little motion interfield processing is employed. This simple approach however, has the major disadvantage that the intrafield band-splitting does not provide the optimal resolution for the low-pass branch, which is of course the compatible signal. Figure 4.16 shows the frequency situation for intrafield processing, where f_{sy} refers to the frame sampling frequency. Due to the fact that the vertical sampling frequency of a field is half that of a frame, the frequency responses of the diagonal and band-splitting filters become compressed. From the viewpoint of the vertical sampling frequency of a frame, an image of these responses is introduced, which results in band-pass filter responses. Compared to Figure 4.2, which is the interfield situation, it is clearly visible that frequencies greater than one quarter and less than three quarter of the vertical Nyquist frequency are suppressed, so the resolutions of the low-pass component is not uniform. For this reason the non-uniform line structure compensation is redundant, because those frequencies introducing distortions are no longer present. The reconstituted signal for this approach is also sub-optimal due to the additional diagonal filter response image(Figure 4.16), which has been introduced.

An even simpler solution is to leave the diagonal and vertical band-splitting filter out for intrafield processing, with only a vertical all-pass filter being implemented to compensate for the non uniform line structure. This proposal ensures the optimal resolution in the compatible signal, which is a uniform vertical response within one half of the Nyquist frequency. Frequencies greater than one half of the Nyquist frequency introduce aliasing that cannot be avoided with intra field processing techniques. A trade-off of this proposal is that a correct up-conversion at the decoder is not possible with simple intra-field processing techniques, which is a well-known lemma within HDTV interpolation principles [26, Chapter 6] [72] [73] [74]. The frequency components greater than half of the Nyquist frequency of the down converted signal are an aliased image of the lower components and only the phase relationship between two consecutive fields provides the appropriate perception (interlace sampling). So an intra-field up-conversion cannot handle these higher frequencies correctly, because they are processed as low frequencies. The result is that in the up-converted signal these components still appear as interlaced components which is equivalent to a frequency shift of two.

A third strategy is a modification of the aforementioned principles, which is to derive the low-pass signal as usual using intra-field filtering. This follows the concept that those frequencies responsible for distortions are suppressed. Therefore a uniform vertical resolution is not possible, neither for the reconstituted nor for the down-converted signal, but in contrast to the previous solution no erroneous frequencies are being generated at the decoder.

Figure 4.17a and b shows the block diagram of the first and second mentioned proposal, respectively. The aforementioned third one is equivalent to Figure 4.17b by substituting the intra-field all-pass with a low-pass filter. From the view point of implementation complexity, it is obvious that the strategy given in Figure 4.17b is superior, however, as will be seen in the simulation section, the implementation of Figure 4.17a provides a better decoded signal.

The decisive information required to select between the two processing methods is obtained from a motion detector. As previously mentioned, this detector is not the basis of the analysis, however a brief overview of appropriate solutions available is now presented, which could be integrated seamlessly in the proposed system.

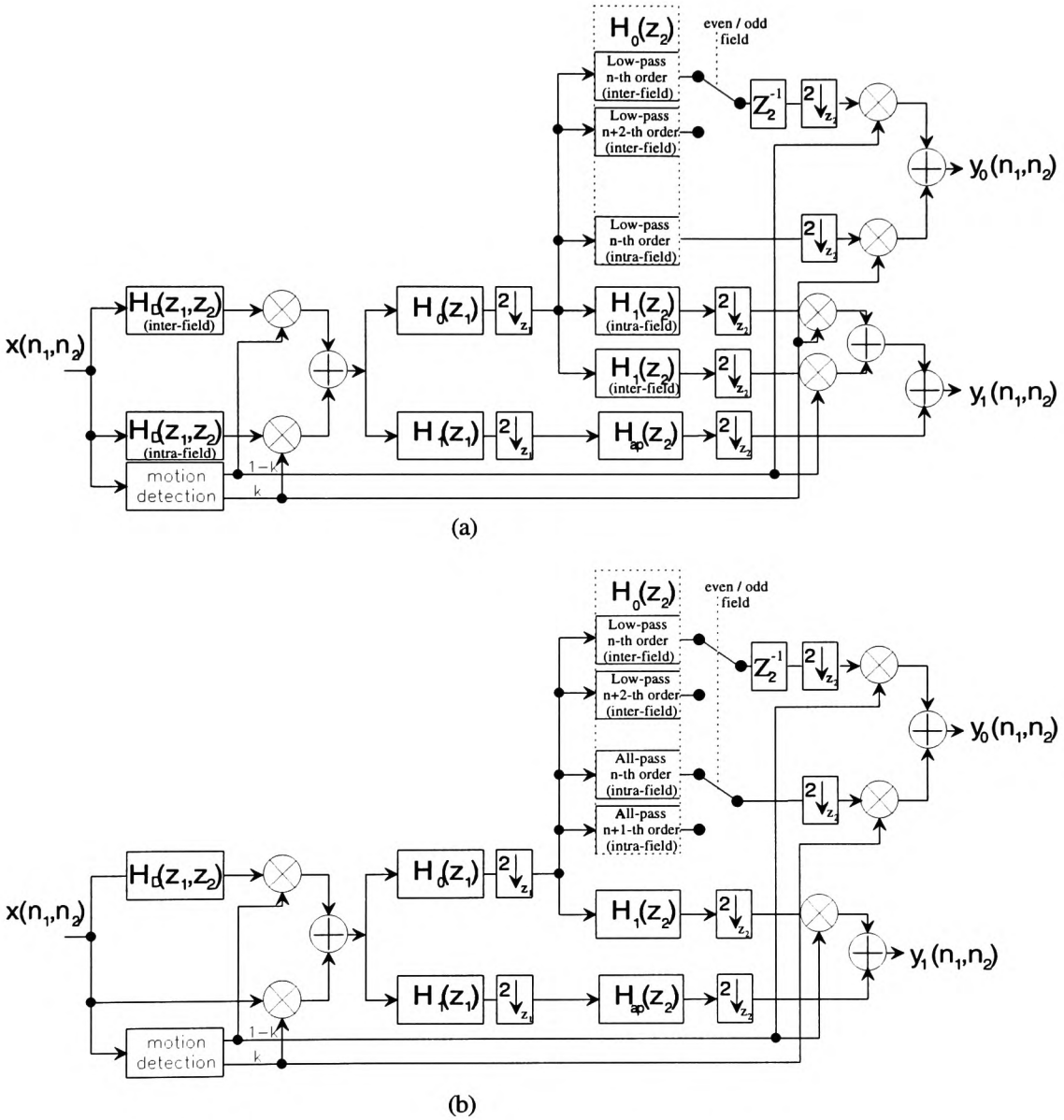

Figure 4.17: Motion adaptive implementation of the dual channel QMF bank strategy (a) straightforward approach (b) reduced complexity approach

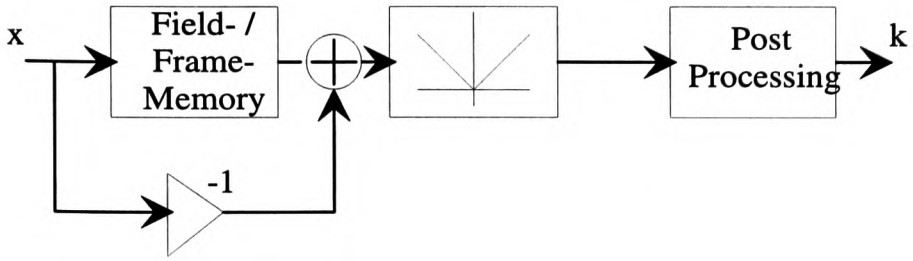

Figure 4.18: Principal block diagram of a motion detector [123, Chapter 3]

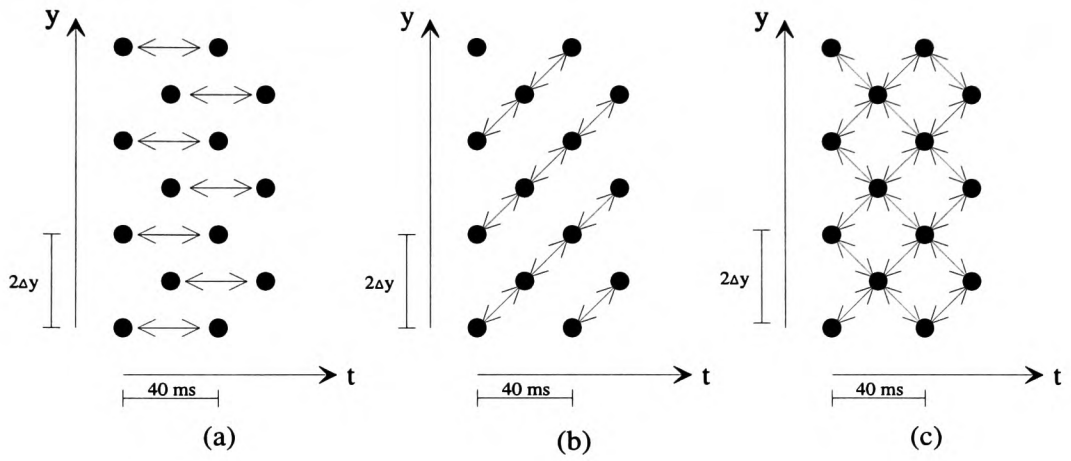

Figure 4.19: Vertical / temporal sampling relation of (a) frame based motion detection (b) field based motion detection (c) same as (b) with line offset compensation [123, Chapter 3]

Figure 4.18 shows the general structure of a motion detector. It is based upon subtracting the corresponding pixel values from consecutive fields or frames followed by deriving the absolute value prior to undertaking post processing. This post processing is usually a low-pass filter to smooth the detection signal and further to provide a soft fading between the two operation modes. Figure 4.19 gives an insight to the differences by using field- or frame store based detection. It is obvious that only with frame store based implementations is a true spatial correct comparison possible (Figure 4.19a). Field based solutions are clearly more attractive because of lower complexity, but the inherent half a line offset between the fields implies the problem that the detection is depended upon the movement direction [123, Chapter 3] (Figure 4.19b). This issue can be resolved by a line-offset compensation similar to that proposed earlier (Figure 4.19c). A very detailed description upon different motion detectors is given by Teichner [25, Section 4.2], who compares field, frame and multiple

frame based implementations and discusses further detection possibilities within a composite PAL signal. The focus is also set upon the post processing of the detection signal especially to the various fading possibilities. Other analysis is performed by Schamel as in [124], where possibilities of separate motion detectors at the encoder and decoder are been investigated. A special implementation example is proposed by Hentschel [125], who derives the decisive information from so called "mouse teeth"; the high vertical frequencies between two fields caused by motion so that only one field memory is necessary. It is proven that this method provides excellent noise robustness, but at the expense of significantly increasing complexity.

In conclusion, the actual motion detector that is incorporated in the system is not the most vital issue, but rather an awareness for its specific function in the successful operation of the system. In terms of hardware complexity, noise performance and efficiency, a simple binary-detector which classifies no-or-little / motion is adequate to enable switching between inter- and intra- field filtering and provide basic operability.

4.2 Embedded data transmission

As given in Section 2.3, the overall PALPLUS signal consists of two different components which are suitable for further digital modulation. The standard video signal, which is PAL-coded using the Colorplus technique and the vertical helper. Figure 4.20 shows the letter box format of a PALPLUS signal.

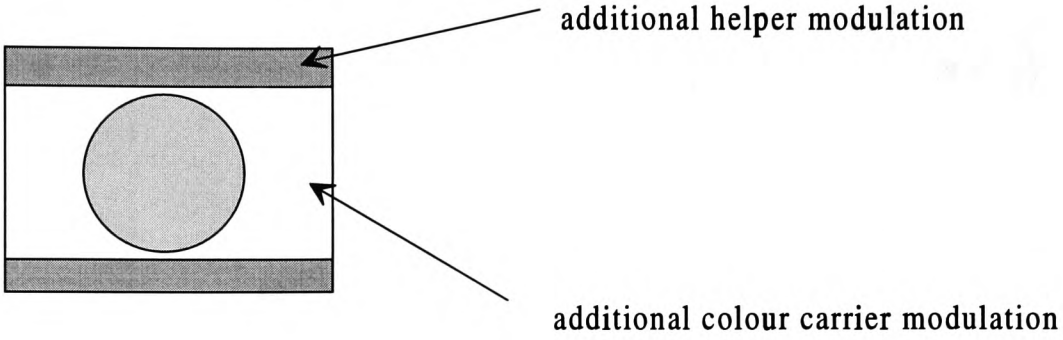

Figure 4.20: Signal parts suitable for additional modulation

The proposed modulation techniques for both signal parts are based upon the principles of QAM methods, where for the additional helper modulation a new carrier is introduced. Both proposals are closely related to each other, taking advantage of the carrier phase alternation, which is inherent in the PAL colour system and introduced within the helper modulation. This allows additional colour carrier and helper modulation for embedded data transmission, respectively. The following sections will discuss this in more detail.

4.2.1 Additional helper modulation

The PALPLUS helper is modulated with the zero degree phase component of the colour sub-carrier, but the idea of using the quadrature component for integrating the additional information, though attractive, is impractical because single sideband modulation is used for the helper signal.

An alternative solution is to introduce a new carrier, so arranged that the greatest distance in the three dimensional spectra between the two subcarriers is chosen. Figure 4.21 gives an

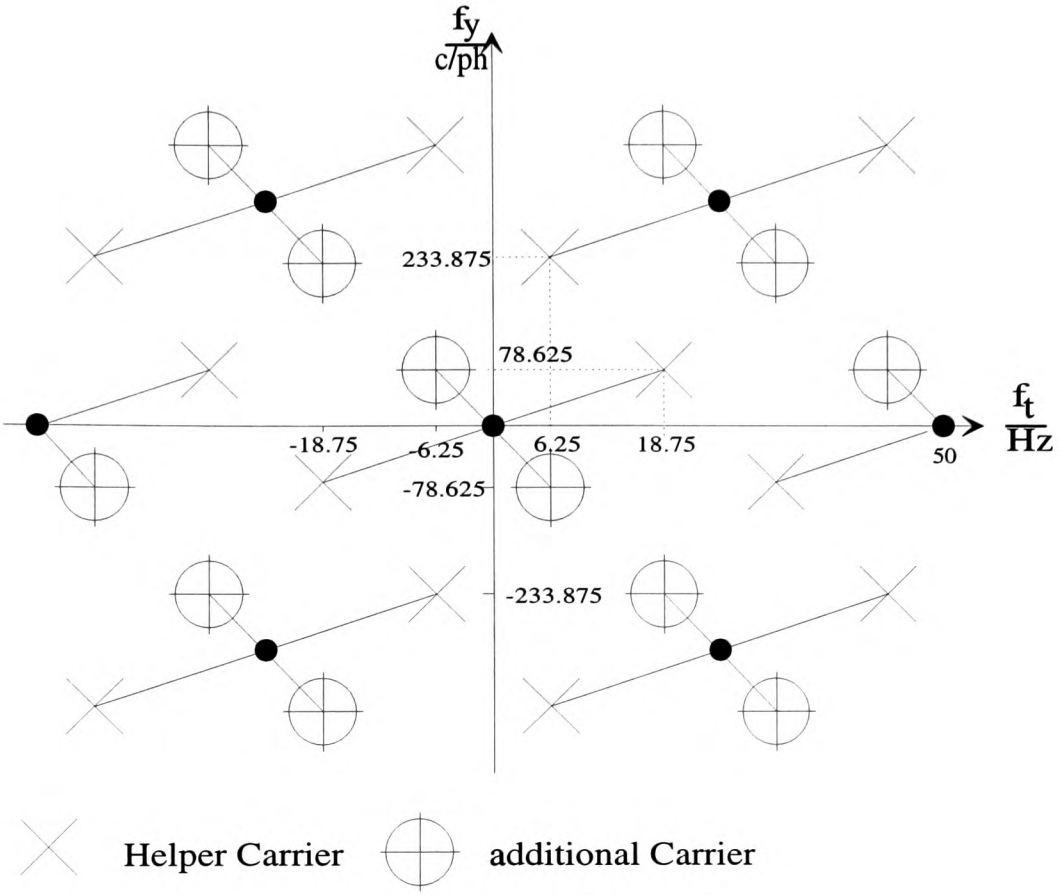

Figure 4.21: Positions of the PALplus helper and the additional carrier in the vertical/temporal plane

insight into this scenario realising a $25Hz$ frequency offset by alternating the helper carrier phase between 0 and 180 degrees, from field to field. This results in identical horizontal and vertical frequency components as for the helper carrier with the only difference that the movement is slower and in the opposite direction. This affords the possibility of using a temporal filter to separate the two components. This separation filter can be easily implemented by applying a field memory, because after a 312 line delay the additional carrier is in-phase, while the helper carrier is in anti-phase.

The digital modulation of this additional carrier is proposed to be a modified PSK technique, where the in-phase component is bandlimited to approximately $0.5MHz$, rather than $3.5MHz$ for the quadrature part. Assuming a roll-off factor of 0.5 and two symbols per data

channel, the data rate provided with this proposal will be approximately $1.2Mbit/s$, taking into account that the helper uses 25% of the standard active video signal.

For the standard PALPLUS receiver, any distortion according to the helper results in critical artefacts. This is firstly due to the reduced amplitude of the helper signal and secondly to the fact that demodulation of this additional data will appear as extraneous noise at high vertical frequencies. This degrades the overall visual quality of the signal because of the imbalance in the signal-to-noise ratio for the helper and standard signal part, which is extremely disadvantageous during camera mode (intra field processing). This phenomenon is analysed by Mench [30], and its effect illustrated in Figure 4.22. During reconstitution of the full 16 : 9 picture format at the PALPLUS decoder, the helper signal is interpolated so that every fourth line within a field is a helper line. Within each frame, these lines are paired because of the intra field processing in camera mode, so if the helper is disturbed this will cause highly visible line structured noise artefacts.

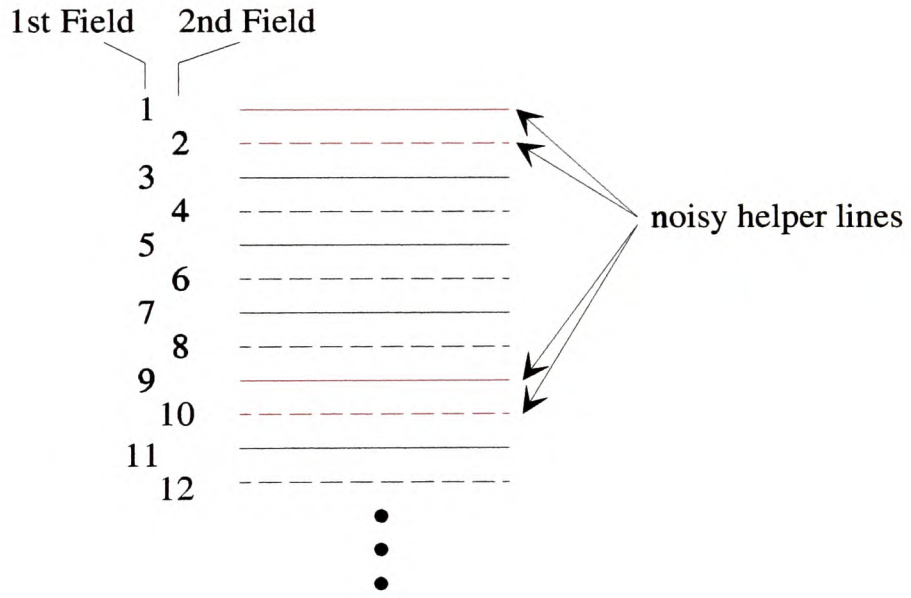

Figure 4.22: Visualisation of the line structured noise artefacts, due to helper distortions [30]

As outlined any modification to the helper will raise compatibility problems, which cannot be solved within an acceptable range of implementation complexity. The same issue arises in the separation of the helper and the additional component, where at least a field

memory must be used. These two reasons combined mean that the additional helper modulation proposal is found to be unsuitable and further analysis is focused upon the additional colour carrier modulation technique.

4.2.2 Additional colour carrier modulation

4.2.2.1 Principles

In contrast to the NTSC-system, where the colour difference signals I and Q are quadrature modulated, PAL alternates the phase of the V-component carrier between 90 and 270 degrees from line to line, where the U-component is fixed to the 0 degree carrier phase. Figure 4.23 shows the location for the two modulated colour components in the horizontal / vertical frequency plot of the PAL television signal. The switching leads to a spectral offset of the two colour components in the three dimensional frequency domain, with the V-carrier modulated on its 90-degree phase and the U-carrier on its 0-degree. Hence, both frequencies can be additionally modulated by using the respective orthogonal components and provide two sub-channels which are suitable for further digital transmission. For realisation, the carrier phase of the "digital U-component" D_U, must alternate between 0 and 180 degrees from line to line during the carrier phase of D_V, which is fixed to 90 degrees. Figure 4.24a displays this graphically for the given colour and data vector F and D in two consecutive lines n and n+1. Their addition forms the output vector S, which undergoes the usual further processing before transmission. In the receiver, at the PAL line delay, the vector sum of two neighbouring lines is derived so that the U and D_V signals are obtained from the in-phase and quadrature components respectively. In the same way, V and D_U are obtained from the colour vector difference (Figure 4.24b). This perfect possibility of separation is only valid if the neighbouring lines have identical content, which is not what happens in reality so that crosstalk distortions will occur.

The block diagram in Figure 4.25 gives an insight into the conceptional implementation realising this technique. The colour signals U and V, are processed as usual with the minor difference that a vertical lowpass, $H_U(f_y)$ and $H_V(f_y)$ is added into each signal path, the

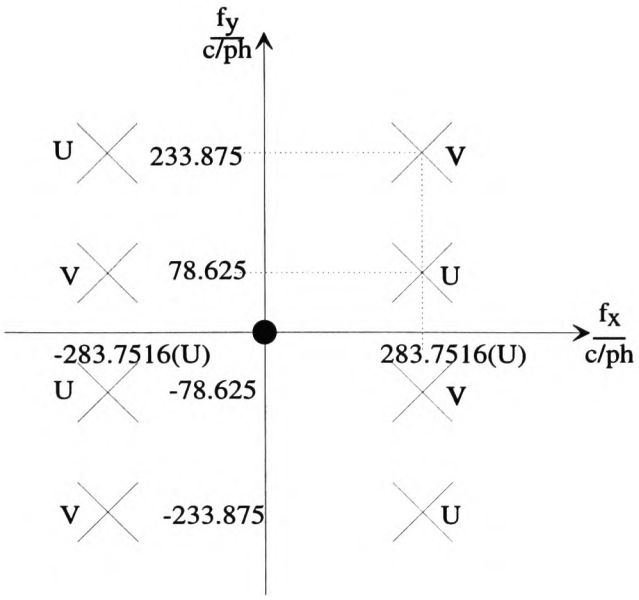

Figure 4.23: Colour carrier positions for U and V components

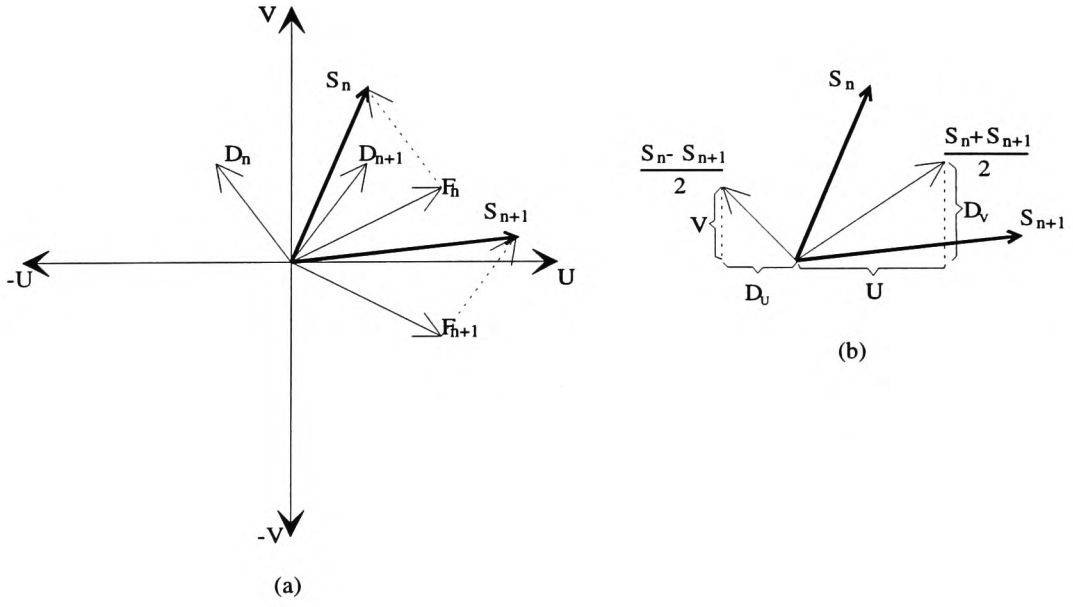

Figure 4.24: (a)Colour and data vector addition at the encoder and (b) demodulation at the receiver

reason for which will be discussed in the next section. The data stream is initially split into two channels of half the original data rate before subsequent form filtering. This form filter together with the following upsampling and vertical interpolation is part of the two dimensional form filtering technique explained fully in Section 4.2.2.3. Following the modulation as described above, the resulting data vector is added to the colour and further multiplexed with the luminance as usual. At the decoder, following luminance / chrominance separation, the colour- / data signal is processed by the PAL line delay, splitting it into those components whose carrier phase is alternated and those, whose carrier phase is fixed (V, D_U and U, D_V respectively). Finally the demodulation provides the reconstruction of each signal. The post filters are necessary to suppress higher order frequency parts from the demodulation and for the data signal parts, to suppress the single sideband components from the colour signal. Finally the two data channels are combined to construct the original data stream.

4.2.2.2 Crosstalk distortions

As defined in the overall objectives for this research, the highest priority must be given to the issue of compatibility with standard TV-sets, which requires that the implemented data stream does not impact upon the ordinary decoded video signal. The previously mentioned crosstalk effects are a major error source for degrading the subjective quality of the compatible video signal.

Two specific forms of crosstalk distortion will be considered. Firstly, intra-carrier crosstalk, where D_U and D_V crossover and appear as their quadrature parts, which are of course the colour signals, and secondly inter-carrier crosstalk, where the two digital components are demodulated at the wrong carrier frequency. In both cases the resulting distortions will appear as visible colour noise, which directly impinges upon the perceived picture quality.

The cause of intra-carrier crosstalk distortion is the non-symmetrical interference of the side-bands around the colour carrier, so that perfect demodulation of the in-phase and quadrature components is limited. This happens either because of the overall frequency response during transmission or the data signals exceed their maximum bandwidth range. Employing

an equalisation filter, as in the well-known peaking technique for the NTSC system [24], will reduce this particular effect. The maximum data channel bandwidth is given from the PAL standard. Its derivatives B,G,H and I define a colour carrier frequency of 4.433 MHz together with an overall video bandwidth of 5 and 5.5 MHz for B,G,H and I respectively. This implies that for colour frequencies higher then approximately 0.5 MHz for PAL B, G,H (1 MHz for PAL I) the modulation becomes single side band and therefore a limitation of the bandwidth where additional quadrature modulation is possible. The design however, has to guarantee that the bandwidth of the additional data streams does not exceed 0.5 MHz.

The inter-carrier crosstalk distortion compromises the compatibility aspect in a very critical manner. The data signal combination D_U/D_V is uncorrelated, so their spectra are uniform within the three dimensional video frequencies f_x, f_y, f_t. The consequence of this is a total spectral overlap between the colour and data signals, and further visible colour noise. Filters must be included to define specific locations for each component and thus attenuate these effects. The U / V separation of the PAL line delay at the receiver also has to be considered, because its poor separation limits the possibility of a perfect overall separation.

Another source of cross distortions is the reverse case of the above discussions, where the colour is crossing over and effects the data channels. These are not as critical, because the issue of compatibility is not touched and the disturbances effect only the digital data stream, which is by nature less sensitive. Two different sources for these distortions can be distinguished. Firstly, the colour signals cross over and secondly intercarrier-crosstalk between the two data channels.

The colour signal crosstalk arises from high vertical frequency components in the picture content. The probability of those components is generally less in a natural scene, however a vertical filter with a cut-off frequency of at least half the vertical Nyquist frequency has still to be included in order to reduce the error rates. As known from the D2MAC TV [50] transmission system, this filtering does not compromise subjective quality, so the same vertical colour prefilter strategy is adopted for this system.

The inter crosstalk between the data channels is limited due to the aforementioned spectral forming. In considering the proposed technique discussed in the following section, the

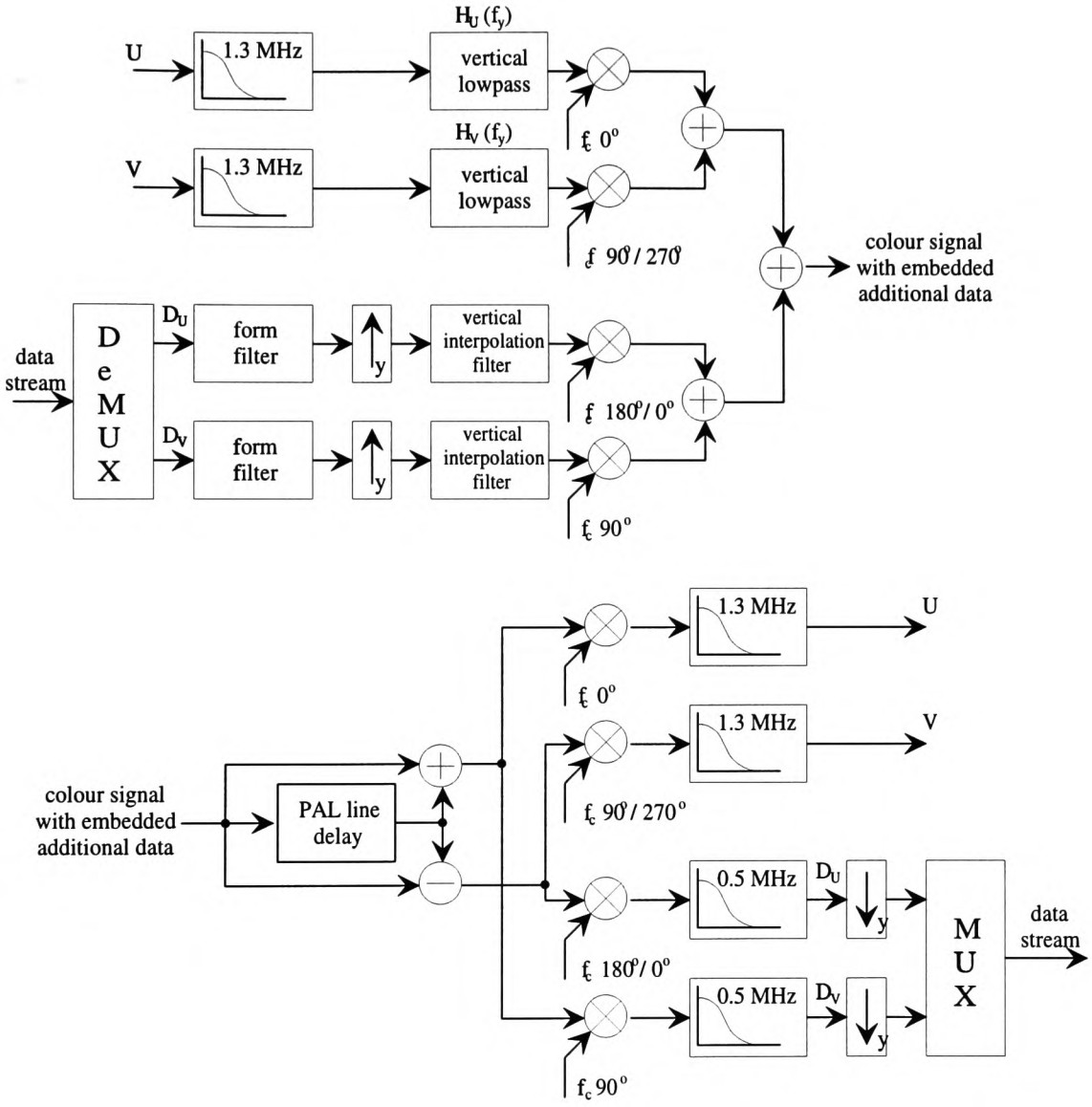

Figure 4.25: Block diagram of the proposed encoder / decoder structure

coder/decoder implementation for the data stream is equivalent to the transmultiplexer structure proposed by Vetterli [126], where by selecting a special set of filter responses, perfect separation is possible. This however excludes the possibility to use the PAL line delay also for data channel separation, so an additional filter set must be included.

4.2.2.3 Encoder design and subjective performance

The encoder design discussed concentrates on the various possibilities of the spectral forming filter of the data signals to avoid inter-carrier and cross colour noise distortions. Their role is the most crucial in the context of compatibility and subjective performance.

Theoretical analysis:- An insight of the three dimensional spectral situation is given in Figure 4.26. The locations of the modulated colour signals U and V, are given with their carrier position in the center. The spectra of the embedded data signals are theoretically uniform along all three axis of the frequency plot, because each data value is uncorrelated within consecutive samples, lines and frames. To limit these spectra to definite locations and thus avoid the aforementioned crosstalk effects, form filters must be included.

The horizontal forming is performed by the usual forming filter to avoid intersymbol interference and ensures that the bandwidth is limited to 0.5 MHz. Further, either vertical or temporal filtering is necessary to provide non-overlapping frequency regions for the data spectra. Due to the fact that the colour signal separation at the decoder is a vertical filter (which is actually the PAL line delay), also for the data channel vertical form filters must be used.

The vertical filters providing these spectral locations for each data component have to be lowpass. Analysing the distortions occurring from crossing over into the colour channels, the data signals pass through the aforementioned vertical lowpass filter before subsequently being processed by the PAL line delay, which is a sine shaped highpass for D_V. The situation for D_U is equivalent, so the crosstalk attenuation response is equal for both cases and can be

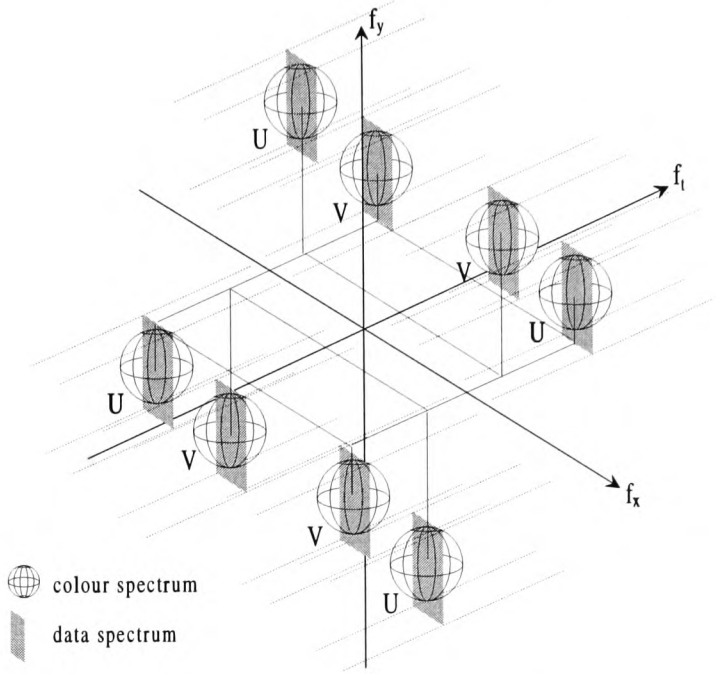

Figure 4.26: Three dimensional spectral location of the PAL colour and additional components

computed from the following relationship:-

$$C_A(f_y) = H_D(f_y)H_P(f_y) \tag{4.10}$$

where $H_P(f_y)$ is the sine shaped PAL line delay separation and $H_D(f_y)$ the vertical low pass form filter for the data signal at the encoder.

Quantifying the aforementioned cross distortions is difficult, because they interfere only in the colour channel, so their appearance is blocky colour noise, which is unusual compared to normal noise degradation and therefore perceptively very annoying. To provide a quantitative measure the noise power is evaluated which accrue from the cross talking data signals, from which either the signal to noise ratio within each colour channel, SNR_U and SNR_V, and the DSNR (Display Signal to Noise Ratio) is derived. The latter is similar to the model that is published in [127]. Any previous noise distortions within the analogue video signal will not impact upon this qualitative evaluation.

Assuming the data signal U_D has a uniform, zero mean PDF (Probability Density Function) within a range from $-\alpha$ to α, the noise power can be computed directly from the vari-

ance σ^2. Depending on the number of symbol levels per data channel, which is for example N=2 for 4 QAM, N=4 for 16 QAM and so on, the following relationship can be derived:-

Starting from the discrete uniform PDF [128]

$$\sigma^2 = \frac{N^2 - 1}{12} \tag{4.11}$$

if the symbols are within the range of $\{0; 1; \ldots; N+1\}$ or $\{-\frac{N-1}{2}; \ldots; \frac{N-1}{2}\}$. To use Equation (4.11) for symbols between $\{-1; \ldots; 1\}$ a multiplication of $\frac{2}{N-1}$ must be performed, so that

$$\sigma^2 = \frac{N^2 - 1}{12}(\frac{2}{N-1})^2 \tag{4.12}$$

and further

$$\sigma^2 = \frac{(N-1)(N+1)}{12}\frac{4}{(N-1)^2} \tag{4.13}$$

Introducing α to consider the data signal amplitude, σ^2 can finally be written as

$$\sigma^2 = \alpha^2 \frac{N+1}{3(N-1)} \tag{4.14}$$

Assuming conditions of ideal transmission, which means perfect filter characteristics for luminance and chrominance splitting as well as chroma demodulation at the receiver, only the colour difference signals are affected by cross colour noise distortions. The noise power in each colour channel introduced from the data signal is then given as:-

$$P_N = \int_0^{f_{sx}} \int_0^{f_{sy}} \sigma^2 |H_F(f_x)^2| |C_A(f_y)^2| df_x df_y \tag{4.15}$$

where $C_A(f_y)$ is the crosstalk attenuation response introduced in Equation (4.10) and $H_F(f_x)$ the horizontal form filter. f_{sx} and f_{sy} are the horizontal and vertical sampling frequency, respectively. If no vertical forming filter is used in the encoder, so that $C_A(f_y) = H_P(f_y)$, Equation (4.15) is simplified to

$$P_R = \frac{\sigma^2}{4} \int_0^{f_{sx}} |H_F(f_x)|^2 df_x \tag{4.16}$$

During usual noise performance discussions the eye weighting function must be taken into account, because the human eye is less sensitive to higher frequency distortions. In this

case however, the crosstalk noise bandwidth is less than $0.5MHz$ where the eye perception has nearly no degradation [129]. The same situation is assumed for the luminance / chrominance separation and also for the colour post filters, so that only $C_A(f_y)$ and $H_F(f_x)$ have to be considered. From Equation (4.15) the signal to noise ratio, SNR, is given as:-

$$\frac{SNR}{[dB]}|_{U,V} = 10log\frac{P_{U,V}}{P_N} \tag{4.17}$$

The maximum peak-to-peak signals for U and V are different and are as follows [130]:-

$$U = 0.612V_{pp} \tag{4.18}$$

$$V = 0.861V_{pp} \tag{4.19}$$

So finally the inter carrier crosstalk can be qualified as:-

$$SNR|_U = 10log\frac{0.375V^2}{P_N} \tag{4.20}$$

$$SNR|_V = 10log\frac{0.74V^2}{P_N} \tag{4.21}$$

From this objective SNR (Signal to Noise Ratio) a more subjective oriented method is derived. It is a modification of the DSNR definition taken from [127]. This method considered the fact that the crosstalk noise encroaches upon the principles of constant luminance. This implies an additional crosstalk in the luminance, because of the non linearity of the picture tube, well known as the gamma law. Equation (4.15) quantifies the distortions within each colour signal, U' and V'. To assess the visibility at the display, the expression for signal plus noise at the output of the decoder matrix must be derived. With $R'-Y' = 1.14V'$ and $B'-Y' = 2.03U'$ the three distorted primary colour signals are given as:-

$$R' + n_R = R' + 1.14\sqrt{P_N} \tag{4.22}$$

$$G' + n_G = G' + 0.96\sqrt{P_N} \tag{4.23}$$

$$B' + n_B = B' + 2.03\sqrt{P_N} \tag{4.24}$$

where $R' = R^{1/\gamma}, G' = G^{1/\gamma}, B' = B^{1/\gamma}$ are the pre gamma corrected colour signals and n_R, n_G, n_B the respective cross colour noise distortions. The displayed luminance Y_D at

the output of the display tube can be obtained by weighting each primary colour signal and adding each term after applying the gamma law [127].

$$Y_D = 0.3(R' + 1.14\sqrt{P_N})^\gamma + 0.59(G' + 0.96\sqrt{P_N})^\gamma + 0.11(B' + 2.03\sqrt{P_N})^\gamma \quad (4.25)$$

Using the relationship $(1+a)^\gamma \approx 1 + \gamma a$, for $a << 1$ Equation (4.25) can be written as:-

$$Y_D = 0.3R + \gamma\frac{0.342R\sqrt{P_N}}{R'} + 0.59G + \gamma\frac{0.566G\sqrt{P_N}}{G'}0.11B + \gamma\frac{0.22B\sqrt{P_N}}{B'} \quad (4.26)$$

and letting $\delta = 1 - \frac{1}{\gamma}$and adding signal terms in voltage and noise terms in power [127]

$$Y_D = 0.3R + 0.59G + 0.11B + \gamma\sqrt{P_N}\sqrt{(0.342R^\delta)^2 + (0.566G^\delta)^2 + (0.22B^\delta)^2} \quad (4.27)$$

The DSNR is then given by

$$DSNR = 20log\frac{Y}{\gamma\sqrt{P_N}\sqrt{(0.342R^\delta)^2 + (0.566G^\delta)^2 + (0.22B^\delta)^2}} \quad (4.28)$$

This ratio can be derived for a given P_N and γ, where P_N is direct related to α, which is the data signal amplitude and the number of symbol levels N. With an increasing N, Equation (4.10) shows that σ^2 moves to threshold of 1/3 for $\alpha = 1$, so a 16-QAM or 64-QAM, N=4 or N= 8 respectively will balance the DSNR gain with complexity.

Filter optimisation:- Two methods will be discussed for the implementation of the vertical spectral form filter, namely vertical partial response coding and a vertical interpolation technique.

Partial response coding performs a spectral forming by introducing more than two symbols and therefore an energy concentration within a smaller bandwidth. To do this, the data flow must be converted using the following relationship ([131],5.4.1):-

$$y(n) = \sum_{m=0}^{N-1} x(m)h(n-m) \quad (4.29)$$

which is a convolution of the input $x(n)$ with the filter impulse response $h(n)$. If Duo-Binary coding is considered for instance, $h(n)$ must be chosen as:-

$$h_{Dduo}(n) = \frac{1}{2}(\delta(n) + \delta(n-1)) \quad (4.30)$$

so that

$$H_{Dduo}(f_y) = cos(\pi \frac{f_y}{f_{sy}}) \tag{4.31}$$

Duo-Binary coding converts the usual two levels per symbols into three and performs a cosine shaped spectral forming which reduces the crosstalk effects. Alternatively a higher order partial response code will achieve better spectral forming properties but also the number of symbol levels will increase, which decreases the transmission robustness.

The other spectral forming technique involves transmitting data only every L^{th} line, where L is the interpolation factor. An interpolation filter fills-in the omitted lines and thus performs the vertical spectral forming by suppressing the imaging introduced due to the up-sampling process of the data signal. The resulting bandwidth is therefore $\frac{1}{L}$ compared to transmitting data every line. To ensure an optimal reconstruction of the data signals at the decoder, the overall vertical filter chain during transmission has to maintain the original data samples. This criterion is fulfilled if every L^{th} sample of the overall filter impulse response is zero, which characterises the design supposition of

$$h_D(n = iL) = 0 \qquad i = 1, 2, 3, \ldots \qquad h_D(n = 0) = 1 \tag{4.32}$$

Equation (4.32) implies an FIR filter design, that need not necessarily be linear phase ([132]7.2). The designed vertical filter responses cover the whole transmission chain, so the vertical form filter must be excluded by deconvolving the other vertical filters of the chain, which is the PAL line delay, if this is to be used for the data channel separation. Otherwise additional filters have applied for the decoding process. The frequency response of the deconvoluted form filter is given as:-

$$H_F(f_y) = \frac{H_D(f_y)}{H_P(f_y)} \tag{4.33}$$

This technique implies a degradation of the overall spectral forming performance and therefore a limitation of the crosstalk attenuation response $C_A(f_y)$. Two critical areas are identified. Firstly the frequency area close to the vertical Nyquist frequency, because $H_P(f_y)$ is cosine shaped filter with a zero at Nyquist. Secondly the region at $1/L$ of the Nyquist frequency. This position indicates the lowest attenuation of $C_A(f_y)$ which is further compromised by $20logsin(\frac{\pi}{2L})$ due to the exclusion of $H_P f_y$(Figure 4.27). The requirements for the

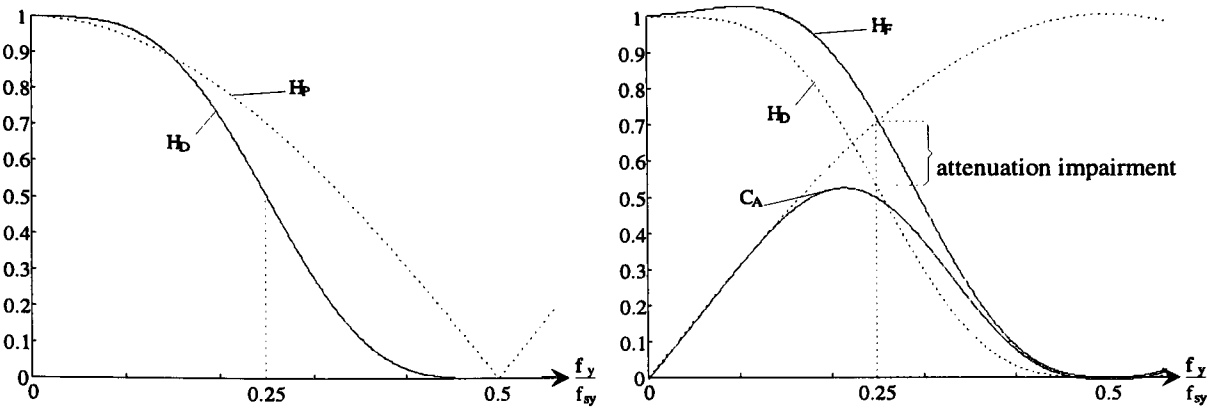

Figure 4.27: Graphical explanation of the vertical form filter situation for $L = 2$

vertical form filter $H_F(f_y)$ using the interpolation technique are direct related to the optimisation of $C_A(f_y)$. So the major requirement for $H_D(f_y)$ which is entirely separate from the general interpolation filter properties are that it must exhibit:-

- sufficient attenuation at $\frac{f_{sy}}{2L}$
- no abnormal behaviour in the frequency area of $\frac{f_{sy}}{2}$ after deconvolution of $h_P(n)$

Several design methods can be found fulfilling these requirements. The ideal interpolation filter provides no passband ripple together with perfect stopband attenuation properties. This only can be achieved with an impulse response given as

$$h_D(n) = \frac{sin(\frac{\pi n}{L})}{\frac{\pi n}{L}} \tag{4.34}$$

for infinite n . For a practical realisation a window must be applied, so that the filter design technique starts from a sinc-function (Equation (4.34)) before subsequently being multiplied by a window. The parameters of the sinc-function must be chosen so that every L^{th} coefficient of the response is zero:

$$h_{Dw}(n) = \frac{sin(\frac{\pi n}{L})}{\frac{\pi n}{L}} w(n) \tag{4.35}$$

The choice of the window must meet these requirements, and Appendix B.2 compares the different window possibilities.

A different interpolation filter design method is the maximally flat filter approach which uses Lagrange polynomials for deriving the filter coefficients. This technique is extensively used in fractional sampling interval delays [133], but is also found in conventional interpolation approaches [132][134].

The Lagrange polynomials are defined as:

$$A^d(m) = \prod_{k=0;k\neq m}^{M} \frac{d-k}{n-k} \qquad m = 0, 1, 2, \ldots, M \tag{4.36}$$

where M is the polynomial order and d the delay to which position the samples should interpolate. For the interpolation filter design a set of polynomials of different order and delay related to filter order and interpolation factor must be derived, from which the final filter coefficients are selected. More detail can be found in [132] and [135]. An algorithm for an interpolation factor of two can be designed with the rules taken from Tonge [134]:

$$\begin{aligned} h_{Dtonge}(0) &= \frac{1}{2} \\ h_{Dtonge}(2n+1) &= \frac{\prod_{m=0}^{M}(2m+1)^2}{4(2n+1)^2 \prod_{m\neq n}((2m+1)^2-(2n+1)^2)} \end{aligned} \tag{4.37}$$

in which $2n+1$ refers to the filter coefficient and M to the filter order, where $M = 0$ stands for an order of 2, $M = 1$ for 6, $M = 2$ for 10, and so on. Due to the symmetry in Equation (4.37), only one half of the filter impulse response needs to be derived, so that the result must be mirrored to get the final version. The problem raised with this filter approach is that it only provides good results for interpolation factors of two, so that for different factors another design method must be used (Appendix B.3).

A third method is of interest because of its higher degree of design freedom, is based on a Tschebyscheff approximation together with a modification proposed by Schaefer and Rabiner [136]. This produces filter results which are comparable with Kaiser window designs [132].

To improve the attenuation at $\frac{1}{L}$ of the Nyquist frequency of $C_A(f_y)$ a combination of the interpolation technique together with the duobinary coding will provide a better solution. A duobinary coded signal spectrum is cosine shaped, so it is zero at the Nyquist frequency. An upsampling of L by introducing zeros will shift this point to $1/L$ of the new Nyquist

frequency and therefore introducing a notch at the aforementioned critical location. The corresponding impulse response can be derived as follows:-

$$h(n) = \sum_{m=0}^{N-1} h_F(m)\frac{1}{2}(\delta(n-m) + \delta(n-L-m)) \tag{4.38}$$

for $L = 2, 3, \ldots$ depending upon the chosen interpolation factor.

4.3 Data compression

The data compression block, in Figure 4.1 has the specific aim of linking the pre-processing section, that is the dual channel subband coding, with the embedded data modulation. Chapters 1 and 2 provide suitable references to the large mass of literature upon date compression techniques and their appropriateness for specific applications. The following discussion will not therefore present a detailed solution, but will instead discuss the general feasibility and the requirements of the data compression within the proposed system and for completeness fulfill one of the original objectives of this research.

The dual channel subband strategy implicitly provides a data compression of two, due to the diagonal filtering, so that the residual signal resolution becomes exactly the same than the standard component.

$$720\frac{pixel}{line}576\frac{line}{frame}25\frac{frame}{s} = 10368000\frac{pixel}{s} \tag{4.39}$$

Considering further a quantisation of $8\frac{Bit}{pixel}$ the resulting data rate increases to:-

$$\rho = 10368000\frac{pixel}{s}8\frac{Bit}{pixel} = 82944000\frac{Bit}{s} \tag{4.40}$$

In the context of the proposed system, it is shown in Section 5.2 that the data rate provided by the embedded data modulation ranges form approximately $200\frac{KBit}{s}$ to $1000\frac{KBit}{s}$, depending upon the selected roll-off factor and the implemented vertical form filter technique. This typically requires a compression ratio between 80 and 400, which is clearly a very high number indeed.

A general impediment in reaching such a high compression ratio is raised by the statistical properties of the residual signal. Due to the bandsplitting process, the residual will be high pass, so is already a differential signal. This implies that those compression techniques which are based upon decorrelating principles, e.g. the DCT and KLT, will be inefficient within this context.

An adaptive quantizing algorithm presented by Amor [137] was implemented and further analysed by Toedtmann [138]. The final compression ratio achieved by this method was proven to be a maximum of ten. A different, non linear quantizing technique based on a DCT is presented by Lipkow [139] with the aim of adapting the coding strategy to the human visual perception. However, this approach also does not provide higher ratios than ten. Enhancements can be expected if motion adaptive solutions are considered. A temporal subsampling strategy as discussed in [2] provides an additional compression of two, while more sophisticated methods such as motion vector based techniques will increase this further, so that an overall realistic achievable compression ratio can be approximately 30.

It is obvious that the data rate provided by a single embedded sub channel is not satisfactory. Combining the techniques presented in this thesis with that proposed by Ruppel [102] (see Section 3.2.3) will give a data rate of approximately $1200\frac{KBit}{s}$ and thus require a compression ratio of 70. This is much more realistic than those values given above however, as outlined this value is far beyond what's currently realistic with contemporary methods.

Another aspect militating against such high compression ratios, is that the residual signal is aimed to enhance the overall picture quality. It is expected that unrealistically high ratios will inevitably lead to additional picture artefacts, for example an insufficient aliasing compensation usually performed by the QMF.

A corollary of this is that while the high compression ratios can in principle be achieved , the inevitable result is of compromising overall picture quality. From the proposed system viewpoint therefore, it is much more appropriate to exploit the potential embedded data capacity for supplementary multimedia services rather than explicitly attempting high or extended definition TV.

4.4 Interim conclusion

This chapter has reviewed the theoretical underpinning of the main areas throughout this work. Firstly, the principles of "dual channel sub-band coding" were introduced whereby only two sub-bands instead of the usual four were derived by implementing a diagonal pre-filter before subsequent band splitting using QMF banks. It was shown that there is significant merit in implementing the horizontal and vertical band-splitting filter banks to be odd and even order respectively, to compensate crosstalk components and thus provide a uniform overall transfer function response. The inherent drawback of this sub band strategy is that no overall alias compensation can be achieved within the reconstituted signal. The design constraints for the diagonal and band-splitting filters were clearly identified. Different filter design methods are introduced and compared. However, only relatively simple methods are applied to verify this theoretical analysis, because these studies relate to verifying the overall principles of the system. For further system improvements several more sophisticated methods are available which were examined. To make the dual channel sub band strategy applicable to moving, interlace scanned video signals, the general problems raised with such an input were reviewed. Three separate motion adaptive modifications were proposed, with different properties for the compatible and the decoded signal quality and corresponding implementation complexities. The actual specific method for motion detection is a degree of freedom for implementation since many solution are available for the proposed system, which all afford different advantages and disadvantages.

The second section presents two different embedded modulation techniques for the two signal components within a PALplus television signal. Trade-offs and distortions were highlighted. The additional helper modulation was identified as being problematic because of its proneness to noise and the necessity of a high order temporal filter to split the two components. The additional colour carrier modulation provides the best potential for embedded data transmission. This technique uses the active video part by modulating the colour subcarrier in such a way that the frequency locations of the modulated colour difference signals are doubly occupied. It is clear that some crosstalk distortion occurs, which degrades compatibility. This had been fully analyzed and quantified using the objective SNR calculation

for each colour difference signal and a more subjectively orientated Display Signal to Noise Ratio (DSNR). This was intended to give a measure of the cross data noise distortion visible. The concept of a two dimensional form filtering was proposed to suppress these degradations and balance the data rate efficiency. Three different filter strategies, namely duo-binary coding, a special interpolation technique and the combination of both, were discussed together with different filter design methods.

Finally the feasibility of the residual data compression, which completes this system has been reviewed. With an actual implementation example given, it was outlined, that it is generally possible to provide a compression technique fulfilling the initial aim of this work. However, the identified high compression ratio implies several trade-offs, so that it is much more appropriate to provide the additional data transmission capacity to other supplementary data services.

Chapter 5

Discussion of practical results

5.1 Simulation of Dual channel sub-band coding

The detailed concept of the dual channel sub-band coding system is given in Section 4.1. The simulations presented concentrate upon the even- order filter scenario for vertical band-splitting. Firstly, before analysing the various filter designs and combinations, a verification of the distortion analysis of Section 4.1.2 is given.

Figure 5.1 compares the input with the output signal, which is derived by the dual channel sub-band algorithm using no diagonal prefilter. A diagonal post filter however, is included. To give a better view of the diagonal sinewave pattern, the screen shots are zoomed by a factor of four and further the graphics underneath provide a helpful visualisation. Finally the measured two dimensional FFT-plots show exactly which frequencies are included in the input and output signals. The processed sinewave is outside the passband of the ideal, not implemented diagonal filter, so it is obvious that aliasing and cross over distortions will occur. Figure 5.1b proves the conclusions derived in Section 4.1.2. The diagonal post filter suppresses post aliasing as well as the original component, so that the two crossover terms covered by the passband remain. The output sinewave pattern is totally different from the input.

Figure 5.2 shows a crossover distortion raised from a frequency within the coverage of the

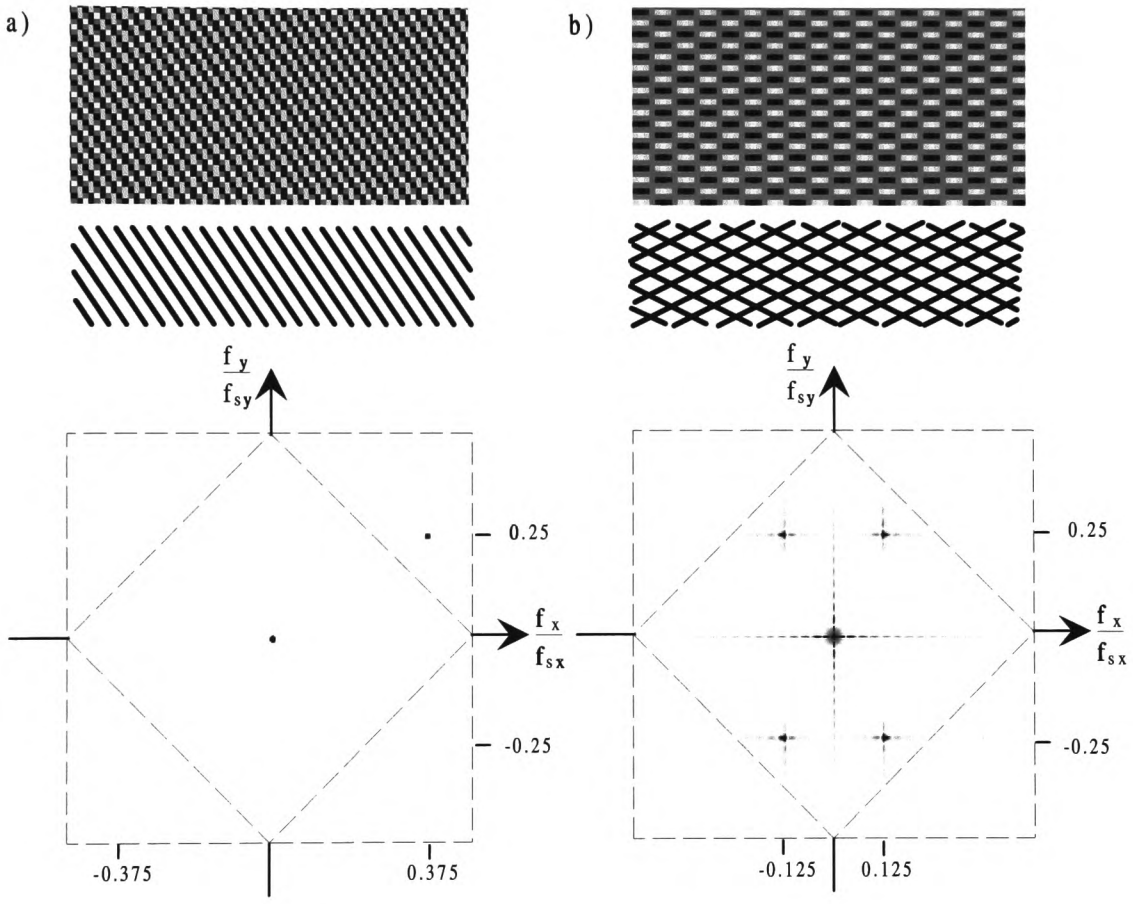

Figure 5.1: Comparison to visualise cross over effects in Input-(a) / Output-(b) image

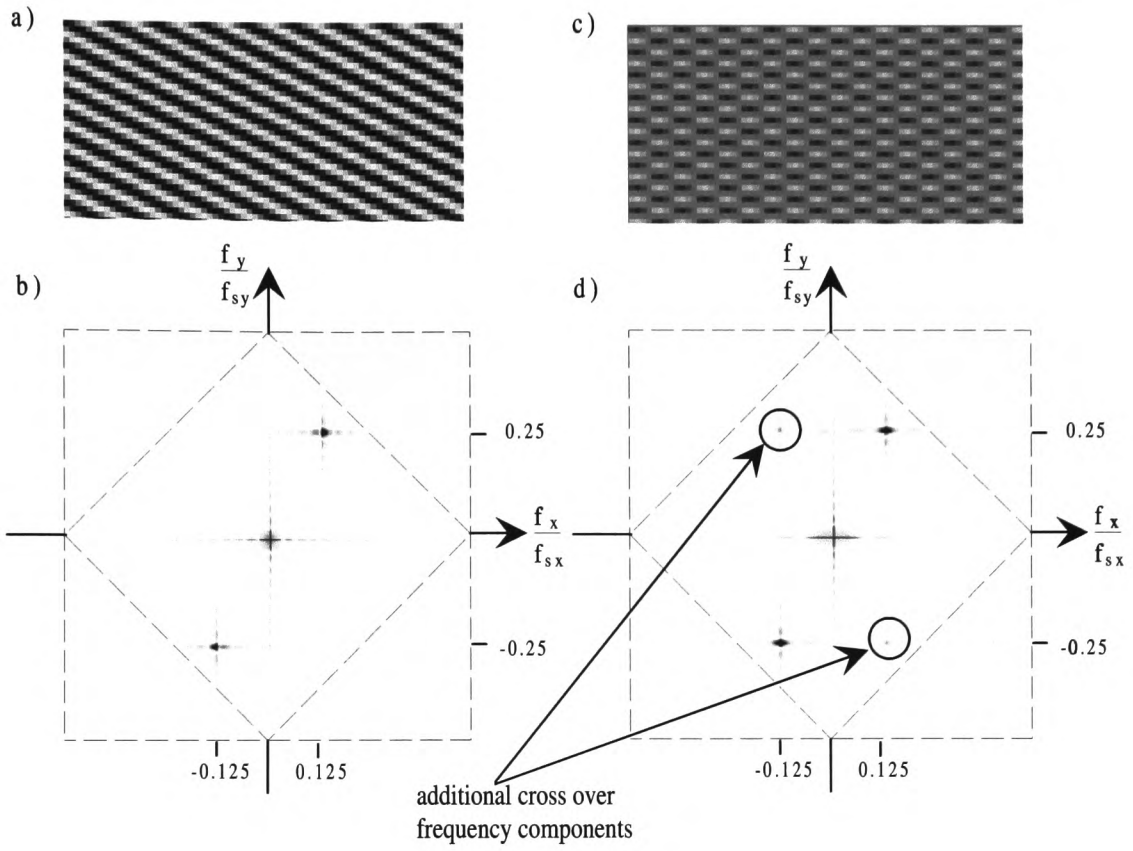

Figure 5.2: Cross over example for frequency components within the passband of the diagonal filter (zoomed and amplified)

passband of the diagonal prefilter. In contrast to the previous example, trivial cosine shaped filters are used for horizontal bandsplitting. The wide passband characteristics of these filters however, means that a wide transition band overlap component C_{A2}, occur. This introduces a horizontal mirrored component of the original frequency as shown in Figure 5.2b, caused by vertical subsampling. For this filter combination this mirrored crossover is attenuated by $9dB$ as can easily be shown with Equation (A.25), so in relation to the original frequency it is still perceptible, but less annoying. The screen shot of Figure 5.2c shows a difference image between the input and output, which is zoomed and amplified by four. If a high input frequency is now considered which is close to the cut-off frequency of the diagonal filter, the attenuation for this distortion will decrease by up to $6dB$. The same situation occurs for horizontal cross over, if the input frequency pattern is rotated by 90^o.

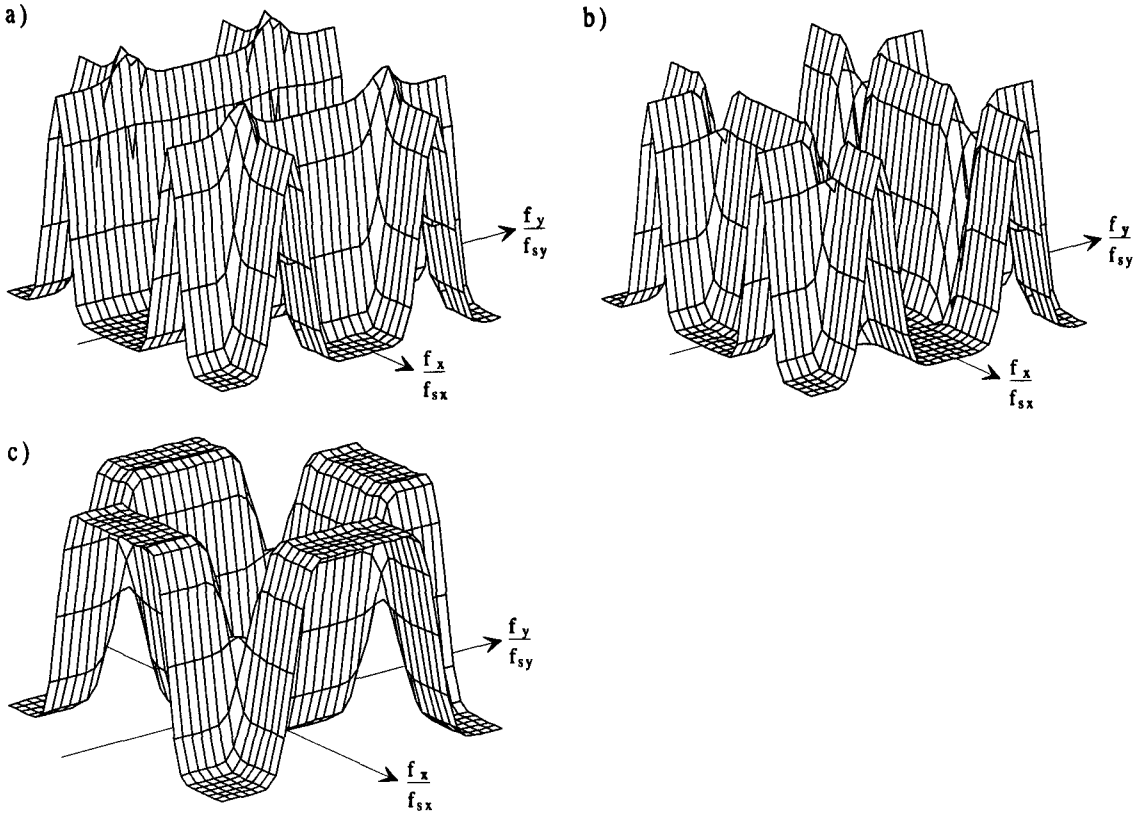

Figure 5.3: Crossover and alias terms responsible for, (a) horizontal (b) vertical (c) diagonal subsampling using no diagonal prefilter

Figure 5.3 shows each crossover and alias term separately, but in contrast to the plots in Figure 4.10 real filter responses of $15^{th}/14^{th}$ order bandsplitting filter are applied. The major alias components in Figure 5.3a and b will be suppressed by implementing the diagonal prefilter however, those parts of the crossover terms within the diagonal passband remain and introduce the effects as discussed previously. A dominant crossover occurs in the diagonal subsampling as shown in Figure 5.3c. These components can be only balanced by the diagonal prefilter. Assuming ideal prefiltering, no aliasing frequencies appear in the passband of this term and so it is distortion free.

The discussions so far focus upon highlighting the various distortion effects. The major role in trying to avoid these distortions is given to the pre and post diagonal filter, because the baseband of the dual-channel subband technique is diamond shaped within the horizontal/vertical frequency plane. Considering ideal filter shapes most of the distortions can

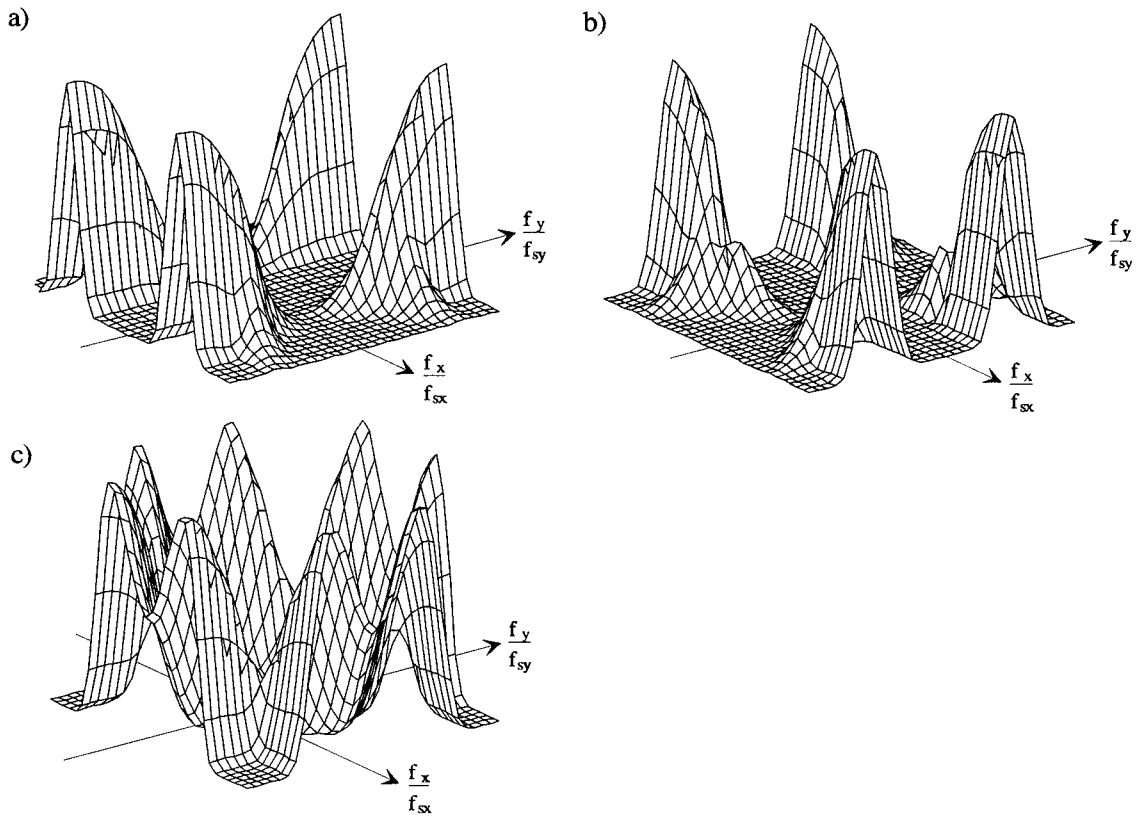

Figure 5.4: Crossover and alias terms from Figure 5.3 using a real, but smooth roll-off diagonal prefilter

be eliminated however, under certain specific conditions in the bandsplitting filter process, some small distortions remain. The effects will now be discussed using realistic diagonal pre filter shapes, $H_{Dpre}(z_1, z_2)$. Each alias component (Equation (A.20) to (A.22)) must be multiplied by the appropriate shifted diagonal filter response, so that

$$A_{1D}(z_1, z_2) = A_1(z_1, z_2)H_{Dpre}(-z_1, z_2) \quad (5.1)$$

$$A_{2D}(z_1, z_2) = A_2(z_1, z_2)H_{Dpre}(z_1, -z_2) \quad (5.2)$$

$$A_{3D}(z_1, z_2) = A_3(z_1, z_2)H_{Dpre}(-z_1, -z_2) \quad (5.3)$$

Integrating a further real diagonal post filter, $H_{Dpos}(z_1, z_2)$, each alias term must be additionally multiplied by $H_{Dpos}(z_1, z_2)$. Figure 5.4 shows the corresponding aliasing terms from Figure 5.3 using a 11 by 11-tap diagonal prefilter.

To analyse the overall performance of the implemented filters, the separate distortions,

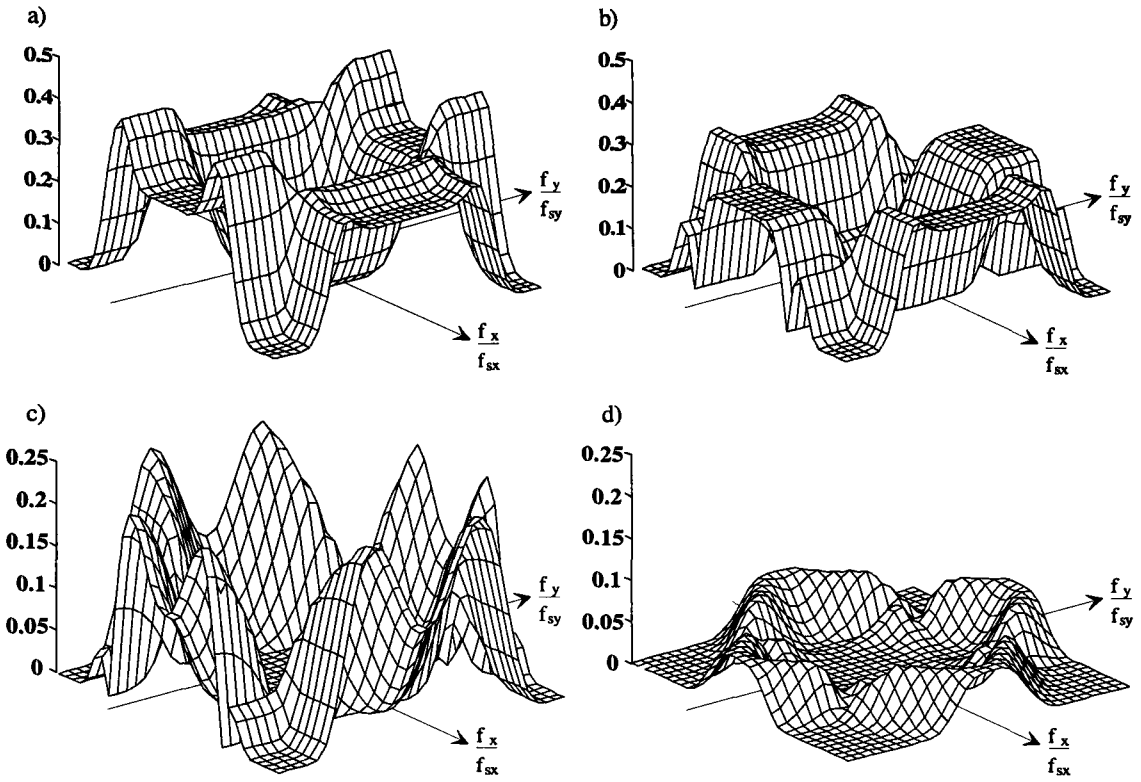

Figure 5.5: Overall crossover and alias frequency response a) with $\frac{N_2}{2}$ is odd, b) with $\frac{N_2}{2}$ is even, and the respective versions of b) including c) diagonal pre filter and d) diagonal pre and post filter

highlighted with Figure 5.3 and Figure 5.4, must be added. Equation (A.20) to (A.26) shows that the phase relation is not unique and further depends upon the order of the vertical band-splitting filter. Figure 5.5a and b gives an insight to this superposition and compares the scenario when $\frac{N_2}{2}$ is odd and even, respectively. The advantage when $\frac{N_2}{2}$ = even is clearly visible. Figure 5.5c gives an insight by implementing $\frac{N_2}{2}$ = even together with the 11 by 11-tap diagonal prefilter. Figure 5.5d additionally includes a diagonal postfilter. For both these plots the amplitude is scaled by two to improve visibility. Finally, Figure 5.5d shows those frequency areas within the horizontal/vertical frequency plane, which are disturbed by aliasing and crossover components. This disturbance response can be directly derived as

$$H_{Dis}(z_1, z_2) = \frac{1}{4}(A_{1D}(z_1, z_2) + A_{2D}(z_1, z_2) + A_{3D}(z_1, z_2))H_{Dpos}z_1, z_2 \qquad (5.4)$$

and will help to evaluate the various filter combinations. For classification ϵ will be defined

Example No.	hor. band-splitting filter	vert. band-splitting filter	diagonal pre filter	diagonal post filter	ϵ	Figure
1	lh_16	lv_15	11x11 tap	11x11 tap	0.0123	5.10
2	lh_16	lv_17	11x11 tap	11x11 tap	0.0097	5.11
3	lh_16	lv_17	19x19 tap	19x19 tap	0.0045	5.12
4	lh_16	lv_17	31x31 tap	31x31 tap	0.0031	5.13
5	lh_16	lv_17	31x31 tap	19x19 tap	0.0039	5.14
6	lh_16	lv_17	31x31 tap	11x11 tap	0.0071	5.15
7	lh_2	lv_17	31x31 tap	31x31 tap	0.0107	5.16
8	lh_8	lv_9	31x31 tap	31x31 tap	0.0079	5.17

Table 5.1: Filter combinations used to analyse overall efficiency

as the volume underneath $H_{Dis}(z_1, z_2)$ so that:

$$\epsilon = \int_{z_1} \int_{z_2} H_{Dis}(z_1, z_2) dz_1 dz_2 \tag{5.5}$$

Three different diagonal filters will be used in the simulations. They are designed by applying the rotation method together with a Kaiser window ($\alpha = 1$) as explained in Section 4.1.3 by Vergin [119]. Figure 5.6 shows the frequency response together with the corresponding contour plot for the 11 by 11 tap version. This represents the case of implementing a filter with a relatively wide transition bandwidth, so that in critical frequency areas insufficient alias attenuation would be expected. A 19 by 19 tap design is given in Figure 5.7, which represents a satisfactory compromise between complexity and attenuation efficiency. For completeness 31 by 31 tap filter from Figure 5.8 has been included as an approximation of the ideal case.

Figure 5.9 shows an insight to the frequency responses of the bandsplitting filters. They are designed with the recursive windowing method as explained in Section 4.1.3 by applying the tools developed by Meissner [122]. These filters conform to the strict rules of a QMF design, but they are suboptimal in that there will exist amplitude distortions in the overall transfer function. This however, touches all subband designs in general and is not the main

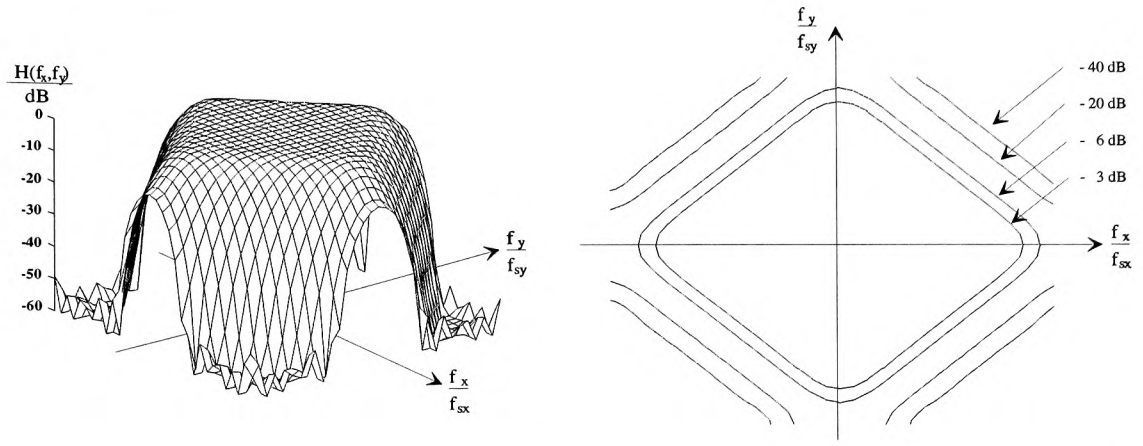

Figure 5.6: Diagonal frequency response with its contour plot for the 11x11 tap filter example

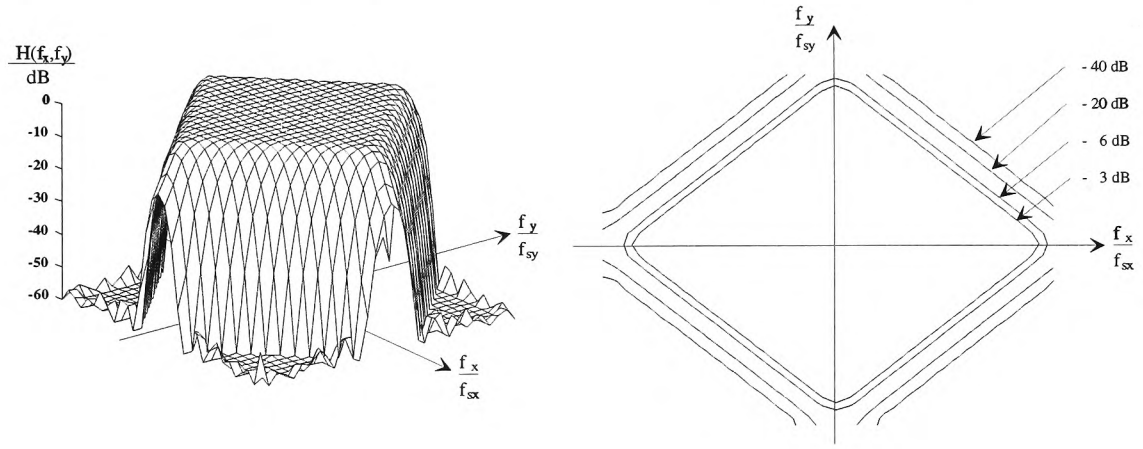

Figure 5.7: Diagonal frequency response with its contour plot for the 19x19 tap filter example

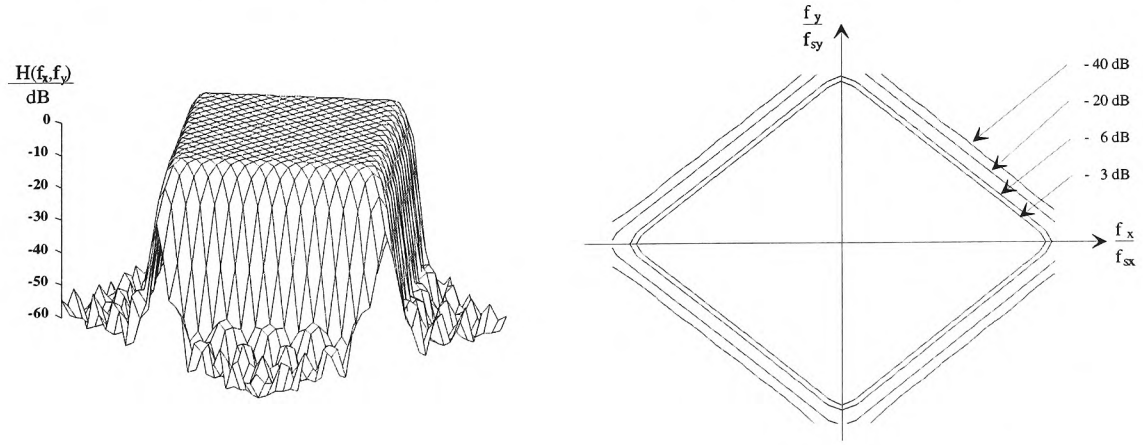

Figure 5.8: Diagonal frequency response with its contour plot for the 31x31 tap filter example

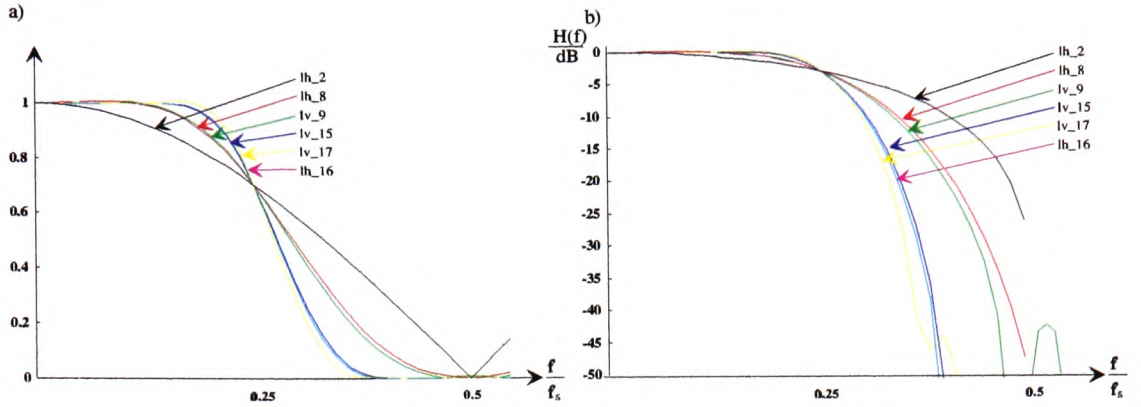

Figure 5.9: a) linear and b) logarithmic frequency response of the used bandsplitting filter

focus for this research into the dual- channel subband strategy. The filters are therefore considered as sufficiently adequate for evaluating this novel implementation. The nomenclature "lh" indicates horizontal filtering and "lv" vertical filtering with following digits represents the number of corresponding filter coefficients.

Table 5.1 summarises the simulations performed to compare the different filter combinations and further to evaluate overall efficiency of these dual channel subband scenarios. Figure 5.10 to Figure 5.17 shows the simulation results for these examples. Here the overall transfer function $T(z_1, z_2)$ and the disturbance response $H_{Dis}(z_1, z_2)$ are displayed together with an encoded / decoded zoneplate test image. To highlight the disturbed regions, the contour plot of the two responses are overlaid with the processed zoneplate.

Example No. 1 and No. 2 compares the $\frac{N_2}{2}$ = odd / $\frac{N_2}{2}$ = even implementation. The value of ϵ shows a slight advantage for Example No.2, which is $\frac{N_2}{2}$ = even. This is also visible with Figure 5.10 and Figure 5.11, where the distortion response (Figure 5.11b)) provides a better attenuation with no peaks higher than $-26dB$ visible. Table 5.1 shows that the remaining Examples all using the $\frac{N_2}{2}$ = even implementation to exploit this advantage. Example No. 2, No. 3 and No. 4 present the three different diagonal filter implementations using the same filter for pre- and post filtering. When viewing their frequency responses, not surprisingly the $31x31$ tap version provides the best result. The comparison of ϵ shows that this filter is only slightly superior to the 19 by 19 tap implementation, so providing a viable

alternative, with significantly less complexity. Figure 5.13 verifies the near ideal case for the $31x31$ tap filter. For the 19 by 19 tap implementation, Figure 5.11b shows also excellent disturbance value, but as can be seen in Figure 5.11d, the disturbance transition bandwidth is wider and therefore more distortion is visible. With the 11 by 11 tap filter, Figure 5.10 provides a good example of what occurs if the transition bandwidth is too wide. Example No. 5 and No. 6 shows the scenario if the diagonal post filter is implemented with less complexity. Comparing the values of ϵ with those pre- and post filter implementing with equal complexity, the importance of an adequate prefilter is clearly visible. Example No. 5 provides an alternative to the implementation of Example No. 4. With Example No. 6 the disturbance increases as seen in Figure 5.15d. Example No. 7 simulates the case where a horizontal bandsplitting filter is implemented with a wide transition bandwidth to highlight again the crossover from frequencies within the passband of the diagonal prefilter. Comparing ϵ with that from Example No. 4 shows, that this is not an appropriate solution. The disturbance response from Figure 5.16b verifies this as the worst filter selection with the $-26dB$ peaks, visible in Figure 5.16d, marking those frequency regions, which were previously identified as critical. A compromise for bandspliting filter complexity is simulated with Example 8, by implementing $7^{th}/8^{th}$ order filters, rather than $15^{th}/16^{th}$ as in the other examples. The value of ϵ and furthermore detailed view with Figure 5.17 shows this could only be a compromise solution.

To assess the performance of these filter examples on real-world images, Figure 5.18 to Figure 5.21 shows the outcome by processing the test images "Lena" and "Bath" with the implementations of Example No. 4 and No. 2. In both cases distortions are only visible in the magnified difference images. To quantify the distortions the root mean squared error, RMSE (Root Mean Square Error) is derived as defined in [70],

$$RMSE = \sqrt{\frac{1}{heightxwidth} \sum_{height} \sum_{width} diff^2} \tag{5.6}$$

from which the SNR can be derived.

$$SNR = 20dBlog\frac{255}{RMSE} \tag{5.7}$$

Table 5.2 summarises this for "Lena" and "Bath". For both images the values are very small, meaning a relatively high SNR which indicates that naturally those frequencies identified

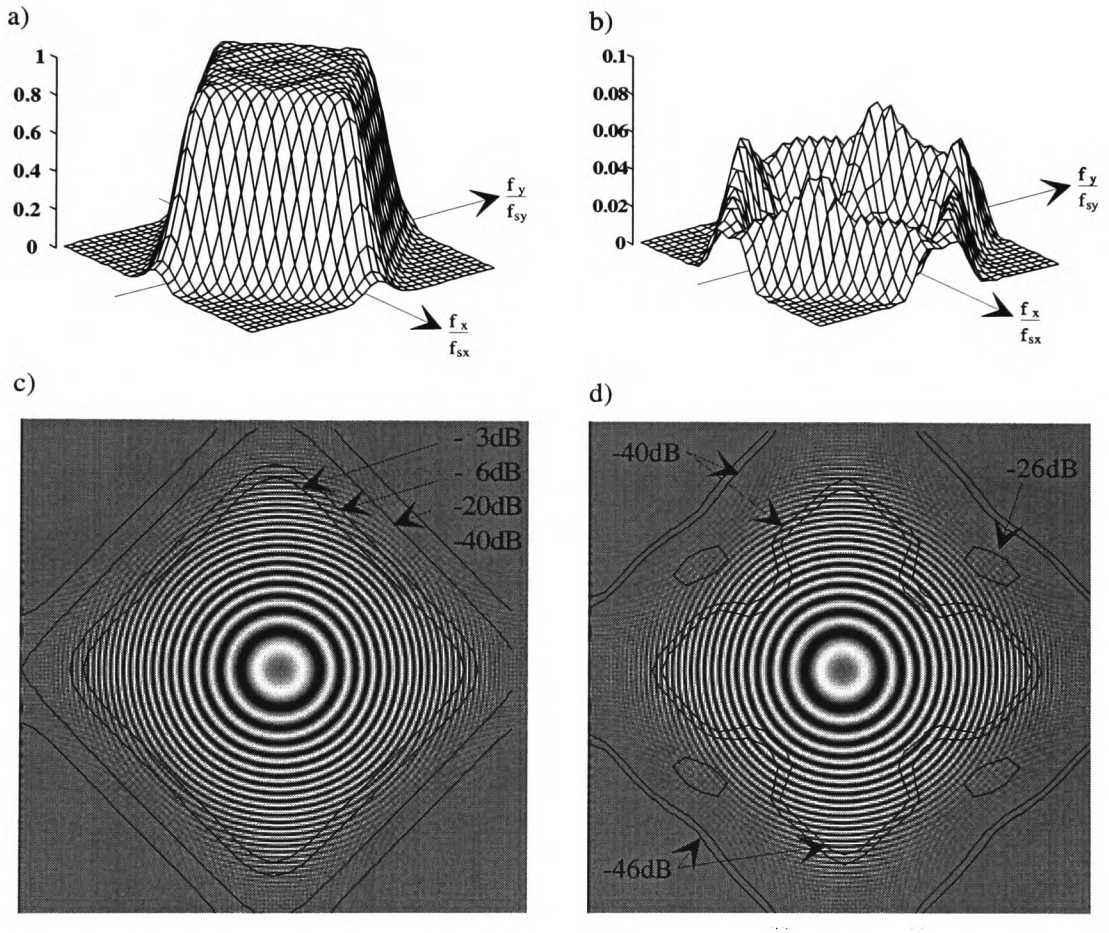

Figure 5.10: Example No. 1: a) overall transfer function $T(z_1, z_2)$ including the diagonal pre- and postfilter responses b) disturbance response $H_{Dis}(z_1, z_2)$ c) output image overlaid with the contour of a) d) output image overlaid with the contour of b)

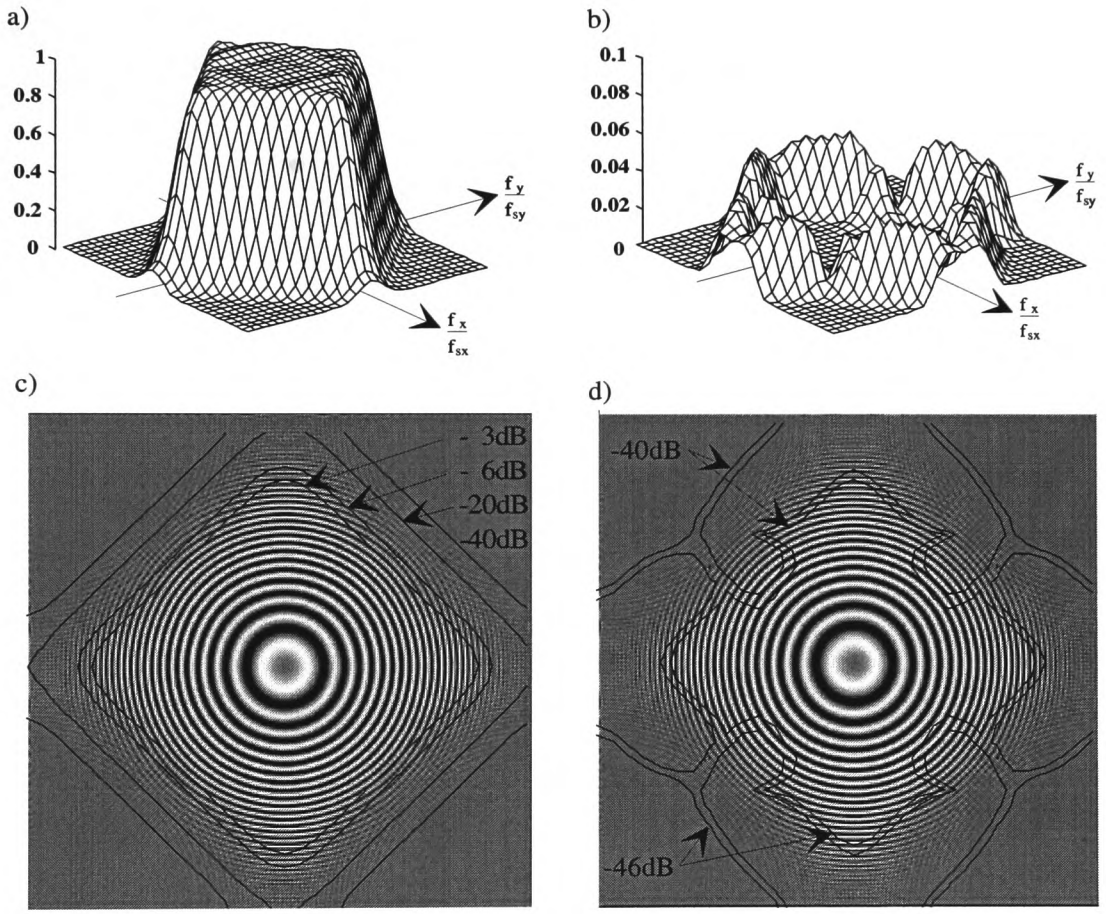

Figure 5.11: Example No. 2: a) overall transfer function $T(z_1, z_2)$ including the diagonal pre- and postfilter responses b) disturbance response $H_{Dis}(z_1, z_2)$ c) output image overlaid with the contour of a) d) output image overlaid with the contour of b)

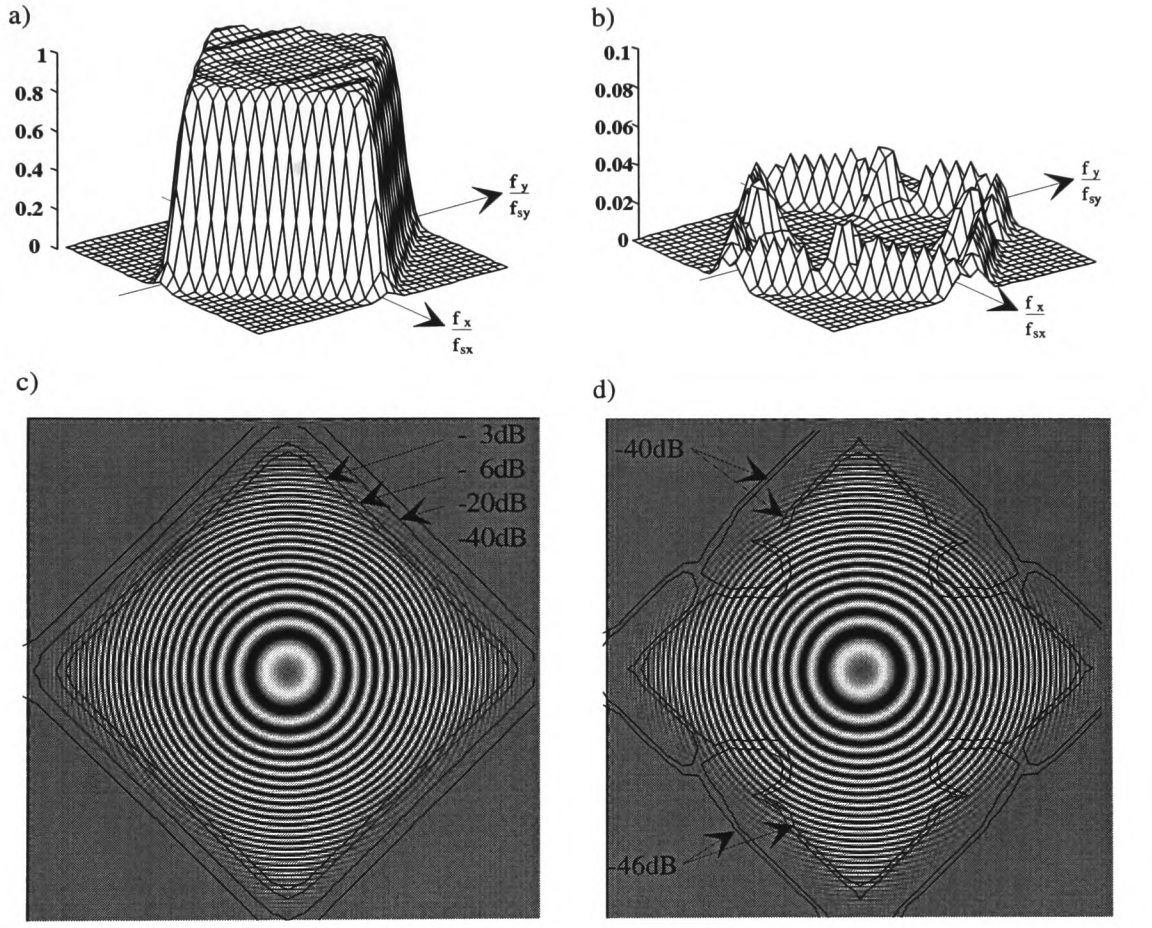

Figure 5.12: Example No. 3: a) overall transfer function $T(z_1, z_2)$ including the diagonal pre- and postfilter responses b) disturbance response $H_{Dis}(z_1, z_2)$ c) output image overlaid with the contour of a) d) output image overlaid with the contour of b)

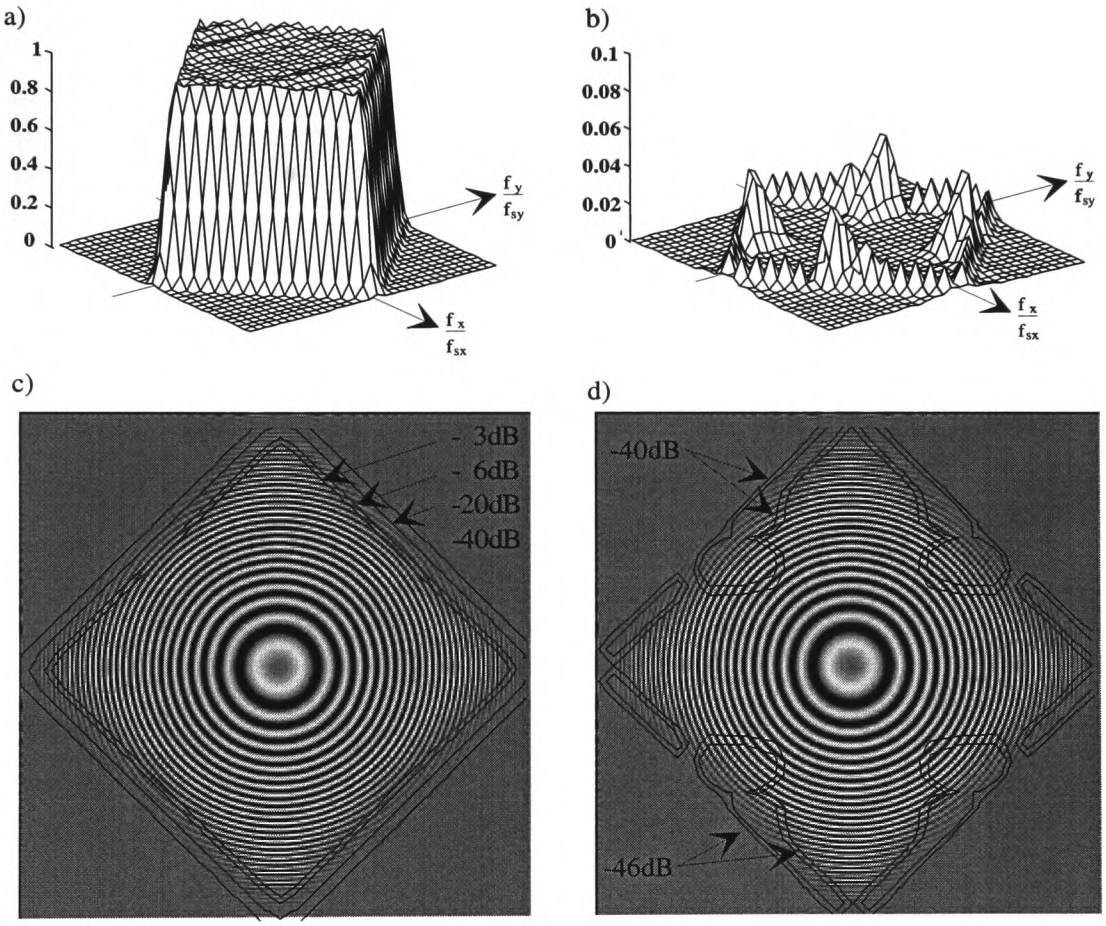

Figure 5.13: Example No. 4: a) overall transfer function $T(z_1, z_2)$ including the diagonal pre- and postfilter responses b) disturbance response $H_{Dis}(z_1, z_2)$ c) output image overlaid with the contour of a) d) output image overlaid with the contour of b)

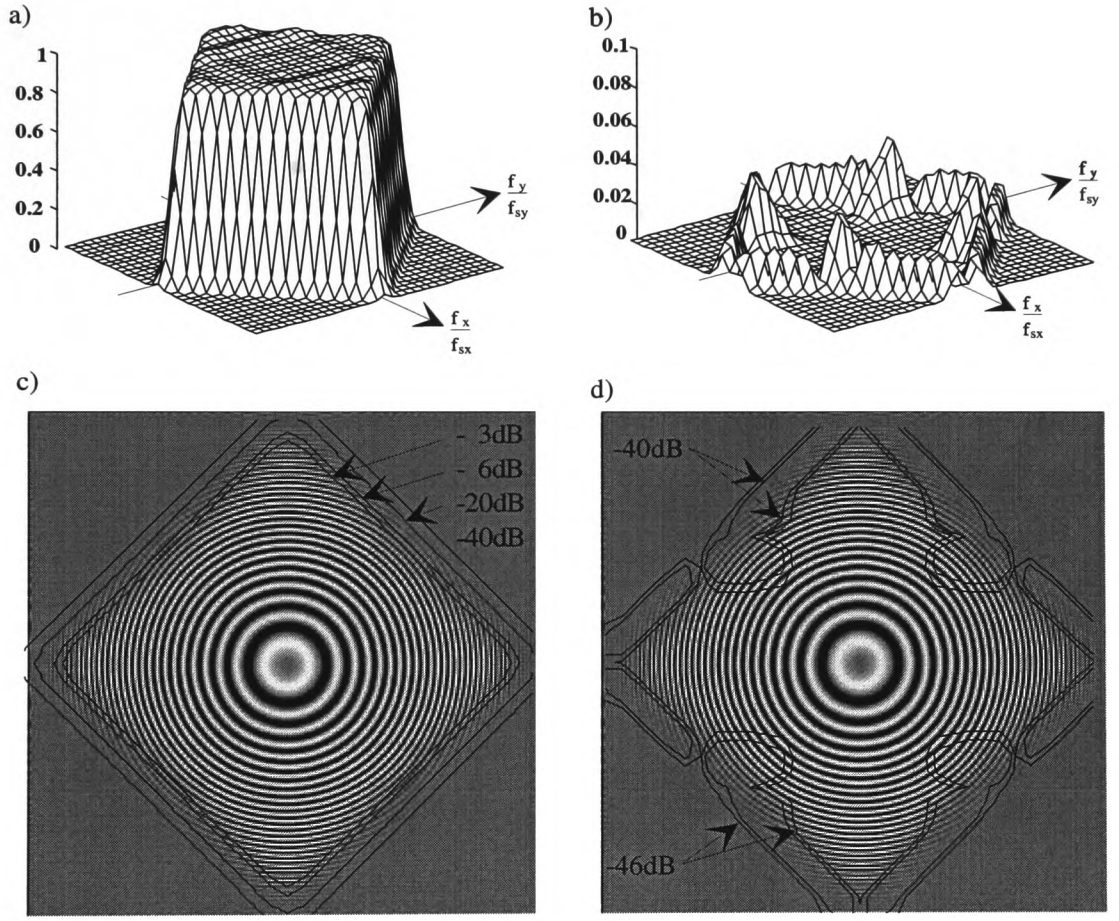

Figure 5.14: Example No. 5: a) overall transfer function $T(z_1, z_2)$ including the diagonal pre- and postfilter responses b) disturbance response $H_{Dis}(z_1, z_2)$ c) output image overlaid with the contour of a) d) output image overlaid with the contour of b)

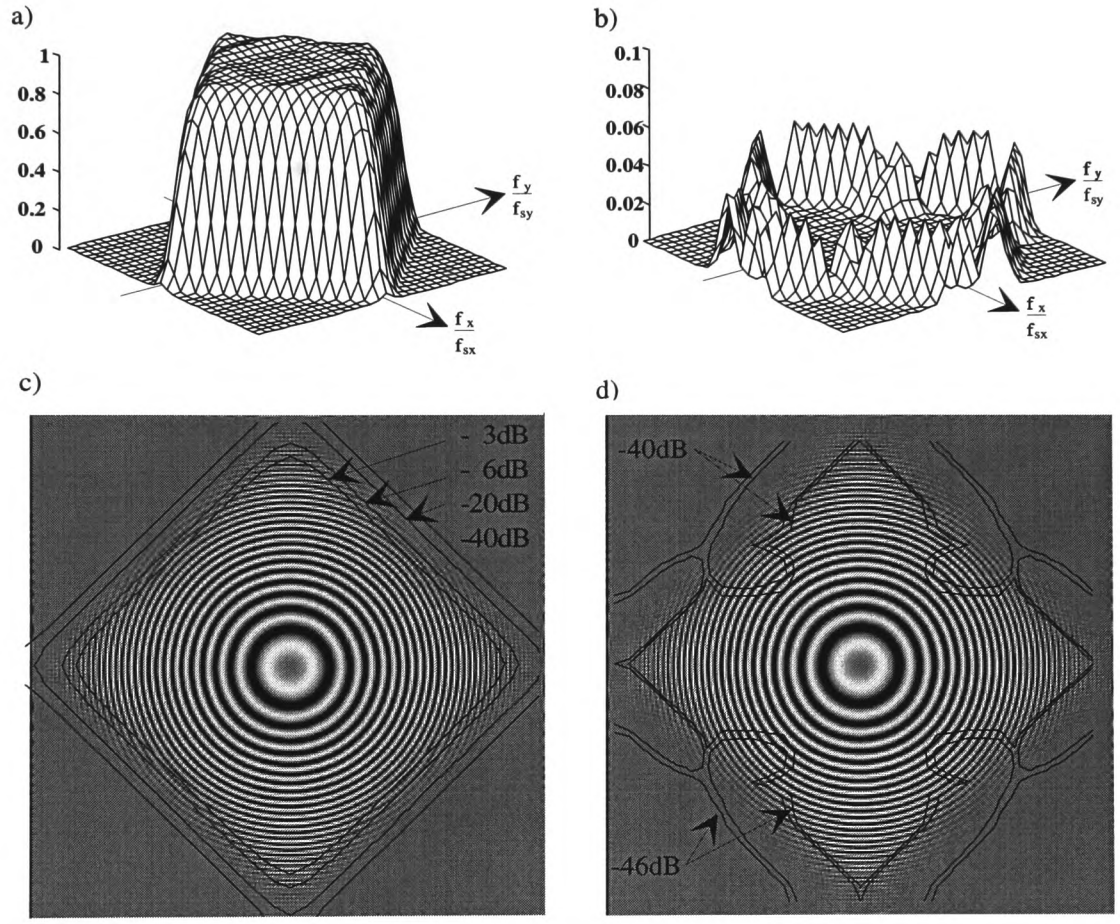

Figure 5.15: Example No. 6: a) overall transfer function $T(z_1, z_2)$ including the diagonal pre- and postfilter responses b) disturbance response $H_{Dis}(z_1, z_2)$ c) output image overlaid with the contour of a) d) output image overlaid with the contour of b)

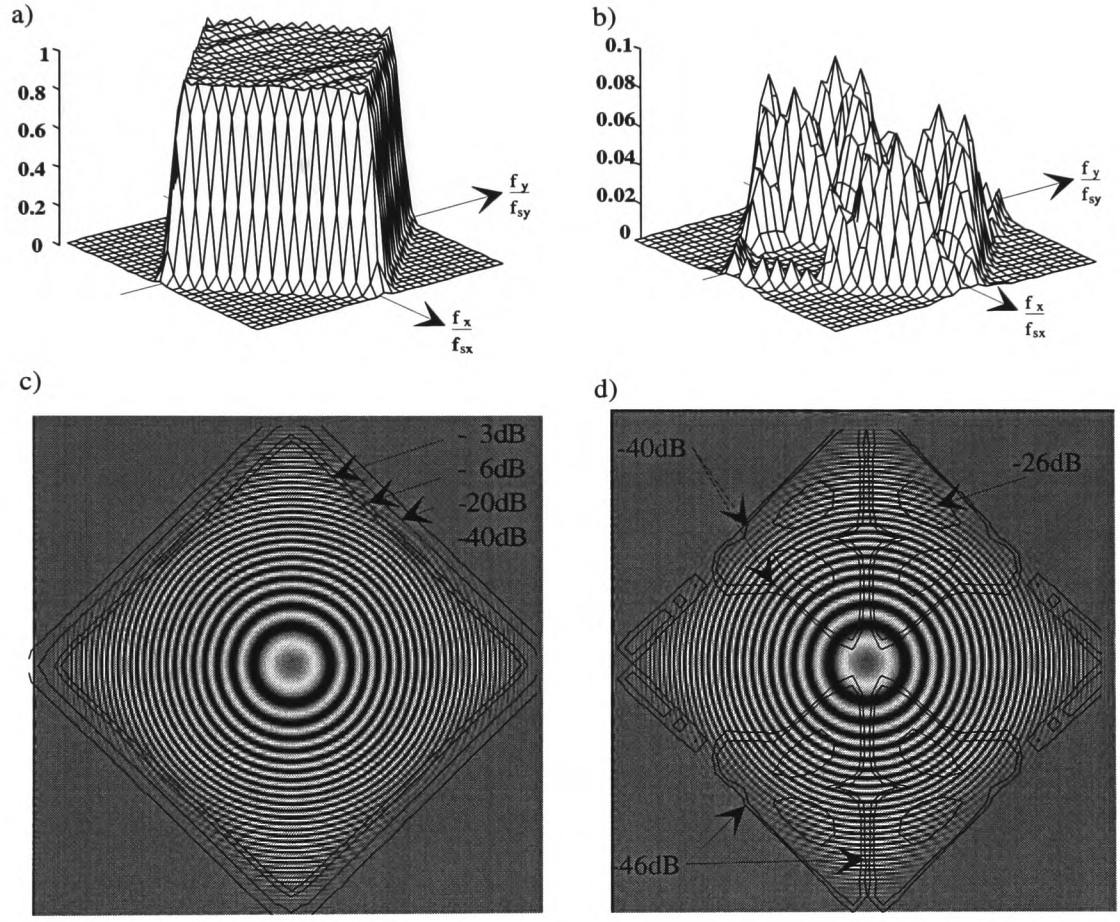

Figure 5.16: Example No. 7: a) overall transfer function $T(z_1, z_2)$ including the diagonal pre- and postfilter responses b) disturbance response $H_{Dis}(z_1, z_2)$ c) output image overlaid with the contour of a) d) output image overlaid with the contour of b)

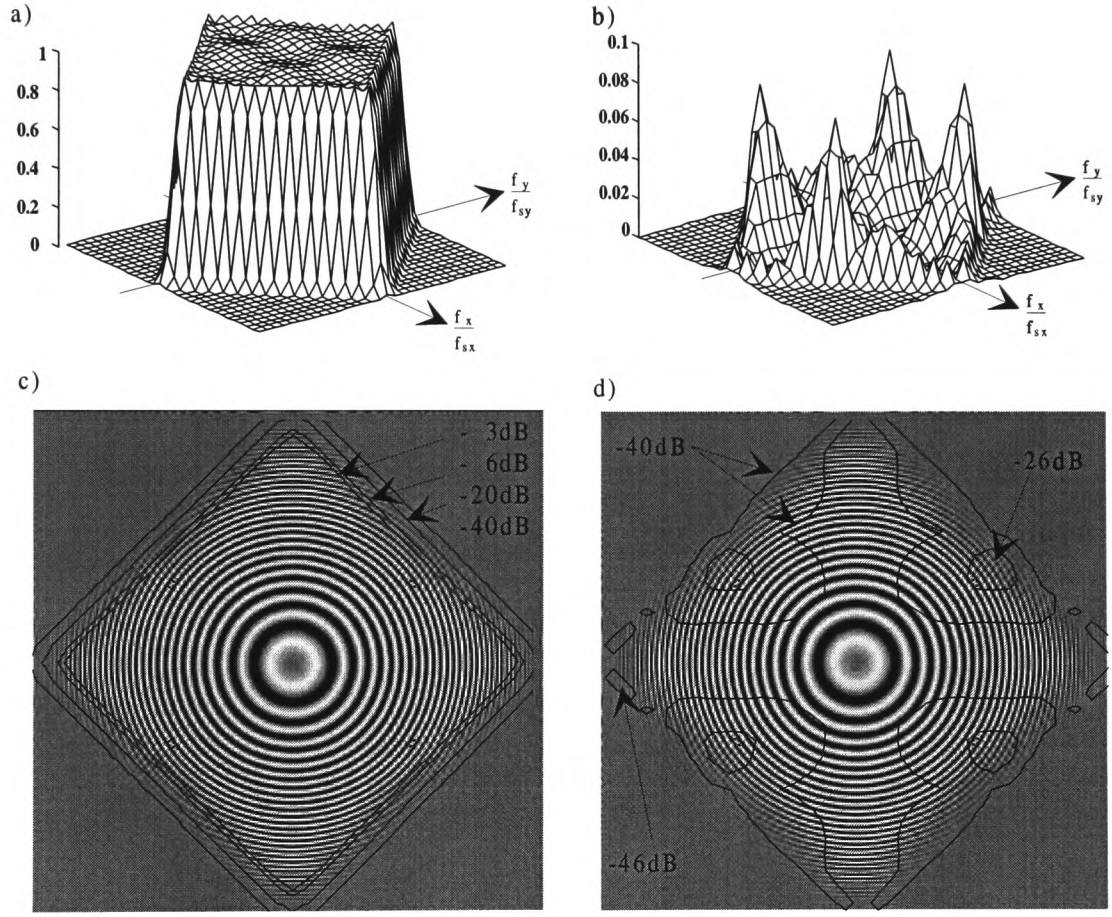

Figure 5.17: Example No. 8: a) overall transfer function $T(z_1, z_2)$ including the diagonal pre- and postfilter responses b) disturbance response $H_{Dis}(z_1, z_2)$ c) output image overlaid with the contour of a) d) output image overlaid with the contour of b)

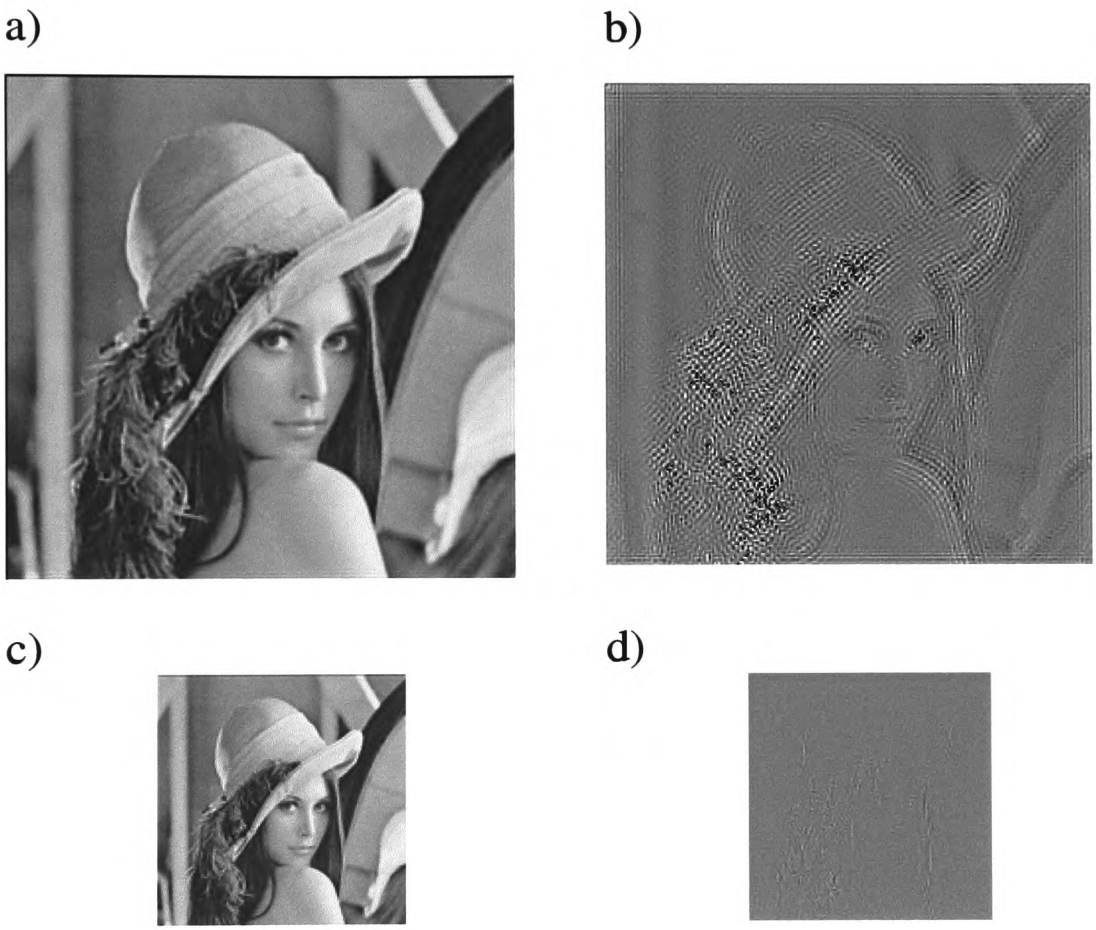

Figure 5.18: Example No. 4: a) output image of Lena b) input/output difference image magnified by 32 c) encoded low resolution component d) encoded residual component

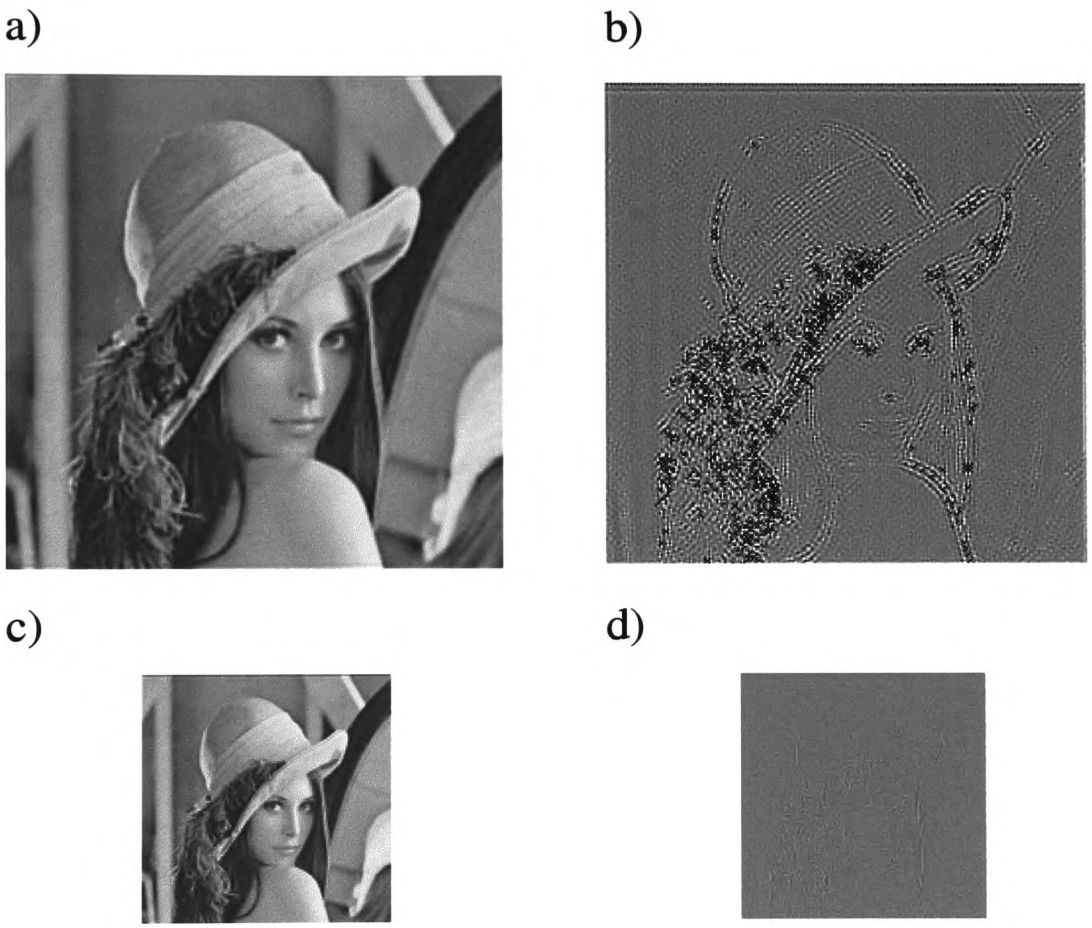

Figure 5.19: Example No. 2: a) output image of Lena b) input/output difference image magnified by 32 c) encoded low resolution component d) encoded residual component

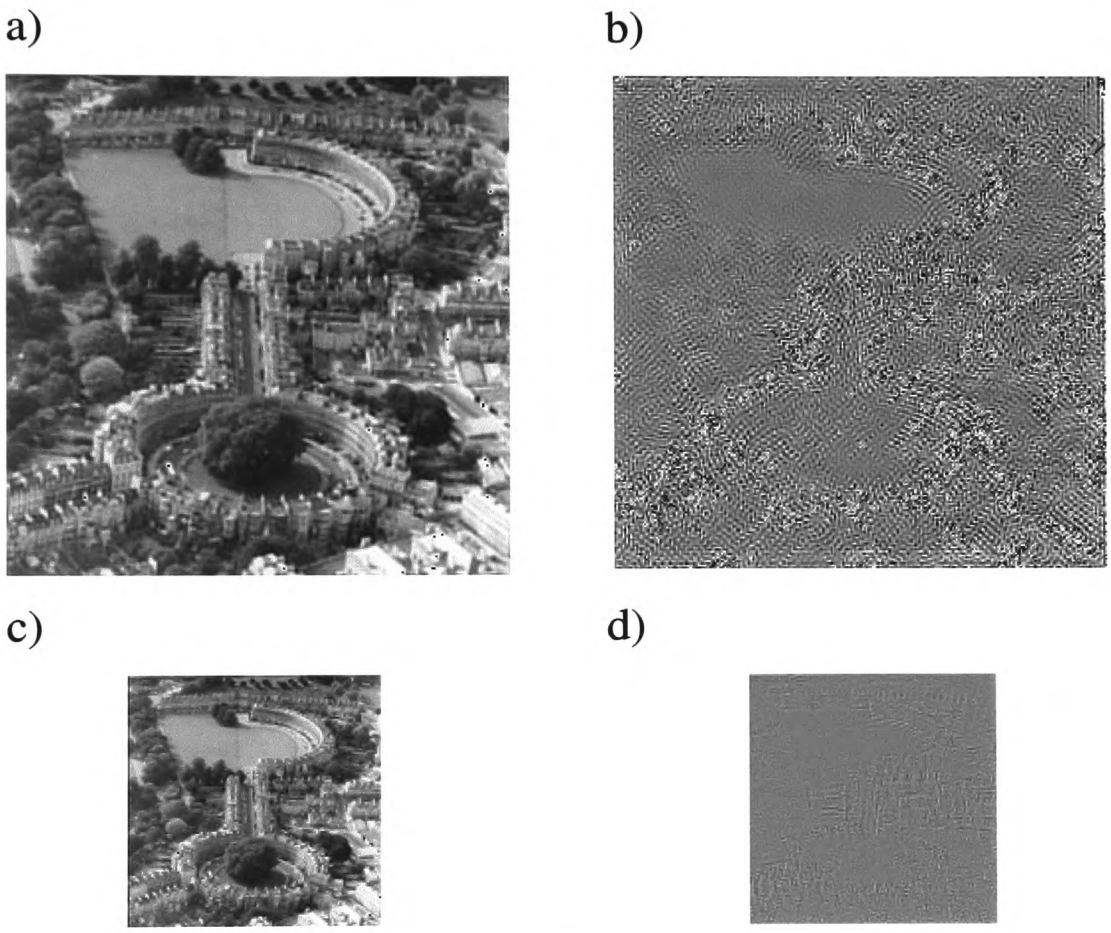

Figure 5.20: Example No. 4: a) output image of Bath b) input/output difference image magnified by 32 c) encoded low resolution component d) encoded residual component

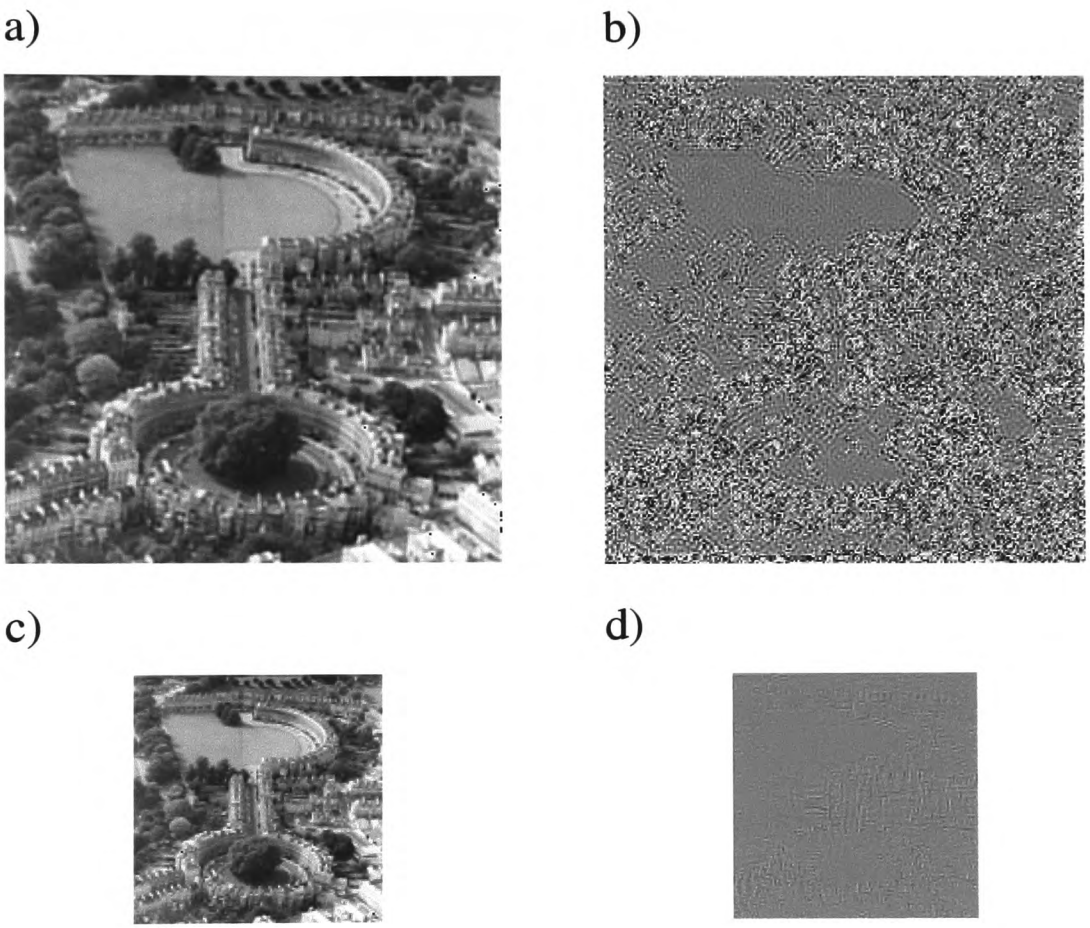

Figure 5.21: Example No. 2: a) output image of Bath b) input/output difference image magnified by 32 c) encoded low resolution component d) encoded residual component

Example No.	Lena RMSE	Lena SNR	Bath RMSE	Bath SNR
4	0.212	61.6 dB	1.524	44.5 dB
2	0.442	55.2 dB	2.889	38.9 dB

Table 5.2: RMSE of the encoded/decoded test images

within the proposed system as critical occurs to performance do not often occur within realistic images.

Section 4.1.4 identified the inherent problems when applying the Dual-Channel Subband strategy to interlaced rather than progressive scanned video signals. As outlined, major problems arise from the vertical subsampling process due to the resulting non uniform line structure. Figure 5.22 compares generally the different subsampling implementations for an interlaced scanned zone plate test image containing a horizontal and a vertical frequency sweep from DC to the Nyquist frequencies. Figure 5.22a and b give an insight to the situation which occurs for an inter field pre filtering with and without non uniform line structure compensation, respectively. It is obvious that frequencies greater than half the vertical Nyquist frequency are well suppressed however, in Figure 5.22a, aliasing distortions are clearly visible for those parts greater than a quarter of the Nyquist frequency due to the non equidistant vertical sampling lattice. The subsequent results obtained by applying an intra field prefilter are given in Figure 5.22c and d. As mentioned in Section 4.1.4, this filter strategy cannot reach values greater than half the Nyquist frequency, because these parts are images within a field. However, as visible in Figure 5.22 c, those frequencies introducing aliasing due to the non uniform line structure are suppressed. This solution provides an aliasing free output, but not the maximal possible resolution. This is improved by the implementation shown in Section 4.1.4 d, where the non uniform line structure is compensated for by applying an all pass rather than a low pass filter, but therefore aliasing distortions greater than half the Nyquist frequency occur.

Not surprisingly, the inter field filtering provides the best resolution for the subsampled component, but as is commonly known this also introduces motion blur. Therefore Section

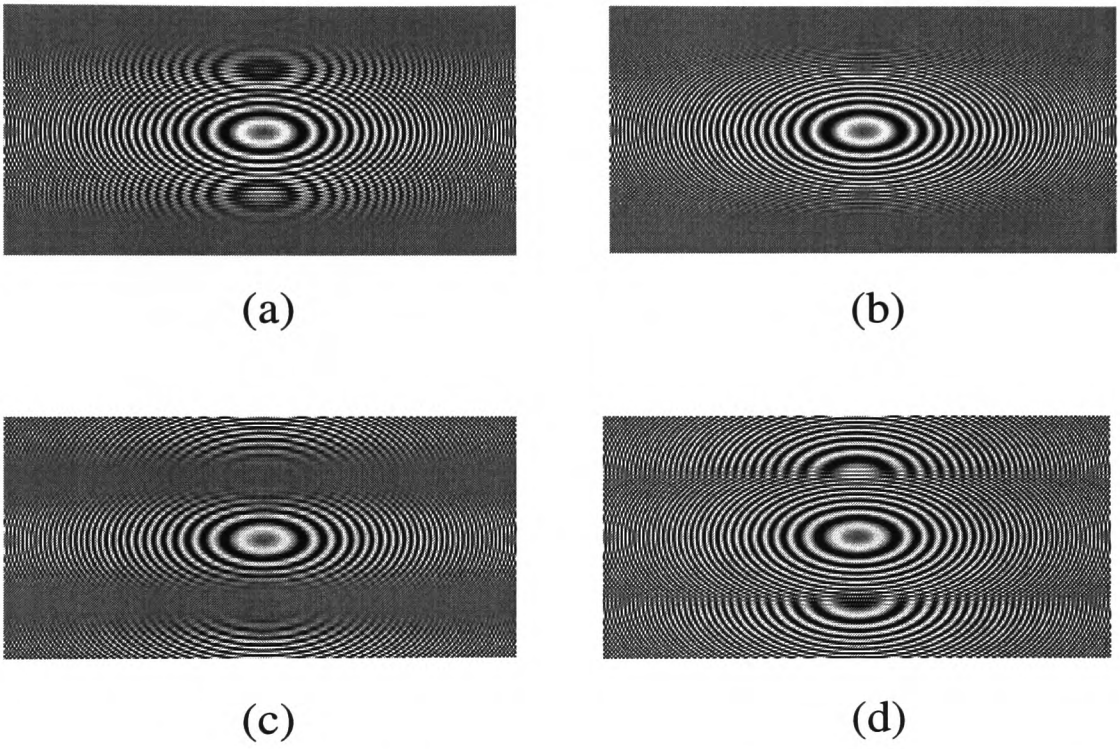

Figure 5.22: Different sub-sampling strategies of the interlaced zone plate input (a) inter field filtering (b) inter field filtering with line offset compensation (c) intra field filtering (d) intra field all-pass filtering with line offset compensation

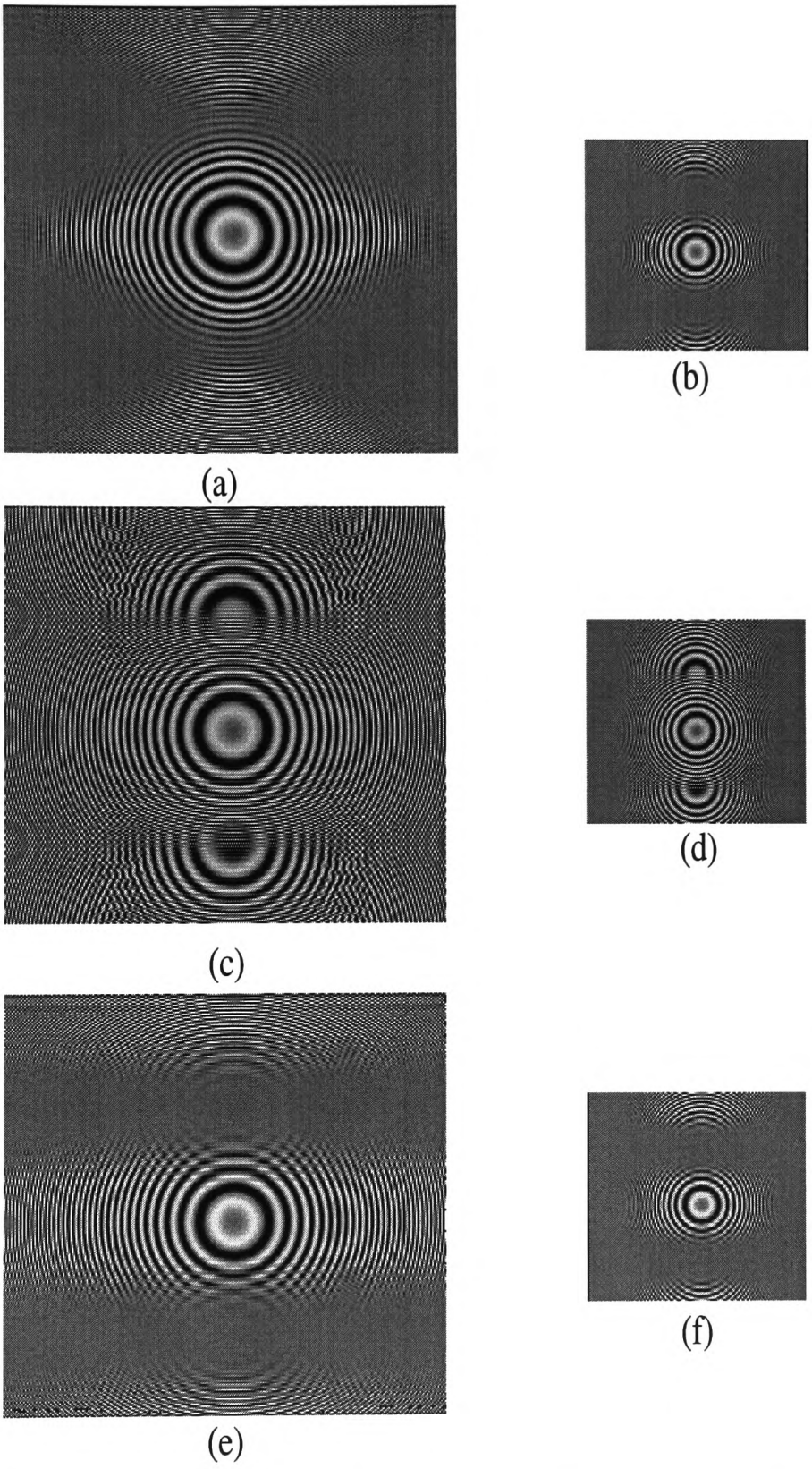

Figure 5.23: Reconstituted and standard image by applying the three different implementation scenarios for intra field processing

4.1.4 envisages a motion adaptive implementation of the dual channel subband approach by applying the similar principles as performed for the progressive scanned images in the case of no or little motion and an intra field modification for areas of motion. Three proposals are distinguished within Section 4.1.4 from which the corresponding reconstituted outputs and standard components for intra field processing are shown in Figure 5.23.

Figure 5.23a and b gives an insight to the strategy applying the same signal processing techniques for the intra field as for the inter field mode. This avoids motion blur, but an insufficient resolution especially for the low-pass compatible signal. In Figure 5.23c and d the results of the second proposal show that maximal vertical resolution in the down converted signal is possible by simply applying the aforementioned all-pass filter structure however, as analysed in Section 4.1.4 these parts cannot be correctly reconstructed at the decoder. Figure 5.23e and f display the third variant, which is a compromise between the two previous implementations. It is obvious that also with this strategy the resolution in both components is suboptimal.

In comparison, the first proposal provides the best result for the reconstituted signal. The lack of resolution in the compatible signal is acceptable, because it occurs only for motioned parts of an image. In the context of implementation complexity, the third strategy will provide a compromise, where for the second option the worse resolution of the reconstituted signals is not acceptable.

5.2 Simulation of embedded data transmission

The embedded data transmission technique discussed here modulates the active video part of a PAL signal. To be compatible with PALPLUS only 432 lines of the total 576 are available, which is the 16 : 9 centre signal, because the remaining 144 lines are reserved for the helper transmission. The given results, discussions and values are related to the 432 line centre signal. The helper parts are left untouched.

The overall data channel bandwidth is, as given in Section 4.2.2.2:

$$f_{Bdata} = 5MHz - 4.433MHz = 0.567MHz \tag{5.8}$$

for PAL -B, -G and -H. For PAL -I, which is used in the UK, the bandwidth is:

$$f_{Bdata-I} = 5.5MHz - 4.433MHz = 1.067MHz \tag{5.9}$$

It is not essential for further considerations to distinguish between the different PAL derivatives, because it effects only the overall data rate. To reflect the worst case the focus is set on PAL -B, -G, -H. For transformation the data rate must be approximately doubled.

From Equation (5.8) the maximum bit duration can be derived with respect to the roll-off factor ρ [131, Section 2.1.3]

$$T_{Bit} = \frac{1}{2f_{Bdata}}(1+\rho) \tag{5.10}$$

With an active line length of $52\mu s$, the maximum number of symbols per line and per additional data channel can be found. For simplification during decoding it is beneficial to synchronise the byte count within each transmission line, so the number of symbols per line is truncated to an integer number of bytes. The overall data rate provided can be derived as follows:-

$$r = trunc_{Byte}(\frac{52\mu s}{T_{Bit}})\frac{symbols}{line}432\frac{line}{frame}25\frac{frame}{s}ldN\frac{Bits}{Symbol}\frac{1}{L} \tag{5.11}$$

where N is the number of symbol levels per channel and L the interpolation factor. For simplification an initial data rate should be defined as follows:

$$r_{Initial} = trunc_{Byte}(\frac{52\mu s}{T_{Bit}})\frac{symbols}{line}432\frac{line}{frame}25\frac{frame}{s} \tag{5.12}$$

ρ	0.2	0.3	0.4	0.5	0.6	0.7	0.8	0.9	1.0
T_{Bit}	1.058	1.146	1.235	1.232	1.411	1.45	1.587	1.676	1.764
$\frac{symbols}{line}$	98	90	84	78	72	68	64	62	58
$trunc_{Byte}$ $(\frac{symbols}{line})$	96	88	80	72	72	64	64	56	56
$\frac{r_{Initial}}{KBits/s}$	1036.8	950.4	864	777.6	777.6	691.2	691.2	604.8	604.8
$\frac{1}{\%}$	97.96	97.78	95.24	92.23	100	94.12	100	90.32	96.55

Table 5.3: Comparision of parameters for a given roll off factor, ρ

so that the data rate is given as:-

$$r = r_{Initial} ldN \frac{Bits}{Symbol} \frac{1}{L} \tag{5.13}$$

Table 5.3 compares the situations derived from different values of the roll-off factor, ρ. Due to the byte truncation the data rate efficiency is not uniform within all values of ρ, so $\rho = 0.8$, $\rho = 0.6$ and $\rho = 0.4$ provide a minimum truncation leakage. Figure 5.24 gives an insight of the overall achievable data rate, given from Equation (5.13) for these three roll-off filter types.

The roll-off filter design is straightforward. From the formula taken from [131, Section 2.1.3], the coefficients for an FIR filter design, following the raised cosine approach, can be derived as:-

$$h_F(n) = \frac{1}{T_{Bit}} \frac{sin(\pi \frac{n}{T_{Bit} f_s})}{\pi \frac{n}{T_{Bit} f_s}} \frac{cos(\pi \rho \frac{n}{T_{Bit} f_s})}{1 - (2\rho \frac{n}{T_{Bit} f_s})^2} \tag{5.14}$$

Figure 5.25 compares the filter responses for different values of ρ and also two different filter orders. The implementation of these form filters is usually separated into a pre- and post filter, the so called root raised cosine filter, at the encoder and decoder, respectively. The effect is a superior noise robustness of the data during transmission, however for this simulation the splitting is not actually implemented, because this addresses specific form filtering design techniques in general and such an optimisation was not critical to the overall implementation.

Considering the vertical form filter, there is not much flexibility in designing this filter,

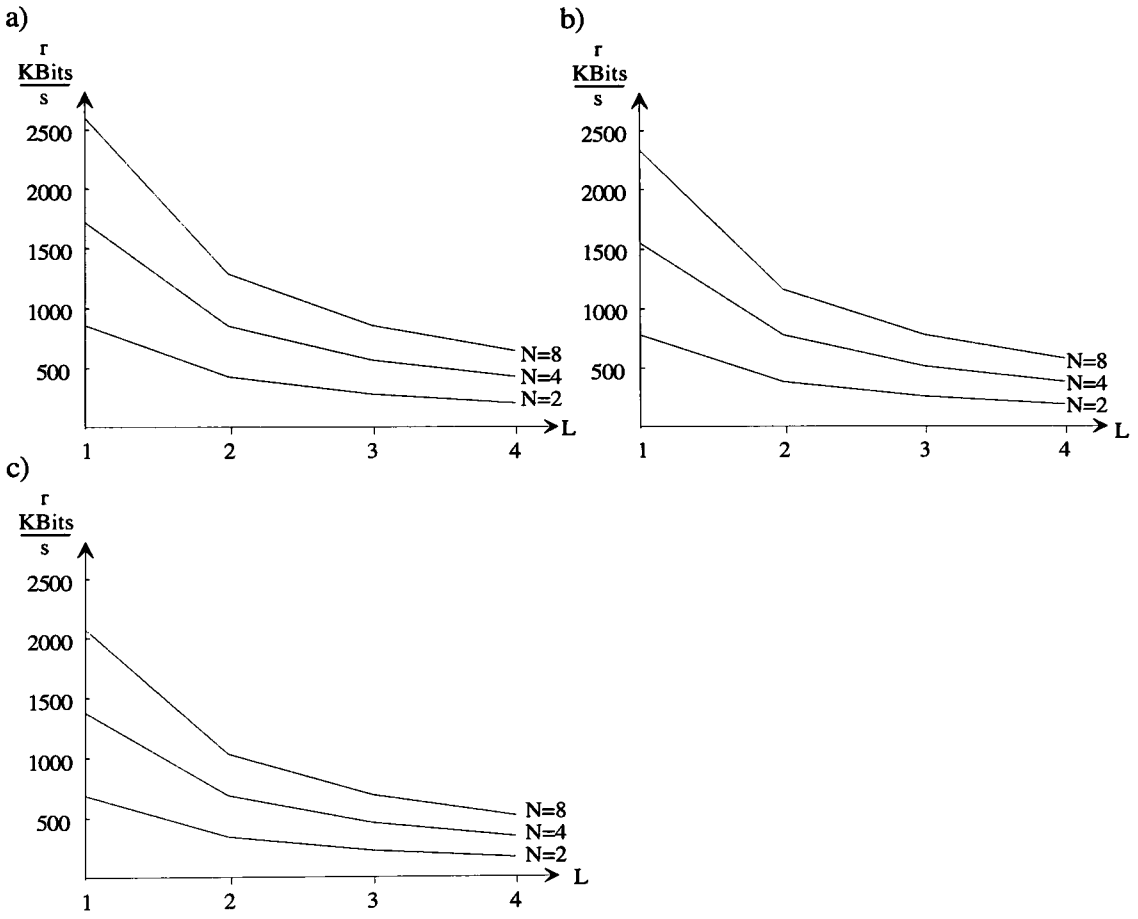

Figure 5.24: Achievable data rates versus interpolation factor for a) $\rho = 0.4$, b) $\rho = 0.6$, c) $\rho = 0.8$

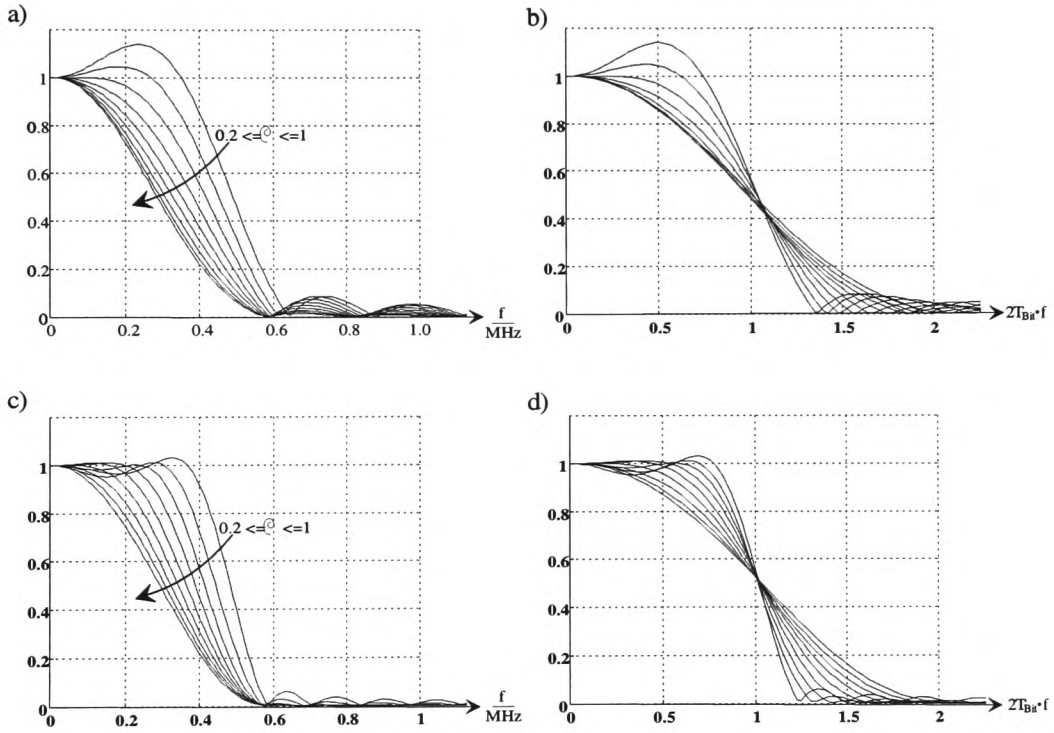

Figure 5.25: Conventional and normalised roll-off filter responses for different values of ρ for filter orders a) and b) 24 c) and d) 48, respectively

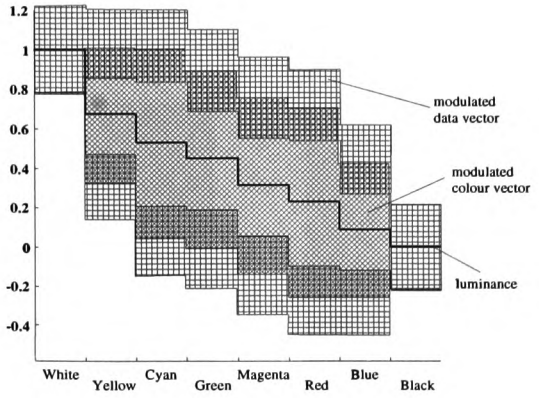

Figure 5.26: Additional data modulated EBU-FBAS colour bar with $\alpha = 0.15$

as neither for the partial response coding, where the vertical filter is fixed due to the chosen order, nor for the interpolation technique. As given in Appendix B the efficiency, that is data rate and subjective quality are nearly equivalent within the design method. Major differences are only visible by the variation of the interpolation factor L. Other important parameters and which have an impact on the overall efficiency are the amplitude of the data signal α and the number of symbol levels, N. Both have an influence upon compatibility and also upon the data channel properties itself. The data amplitude α should be within the limits of 0.075 and 0.15 in relation to the normalised video range. A value of 0.15 causes an overshoot of 20% of the resulting video signal (Figure 5.26), which is a slightly less than for saturated yellow and therefore acceptable. Further α should not be below 0.075, because of an increasing data error rate in noisy transmission channels.

Figure 5.27 shows a screen shot of a normal and EBU (European Broadcasting Union) colour bar together with their corresponding oscillograms. These signals are further used as test inputs, because they provide a good possibility to evaluate the compatibility aspects of the proposed system. Figure 5.28 gives an insight to the additional modulated colour bars from Figure 5.27 using $\alpha = 0.15$, so the EBU version shows the real view of Figure 5.26.

Three different vertical form filter design methods will be further analysed as an example, namely partial response coding, the interpolation approach and the combination of both, as explained in Section 4.2.2.3. For the partial response coding, the three and five level version from Appendix B.1, namely $P1$ and $P2$ are used. For the interpolation approach two filters,

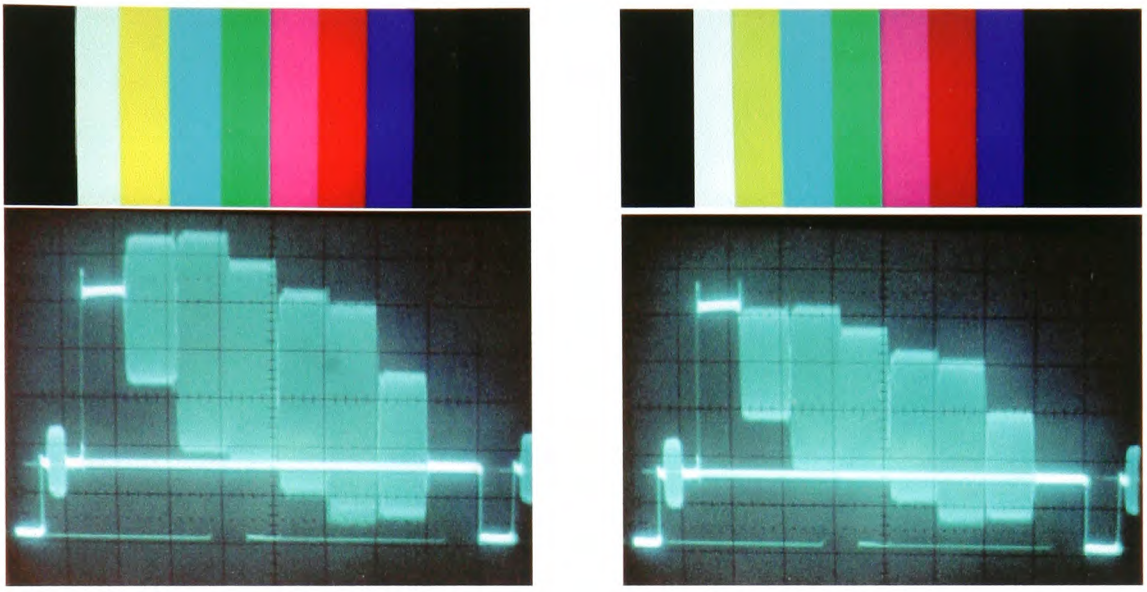

Figure 5.27: Normal and EBU colour bar and their oscillograms

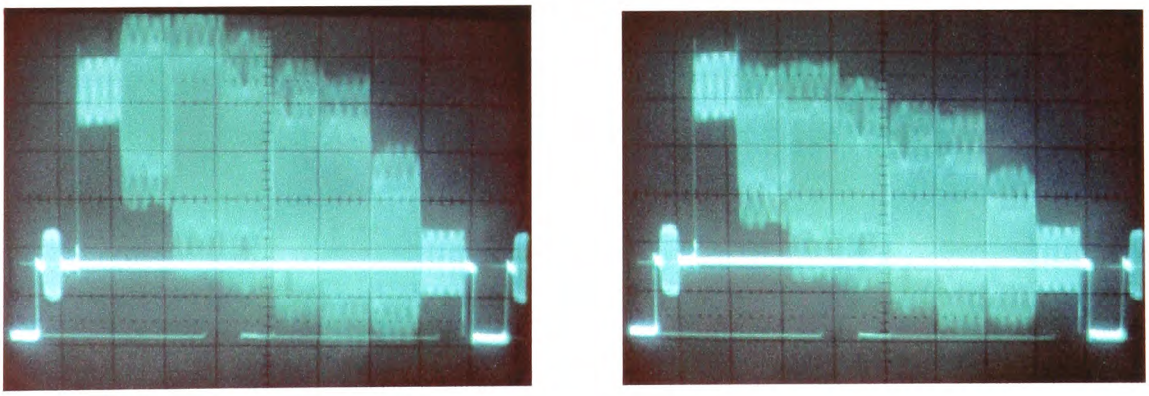

Figure 5.28: Normal and EBU colour bar with modulated data

Ex.	N	L	$\frac{r}{KBits/s}$	$\frac{P_N}{10^{-4}}$ α=0.15	$\frac{SNR\|_U}{dB}$ α=0.15	$\frac{SNR\|_V}{dB}$ α=0.15	$\frac{P_N}{10^{-4}}$ α=0.075	$\frac{SNR\|_U}{dB}$ α=0.075	$\frac{SNR\|_V}{dB}$ α=0.075
P1	2	1	777.6	3.574	30.21	33.17	0.934	33.17	39.19
P2	2	1	777.6	1.768	33.22	36.17	0.447	39.24	42.20
I1	2	2	388.8	3.015	30.94	33.91	0.753	36.97	39.52
I1	4	2	777.6	1.675	33.50	36.46	0.419	39.93	42.48
I4	2	3	259.2	0.392	37.26	42.77	0.176	45.83	46.24
I4	4	3	518.4	0.705	39.82	40.22	0.098	43.28	48.79
P1/I1	2	2	388.8	0.628	37.76	40.72	0.157	43.78	46.73
P1/I4	2	3	259,2	0.160	43.69	46.65	0.040	49.71	52.67

Table 5.4: Comparison of different crosstalk noise using a horizontal form filter with $\rho = 0.6$

$I1$ and $I4$, relating to an interpolation factor of $L = 2$ and $L = 3$ are designed, using Kaiser window with an amplification of L, to keep the data signal power independent from the interpolation factor. Finally the combination of $P1/I1$ and $P1/I4$ is analysed. The corresponding filter responses $H_D(f_y)$ and $C_A(f_y)$ are given in Figure 5.29.

From Equation (4.15) the power of the intercarrier crosstalk within each colour channel can be derived, where an objective quality is given using the DSNR from Equation (4.28). Table 5.4 summarises these results for the mentioned vertical filters using an 24 order horizontal form filter with an roll-off factor of $\rho = 0.6$. Is obvious that with an increasing cross talk attenuation the achieving data rate decreases. Giving the priority to the subjective picture quality, the values from example $I4$, $P1/I1$ and $P1/I4$ produce the lowest crossover noise power, where the 16 QAM version of $I4$ provides the best compromise for crossover noise and bit rate efficiency.

Table 5.5 shows the DSNR of an EBU colour bar for the examples given in Table 5.4. It gives a very good impression of what distortions are actually visible within the possible signal parts of a video signal. The degradations tend to be more visible in dark uniform areas than in bright regions. The DSNR varies within a range of approximately $20dB$ depending on the form filtering. For values of better than $35dB$ nearly no distortions are visible.

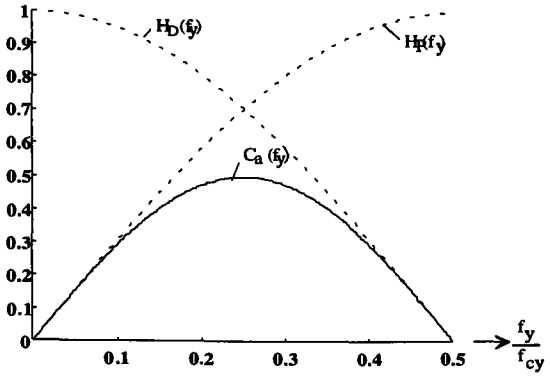

Vertical filter responses from Ex. P1

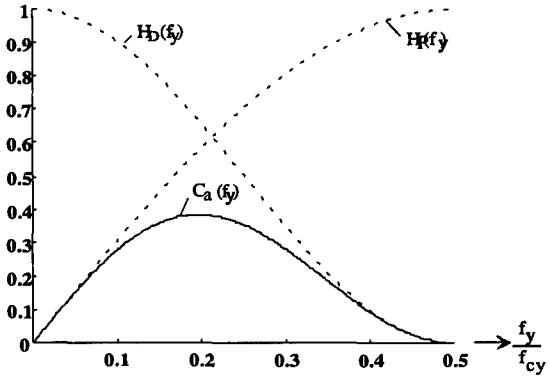

Vertical filter responses from Ex. P2

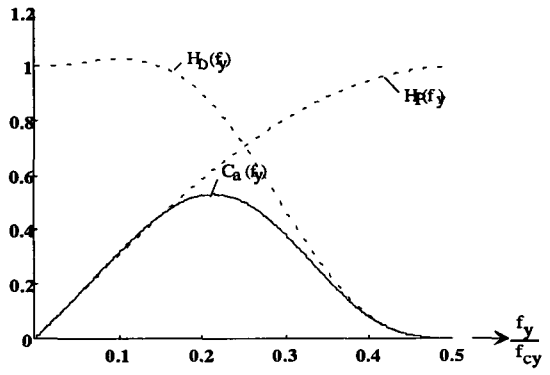

Vertical filter responses from Ex. I1

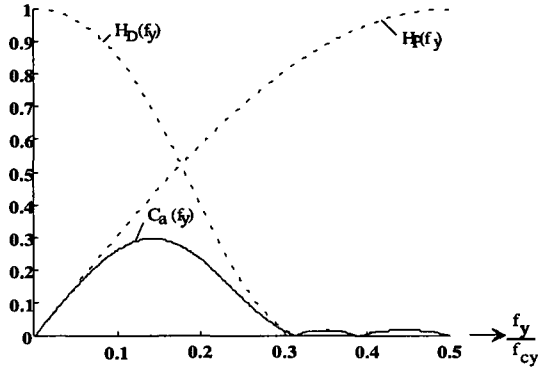

Vertical filter responses from Ex. I4

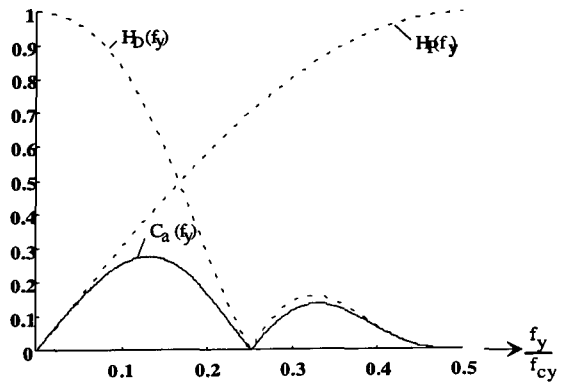

Vertical filter responses from Ex. P1/I1

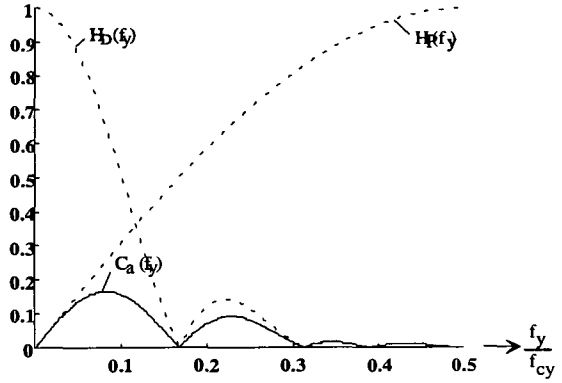

Vertical filter responses from Ex. P1/I4

Figure 5.29: Vertical filter responses used within the simulation examples

Example	White $\frac{DSNR}{dB}$	Yellow $\frac{DSNR}{dB}$	Cyan $\frac{DSNR}{dB}$	Green $\frac{DSNR}{dB}$	Magenta $\frac{DSNR}{dB}$	Red $\frac{DSNR}{dB}$	Blue $\frac{DSNR}{dB}$
P1 α=0.15 N=2	30.75	29.08	27.72	26.86	26.51	25.34	20.33
P1 α=0.0.75 N=2	36.58	34.90	33.55	32.69	32.34	31.17	26.16
P2 α=0.15 N=2	33.81	32.13	30.77	29.92	29.57	28.40	23.39
P2 α=0.0.75 N=2	39.78	38.10	36.75	35.89	35.54	34.37	29.36
I1 α=0.15 N=2	31.49	29.82	28.46	27.60	27.25	26.08	21.07
I1 α=0.0.75 N=2	37.52	35.84	34.48	33.63	33.28	32.10	27.09
I1 α=0.15 N=4	34.05	32.37	31.01	30.16	29.80	28.63	23.62
I1 α=0.0.75 N=4	40.06	38.39	37.03	36.17	35.82	34.65	29.64
I4 α=0.15 N=2	37.80	36.13	34.77	33.91	33.56	32.39	27.38
I4 α=0.0.75 N=2	43.83	42.15	40.79	39.94	39.59	38.42	33.41
I4 α=0.15 N=4	40.35	38.68	37.32	36.46	36.11	34.94	29.93
I4 α=0.0.75 N=4	46.37	44.70	43.34	42.48	42.13	40.96	35.95
P1/I1 α=0.15 N=2	38.31	36.63	35.27	34.42	34.06	32.89	27.88
P1/I1 α=0.0.75 N=2	44.33	42.65	41.29	40.44	40.08	38.91	33.90
P1/I4 α=0.15 N=2	44.24	42.57	41.21	40.35	40.00	38.83	33.82
P1/I4 α=0.0.75 N=2	50.26	48.59	47.23	46.37	46.02	44.85	39.84

Table 5.5: DSNR of an EBU Colour bar for the various examples

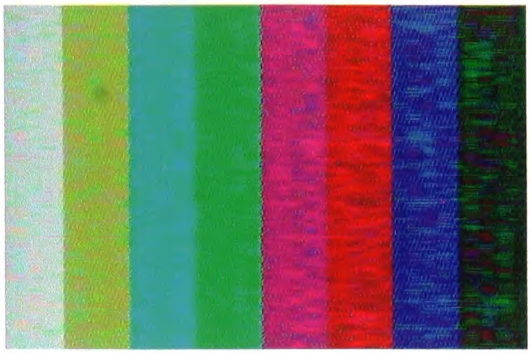

Figure 5.30: Screen shot using no vertical prefilter ($\alpha = 0.15$)

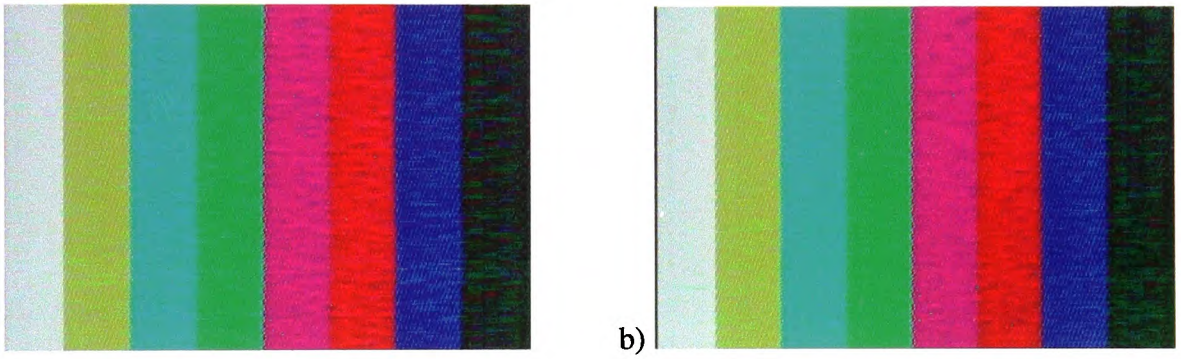

Figure 5.31: Screen shots for example a) P1 and b) P2 ($\alpha = 0.15$)

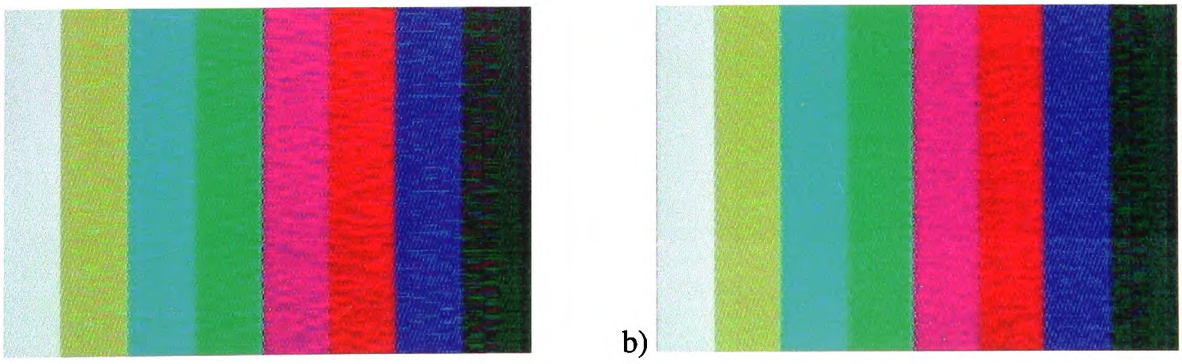

Figure 5.32: Screen shots for example a) I1 ($\alpha = 0.15/N = 2/L = 2$) and b) I1 ($\alpha = 0.075/N = 2/L = 2$)

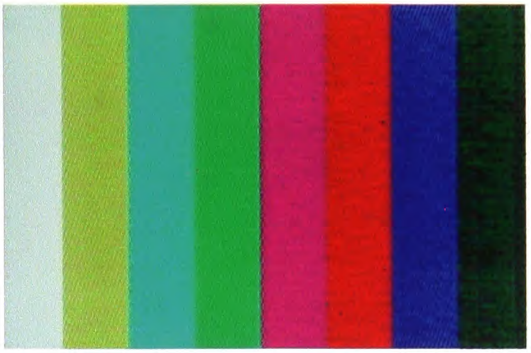

Figure 5.33: Screen shot for example I4 ($\alpha = 0.075/N = 2/L = 3$)

a) 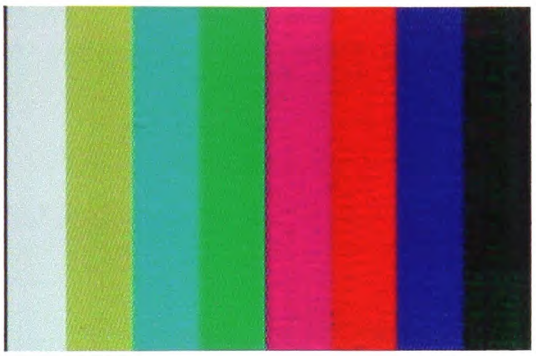

b) 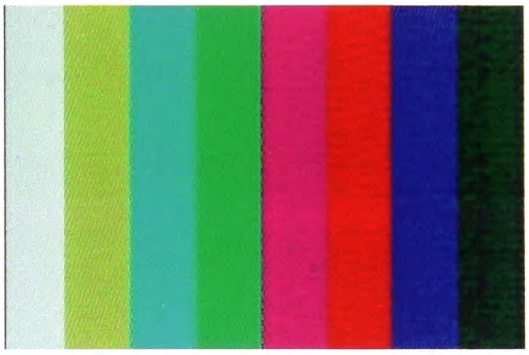

Figure 5.34: Screen shots for example a) I1 ($\alpha = 0.075/N = 4/L = 2$) and b) I4 ($\alpha = 0.075/N = 4/L = 3$)

a) 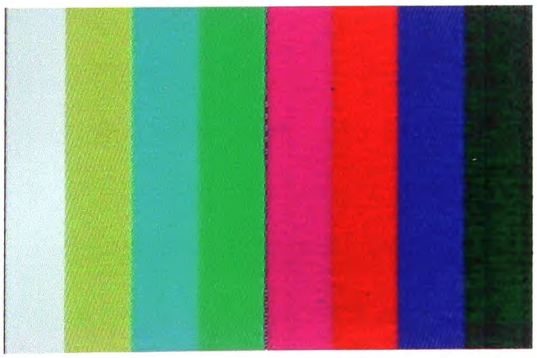

b) 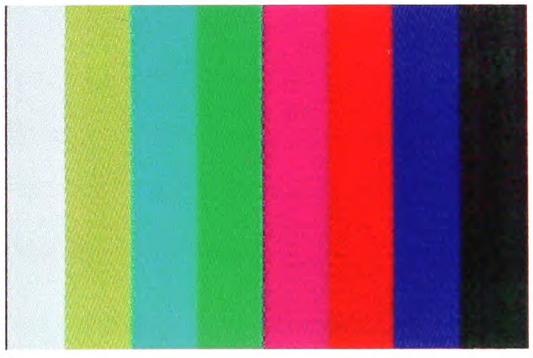

Figure 5.35: Screen shots for example a) P1/I1 ($\alpha = 0.075/L = 2$) and b) P1/I4 ($\alpha = 0.075/L = 3$)

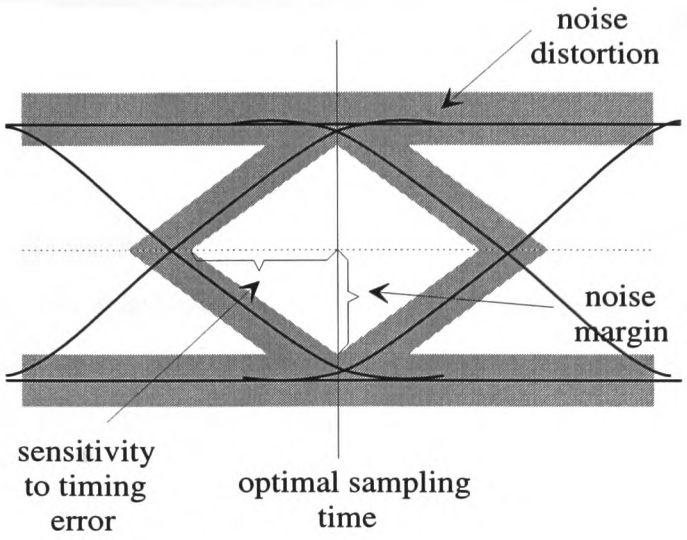

Figure 5.36: Graphical illustration of an eye pattern [140]

Figure 5.30 to Figure 5.35 provides an impression of the subjective quality enabled with the previously presented vertical form filter scenarios. Figure 5.30 shows the worst case, where no vertical filtering is employed. Figure 5.31 compares the two partial response coding implementations. It is visible that the five level approach provides a better cross talk attenuation than duo binary coding. However, this is also insufficient. Figure 5.32 shows the performance of the interpolation method for $L = 2/N = 2$ and displays the difference between a data signal amplitude of $\alpha = 0.15$ and $\alpha = 0.075$. The subjective quality is close to the five level partial response coding example. The cross talk attenuation increases with an interpolation factor of $L = 3$ as shown in Figure 5.33. Figure 5.34 compares the situation for a 16 QAM implementation ($N = 4$), where as expected for the theoretical evaluation, the quality is slightly better than for the 4 QAM counterparts. The examples presented in Figure 5.35 demonstrate the best results. Only minor cross talk distortions are visible, however under normal viewing conditions no subjective degradation can be seen.

The previous discussions relate only to the aspects of compatibility, on which the priority is set, so the parameters are chosen explicitly under this premise. Also of interest are the properties of the data channels, which are namely the achievable data rate and the BER (Bit Error Rate). The data rate issue have already discussed, the BER is directly dependent upon the data signal amplitude α, and the number of signal levels, N.

A common method for the quality evaluation of data transmission channels is to quantify the openness of the eye pattern measured at the receiver. Figure 5.36 graphically illustrates such an eye pattern and gives an insight to the actual information that can be derived from it. The openness defines a margin, so that each symbol level can be clearly identified. This margin is compromised by inter symbol interference or noise distortions during transmission, either in the horizontal or vertical directions, respectively. A decreasing horizontal openness requires an increasing timing accuracy of the resampling at the receiver, where vertically a definite symbol level assignment becomes impossible.

For QAM it is customary to display the eye pattern as two dimensional scatter diagrams [140]. The larger the intersymbol interference and noise the larger the scattering of the received symbol samples.

Figure 5.37 and Figure 5.38 shows the measured eye pattern and scatter diagram for 3 and 5 level partial response coding per data channel, respectively. The asymmetric nature of the shape of the symbol positions is due to rounding during signal processing however, in this example perfect data reconstitution is possible. This ideal situation is lost after additive white gaussian noise occurs during transmission. It is clear that due to noise degradation the symbol positions within the signal space become more and more undefined and the eye openness is corresponding smaller, so the prone to bit errors increases. Figure 5.39 shows the situation for duobinary coding with a signal to noise ratio of $30dB$.

Figure 5.40 to 5.42 gives an insight into the scenario using interpolation technique with 4 QAM and $\alpha = 0.15$. It is clearly visible that no problems are identified within normal transmission conditions. The situation becomes different using $\alpha = 0.075$ (Figure 5.43 to 5.46) however, where with a signal to noise ratio of $30dB$ stably distinguishing between the symbol levels is possible. Figure 5.47 to 5.50 compare the scenario for 16 QAM and $\alpha = 0.15$. It is shown that the relations become more critical with lower SNR of the transmission channel due to more symbol levels. A threshold of a definite symbol reconstitution is given using $\alpha = 0.075$ (Figure 5.53 and Figure 5.54) between 35 and $30dB$ SNR.

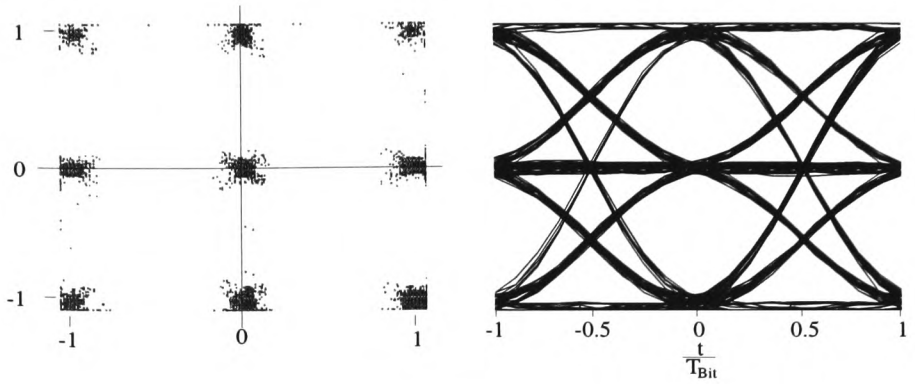

Figure 5.37: Scatter diagram and eye pattern implementing duo binary coding for vertical spectral forming

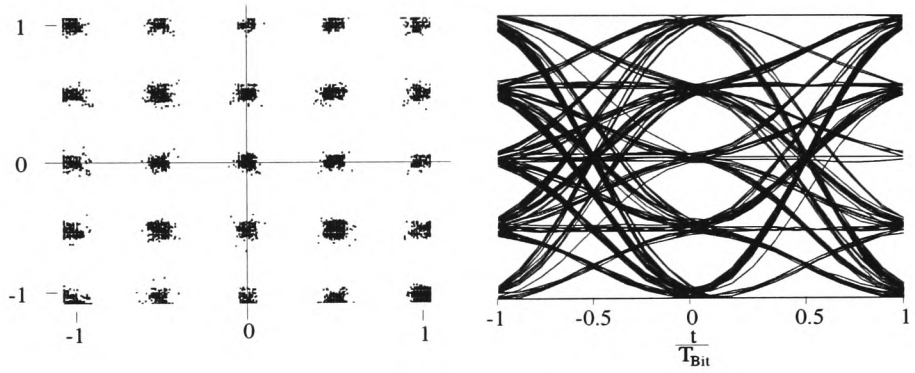

Figure 5.38: Scatter diagram and eye pattern implementing 5-level partial response coding for vertical spectral forming

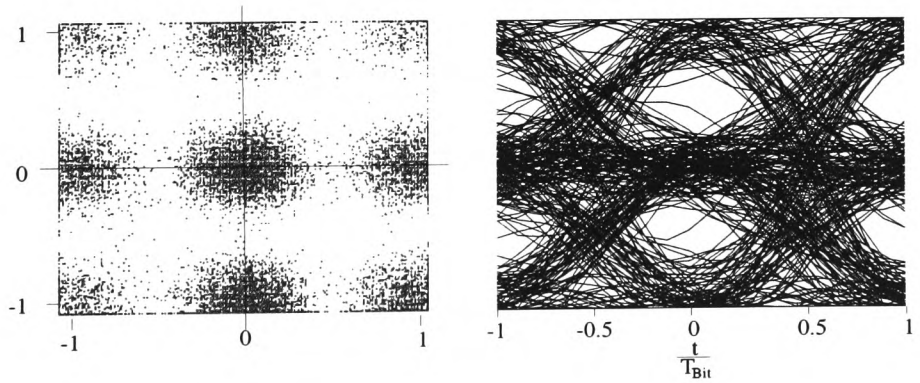

Figure 5.39: Scatter diagram and eye pattern for the duobinary case introducing $30dB$ noise during transmission

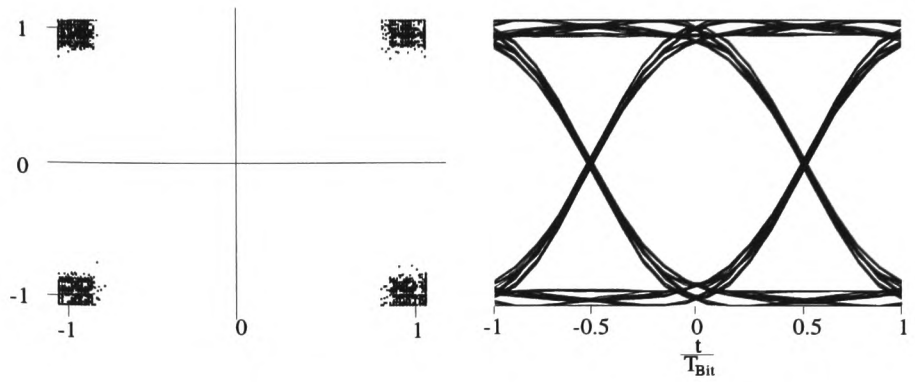

Figure 5.40: Scatter diagram and eye pattern implementing interpolation technique with 4 QAM and $\alpha = 0.15$

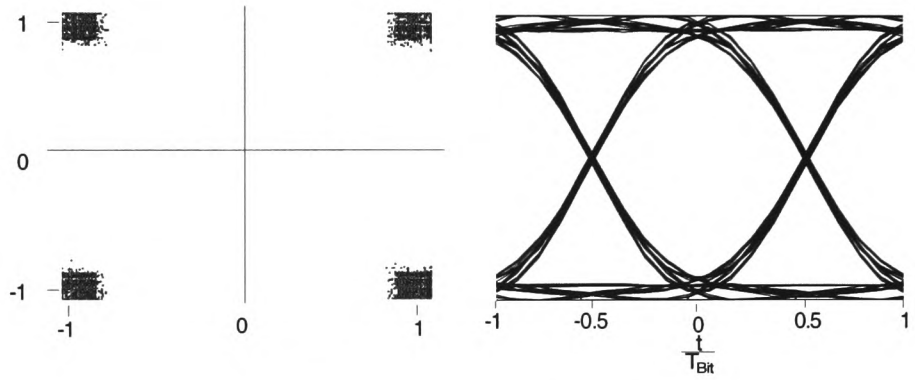

Figure 5.41: Scatter diagram and eye pattern of Figure 5.40 introducing $40dB$ noise during transmission

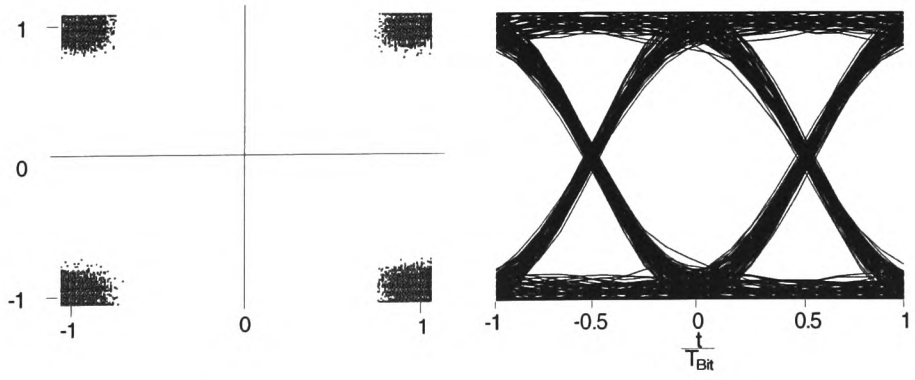

Figure 5.42: Scatter diagram and eye pattern of Figure 5.40 introducing $35dB$ noise during transmission

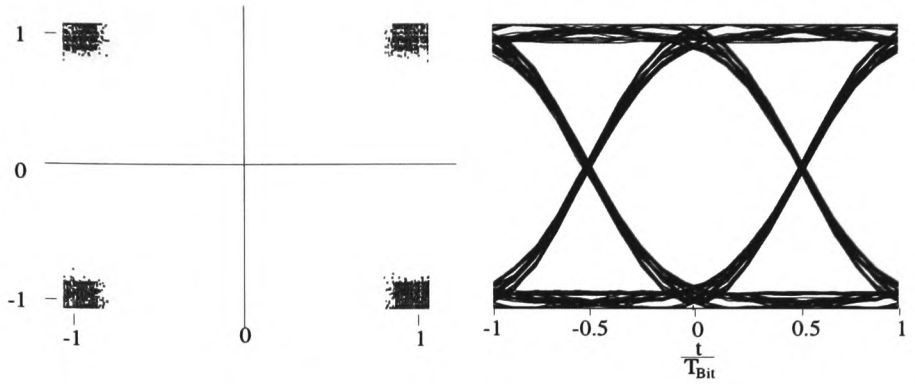

Figure 5.43: Scatter diagram and eye pattern implementing interpolation technique with 4 QAM and $\alpha = 0.075$

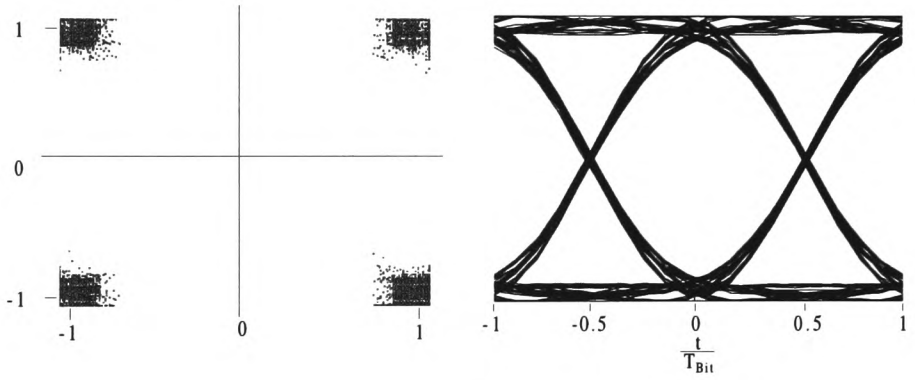

Figure 5.44: Scatter diagram and eye pattern of Figure 5.43 introducing $40dB$ noise during transmission

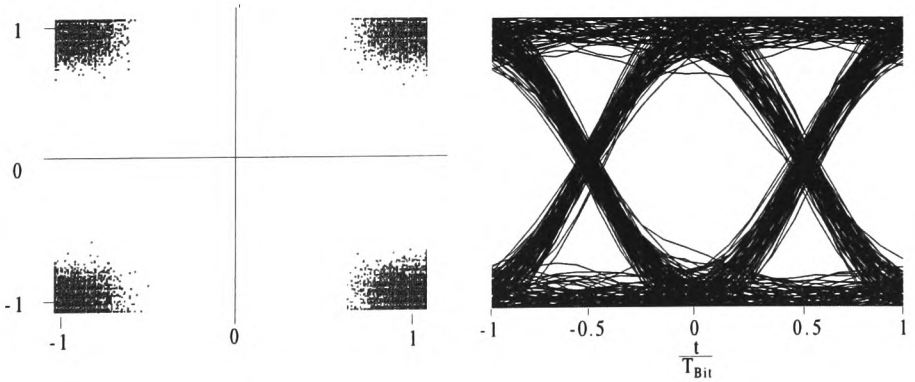

Figure 5.45: Scatter diagram and eye pattern of Figure 5.43 introducing $35dB$ noise during transmission

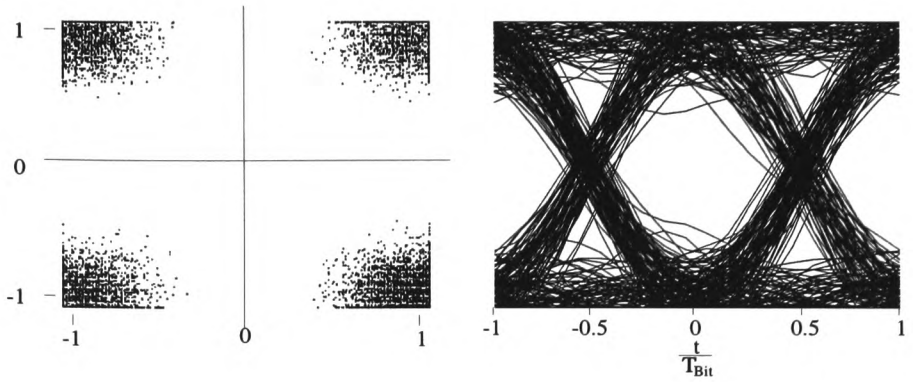

Figure 5.46: Scatter diagram and eye pattern of Figure 5.43 introducing $30dB$ noise during transmission

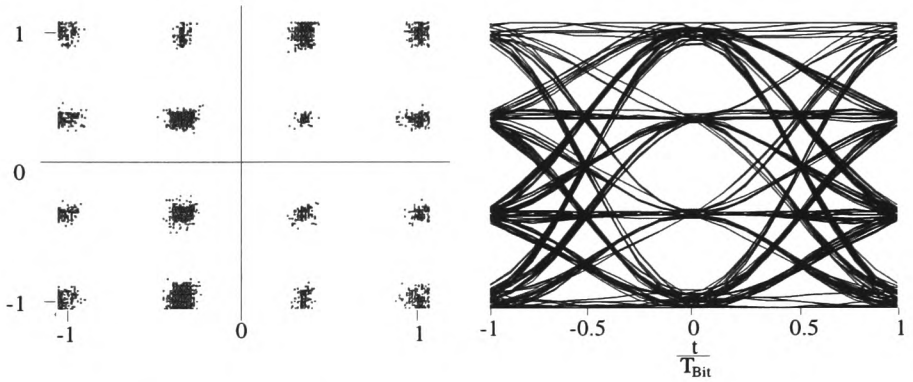

Figure 5.47: Scatter diagram and eye pattern implementing interpolation technique with 16 QAM and $\alpha = 0.15$

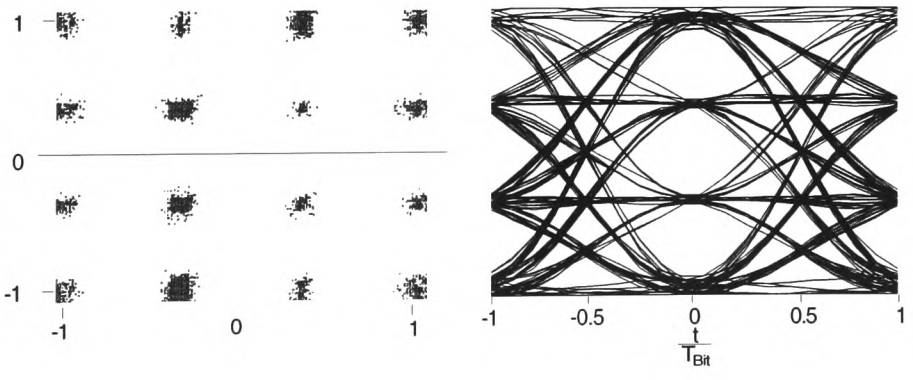

Figure 5.48: Scatter diagram and eye pattern of Figure 5.47 introducing $40dB$ noise during transmission

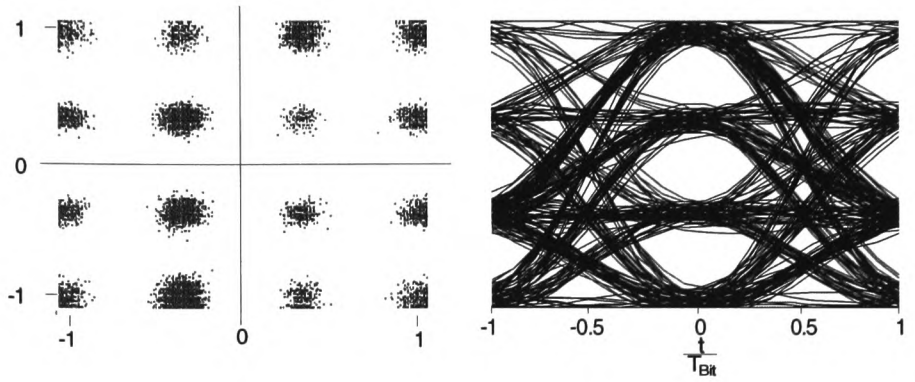

Figure 5.49: Scatter diagram and eye pattern of Figure 5.47 introducing $35dB$ noise during transmission

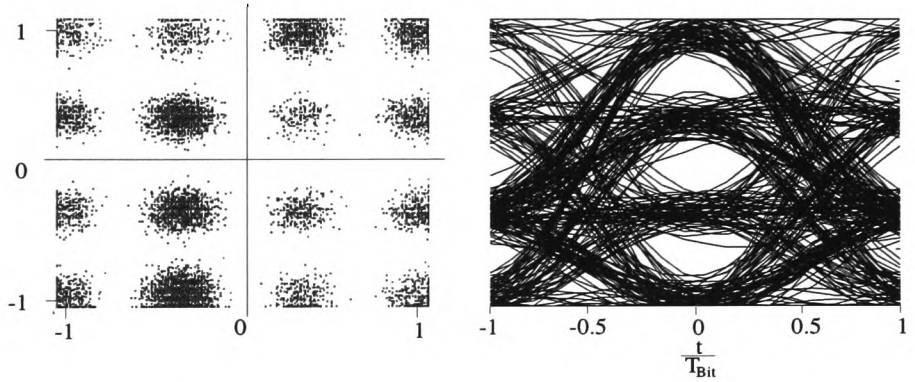

Figure 5.50: Scatter diagram and eye pattern of Figure 5.47 introducing $30dB$ noise during transmission

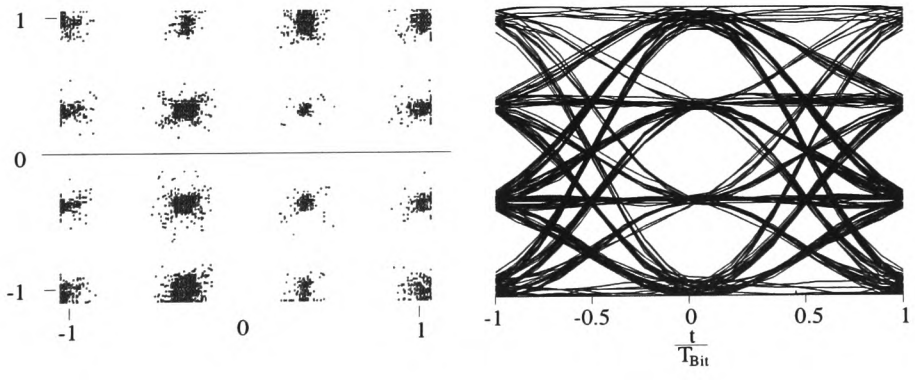

Figure 5.51: Scatter diagram and eye pattern implementing interpolation technique with 16 QAM and $\alpha = 0.075$

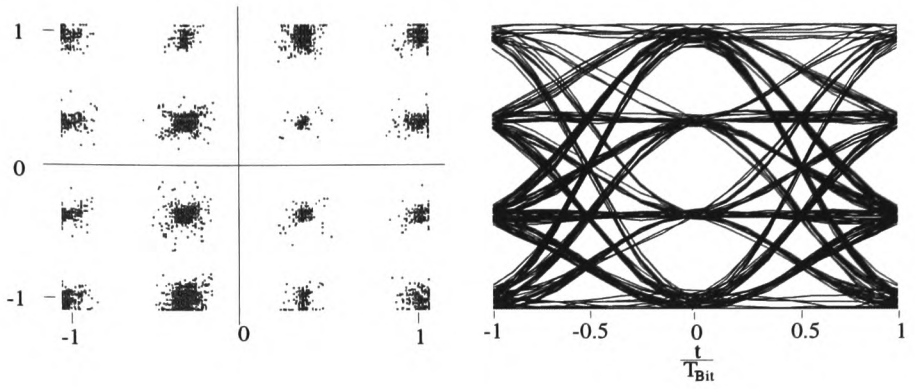

Figure 5.52: Scatter diagram and eye pattern of Figure 5.51 introducing $40dB$ noise during transmission

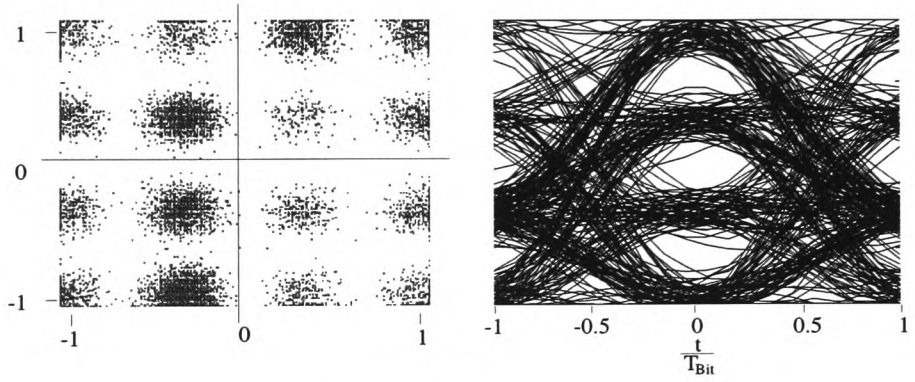

Figure 5.53: Scatter diagram and eye pattern of Figure 5.51 introducing $35dB$ noise during transmission

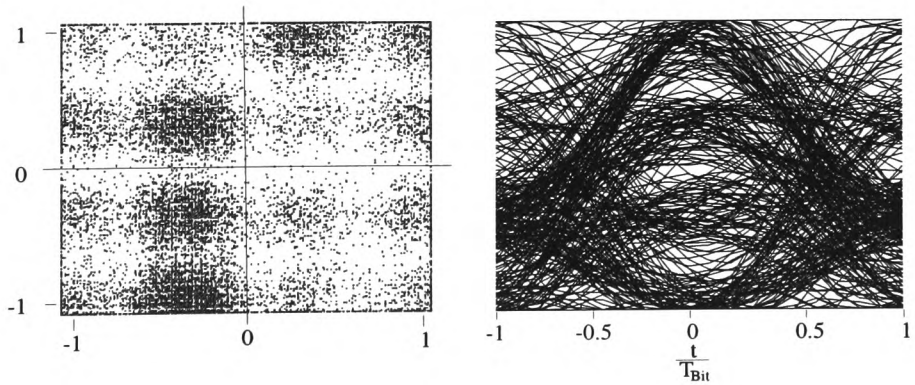

Figure 5.54: Scatter diagram and eye pattern of Figure 5.51 introducing $30dB$ noise during transmission

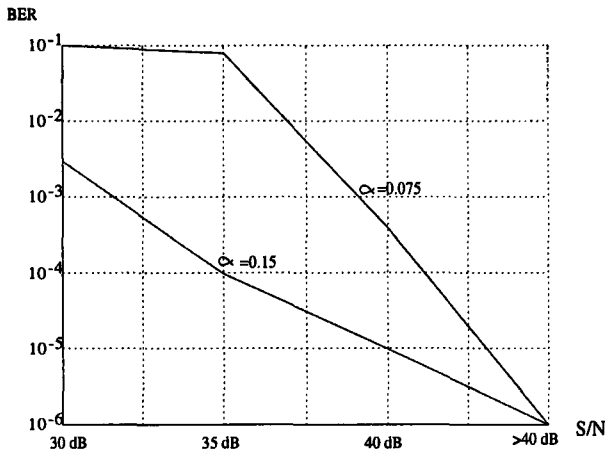

Figure 5.55: Bit error rate summarised from the previous examples

Figure 5.55 summarises the previous examples by plotting the measured BER for 16 QAM versus the transmission channel signal to noise ratio. The examples for 4 QAM are omitted, because no error occurred within the measured time period.

It should mentioned that another source of bit error is introduced from high vertical colour frequencies, which cross over into the data channel. Due to the probability of occurrence of these frequencies the resulting errors appear as burst errors. The previously mentioned vertical filter in the colour signal paths will prevent these effects, so that throughout the simulations no such errors occurred.

5.3 Interim conclusion

Within this Chapter the simulation results of the "Dual channel sub-band" strategy and the "Additional colour carrier" modulation are presented. Both Sections confirm practically the theoretical development outlined throughout Chapter 4 and further to provide an insight to the impact of various system parameters.

Section 5.1 reviews initially the crossover effects, similar to Section 4.1, but in contrast real filters were applied. Three diagonal filters with different complexity together with three bandsplitting filter banks were introduced to analyse the cross effects in relation to filter

complexity. With the main focus upon the diagonal filters, which were previously identified to be the most critical, eight different combinations were presented to study the effects of these essential parameters.

The results prove the important role of the two dimensional diagonal filter however, they also clearly show that a moderate filter order, for example 19 by 19 taps, will provide a sufficient outcome. The same is valid for the bandsplitting filter, but due to wide transition bandwidth between pass- and stop-band , they should be not less than eight taps. It is also not necessary to have such a complex diagonal post filter at the decoder compared with that for the encoder. If a sufficient attenuation of those frequencies which are identified to be critical is performed, a lower diagonal filter order can be applied at the receiver. The investigation upon real images shows that visible effects are much less than expected, so that the filter specifications at the receiver can be more relaxed, than those for the encoder.

In summarising the results in Section 5.1, it was found that the dual channel subband strategy is a viable way to derive only two sub-bands, instead the usual four. Only a moderate filter complexity is necessary to provide an acceptable output, especially for real images, where extensive tests revealed that no perceptual distortions appeared. For the processing of interlaced scanned video signals a motion adaptive implementation is proposed. The achievable performance is again mainly balanced with complexity. However, with some compromises for the down converted component a satisfactory solution has been demonstrated.

The analysis throughout Section 5.2 concentrated upon the two dimensional form filter to avoid inter symbol and inter carrier crosstalk distortions due to the additional embedded data channels. After an initial study of the achievable data rate in relation to the different filter strategies and a discussion of possible data signal amplitudes, eight different form filter implementations with two different data amplitudes were further investigated.

Three different categories were distinguished within the filter implementations, namely a partial response coding, an interpolation technique and a combination of both. The partial response coding is found to be insufficient in terms of cross talk attenuation. An acceptable result was performed by the interpolation technique implemented with an interpolation factor of three however, to keep a sufficient data rate a 16 QAM must be employed. A superior

cross talk attenuation is provided by the combination strategy, but with loss of data rate capacity. Further analysis focused upon the noise susceptibility of the data channels. Within a range down to $30dB$ signal to noise ratio during transmission, no error was measurable for the 4 QAM implementation. For 16 QAM the situation changes, so that for low data amplitudes a signal to noise ratio of at least $40dB$ must be available.

The results of Section 5.2 clearly outline that the additional colour carrier modulation is a possible strategy for embedded data modulation. It was shown that the cross talk distortions can be suppressed under a perceptual threshold, nevertheless providing a data rate of at least $500\frac{KBit}{s}$ together with acceptable noise robustness.

Chapter 6

Conclusions

This thesis has presented the details of a novel encoder design which enables PAL / PALPLUS compatible enhanced quality television distributions. A dual channel subband strategy is employed which supplements the analogue TV signal with an embedded digitally modulated data stream, to transmit a residual component for signal reconstitution at the receiver. Simulation results demonstrate the overall feasibility of the underlying system design principles.

An optimal dual channel subband arrangement was developed by combining a diagonal prefilter together with a Quadrature Mirror Filter bank pair. The initial diagonal filtering generates only two high pass, wedge shaped frequency areas, which are subsequently added to form a single high pass band. This addition leads to a principal source of error due to two components. Firstly, cross-over elements and secondly only the partial effectiveness of the QMF alias compensation. Within the analysis, it was shown that by applying the band-splitting filter to be odd and even order for horizontal and vertical filtering respectively (or vice-versa), certain crosstalk distortions can be eliminated and thus an optimal overall transfer function achieved. The remaining artefacts were identified and their subjective effects balanced with the filter designs. Extensive tests showed that a typical order of the diagonal filter, for example 19 by 19 taps, provides a sufficient compromise when processing zone plate signals. For real world images however, the situation in comparison becomes much less critical. Hence, the filter order at the decoder can be reduced without visible degradations.

A similar reduction in order for the band-splitting filter is also possible. However, due to the problems raised from the wide transition bandwidth, the complexity of these filters should be a minimum of at least seven taps.

A direct benefit accruing from this solution is the relatively low resultant complexity of both the encoder and decoder, whose performance guarantees perceptually acceptable picture quality for the selected filter solution.

A modification of the dual channel sub-band technique was analysed to handle the inherent problems of applying this strategy to interlaced video signals. A motion detector was incorporated to switch between inter- and intra-field processing in combination with a line offset compensation. This solution provides the best compromise in the intra-field mode, meaning a reasonable quality for the reconstituted and the compatible signal, whereas other solutions produce superior quality for only one component at the direct expense of the other.

For the embedded digital modulation, two different techniques for the two signal parts, namely the helper and the centre component within the PALPLUS signal, were presented. Both systems insert the supplementary information into the active video portion, meaning the visible part of the video signal. This strategy provides the best potential in exploiting supplementary capacity, because other techniques already allocate different parts, for example the blanking periods or additional sub-carrier outside the video signal. The additional helper modulation is identified as being problematic because of the proneness to any distortions which afflict the helper signal and the necessity of a higher order temporal filter to split the two components. A novel modulation strategy, however, was presented by employing an additional colour carrier modulation and shown to afford much greater potential. This technique occupies the same frequency location as for the colour signals, which is possible due to the inherent PAL colour carrier phase alternation, using an additional quadrature amplitude modulation. To suppress crosstalk effects the concept of a two dimensional form filtering is developed. The work compares the results by selecting different parameter combinations and analysing the critical balance between perceptual distortions and data rate. It was proved that a data rate of $500\frac{KBits}{s}$ is feasible with nearly no visible trade-offs. In noisy transmission channels, the proposed system provides a bit error rate of 10^{-3} for more than $30dB$ SNR.

In respect of encoder and decoder complexity, as in the dual channel subband system, there is considerable flexibility in the design of the two dimensional form filters and a higher embedded transparent date rate is achievable but at the expense of higher order designs.

The large gap between the residual data rate and those provided by the embedded digital modulation should be balanced by employing an appropriate data compression method. It was shown, that a very high compression ratio is necessary to fulfill this original aim of the work. As outlined, it is not impossible to achieve this, but however the overall quality is insufficient for an enhanced definition reconstituted picture. With regard to this issue, it is more propitious to employ the provided digital data channels for the transmission of supplementary multimedia services.

Summarising, this thesis has proved the validity of a novel flexible framework which will provide provision for integrated embedded multimedia services within standard PAL / PALPLUS television transmissions.

Points for further research:-

- Specific design issues in the framework could be optimised in respect of both the filter bank and form-filtering, which could potentially improve the data rate, but simultaneously increase complexity of the entire system.
- integration of additional data reduction techniques for the high pass residual signal, for example applying vector quantization methods.
- exploration of biorthogonal filters from wavelet theory and their performance within the dual channel subband strategy and the possibility of perfect signal reconstitution.
- possible enhancements and optimisations of the embedded data modulation technique in respect of the roll-off characteristics and its effect upon the data rate efficiency. The potential for a lower roll-off form filter exists by keeping the data rate synchronous with the line frequency and using a simple symbol reconstruction at the receiver.

Bibliography

[1] K. B. Benson and D. G. Fink. *HDTV Advanced Television for the 1990s*. McGraw-Hill Publishing Company, INC, 1991.

[2] G. Schmidt, L.S. Dooley, and W.P. Buchwald. A PALplus compatible HDTV encoder system. *IEEE Transactions on Consumer Electronics*, 40(3):207–215, 1994.

[3] L.S. Dooley, W.P. Buchwald, and G. Schmidt. An HDTV encoder design for the transmission of PALplus signals, supplement with a digital residual component. In *3rd international conference on signal processing 1996, Beijing, China*, pages 1134–1135, 1996.

[4] R. J. Clarke. *Digital Compression of still images and video*. Signal processing and its Applications. Academic Press, 1995.

[5] G. Schmidt, L.S. Dooley, and W.P. Buchwald. Design of 2–D digital video filters for PALplus compatible HDTV transmission encoder. *Presented at the fourteenth Annual Saraga Colloquium on Digital and Analogue filters and filtering systems, London*, November 30 1994.

[6] G. Schmidt, W.P. Buchwald, and L.S. Dooley. Optimal design of dual-channel sub-band filter structures for video and image applications. In *3rd international conference on signal processing 1996, Beijing, China*, pages 373–376, 1996.

[7] G. Schmidt, W.P. Buchwald, and L.S. Dooley. A comparative review of modulation techniques for integrating digital components within a PALplus signal. In *Digest of technical papers, ICCE '96*, pages 12–13, 1996.

[8] G. Schmidt, W.P. Buchwald, and L.S. Dooley. A modulation technique for integrating digital subchannels within a PAL/PALplus signal. *IEEE Transactions on Consumer Electronics*, 44(3):793–802, 1998.

[9] H. Schroeder. *Mehrdimensionale Signalverarbeitung*. B.G. Teubner, 1998.

[10] D.E. Pearson. *Transmission and display of pictoral Information*. Pentech Press, 1975.

[11] D.E. Dudgeon and R.M. Mersereau. *Multidimensional digital signal processing*. Prentice – Hall, INC, 1984.

[12] H. Schoenfelder. *Digitale Filter in der Videotechnik, German*. Drei–R–Verlag, 1988.

[13] P. Vaidyanathan. *Multirate systems and filter banks*. Prentice – Hall, INC, 1992.

[14] P.P. Vaidyanathan. Quadrature mirror filter banks, M–band extentions and perfect reconstruction techniques. *IEEE ASSP magazine*, 4(3):4–20, 1987.

[15] R.E. Crochiere and L.R. Rabiner. *Multirate digital signal processing*. Prentice – Hall, INC, 1983.

[16] J. D. Johnston. A filter family designed for use in quadrature mirror filter banks. *Proc. IEEE Int. Conf. ASSP*, pages 291–294, April 1980.

[17] M. Smith and T.P. Barnwell. Exact reconstruction techniques for tree–structured subband coders. *IEEE Transactions on ASSP*, 34(3):434–440, 1986.

[18] M. Vetterli. Multi-dimenstional sub-band coding: some theory and algorithms. *Signal Processing*, 6(2):97–112, 1984.

[19] S-C. Pei and S-B. Jaw. Design of 2-D quadrature mirror FIR filter for image subband coding. *IEEE Transactions on circuits and systems*, 34(4):438–441, 1987.

[20] T. Chen and P.P. Vaidyanathan. Multidimensional multirate filters and filterbanks derived from one dimensional filters. *IEEE Transactions on Signal Processing*, 41(5):1749–1765, 1993.

[21] E.P. Simoncelli and E.H. Adelson. Non separable extensions of quadrature mirror filters to multiple dimensions. *Proc. IEEE*, 78(4):652–664, 1990.

[22] E. Viscito and J.P. Allebach. The analysis and design of multidimensional FIR perfect reconstruction filter banks for arbitrary sampling lattices. *IEEE Transactions on circuits and systems*, 38(1):29–41, 1991.

[23] G.J. Tonge. Three-dimensional filters for television sampling. *IBA Experimental & Development Report*, (117/82), June 1982.

[24] H. Schönfelder. *Bildkommunikation, German*. Springer-Verlag, 1983.

[25] D. Teichner. *Bildinhaltsabhängige Filterung von PAL-Signalen zur Verbesserung der Luminanz-Chrominanz-Trennung, German*. PhD thesis, TU-Braunschweig, 1989.

[26] C. P. Sandbank. *Digital Television*. John Wiley and Sons, 1990.

[27] A.Ebner, E.Matzel, R.Marcom, R.Ochs, U.Riemann, M.Silverberg, R.Storey, F.Vreeswijk, and D.Westerkamp. PALplus: transmission of 16:9 pictures in a terrestrial PAL-Channel (German). *FKT*, 46(11):733–739, 1992.

[28] Chr. Hentschel. Bandsplitting for sampling rate conversion for a PALplus transmission (German). *FKT*, 46(11):742–754, 1992.

[29] T. Herfet. Band–splitting for compatible 16:9 transmission (German). *Rundfunktech. Mitteilungen*, 35(1):29–35, 1991.

[30] A. Mench. *Stoerabstandsverbesserung bei der frequenzmodulierten Satellitenuebertragung von Fernsehsignalen, German*, volume 470 of *Information / Communication technology*. VDI, 1996.

[31] ETSI. Television systems; enhanced 625-line phase alternate line (pal) television; PALplus. *prETS 300731*, February 1996.

[32] ITU-R. Encoding parameters of digital television for studios. *Recommendation 601 MOD F*, 1985.

[33] A.Ebner. PALplus: a new transmission standard for wide screen picture format(German). *FKT*, 49(7-8):435–428, 1995.

[34] R. Kays. A technique for improved PAL–coding and decoding (German). *FKT*, 44(11):595–602, 1990.

[35] Y. Ninomiya. High definition television system. *Proceedings of the IEEE*, 83(7):1086–1093, 1995.

[36] G. Tonge. The television scanning process. *SMPTE Journal*, pages 657 – 666, July 1984.

[37] T.J. Long. Why noncompatible high–definition television. *IBA technical review*, pages 4–12, 1983.

[38] C. Hentschel and W.P. Buchwald. Augencharakteristik in der verticalen-/temporalen Frequenzebene, German. *FKT*, 45(4):181–187, 1991.

[39] T. Kummerow. Aspects of digital HDTV systems (German). *Frequenz*, 37(11/12):278–285, 1983.

[40] ITU-R. Basic parameter values for the HDTV standard for the studio and for international program exchange. *Recommendation 709*, 1990.

[41] R. Bucken. High definition television (HDTV):quarrels about the future of television (German). *Funkschau*, (16):87–91, 1986.

[42] B. Wendland and M. Silverberg. From PAL via HD-MACto HDTV (German). *Funkschau*, (18):24–29, 1989.

[43] N. Bolewski. MAC †. *FKT*, 47(4):225, 1993.

[44] R. Hopkins. Digital terrestrial HDTV for North America: The Grand Alliance HDTV System. *IEEE Transactions on Consumer Electronics*, 40(3):185–198, 1994.

[45] J. S. Lim K. Challapali, X. Lebegue et al. The grand alliance system for US HDTV. *Proceedings of the IEEE*, 83(2):158–174, 1995.

[46] E. Petajan. The HDTV grand alliance system. *Proceedings of the IEEE*, 83(7):1094–1105, 1995.

[47] B. Ghatt, D. Birks, and D. Hermreck. Digital television: making it work. *IEEE Spectrum*, 34(10):19–28, 1997.

[48] D. Wood. The DVB project: philosophy and core system. *Electronics & Communication Engineering Journal*, 9(1):5–10, 1997.

[49] ATSC Recommended Practice. Harmonization with DVB SI in the use of the ATSC digital television standard. *ATSC Standards*, (A/58), 1998.

[50] IRT. Handbook for the d2-mac/packet - transmissionsystem, German. *Institut fuer Rundfunktechnik, Muenchen*, 1988.

[51] NHK Science and technical research laboratories. *High definition television, hi-vision technology*. Van Nostrand Reinhold, 1993.

[52] W. Boie. TV-Systeme mit erhöhter Bildqualität (III), German. *FKT*, 46(2):128–131, 1992.

[53] H. Schönfelder. *Fernsehtechnik im Wandel, German*. Springer-Verlag, 1996.

[54] W. Boie. TV-Systeme mit erhöhter Bildqualität (I), German. *FKT*, 45(12):671–680, 1991.

[55] W. Boie. TV-Systeme mit erhöhter Bildqualität (II), German. *FKT*, 46(1):41–52, 1992.

[56] ITU-R Study Group 11/3. A guide to digital terrestrial television broadcasting in the VHF/UHF bands. *Document 11-3/3-E*, 1996.

[57] Technical University Braunschweig. Digital television broadcasting – (DTVB, German). 1994.

[58] ISO/IEC DIS 13818-2. Information Technology - Generic coding of moving pictures and associated audio information - Part 2: Video. *Draft international standard*, 1994.

[59] ISO/IEC DIS 13818-1. Information Technology - Generic coding of moving pictures and associated audio information - Part 1: Systems. *Draft international standard*, 1994.

[60] ISO/IEC DIS 13818-3. Information Technology - Generic coding of moving pictures and associated audio information - Part 3: Audio. *Draft international standard*, 1994.

[61] ATSC Recommended Practice. Digital audio compression AC-3. *ATSC Standards*, (A/52), 1998.

[62] B. Fox. Digital TV comes down to earth. *IEEE Spectrum*, 35(10):23–29, 1998.

[63] R. Hopkins. Advanced television systems. *IEEE Transactions on Consumer Electronics*, 34(1):1–15, 1994.

[64] G. J. Tonge. Image processing for higher definition television. *IEEE Transactions on Circuits and Systems*, 34(11):1385–1398, 1987.

[65] Chr. Hentschel. Theoretischer und subjektiver Vergleich verschiedener Flimmerreduktionsverfahren (German). *Rundfunktech. Mitteilungen*, 32(2):75–82, 1987.

[66] T. Okada, M. Hongu, and Y. Tanaka. Flicker-free non-interlaced receiving system for standard color TV signals. *IEEE Transactions on Consumer Electronics*, 31(3):240–254, 1985.

[67] B. Wendland. Bildabtastung und subjektive Bildqualitaet, German. *FKT*, 39(2):57–63, 1985.

[68] H. Amor. Untersuchungen zur kompatiblen Uebertragung hochaufloesender Bilder. *FKT*, 36(3):99–102, 1982.

[69] E. Fischer. Bandsplitting of video signals for 2-channel transmission. *IEEE Transactions on Consumer Electronics*, 34(3):474–483, 1988.

[70] Majid Rabbani and Paul M. Jones. *Digital image compression techniques*, volume TT 7 of *Tutorial Texts in optical engineering*. SPIE Optical engineering press, 1991.

[71] H. Sauerburger and L. Stenger. Preprocessing and digital coding of HDTV signals (German). *Frequenz*, 37(11/12):288–298, 1983.

[72] G. Schamel. Pre- and postfiltering of HDTV signals for sampling rate reduction and display up-conversion. 34(11):1432–1439, 1987.

[73] G. Schamel. Mehrdimensionale Vorfilterung, Reduktion der Abtastrate und Interpolation von HDTV Signalen (Teil 1), German. *Rundfunktech. Mitteilungen*, 42(10):284–288, 1988.

[74] G. Schamel. Mehrdimensionale Vorfilterung, Reduktion der Abtastrate und Interpolation von HDTV Signalen (Teil 2), German. *Rundfunktech. Mitteilungen*, 42(11/12):300–304, 1988.

[75] H. Sauerburger and L. Stenger. Transmissions of HDTV signals using two satellite channels(German). *Rundfunktech. Mitteilungen*, 28(5):235–240, 1984.

[76] B.G. Haskell. High Definition Television (HDTV)–Compatibility and distribution . *IEEE Transactions on Communications*, 31(12):1308–1317, 1983.

[77] B.G. Haskell. Semicompatible High Definition Television using field differential signals. *IEEE Transactions on Communications*, 34(10):1031–1037, 1986.

[78] T. Fukinuki, Y. Hirano, and H. Yoshigi. Experiments on proposed extended definition tv with full NTSC compatible. *SMPTE Journal*, pages 923–929, October 1984.

[79] T. Fukinuki and Y. Hirano. Extended definition tv fully compatible with existing standards. *IEEE Transactions on Communications*, 32(3), 1984.

[80] M. A. Isnardi. Exploring and exploiting subchannels in the NTSC spectrum. *SMPT Journal*, pages 526–532, July 1988.

[81] M.A. Isnardi, J.S. Fuhrer, et al. A single channel NTSC compatible widescreen EDTV system. *Image Technology*, 70(4):118–119, 1988.

[82] M.A. Isnardi, C.B. Dieterich, and T.R. Smith. Advanced compatible television: A Progress report. *SMPTE Journal*, pages 484–495, July 1988.

[83] A.G. Toth, M. Tsinberg, and C.W. Rhodes. Hierarchical NTSC compatible HDTV system architecture – a North America perspective. *Int. J. Digit. Analog Cable Systems*, 1(2):65–72, 1988.

[84] W.E. Glenn and K.G. Glenn. HDTV compatible transmission system. *SMPTE Journal*, 96(3):242–246, 1987.

[85] Mikhail Tsinberg. ENTSC two–channel compatible HDTV sytem. *IEEE Transactions on Consumer Electronics*, 33(3):146–153, 1987.

[86] M. D. Windram, R. Morcom, and T. Hurley. Extended definition MAC. *IBA Technical Review*, 21:27–41, 1983.

[87] R.V. Ducey. Multimedia broadcasting and the internet. In *6th annual internet society conference*, 1996.

[88] NDBC. Final report. *www.nab.org*, 1997.

[89] J.G.W. Pledge. The AUDETEL audio description service for visually impaired people. In *Time between pictures - the vertical blanking interval*, pages 3/1–3/7, 1994.

[90] M. Schneider. What is teletext. *Philips Technical Document No.8129*, 1994.

[91] N.W. Green. PDC programme delivery control. In *Time between pictures - the vertical blanking interval*, pages 6/1–6/5, 1994.

[92] G. Berry. Teletext services - cant't they go any faster. In *Time between pictures - the vertical blanking interval*, pages 1/1–1/12, 1994.

[93] Technischer Richtlinie ARD / ZDF. Fernsehtext Spezifikation. In *Nr. 8 R4*, 1986.

[94] BDS Ltd. Datacast as used by the BBC. *www.bdsltd.co.uk*, 1997.

[95] P. Buchner. Line 23 signalling. In *Time between pictures - the vertical blanking interval*, pages 8/1–8/8, 1994.

[96] Reportl. NAB '95 conference & exhibition. *Rundfunktech. Mitteilungen*, 39(2):78–82, 1995.

[97] A. Finger, H. Hiller, O. Goetting, and J. Schoenthier. A new digital add on data transmission within analogue television channels, German. *Proceedings of the 17. FKTG Annual Conference*, pages 476–485, 1996.

[98] EBU. Nicam 728: transmission of two-channel digital sound with terrestrial television systems b, g, h, i, k1 and l. *EN 300163*, 1998.

[99] S. Dinsel. Tv-datacast a compatible digital data system for analogue tv networks, German. *Proceedings of the 17. FKTG Annual Conference*, page 496, 1996.

[100] W. Szepanski. *Uebertragung nichtorthogonaler Zusatzsignale in Bildkanaelen, German*. PhD thesis, Technical University Aachen, 1979.

[101] A. Stoetera. *Synthese und Dedektion von Zusatzsignalen in Fernsehbildkanaelen*. PhD thesis, Technical University Aachen, 1985.

[102] W. Ruppel. *Kompatible Uebertragung eines digitalen Zusatzsignals bei konventionellen Fernsehsystemen, German*, volume 304 of *Information / Communication technology*. VDI, 1994.

[103] W. Ruppel. Compatible transmission of additional digital signals with conventional tv systems, German. *Frequenz*, 48(5-6):133–138, 1994.

[104] M. Plantholt. *German Patent DE 3841073 A1*, 1988.

[105] U. Riemann and M. Plantholt. *European Patent EP 0521028 B1*, 1991.

[106] U. Kraus, U. Riemann, and M. Plantholt. *European Patent EP 0542812 B1*, 1991.

[107] A.N. Netravali and B.G. Haskell. *Digital Pictures (Representation and Compression)*. Plenum Pess, 3 edition, 1991.

[108] W.P. Pennebaker and J.L Mitchell. *JPEG still image data compression standard*. Van Nostrand Reinhold, 1988.

[109] J.L. Mitchell, W.P. Pennebaker, C.E. Fogg, and D.J. LeGall. *MPEG video compression standard*. Chapman & Hall, 1996.

[110] S. Hartwig and W. Endemann. Digitale bildcodierung. *FKT*, (2), 1992.

[111] ISO/IEC DIS 10918-1. digital compression and coding of continuous-tone still images. *Draft international standard*, 1992.

[112] Gregory K. Wallace. The JPEG still picture compression standard. *IEEE Transactions on Consumer Electronics*, 38(1), February 1992.

[113] T. Micke and F. Fell-Bosenbeck. Datenkompression bei der professionellen Videoaufzeichnung, German. *FKT*, 50(6):309–314, 1996.

[114] S. Hartwig and W. Endemann. Digitale bildcodierung. *FKT*, (6), 1992.

[115] T. Milde. *Videokompressionsverfahren im Vergleich, German.* dpunkt, 1995.

[116] ISO/IEC DIS 11172. Coding of moving pictures and associated audio for digital storage media up to about 1,5 Mbits. *Draft international standard*, 1992.

[117] H. Schroeder and H. Elsler. Planare Vor- und Nachfilterung fuer Fernsehsignale, German. *ntzArchiv*, (4):303–312, 1984.

[118] V. Cappellini, A.G. Constantinides, and P. Emiliani. *Digital Filters and their Applications*. Acedemic Press, 1978.

[119] B. Vergin. Image data compression by subsampling using two dimensional spatial filters. *Dipl. thesis at University of Glamorgan / Fachhochschule Wolfenbuettel*, 1994.

[120] M. Vetterli and J. Kovacevic. *Wavelets and Subband Coding*. Signal Processing. Prentice Hall, 1995.

[121] J. D. Villasenor, B. Belzer, and J. Liao. Wavelet filter evaluation for image compression. *IEEE Transactions on Image Processing*, 4(8):1053–1060, 1995.

[122] M. Meissner. Quadrature-mirror-filter design for subband coding of video signals. *Dipl. thesis at University of Glamorgan / Fachhochschule Wolfenbuettel*, 1995.

[123] Ch. Hentschel. *Video-Signalverarbeitung, German.* Informationstechnik. B.G. Teubner, 1998.

[124] G. Schamel. Motion detection of subsampled HDTV fields. *Poc. Int. Conf. Digital Signal Processing*, pages 522–526, 1987.

[125] C. Hentschel. High quality noise insensitive motion detector using one field memory. *IEEE Transactions on Consumer Electronics*, 42(3):696–704, 1996.

[126] M. Vetterli. Perfect transmultiplexers. *Proc. IEEE Int. Conf. Acoust. Speech and Signal Proc.*, pages 2567–2570, 1986.

[127] B. Selvan and R.J. Green. Objective noise evaluation of component video signals using an electric colour video simulator. *IEEE Transactions on Broadcasting*, 39(3):327–330, 1993.

[128] H. L. Hartmann. *Berichte zur Systematik und Analyse von Nachrichtensystemen, German.* TU-Braunschweig, 1977.

[129] ITU-R. Transmission performance of television circuits designed for use in international connections. *Recommendation 567 Annex II to Part C*, 1990.

[130] K. P. Wendler. *Zeitmultiplexverfahren fuer die Uebertragung und Aufzeichnung von Farbfernsehsignalen, German.* PhD thesis, TU-Braunschweig, 1986.

[131] K. D. Kammeyer. *Nachrichtenuebertragung, German.* Informationtechnology. B. G. Teubner, 1992.

[132] W. Hess. *Digitale Filter, German.* Electronics. B. G. Teubner, 1993.

[133] T. I. Laakso, V. Vaelimaeki, M. Karjalainen, and U. K. Laine. Splitting the unit delay. *IEEE Signal Processing Magazine*, 13(1):30–60, January 1996.

[134] G.J. Tonge. The sampling of television images. *IBA Experimental & Development Report*, (112/81), May 1981.

[135] MATH WORKS. MatLab Signal Processing Tollbox.

[136] R. W. Schaefer and L. R. Rabiner. A digital signal processing approach to interpolation. *Proceedings of the IEEE*, 61:692–702, 1973.

[137] H. Amor. *Contribution to a compatible transmission of high resolution TV pictures (German).* PhD thesis, Technical University Aachen, June 1982.

[138] U. Toedtmann. Image data compression using adaptive quantisation. *Dipl. thesis at University of Glamorgan / Fachhochschule Wolfenbuettel*, 1995.

[139] M. Lipkow. Data compression of video signals by non-linear quantisation. *Dipl. thesis at University of Glamorgan / Fachhochschule Wolfenbuettel*, 1995.

[140] J. D. Gibson. *The mobile Communication Handbook.* PRC Press / IEEE Press, 1996.

[141] K. Konstantinides and J.R. Rasure. The khoros software development environment for image and signal processing. *IEEE Transactions on Image Processing*, 3(3):243–252, 1994.

Appendix A

Derivation of dual channel crosstalk

As alluded to in Section 2.2, the general case for a separable analysis section with orthogonal subsampling results into four subbands. Figure 4.4 gives the block diagram of the analysis / synthesis filter bank for processing only two bands by using an additional diagonal pre- and postfilter. So for the following subband decomposition the input signal is referred to $X_D(z_1, z_2)$, which stands for the diagonal filtered $X(z_1, z_2)$.

A.1 Conventional scheme using odd filter orders

The two subbands $y_0(n_1, n_2)$,$y_1(n_1, n_2)$ can be written in the z-domain

$$\begin{aligned} Y_0(z_1\prime, z_2\prime) = &\tfrac{1}{4}[H_0(z_1^{\frac{1}{2}})H_0(z_2^{\frac{1}{2}})X_D(z_1^{\frac{1}{2}}, z_2^{\frac{1}{2}}) + \\ &H_0(-z_1^{\frac{1}{2}})H_0(z_2^{\frac{1}{2}})X_D(-z_1^{\frac{1}{2}}, z_2^{\frac{1}{2}}) + \\ &H_0(z_1^{\frac{1}{2}})H_0(-z_2^{\frac{1}{2}})X_D(z_1^{\frac{1}{2}}, -z_2^{\frac{1}{2}}) + \\ &H_0(-z_1^{\frac{1}{2}})H_0(-z_2^{\frac{1}{2}})X_D(-z_1^{\frac{1}{2}}, -z_2^{\frac{1}{2}})] \end{aligned} \tag{A.1}$$

$$\begin{aligned} Y_1(z_1\prime, z_2\prime) =& \tfrac{1}{4}[(H_0(z_1^{\frac{1}{2}})H_1(z_2^{\frac{1}{2}}) + H_1(z_1^{\frac{1}{2}})H_{ap}(z_2^{\frac{1}{2}}))X_D(z_1^{\frac{1}{2}}, z_2^{\frac{1}{2}}) + \\ & (H_0(-z_1^{\frac{1}{2}})H_1(z_2^{\frac{1}{2}}) + H_1(-z_1^{\frac{1}{2}})H_{ap}(z_2^{\frac{1}{2}}))X_D(-z_1^{\frac{1}{2}}, z_2^{\frac{1}{2}}) + \\ & (H_0(z_1^{\frac{1}{2}})H_1(-z_2^{\frac{1}{2}}) + H_1(z_1^{\frac{1}{2}})H_{ap}(-z_2^{\frac{1}{2}}))X_D(z_1^{\frac{1}{2}}, -z_2^{\frac{1}{2}}) + \\ & (H_0(-z_1^{\frac{1}{2}})H_1(-z_2^{\frac{1}{2}}) + H_1(-z_1^{\frac{1}{2}})H_{ap}(-z_2^{\frac{1}{2}}))X_D(-z_1^{\frac{1}{2}}, -z_2^{\frac{1}{2}})] \end{aligned} \tag{A.2}$$

Describing the synthesis bank $\hat{X}(z_1, z_2)$ is expressed as

$$\begin{aligned} \hat{X}(z_1, z_2) = & G_0(z_1)G_0(z_2)Y_0(z_1\prime^2, z_2\prime^2) + \\ & (G_0(z_1)G_1(z_2) + G_1(z_1)G_{ap}(z_2))Y_1(z_1\prime^2, z_2\prime^2) \end{aligned} \tag{A.3}$$

The substitution of Equation(A.1) and Equation(A.2) in Equation(A.3) results in the overall formulation

$$\begin{aligned} \hat{X}(z_1, z_2) = & \tfrac{1}{4}[H_0(z_1)H_0(z_2)G_0(z_1)G_0(z_2) + H_0(z_1)H_1(z_2)G_0(z_1)G_1(z_2) + \\ & \boldsymbol{H_0(z_1)H_1(z_2)G_1(z_1)G_{ap}(z_2) + H_1(z_1)H_{ap}(z_2)G_0(z_1)G_1(z_2)} + \\ & H_1(z_1)H_{ap}(z_2)G_1(z_1)G_{ap}(z_2)]X_D(z_1, z_2) + \\ & \tfrac{1}{4}[H_0(-z_1)H_0(z_2)G_0(z_1)G_0(z_2) + H_0(-z_1)H_1(z_2)G_0(z_1)G_1(z_2) + \\ & \boldsymbol{H_0(-z_1)H_1(z_2)G_1(z_1)G_{ap}(z_2) + H_1(-z_1)H_{ap}(z_2)G_0(z_1)G_1(z_2)} + \\ & H_1(-z_1)H_{ap}(z_2)G_1(z_1)G_{ap}(z_2)]X_D(-z_1, z_2) + \\ & \tfrac{1}{4}[H_0(z_1)H_0(-z_2)G_0(z_1)G_0(z_2) + H_0(z_1)H_1(-z_2)G_0(z_1)G_1(z_2) + \\ & \boldsymbol{H_0(z_1)H_1(-z_2)G_1(z_1)G_{ap}(z_2) + H_1(z_1)H_{ap}(-z_2)G_0(z_1)G_1(z_2)} + \\ & H_1(z_1)H_{ap}(-z_2)G_1(z_1)G_{ap}(z_2)]X_D(z_1, -z_2) + \\ & \tfrac{1}{4}[H_0(-z_1)H_0(-z_2)G_0(z_1)G_0(z_2) + H_0(-z_1)H_1(-z_2)G_0(z_1)G_1(z_2) + \\ & \boldsymbol{H_0(-z_1)H_1(-z_2)G_1(z_1)G_{ap}(z_2) + H_1(-z_1)H_{ap}(-z_2)G_0(z_1)G_1(z_2)} + \\ & H_1(-z_1)H_{ap}(-z_2)G_1(z_1)G_{ap}(z_2)]X_D(-z_1, -z_2) \end{aligned} \tag{A.4}$$

The bold written terms in Equation(A.4) will highlight the signal parts, which occur due to the addition of the two subbands to form $y_1(n_1, n_2)$ and consists of vertical high frequency components, which are crossed over to become horizontal and vice versa. The dotted arrows

in Figure 4.4 visualize this phenomena. So Equation(A.4) will be further written as

$$\begin{aligned}\hat{X}(z_1,z_2) &= \frac{1}{4}[T(z_1,z_2)+C_T(z_1,z_2)]X_D(z_1,z_2)+\\ &\frac{1}{4}[A_1(z_1,z_2)+C_{A1}(z_1,z_2)]X_D(-z_1,z_2)+\\ &\frac{1}{4}[A_2(z_1,z_2)+C_{A2}(z_1,z_2)]X_D(z_1,-z_2)+\\ &\frac{1}{4}[A_3(z_1,z_2)+C_{A3}(z_1,z_2)]X_D(-z_1,-z_2)\end{aligned}$$

where $T(z_1,z_2)$ and $A_1(z_1,z_2)\cdots A_3(z_1,z_2)$ denotes what is usually referred to the transfer function and the alias parts respectively and

$$\begin{aligned}C_T(z_1,z_2) =& H_0(z_1)H_1(z_2)G_1(z_1)G_{ap}(z_2)+H_1(z_1)H_{ap}(z_2)G_0(z_1)G_1(z_2)\\ C_{A1}(z_1,z_2) =& H_0(-z_1)H_1(z_2)G_1(z_1)G_{ap}(z_2)+H_1(-z_1)H_{ap}(z_2)G_0(z_1)G_1(z_2)\\ C_{A2}(z_1,z_2) =& H_0(z_1)H_1(-z_2)G_1(z_1)G_{ap}(z_2)+H_1(z_1)H_{ap}(-z_2)G_0(z_1)G_1(z_2)\\ C_{A3}(z_1,z_2) =& H_0(-z_1)H_1(-z_2)G_1(z_1)G_{ap}(z_2)+H_1(-z_1)H_{ap}(-z_2)G_0(z_1)G_1(z_2)\end{aligned} \tag{A.5}$$

will be further referred as the crossover terms.

For convenience $H_0(z)$ is set to $H(z)$ and $G_0(z)$ to $G(z)$. Similar to Equation (2.20) the filters are chosen as $H_1(z)=G(-z)$ and $G_1(z)=-H(-z)$. Equation(A.4) becomes

$$\begin{aligned}T(z_1,z_2) = H(z_1)H(z_2)G(z_1)G(z_2) - H(z_1)G(-z_2)G(z_1)H(-z_2) -\\ G(-z_1)H_{ap}(z_2)H(-z_1)G_{ap}(z_2)+C_T(z_1,z_2)\end{aligned} \tag{A.6}$$

$$\begin{aligned}A_1(z_1,z_2) = H(-z_1)H(z_2)G(z_1)G(z_2) - H(-z_1)G(-z_2)G(z_1)H(-z_2) -\\ G(z_1)H_{ap}(z_2)H(-z_1)G_{ap}(z_2)+C_{A1}(z_1,z_2)\end{aligned} \tag{A.7}$$

$$\begin{aligned}A_2(z_1,z_2) = H(z_1)H(-z_2)G(z_1)G(z_2) - H(z_1)G(z_2)G(z_1)H(-z_2) -\\ G(-z_1)H_{ap}(-z_2)H(-z_1)G_{ap}(z_2)+C_{A2}(z_1,z_2)\end{aligned} \tag{A.8}$$

$$\begin{aligned}A_3(z_1,z_2) = H(-z_1)H(-z_2)G(z_1)G(z_2) - H(-z_1)G(z_2)G(z_1)H(-z_2) -\\ G(z_1)H_{ap}(-z_2)H(-z_1)G_{ap}(z_2)+C_{A3}(z_1,z_2)\end{aligned} \tag{A.9}$$

Setting furthermore $G(z) = H(z)$ and $H_{ap}(z) = G_{ap}(z) = H(z)$ and substituting $H(z) = e^{-j\omega\frac{N}{2}}|H(z)|$ the equations reduces due to alias cancellation to

$$T(z_1, z_2) = e^{-j(\omega_1 N_1 + \omega_2 N_2)}[|H(z_1)|^2|H(z_2)|^2 - (-1)^{N_2}|H(z_1)|^2|H(-z_2)|^2 - (-1)^{N_1}|H(-z_1)|^2|H(z_2)|^2 + |C_T(z_1, z_2)|] \quad \text{(A.10)}$$

$$A_1(z_1, z_2) = e^{-j(\omega_1 N_1 + \omega_2 N_2)}[-e^{-j\pi\frac{N_1}{2}}(-1)^{N_2}|H(-z_1)||H(z_1)||H(-z_2)|^2 + |C_{A1}(z_1, z_2)|] \quad \text{(A.11)}$$

$$A_2(z_1, z_2) = e^{-j(\omega_1 N_1 + \omega_2 N_2)}[-e^{-j\pi\frac{N_2}{2}}(-1)^{N_1}|H(-z_1)|^2|H(-z_2)||H(z_2)| + |C_{A2}(z_1, z_2)|] \quad \text{(A.12)}$$

$$A_3(z_1, z_2) = e^{-j(\omega_1 N_1 + \omega_2 N_2)}[-e^{-j\pi(\frac{N_1}{2}+\frac{N_2}{2})}|H(z_1)||H(-z_2)||H(-z_1)||H(z_2)| + |C_{A3}(z_1, z_2)|] \quad \text{(A.13)}$$

The cross over terms then become:

$$|C_T(z_1, z_2)| = -e^{-j\pi(\frac{N_1}{2}+\frac{N_2}{2})}[|H(z_1)||H(-z_2)||H(-z_1)||H(z_2)| + |H(z_1)||H(-z_2)||H(-z_1)||H(z_2)|] \quad \text{(A.14)}$$

$$|C_{A1}(z_1, z_2)| = -e^{-j\pi\frac{N_2}{2}}(-1)^{N_1}|H(-z_1)|^2|H(-z_2)||H(z_2)| - e^{-j\pi\frac{N_2}{2}}|H(z_1)|^2|H(-z_2)||H(z_2)| \quad \text{(A.15)}$$

$$|C_{A2}(z_1, z_2)| = -e^{-j\pi\frac{N_1}{2}}|H(z_2)|^2|H(-z_1)||H(z_1)| - e^{-j\pi\frac{N_1}{2}}(-1)^{N_2}|H(-z_2)|^2|H(-z_1)||H(z_1)| \quad \text{(A.16)}$$

$$|C_{A3}(z_1, z_2)| = -(-1)^{N_1}|H(-z_1)|^2|H(z_2)|^2 - (-1)^{N_2}|H(z_1)|^2|H(-z_2)|^2 \quad \text{(A.17)}$$

It is clear that no overall alias cancellation can occur, thus apart from the addition of the two subbands, the system is close to a standard four band implementation, where the fourth

band (high diagonal frequencies) is left out. Therefore the remaining aliasing terms in Equation(A.11)-(A.13) can not be compensated for.

The crosstalk signal part from Equation (A.14) leads to additional amplitude distortions depending on the analysis / synthesis filter shape. As introduced in Section 2.2, a slightly modification will cancel this term.

A.2 Modified scheme using even filter orders for vertical bandsplitting

Considering the vertical bandsplitting by using even filter orders, rather than odd ones, the vertical filters have to be chosen similar to Equation (2.24) so that $G_1(z_2) = H(-z_2)$, with the result, that the crosstalk term $C_T(z_1, z_2)$ will be cancelled. Figure 4.8 gives the modified block diagram of the analysis / synthesis filter bank. Equation (A.4) can then be written as:

$$\begin{aligned}
\hat{X}(z_1,z_2) = \tfrac{1}{4}[&H_0(z_1)z_2^{-1}H_0(z_2)G_0(z_1)G_0(z_2) + H_0(z_1)H_1(z_2)G_0(z_1)z_2^{-1}G_1(z_2) + \\
&H_0(z_1)H_1(z_2)G_1(z_1)z_2^{-1}G_{ap}(z_2) + H_1(z_1)H_{ap}(z_2)G_0(z_1)z_2^{-1}G_1(z_2) + \\
&H_1(z_1)H_{ap}(z_2)G_1(z_1)z_2^{-1}G_{ap}(z_2)]X_D(z_1,z_2) + \\
\tfrac{1}{4}[&H_0(-z_1)z_2^{-1}H_0(z_2)G_0(z_1)G_0(z_2) + H_0(-z_1)H_1(z_2)G_0(z_1)z_2^{-1}G_1(z_2) + \\
&H_0(-z_1)H_1(z_2)G_1(z_1)z_2^{-1}G_{ap}(z_2) + H_1(-z_1)H_{ap}(z_2)G_0(z_1)z_2^{-1}G_1(z_2) + \\
&H_1(-z_1)H_{ap}(z_2)G_1(z_1)z_2^{-1}G_{ap}(z_2)]X_D(-z_1,z_2) + \\
\tfrac{1}{4}[&H_0(z_1)(-z_2^{-1})H_0(-z_2)G_0(z_1)G_0(z_2) + H_0(z_1)H_1(-z_2)G_0(z_1)z_2^{-1}G_1(z_2) + \\
&H_0(z_1)H_1(-z_2)G_1(z_1)z_2^{-1}G_{ap}(z_2) + H_1(z_1)H_{ap}(-z_2)G_0(z_1)z_2^{-1}G_1(z_2) + \\
&H_1(z_1)H_{ap}(-z_2)G_1(z_1)z_2^{-1}G_{ap}(z_2)]X_D(z_1,-z_2) + \\
\tfrac{1}{4}[&H_0(-z_1)(-z_2^{-1})H_0(-z_2)G_0(z_1)G_0(z_2) + H_0(-z_1)H_1(-z_2)G_0(z_1)z_2^{-1}G_1(z_2) + \\
&H_0(-z_1)H_1(-z_2)G_1(z_1)z_2^{-1}G_{ap}(z_2) + H_1(-z_1)H_{ap}(-z_2)G_0(z_1)z_2^{-1}G_1(z_2) + \\
&H_1(-z_1)H_{ap}(-z_2)G_1(z_1)z_2^{-1}G_{ap}(z_2)]X_D(-z_1,-z_2) \qquad \text{(A.18)}
\end{aligned}$$

and further after substitution:

$$T(z_1,z_2) = e^{-j(\omega_1 N_1+\omega_2 N_2)}[z_2^{-1}|H(z_1)|^2|H(z_2)|^2 + (-1)^{N_2}z_2^{-1}|H(z_1)|^2|H(-z_2)|^2 - (-1)^{N_1}z_2^{-1}|H(-z_1)|^2|H(z_2)|^2 + |C_T(z_1,z_2)|] \quad \text{(A.19)}$$

$$A_1(z_1,z_2) = e^{-j(\omega_1 N_1+\omega_2 N_2)}[e^{-j\pi\frac{N_1}{2}}(-1)^{N_2}z_2^{-1}|H(-z_1)||H(z_1)||H(-z_2)|^2 + |C_{A1}(z_1,z_2)|] \quad \text{(A.20)}$$

$$A_2(z_1,z_2) = e^{-j(\omega_1 N_1+\omega_2 N_2)}[-e^{-j\pi\frac{N_2}{2}}(-1)^{N_1}z_2^{-1}|H(-z_1)|^2|H(-z_2)||H(z_2)| + |C_{A2}(z_1,z_2)|] \quad \text{(A.21)}$$

$$A_3(z_1,z_2) = e^{-j(\omega_1 N_1+\omega_2 N_2)}[-e^{-j\pi(\frac{N_1}{2}+\frac{N_2}{2})}z_2^{-1}|H(z_1)||H(-z_2)||H(-z_1)||H(z_2)| + |C_{A3}(z_1,z_2)|] \quad \text{(A.22)}$$

with their crossover terms:

$$|C_T(z_1,z_2)| = -e^{-j\pi(\frac{N_1}{2}+\frac{N_2}{2})}[z_2^{-1}|H(z_1)||H(-z_2)||H(-z_1)||H(z_2)| - z_2^{-1}|H(z_1)||H(-z_2)||H(-z_1)||H(z_2)|] \quad \text{(A.23)}$$

$$|C_{A1}(z_1,z_2)| = -e^{-j\pi\frac{N_2}{2}}(-1)^{N_1}z_2^{-1}|H(-z_1)|^2|H(-z_2)||H(z_2)| + e^{-j\pi\frac{N_2}{2}}z_2^{-1}|H(z_1)|^2|H(-z_2)||H(z_2)| \quad \text{(A.24)}$$

$$|C_{A2}(z_1,z_2)| = -e^{-j\pi\frac{N_1}{2}}z_2^{-1}|H(z_2)|^2|H(-z_1)||H(z_1)| + e^{-j\pi\frac{N_1}{2}}(-1)^{N_2}z_2^{-1}|H(-z_2)|^2|H(-z_1)||H(z_1)| \quad \text{(A.25)}$$

$$|C_{A3}(z_1,z_2)| = -(-1)^{N_1}z_2^{-1}|H(-z_1)|^2|H(z_2)|^2 + (-1)^{N_2}z_2^{-1}|H(z_1)|^2|H(-z_2)|^2 \quad \text{(A.26)}$$

It is obvious (Equation A.23) that $C_T(z_1,z_2)$ is cancelled and thus $T(z_1,z_2)$ reduces to

$$T(z_1,z_2) = e^{-j(\omega_1 N_1+\omega_2 N_2)}[z_2^{-1}|H(z_1)|^2|H(z_2)|^2 + (-1)^{N_2}z_2^{-1}|H(z_1)|^2|H(-z_2)|^2 - (-1)^{N_1}z_2^{-1}|H(-z_1)|^2|H(z_2)|^2] \quad \text{(A.27)}$$

Appendix B

Vertical form filter comparison

This appendix will compare the possibilities for the vertical form filter design to approximate the best crosstalk attenuation response $C_A(f_y)$. To classify the filter designs, the area underneath $C_A(f_y)$ is used, which can derived as

$$C = \int_{f_y=0}^{\frac{f_{sy}}{2}} |C_A(f_y)| df_y \tag{B.1}$$

The lowest value of C indicates the optimal approximation to the requirement found in Section 4.2.2.3. The filter order is chosen so that the number of taps is always odd and further, so that the filter length is truncated just before the zero crossing points of the sinc function.

The following sections analyse the design methods introduced in Section 4.2.2.3, so that B.1 focuses upon partial response coding and B.2 and B.3 on the interpolation technique using the window and the maximally flat approach, respectively.

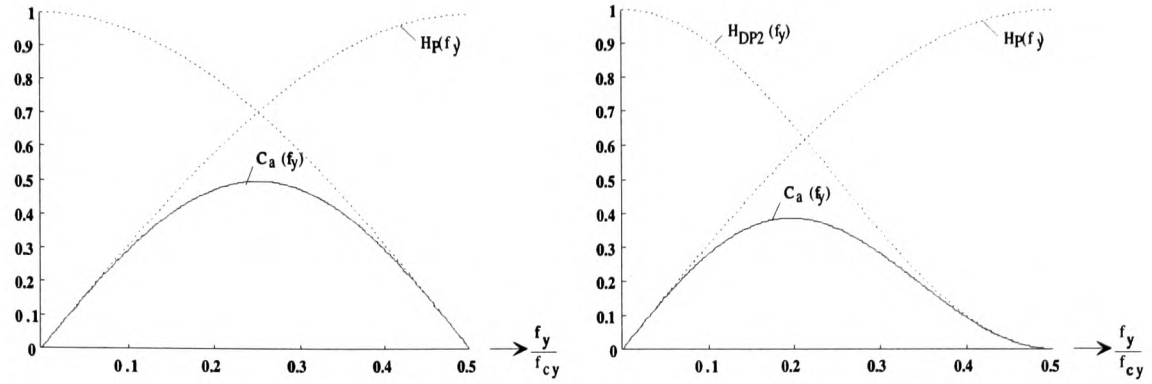

Figure B.1: Filter responses using for a) Duobinary and b) five level partial response coding

B.1 Partial Response approach

The design rule for this approach is taken from Equation 4.29. Two filters of the partial response technique will be analysed:

$$h_{DP1}(n) = \frac{1}{2}(\delta(n) + \delta(n-1)) \tag{B.2}$$

$$h_{DP2}(n) = \frac{1}{4}\delta(n+1) + \frac{1}{2}\delta(n) + \frac{1}{4}\delta(n-1) \tag{B.3}$$

Px refers to partial response coding, where h_{DP1} performs duobinary coding. h_{DP2} transforms the data flow into five levels per symbol. Figure B.1 shows the corresponding frequency responses together with $C_A(f_y)$. The classification C can be derived as $C_{P1} = 0.318$ or $C_{P2} = 0.212$ for three or five levels respectively.

B.2 Windowing approach

The filter coefficients used for this design are derived from Equation (4.35). Three different cosine based windows are used in this comparison:

Blackman $w_{Blackman}(n) = 0.42 - 0.5cos(2\pi\frac{\frac{N}{2}-n}{N}) + 0.08cos(4\pi\frac{\frac{N}{2}-n}{N})$

Hamming $w_{Hamming}(n) = 0.54 - 0.46cos(2\pi\frac{\frac{N}{2}-n}{N})$

Hanning $w_{Hanning}(n) = 0.5(1 - cos(2\pi\frac{\frac{N}{2}-n}{N}))$

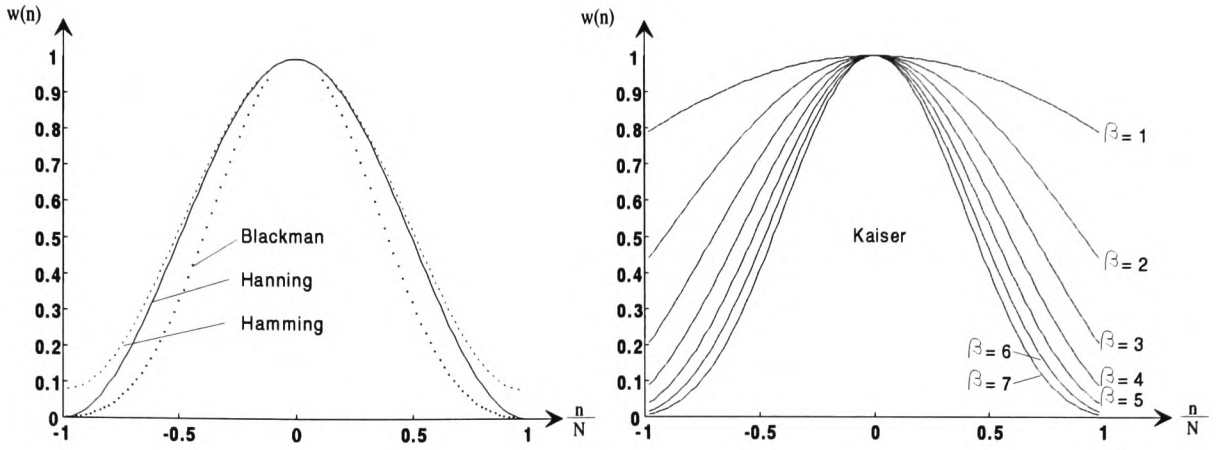

Figure B.2: Window functions used for filter design

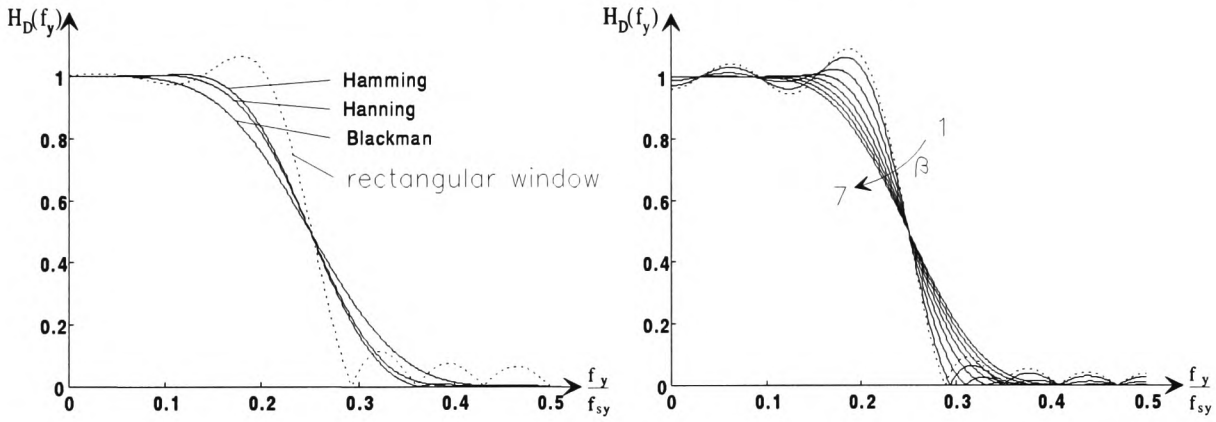

Figure B.3: Filter responses using different windows

and the Kaiser window for seven different values of β.

$$w_{Kaiser}(n,\beta) = \frac{I_0(\beta\sqrt{1-\frac{4(\frac{N}{2}-n)^2}{N^2}})}{I_0(\beta)}$$

for

$$-\frac{N}{2} \leq n \leq \frac{N}{2}$$

Figure B.2 shows the various window functions. Figure B.3 gives an insight to the frequency responses of the filters derived by using the different windows, where Figure B.4 displays the final form filter $H_F(f_y)$ together with the crosstalk attenuation $C_A(f_y)$. The filter order is chosen to 14, but is not so important for this qualitative comparison.

$L = 2$					
Filter taps	7	11	15	19	23
Hanning	0.28	0.250	0.237	0.231	0.222
Hamming	0.33	0.260	0.242	0.234	0.231
Blackman	0.46	0.285	0.243	0.237	0.232
Kaiser	0.26 ($\beta = 2$)	0.240 ($\beta = 3$)	0.234 ($\beta = 4$)	0.229 ($\beta = 4$)	0.227 ($\beta = 4$)
$L = 3$					
Filter taps		11		17	23
Hanning		0.110		0.100	0.096
Hamming		0.118		0.103	0.098
Blackman		0.129		0.098	0.096
Kaiser		0.105 ($\beta = 3$)		0.098 ($\beta = 4$)	0.096 ($\beta = 4$)
$L = 4$					
Filter order			15		23
Hanning			0.059		0.054
Hamming			0.063		0.056
Blackman			0.066		0.057
Kaiser			0.058 ($\beta = 4$)		0.054 ($\beta = 4$)

Table B.1: Efficiency of different windows and filter order for $L = 2, 3, 4$

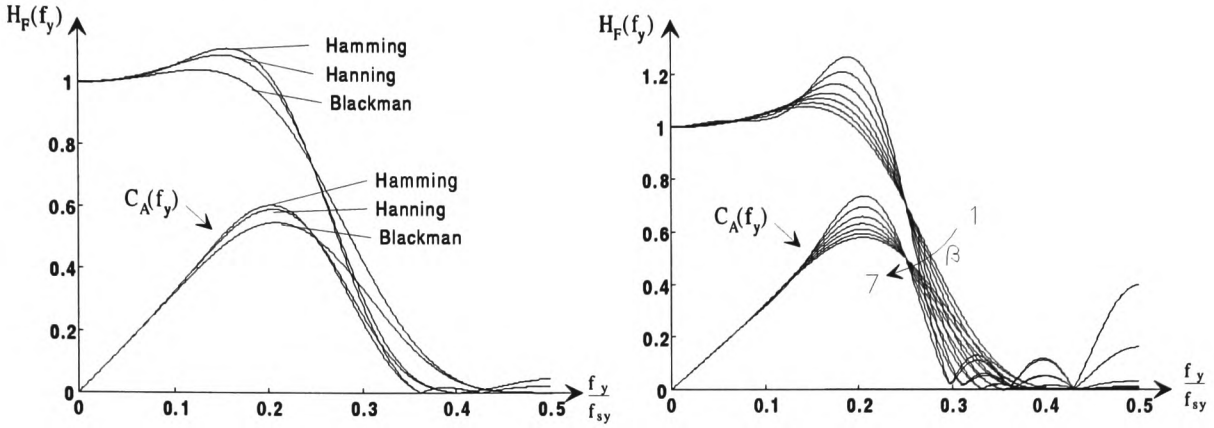

Figure B.4: Form filter responses together with their corresponding $C_A(f_y)$

Table B.1 shows the classification for different windows and filter orders, derived for an interpolation factor from $L = 2$ to $L = 4$. It can be found, that the Kaiser window is slightly superior compared to the Hanning window however, only minor changes are possible within the variations of window types and filter order. The major effects occur due to increasing the interpolation factor.

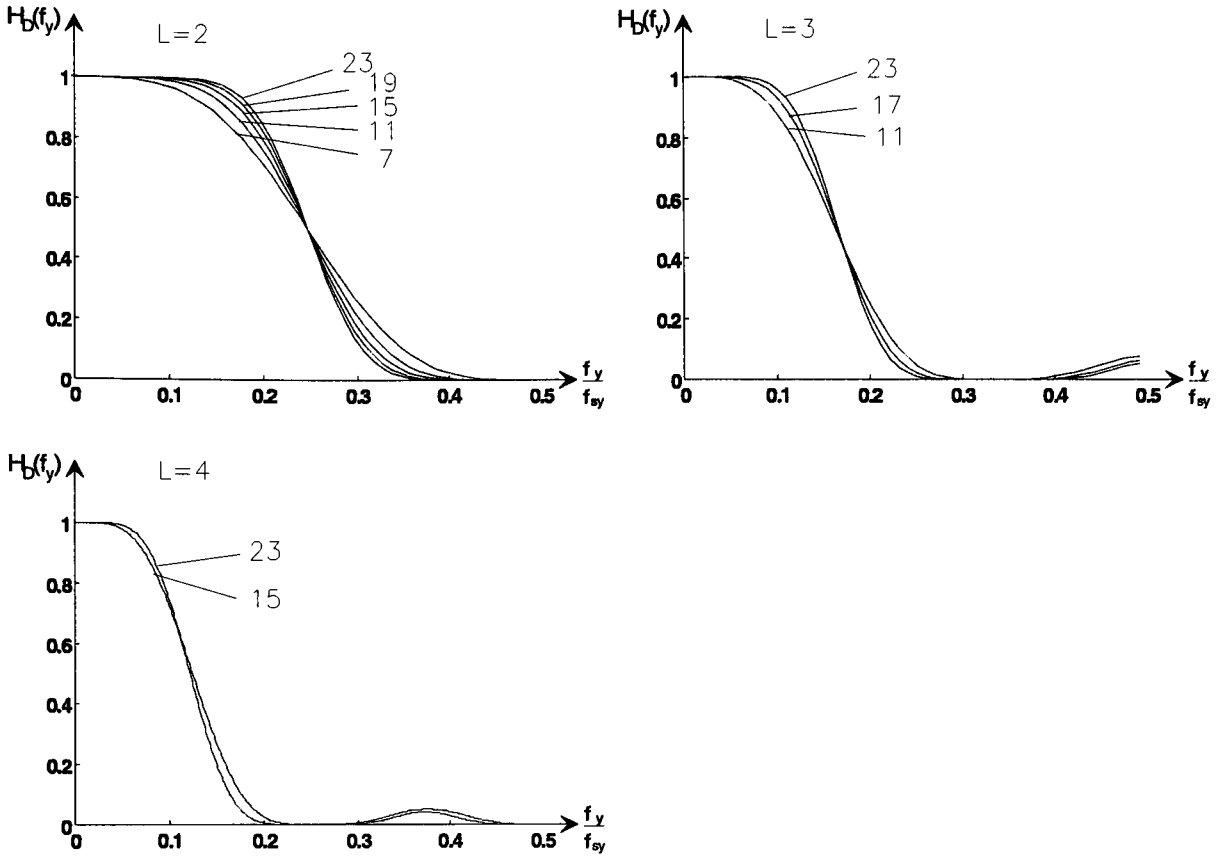

Figure B.5: Filter responses of different filter order for $L = 2$, $L = 3$ and $L = 4$, respectively

B.3 Maximally flat approach

The comparison of the filter design using Lagrange polynomials for interpolation factors of $L = 2$, $L = 3$ and $L = 4$, given in Figure B.5 and Figure B.6, shows clearly that for $L = 2$ the results are similar to that using window design. For $L = 3$ the filters become worse, because of their behaviour in the region of the Nyquist frequency. Also for $L = 4$ this design approach is not efficient enough as shown in Table B.2.

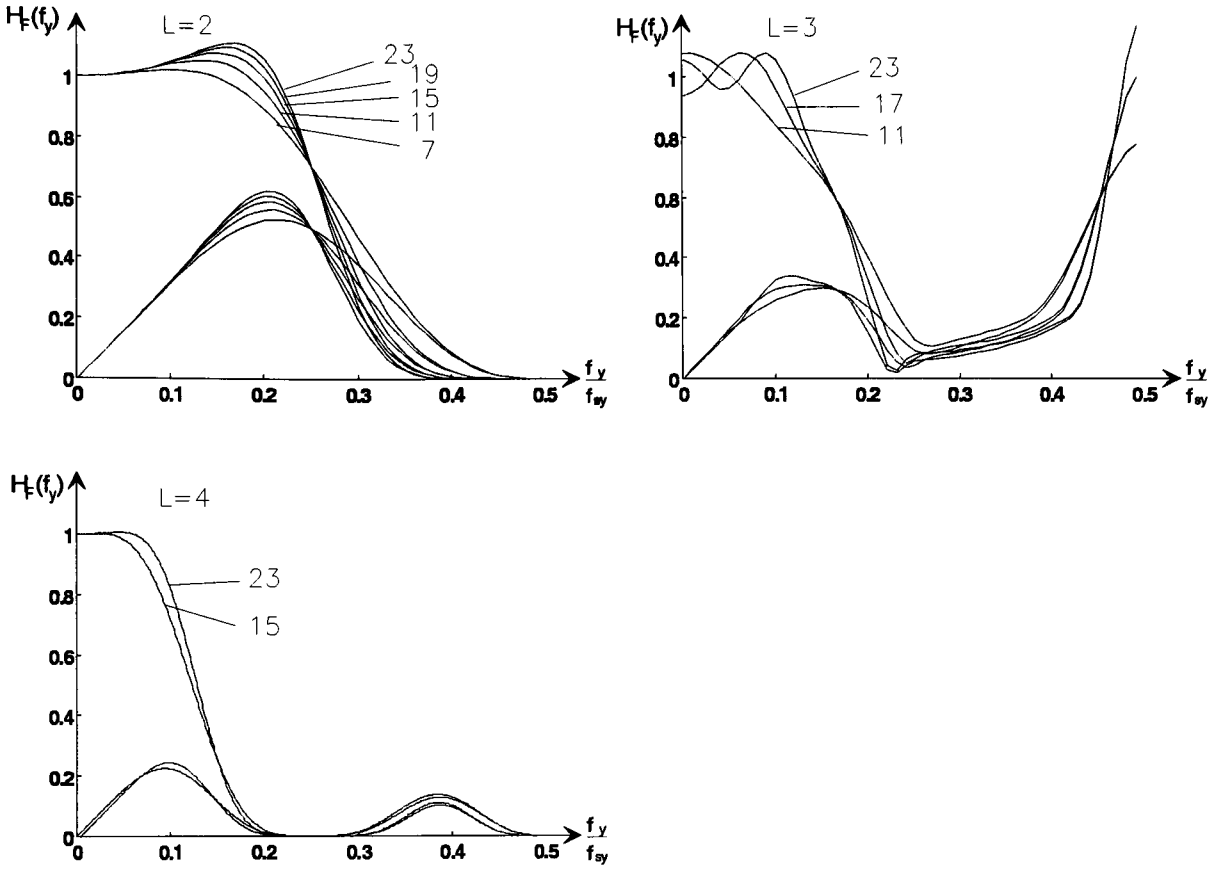

Figure B.6: Form filter responses together with their corresponding $C_A(f_y)$

Filter taps	7	11	15	19	23
$L = 2$	0.265	0.249	0.242	0.237	0.234
Filter taps		11		17	23
$L = 3$		0.249		0.240	0.230
Filter taps			15		23
$L = 4$			0.077		0.068

Table B.2: Efficiency of Lagrange filter design for different filter order and $L = 2$, $L = 3$ and $L = 4$

Appendix C

Real time simulation system

Simulation plays a vital role throughout all research activities. In the initial phase of this work, no suitable environment for video signal simulations was available in the laboratory, so one of the first things was to establish an appropriate engine for real-time simulations. The simulation of moving sequences requires a large amount of memory with the essential feature of real time review and powerful computers to process the enormous data set in an acceptable time. The proposed system can be divided into two parts, namely the software tool to perform the simulation and the sequence storage to provide the real time facility. To be compatible with other activities in the laboratory and further to supply a common environment across the collaborating establishments, the Khoros software package [141] was employed, so that the sequence storage must be integrated into this environment. To provide such test equipment, the development and realisation of a sequence storage unit was undertaken to store and display at least 1.2 seconds of real time video data together with a fast data interface unit. The following functions are defined to be supported by the sequence storage:-

- R-G-B and composite signal input / output,
- real time recording and playback conformance to ITU-R 601,
- full video signal recording (including blanking intervals),

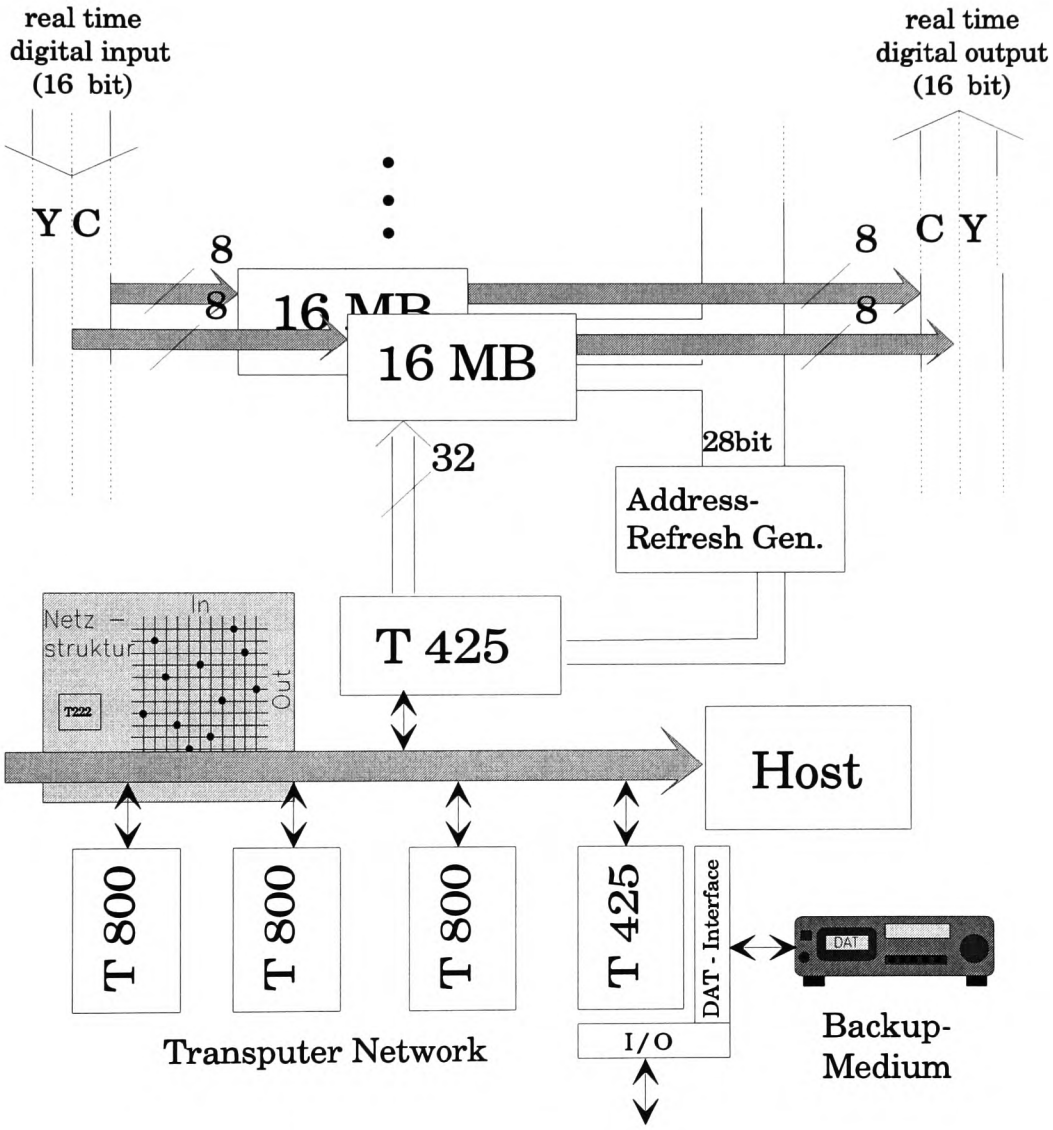

Figure C.1: Block diagram of the sequence storage with multi–transputer support for simulation

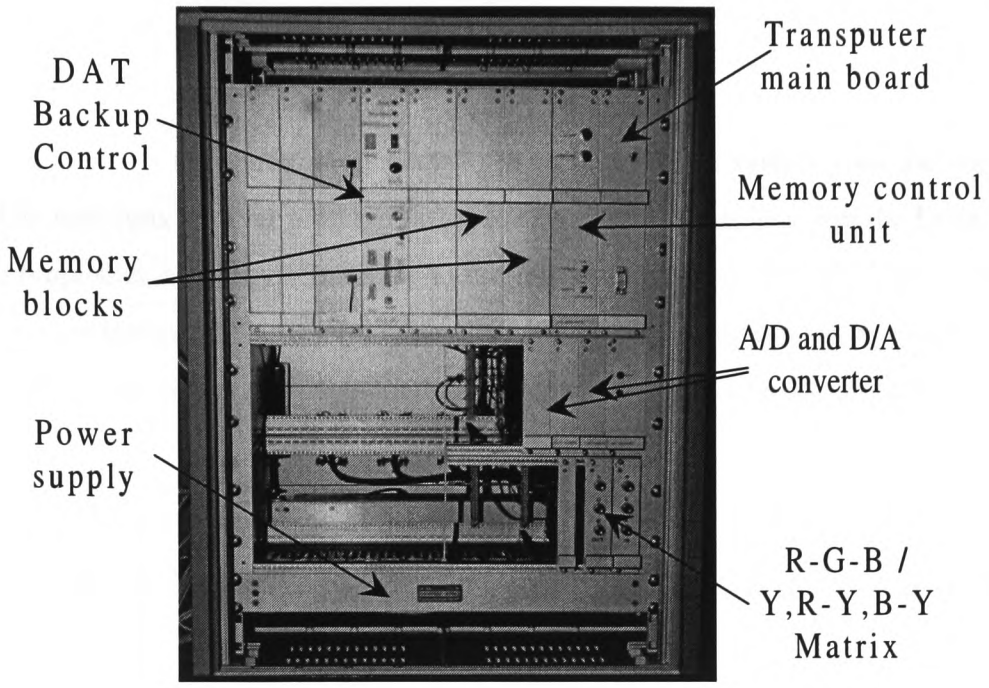

Figure C.2: Simulation system

- modular and extendable memory configuration,
- fast direct memory access,
- comfortable user interface,
- interface to the Khoros simulation environment.

Figure C.1 shows the structure of the realised hardware system. Two 16 Bit real time data busses, for input and output respectively, transfer the digital video in and out of the high speed memory. An additional 32 Bit non real time I/O bus allows random data access through the DMA (Direct Memory Access) interface of the controlling transputer. The address- and refresh generator handles the memory specific signals and generates the addressing to ensure the correct real- and non real-time data flow. The memory itself, is divided into $16MByte$ blocks, which are realised by 16 common $1MByte$ computer memory modules, so an upgrade can be easily achieved. Two memory blocks are currently implemented to support the 16 Bit real time bus. For the ITU-R 601 interface this bus is split into two halves,

allocated to the luminance and the two multiplexed chrominance signals respectively, where for composite inputs a more accurate resolution is applicable.

The controlling transputer is connected via an internal bus system with the host computer. The host runs a server program that provides distributed access over the Ethernet and thus accomplishes a common interface to the real time memory storage from the Khoros simulation environment. The internal transputer bus system is designed to be extendable and configurable. This allows a multi-processor implementation and provides parallel simulation conditions.

Figure C.2 shows the picture of the system and Figure C.3 the main individual components. The standard computer memory modules are clearly visible. The transputer main board, shown in Figure C.2b, is designed to carry eight transputer modules (TRAMs), however only two were currently implemented, because the parallel simulations facility are not used. Figure C.3c shows two different host interface cards, an active and a passive version, where only the active full transputer system included with the aim of occupying no host CPU resource during operation.

Finally Figure C.4 gives an insight to the complete simulation work place.

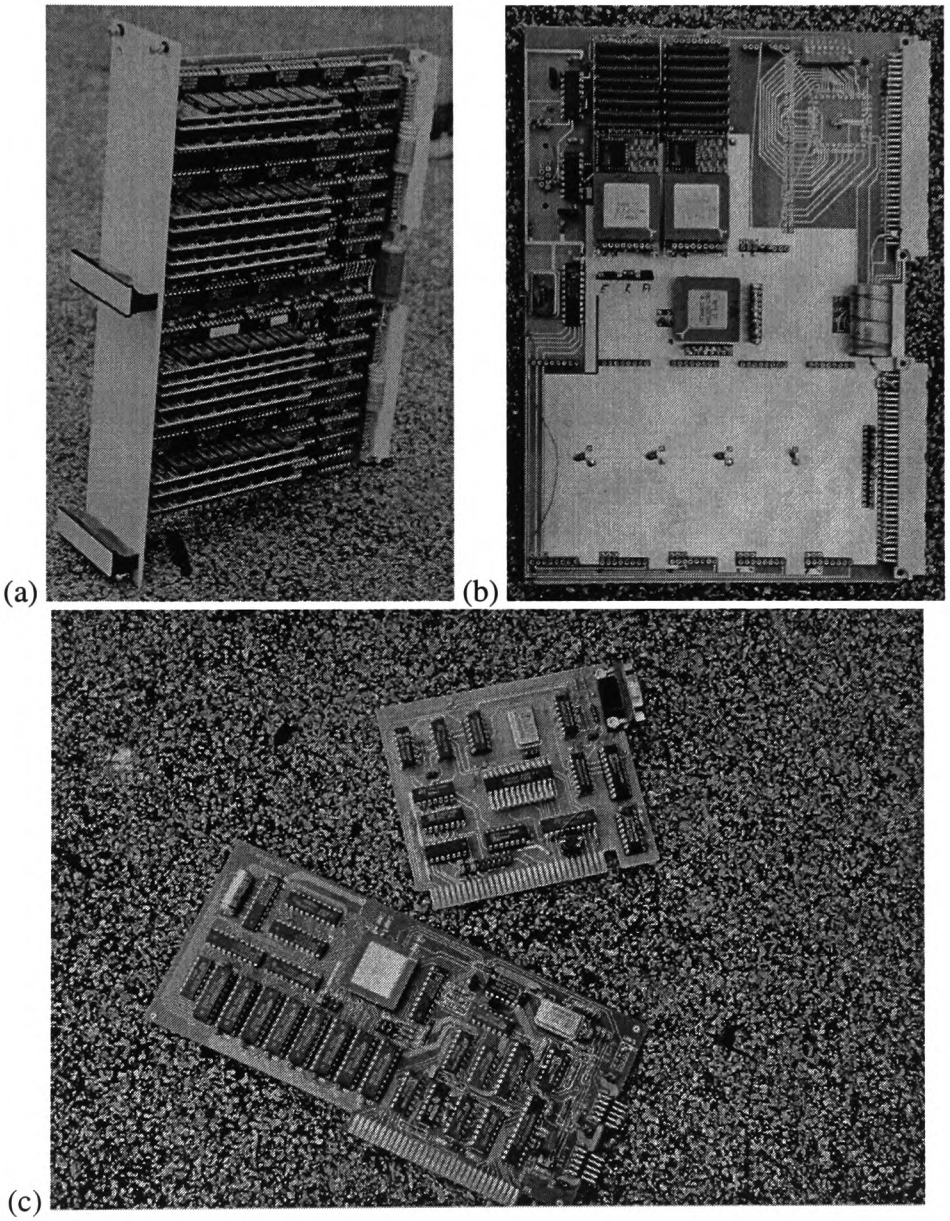

Figure C.3: (a) Sequence storage memory block (b) Transputer main board (c) Transputer / Host interface cards

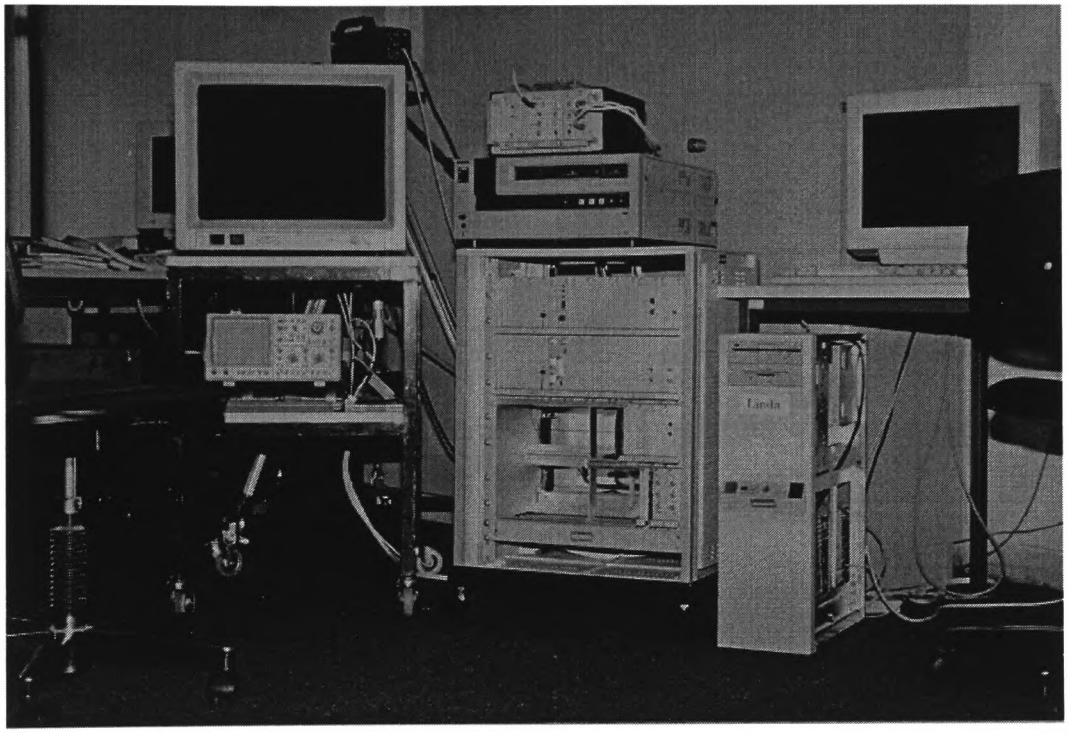

Figure C.4: Simulation working place

Appendix D

Selected Journal Paper Publications

A PALPLUS COMPATIBLE HDTV ENCODER SYSTEM

G. Schmidt,[1] L. S. Dooley,[2] and W. P. Buchwald[1]
[1]FH-Wolfenbuettel, Fb-Elektrotechnik, Germany
[2]University of Glamorgan, Dept. of Electronics & I. T., Wales, UK

ABSTRACT

This paper presents a new implementation for realising PALplus signals from High-Definition Television (HDTV) transmissions. A proposed encoder design is introduced, which decomposes the HDTV input into two separate channels, the first of which subsamples the input signal to produce the standard resolution TV signal, and the second derives a digitally compressed residual component. The problems of non-uniform line structure due to the decimation of an interlaced signal are addressed, as are the visible distortions caused by aliasing and cross-talk effects, with appropriate solutions presented. Finally the important issues of colour enhancement and the composition of the compatible signal are briefly discussed.

1. Introduction

PALplus is a recent European development aimed at overcoming the system dependent limitations inherent in normal PAL TV systems. It was developed primarily as a terrestrial counterpart to the D2MAC (Multiplexed Analog Components) standard, which is used in satellite communications. The normal 4:3 aspect ratio for PAL signals has been widened to 16:9, so it has the same format as D2MAC, but without the corresponding loss of compatibility with standard TV receivers [1]. It also means however, that PALplus does not provide any overall improvement in picture resolution, in comparison with HD-MAC (High Definition MAC), the D2MAC compatible HDTV broadcasting proposal.

The failure of MAC to be universally accepted as the future TV-standard has once again focussed attention upon high definition transmission systems, with the main areas of activity being predominantly concerned with seeking replete digital solutions. This paper deals with the equally important issue of compatibility, in particular between PALplus and HDTV signals. In contrast to earlier research [2][3][4][5] into HDTV compatibility, the solution presented in this paper requires no additional channel capacity for transmission. Using a PALplus signal as the compatible reference, instead of a standard PAL signal implies a consistent 16:9 aspect ratio format, together with the added benefits of less cross-colour and cross-luminance distortion. It is the combination of the PALplus coded signal together with a high resolution, digitally compressed component, which is derived from efficient data compression techniques, that affords the opportunity of transmitting an HDTV signal in a compatible manner.

Fig. 1 shows the complete block diagram of the proposed encoder. The input HDTV signal is decomposed into two main components. Firstly, the down-conversion (decimation) section, which generates the standard resolution TV element to be subsequently PALplus coded to form the compatible signal. The second component is a digital augmentation or residual signal, which undergoes further digital compression before being integrated together with the analogue PALplus signal to form the composite HDTV signal.

This paper will concentrate upon the two processing blocks, decimation and residual processing. These will be fully elucidated in section two, following a brief overview of the characteristics of the PALplus system. In the decimator section, the effect of subsampling an interlaced signal is considered and the necessity for motion adaptive prefiltering discussed. The use of Quadrature Mirror Filter (QMF) techniques, in order to eliminate aliased artefacts in the reconstructed signal is also explored. As for the residual processing module, the performance of diagonal filtering methods will be analysed as the initial stage in deriving a compressed augmentation signal.

2. System parameters

2.1. The PALplus signal

In 1989, a European initiative commenced to try and improve the viewing experience of the standard colour PAL TV system. The resulting proposal, called PALplus, embraces a number of significant enhancements, including a wider 16:9 picture format, which is better

The authors wish to acknowledge the funding received under the ARC collaboration from the British Council and the DAAD (Grant No 443)

Manuscript received June 27, 1994

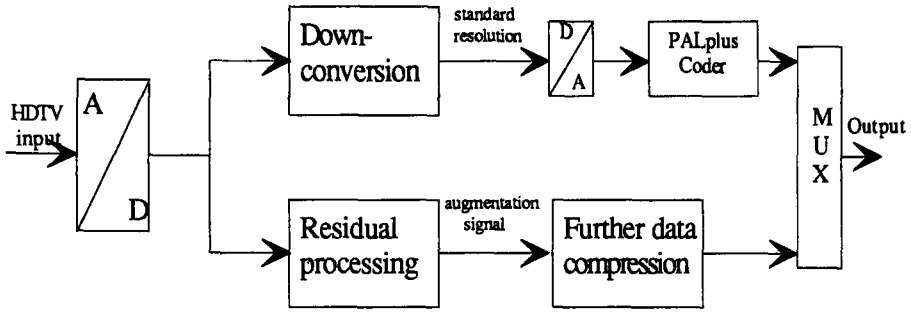

Figure 1: Block diagram of the proposed encoder

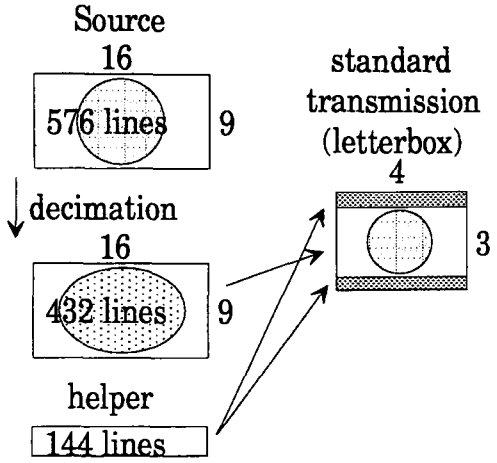

Figure 2: Example of a PAL compatible 16:9 transmission using the "Letterbox" format

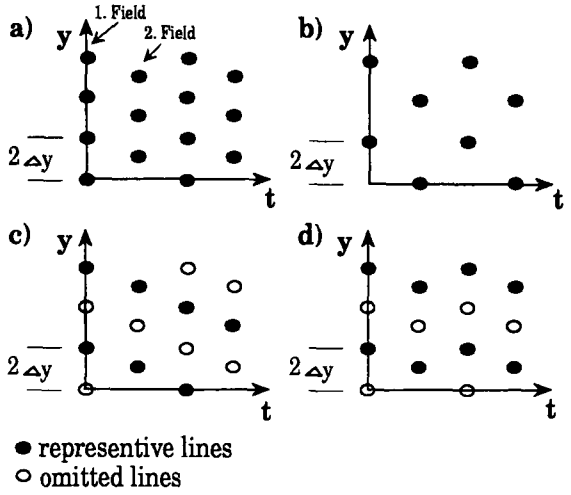

Figure 3: vertical/temporal sampling lattice of a) the input HDTV signal. b) the standard signal. c) the vertically decimated signal without respect to the field. d) as in c) but with the field reset.

suited to the human field of vision, together with a decrease in the cross distortions which afflict ordinary PAL pictures [1]. The other major aim of PALplus is that it should be fully compatible with the standard PAL system.

The issue of compatibility requires that PALplus has to support two different picture geometries, namely 16:9 and 4:3. To avoid visual distortion in standard TV receivers, the coder performs a vertical decimation from 576 active lines down to 432, so providing the correct aspect ratio on all 4:3 tubes, but with black bars appearing at the top and bottom of the screen, in the well known "Letterbox" format, as witnessed in Fig. 2. The additional vertical information necessary for reconstruction in the PALplus decoder, is referred to as the "vertical helper", and is transmitted in the 144 lines which comprise the unused black bars. To ensure that this information is not visible, it is modulated with the colour sub-carrier and attenuated in amplitude. A treatise upon this vertical band-splitting process is given in [6] and [7].

To reduce the effect of both cross luminance and cross colour distortion and thus provide maximum luminance resolution, changes to the PAL coder and decoder have to made, but without compromising the picture quality in standard TV receivers. The requisite signal processing in the PALplus coder and decoder is based on the "Colour plus" technique, details of which are delineated in [8].

2.2. The Down-conversion process

The European HDTV proposed standard is defined as; 1250 lines per frame, 50 fields per second and a 2:1 interlace. Compared with standard TV parameters, it possesses twice the horizontal and vertical resolution, which means that in order to subsample, each dimension has to be decimated by a factor of two.

In contrast to decimation in the horizontal plane, which is straightforward, down-sampling in the vertical plane raises a number of problems because of the

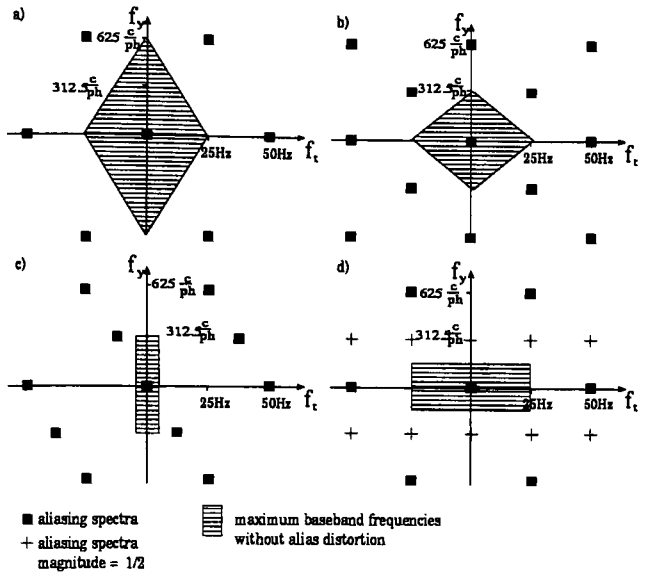

Figure 4: Corresponding spectra for Fig. 3

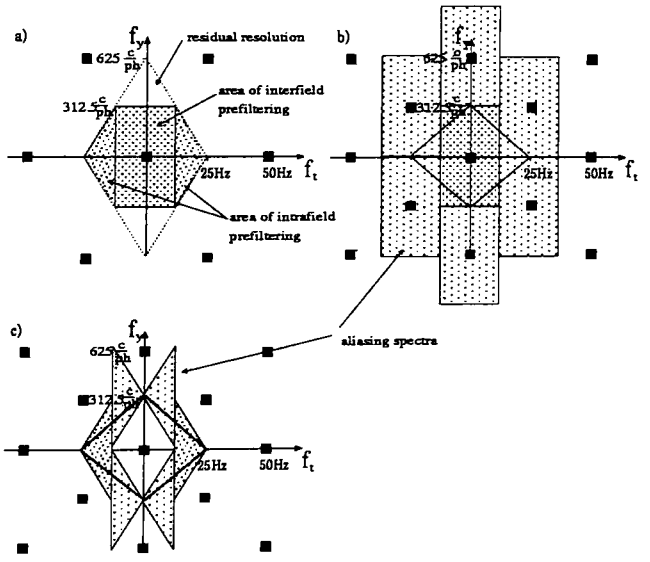

Figure 5: Spectrum of a) the motion adaptive filtered HDTV input. b) the subsampled "little-or-no" motion frequency region. c) the subsampled high motion frequency region.

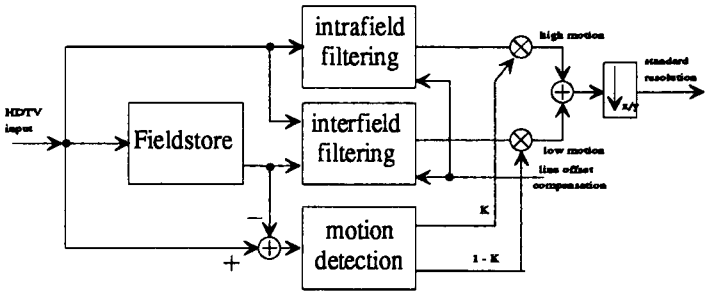

Figure 6: Block diagram of the motion adaptive down-converter used for this application

interlaced nature of the HDTV signal. Fig. 3a shows the vertical/time sampling lattice of such an input signal, while Fig. 3b evinces the equivalent standard resolution. Fig. 4 illustrates the respective spectra corresponding to the line positions given in Fig. 3 [9]. The line positions of the second field in the compatible image are clearly not a subset of those of the input. If this anomaly, caused by the decimation process is ignored, a non-uniform line structure will result as shown in Figs. 3c and d. This leads to additional aliased components being generated (see Figs 4c and 4d), which reduces the resolution to only a quarter, instead of half the input signal.

To obviate this non-uniform line structure, the two fields have to be processed separately. Two distinct prefilters, derived from the same prototype function, are designed to have an identical amplitude response, but different group delays. Switching synchronously with each field between the two filter coefficient sets, will interpolate the lines in every second field to their correct position. Fig. 7a illustrates the loss of resolution which occurs during subsampling without compensating for the line offset. The zone-plate picture represents the full resolution of the HDTV input signal shown in Fig. 4a. After subsampling by two, only a quarter actually remains free from aliasing (Fig. 4d). Fig. 7b shows the same input signal, but now with line offset compensation. The prefilters used in this example are derived from the impulse response given by:

$$h(n) = \frac{sin(\pi * n - 3 + \alpha)}{\pi * n - 3 + \alpha} \qquad n = 0 \ldots 6 \qquad (1)$$

which is an all-pass response, so there is no amplitude distortion. The value of α is respectively chosen as -0.25 and 0.25 for each field, so that the difference in the group delay compensates for the line offset.

When using intrafield filtering, the phase relationship between the two consecutive fields within a frame is not taken into account, so that frequencies greater than half the Nyquist frequency (312.5 c/ph) of the in-

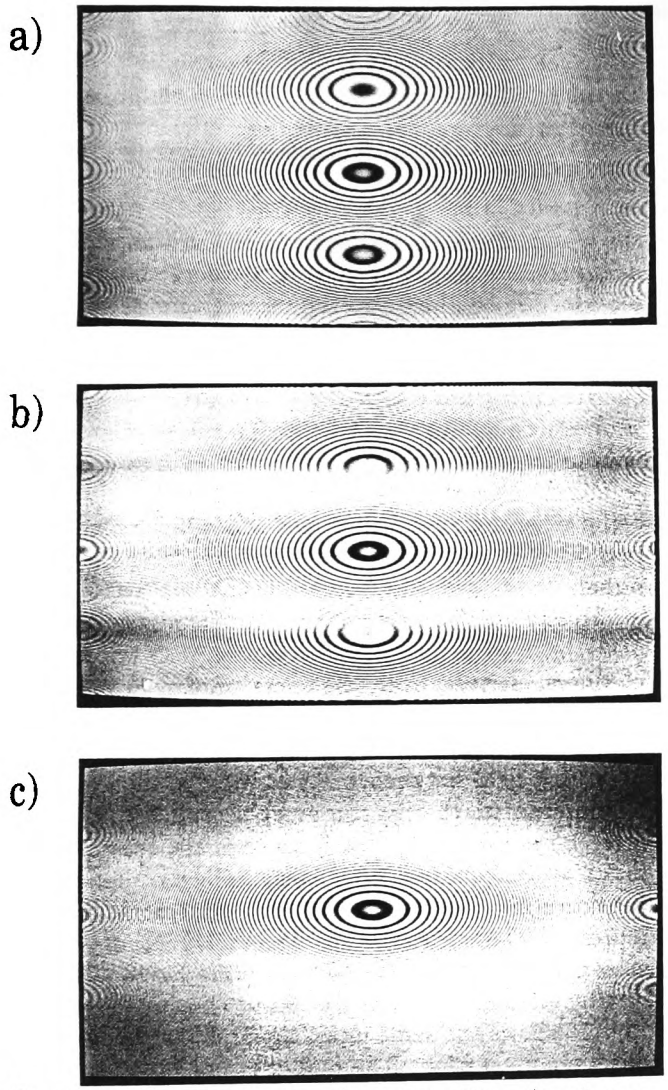

Figure 7: Zone–plate for demonstrating a) subsampling without prefiltering b) subsampling with line offset compensation c) interfield prefiltering with line offset compensation

put signal, are not suppressed and are clearly visible as aliased components. To prevent this unacceptable distortion, an interfield prefilter has to be used. Fig. 7c shows the effect of using such a filter pair. This approach achieves for the down-converted signal, the maximum vertical resolution without any aliasing artefacts, however a feature of interfield filtering, is that it introduces motion blur in moving (non-stationary) scenes.

To combine the advantages of the two prefiltering techniques, that is no motion artefacts in intrafield and maximum vertical resolution in interfield processing, a motion adaptive algorithm is employed in the design. For the case where little-or-no motion is detected, interfield prefiltering is used, whereas if high motion is detected, intrafield processing is performed. Fig. 5 graphically explains the situation. The HDTV input spectrum in Fig. 4a is processed exactly as described above. If it is assumed that an ideal motion detection is present at a temporal frequency of $12.5Hz$, the resultant spectrum will be as shown in Fig. 5a, with the subsampled versions of the spectra for little-or-no motion and high motion shown in Fig. 5b and 5c respectively. Neither of these spectra fit entirely into the aliasing-free frequency region of standard TV receivers, so in certain instances aliased distortion will be visible. In reconstituting the full resolution picture however, these artefacts are not important, since there is no frequency overlap.

The decisive information required to select between the two processing methods, is obtained from a simple motion detector, based upon subtracting the corresponding pixel values from consecutive fields. Fig. 6 provides an insight into the complete down-conversion process.

2.3. Residual processing

Examination of the typical HDTV spectrum in Fig. 8a, reveals that the bandwidth requirement for transmission is at least four times that of the standard TV signal. This means that in the proposed implementation discussed above, the augmentation signal would be responsible for the remaining 75% of picture resolution. To reduce this unrealistic value, efficient data reduction techniques are employed. Two-dimensional diagonal filtering is initially performed to suppress all oblique frequencies in the spatial plane. Subjectively, the loss of such information is acceptable, since the probability of diagonal components occurring is generally much less than for either horizontal or vertical frequencies. The spectral effect of diagonal filtering is illustrated in Fig. 8. It can be seen that the input signal bandwidth is halved without compromising either horizontal or vertical resolution. The standard resolu-

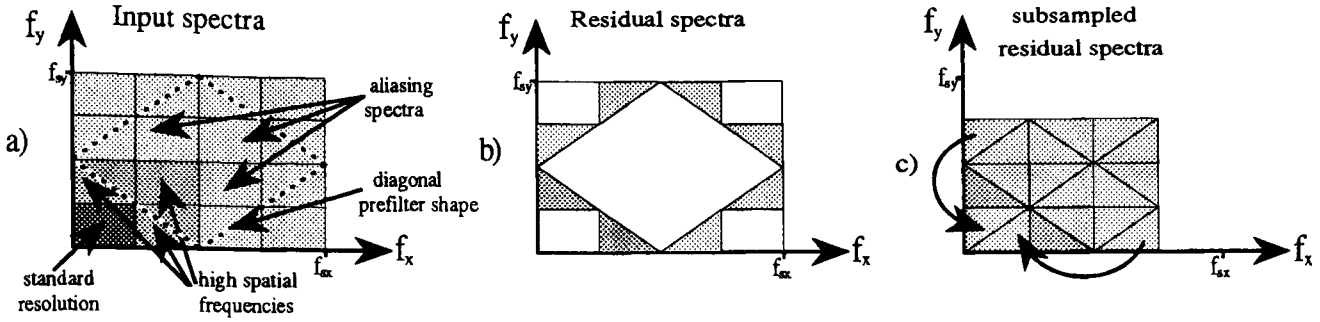

Figure 8: a) typical spectrum of an HDTV source; b) diagonally filtered residual spectrum (without the standard component); c) decimated residual spectrum

tion signal is obtained, with the residual spectrum consisting of only the wedge-shaped high frequency components shown in Fig. 8b. Following decimation by a factor of two, these spectral wedges fold back into the same frequency range as the standard signal, so the requisite bandwidth for the augmentation signal becomes equivalent to that of the normal resolution signal (see Fig. 8c).

The non-ideal characteristics of the prefilters, together with the decimation process in both paths of the proposed encoder in Fig. 1, lead to two different forms of aliased picture distortion. The first results from the band-splitting, highpass-lowpass filter combination, which precedes the subsampling process. The finite transition bandwidth of the two complementary filters means that aliased components, denoted by the horizontal and vertical criss-cross pattern in Fig. 9 are introduced, and will encroach upon the normal resolution signal, as well as the residual spectrum. Such aliasing is clearly visible in standard resolution pictures, so the design of the band-splitting filters has to balance the subjective picture quality with filter complexity, that is the order of the filters. Under a specific set of design conditions, this particular distortion can be eradicated from the reconstituted signal at the receiver, by using a QMF approximation [10]. The QMF filter family exhibit the unique perfect- reconstruction property, with the reconstituted signal being free from aliasing, as well as amplitude and phase distortion, which is a very propitious attribute in this particular application.

The second major source of aliasing error is found only in the residual path and is due to the non-ideal response of the diagonal filter. When the high resolution horizontal and vertical wedges are folded back after subsampling (see Fig. 8c), an overlapping occurs along the diagonal frequency components. The effect of this error upon the residual spectrum is indicated by

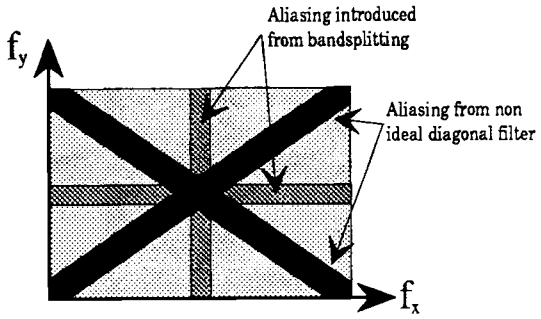

Figure 9: Frequency overlap following the subsampling of the residual signal

the dark oblique criss-cross pattern in Fig. 9, and leads to cross-talk. This is a perceptibly critical and highly visible distortion, since high horizontal frequency components become crossed-over and appear as vertical frequencies and vice versa. The worst possible example of this distortion is shown in Fig. 10, where a horizontal sweep is used as the input signal, that is a signal which comprises only x-direction frequencies between DC and half the sampling rate. The reconstructed picture shows the high vertical frequencies generated by cross-talk. The visibility of these errors is further exacerbated by the interlace, since an additional $25Hz$ flicker is also introduced.

Various diagonal filter designs have been investigated in an attempt to minimise cross-talk distortion, without either compromising overall picture quality or significantly increasing the order of the filter to improve the rate of roll-off. For this implementation, a high-order prefilter is desirable for the coder, such as a 31 by 31 tap response, to ensure maximum cross-talk attenuation, while a much lower filter order is used at the receiver for post-processing. Fig. 11 shows the results of using an 7 by 7 and a 15 by 15 tap linear-phase FIR diagonal filter, designed using a Kaiser window. The re-

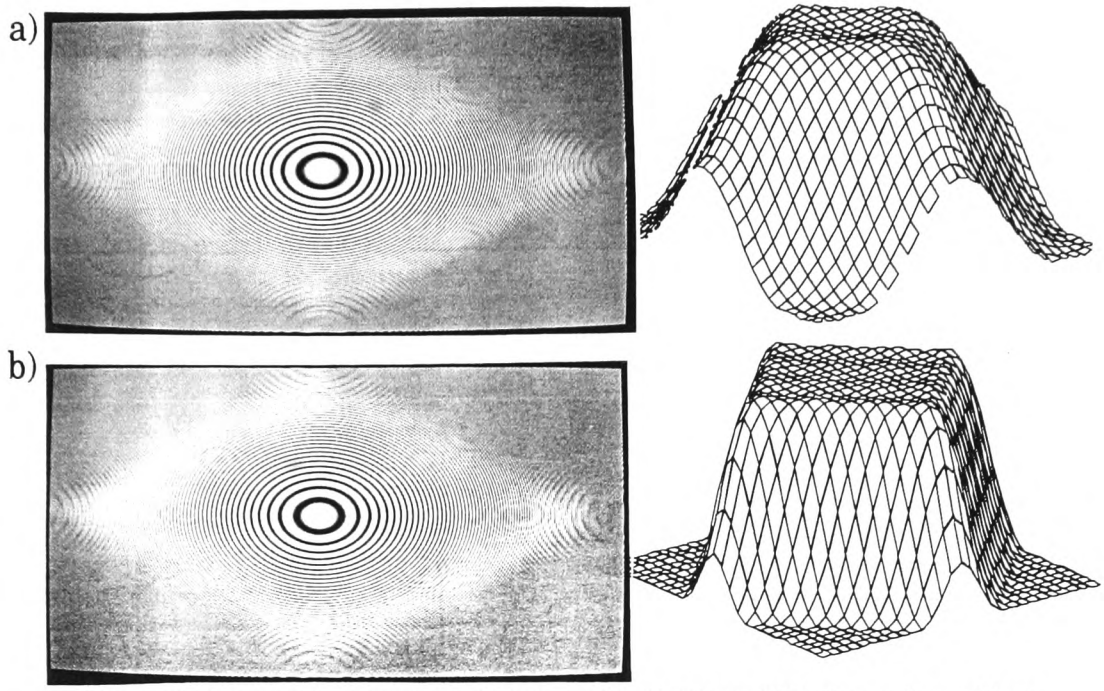

Figure 11: Reconstruction using a) 7x7 tap; b) 15x15 tap FIR diagonal post-filter

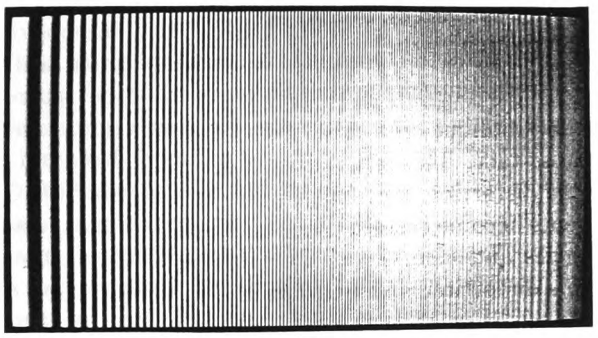

Figure 10: Horizontal/vertical frequency cross-talk

spective filter parameters and frequency responses are furnished in Fig. 12. The 31 by 31 tap FIR prefilter response is plotted in Fig. 12. The higher-order response clearly generates less overlap error because the transition bandwidth of the filter is narrower, though the processing overhead is commensurately greater.

2.4. Further data compression

As alluded in the previous section, the bandwidth of the residual component is equivalent to that of the standard resolution signal, so when amalgamating these two signals together, supplementary compression techniques are required, in order to achieve as high a data reduction ratio as possible. The merits and demerits of

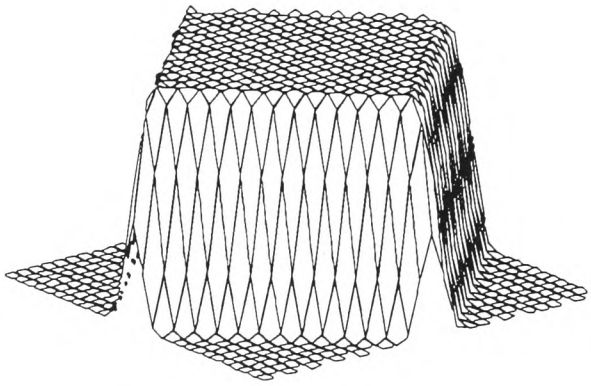

Figure 12: Frequency response of a 31x31 tap FIR diagonal prefilter

applying traditional lossless and lossy compression algorithms will now be analysed. Contemporary lossless techniques typically provide a maximum compression rate of only two, which is clearly not sufficient for this particular application. The generic family of Differential Pulse Code Modulation (DPCM) schemes is not very efficient either, because the residual component is already a differential signal. In essence therefore, the minimum compression ratio that has to be achieved is at least 30, so a more sophisticated approach is necessary. Using intrafield methods, such as the ubiquitous Discrete Cosine Transformation (DCT), which is defined in the Joint Picture Expert Group (JPEG) still-image compression standard [12], raises a number of problems. The most fundamental of these is that the quantizing tables used for the DCT coefficients, are no longer consistent with the spectral properties of the residual signal. The subsampling process illustrated in Fig. 8c, exchanges the spectral locations, so that for example, the DC level now represents the highest frequency component. This means that the DCT quantizing tables have to be modified, as they are normally optimized for the complete reverse situation, where the DC level is the average brightness and the AC coefficients represent the horizontal, vertical and diagonal frequency components. In comparison to these lossless schemes, considerably more care has to be exercised in general, when using lossy intrafield compression techniques, because both the residual component and the standard resolution signal, consist of spectral elements which are intended for alias compensation at the TV receiver. Distortions introduced by the lossy nature of a compression algorithm can very easily compromise picture quality by introducing additional aliasing artefacts. It is not always the case that such distortion is visually apparent, but the viewer's subjective impression of the picture quality must be taken into account in the course of realising any such algorithm.

Of much greater promise are the data compression techniques that are based upon interfield methods and temporal subsampling. Fig. 5a shows that the residual signal component has a maximum temporal resolution of only $12.5Hz$, which affords the possibility of decimating by a factor of two. In addition, bi-directional temporal prediction, which is well known in the context of the Motion Picture Expert Group (MPEG) standard [13], provides considerable potential for reaching the requisite data compression rate. These particular techniques are currently under active investigation.

3. Future Enhancements

3.1. Colour processing

This paper has solely concentrated upon the processing of the luminance signal and the ensuing attempts at achieving high picture quality at low data rates. To date, no colour resolution enhancements have been implemented, which means that the high resolution output signal from the encoder will only possess the colour resolution of a normal PAL transmission. In the vertical direction the effect of this limitation is not too dramatic, since the human eye perceives the luminance components, which compensate somewhat for the hiatus. In the horizontal direction however, the effect it is very poor and the loss of colour resolution clearly visible. Hence, in the final implementation of the PALplus compatible encoder, a second residual signal path is derived which will contain all the necessary horizontal colour resolution information, in order to provide a balanced colour impression at the receiver.

3.2. Composite Signal Format

The other major task required in the proposed system, is the final integration phase of the digital residual component, with the standard analogue PALplus signal, without compromising compatibility. Modern digital multiplexing and modulation techniques appear to afford considerable potential to solve this particular issue and research is continuing in order to achieve the best overall format for the compatible signal.

4. Conclusions

This paper has proposed a new processing system, which affords the possibility of deriving a compact encoded signal, which facilitates HDTV transmissions that are PALplus compatible. The encoder design has been fully elucidated, together with the various constituent modules that have been implemented. The important perceptual errors of aliasing and cross-talk in the residual processing path have been highlighted and solutions presented to minimise their deleterious effects. The introduction of a motion-adaptive prefilter has also been discussed, to enable the encoder to combine the epithets of both intrafield and interfield processing in the subsampling signal path. Finally, two prospective developments, which are necessary for full compatibility were introduced, namely enhanced colour resolution and the format of the composite output signal.

5. References

[1] A.Ebener, E.Matzel, R.Marcom, R.Ochs, U.Riemann, M.Silverberg, R.Storey, F.Vreeswijk, and D.Westerkamp. PALplus: transmission of 16:9 pictures in a terrestrial PAL-Channel (german). *FKT*, 46(11):733–739, 1992.

[2] H. Sauerburger and L. Stenger. Transmissions of HDTV signals using two satellit channels(German). *Rundfunktech. Mitteilungen*, 28(5):235–240, 1984.

[3] H. Sauerburger and L. Stenger. Preprocessing and digital coding of HDTV signals (German). *Frequenz*, 37(11/12):288–298, 1983.

[4] B.G. Haskell. High definition Television (HDTV)–Compatibility and distribution . *IEEE Transactions on Communications*, 31(12):1308–1317, 1983.

[5] Mikhail Tsinberg. ENTSC two–channel compatible HDTV sytem. *IEEE Transactions on Consumer Electronics*, 33(3):146–153, 1987.

[6] Chr. Hentschel. Bandsplitting for sampling rate conversion for a PALplus transmission (German). *FKT*, 46(11):742–754, 1992.

[7] T. Herfet. Band–splitting for compatible 16:9 transmission (German). *Rundfunktech. Mitteilungen*, 35(1):29–35, 1991.

[8] R. Kays. A technique for improved PAL–coding and decoding (German). *FKT*, 44(11):595–602, 1990.

[9] D.E. Dudgeon and R.M. Mersereau. *Multidimensional digital signal processing.* Prentice – Hall, INC, 1984.

[10] P.P. Vaidyanythan. Quadrature mirror filter banks, M–band extentions and perfect reconstruction techniques. *IEEE ASSP magazine*, 4(3):4–20, 1987.

[11] B. Vergin. Image data compression by subsampling using two dimensional spatial filters. *Dipl. thesis at University of Glamorgan / Fachhochschule Wolfenbuettel*, 1994.

[12] W.P. Pennebacker and J.L Mitchell. *JPEG still image data compression standard.* Van Nostrand reinhold, 1988.

[13] ISO/IEC DIS 11172. Coding of moving pictures and associated audio for digital storage media up to about 1,5 Mbits. *Draft international standard*, 1992.

Biographies

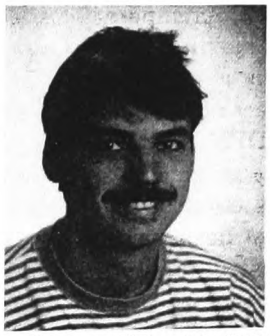

Gunnar Schmidt (M'93) was born in Braunschweig, Germany in 1966. He received his Dipl-Ing. degree in Electronics and Communication Technology in 1990 from the Fachhochschule Braunschweig/Wolfenbuettel, Germany. Since 1990 he has been working with the video signal & picture processing group in the Department of Communication Technology at the Fachhochschule Braunschweig/Wolfenbuettel. He is currently a registered research student in the Department of Electronics and Information Technology at the University of Glamorgan, Wales, studying for his Ph.D. degree.

His main research interests are in the fields of digital signal processing, HDTV systems, video technology and digital data compression techniques.

Laurence S. Dooley (M'81-SM'92) was born in Cwmbran, Wales in 1959. He received his B.Sc., M.Sc. and Ph.D. degrees in Electrical and Electronic Engineering from the University College of Wales, Swansea in 1981, 1983 and 1987 respectively. He worked as a consultant engineer for industry, principally in the area of digital sound synthesiser design for Marine and Bridge simulator systems, before joining the Department of Electronics and Information Technology at the University of Glamorgan in 1986, where he is currently a Senior Lecturer. In 1989 he was a Visiting Scholar in the Department of Electrical Engineering at the University of Sydney, NSW, Australia.

His main research interests are in the fields of digital signal processing, HDTV and video technology, wavelets and neural networks. He is a Senior Member of the IEEE, a Chartered Engineer (C.Eng), a corpo-

rate member of the British Computer Society, the Society for Computer Simulation and the European Society of Signal Processing.

Prof. Dr. Wolf-Peter Buchwald was born in 1954. He studied Communication Technology at the Technical University of Braunschweig, Germany, where he received his Ph.D. degree in 1986. In 1989 he was appointed Professor in Communication Technology and Digital TV techniques at the Fachhochschule Braunschweig/Wolfenbuettel, Germany. He has provided a number of course for industry in the general area of digital video technology.

His main research interests are in the fields of digital signal processing, in particular relating to CCD sensors and digital video signal processing.

A NOVEL MODULATION STRATEGY FOR INTEGRATING DIGITAL SUB-CHANNELS WITHIN A PAL/PAL PLUS SIGNAL

G. Schmidt[1], W. P. Buchwald[2] and L. S. Dooley[3]
[1,2]Fachhochschule Braunschweig/Wolfenbuettel, Fb-Elektrotechnik, Germany
[3]University of Glamorgan, Dept. of Electronics & I.T., Wales, UK

Abstract—**This paper presents an original methodology which facilitates the modulation of digital signals within the active video portion of a conventional analogue PAL/ PALplus television signal. The resultant crosstalk distortion errors which ensue are analysed and a model postulated that enables optimization of a number of important system parameters. It will also be shown that applying this model enables a balancing of subjective quality with data-rate.**

I. Introduction

Substantial research has been undertaken over the last few decades with the explicit goal of enabling digital data transmissions to be embodied within a standard analogue television (TV) channel. The potential benefits accruing from such an intent are manifold, since for a given infrastructure extra multimedia services are feasible. Supplementary programme information, electronic TV guides, multi-lingual high quality audio and special Personal Computer (PC) downloading services are only a flavour of some of the possibilities afforded.

Previous research activities which have explored the use of sub-channels within a television signal, have primarily focused upon high definition (HDTV) and extended definition (EDTV) compatibility approaches [1,2], where the extra resolution is analogue modulated, so that it can be transmitted within these channels. The crucial compatibility issue when attempting to integrate digital data within a TV signal, is to ensure that the appearance of any picture distortions is not perceptible, which in reality tends to involve a trade-off between subjective quality and achievable data rate. To accomplish this objective three distinct possibilities can be identified :

(1) data insertion in the blanking period,

(2) data insertion in the active video,

(3) data insertion outside the video signal, but within the same channel.

In Europe, a practical example of TV data transmission from the first category, is the well-known Teletext system, which modulates digital information on the unused lines in the vertical blanking period. The maximum data rate that can be achieved however is far too low for multimedia applications. Another fully compatible system presented in [3], provides a raw 150kBit/s data rate using spread spectrum technology, while a proposition for the American NTSC television system, called VBI (Vertical Blanking Interval) [4], was made by WavePhore, USA. This system occupies the first ten lines of each field and thus also provides a 150kBit/s data rate.

Interestingly, another WavePhore system, called TVT1 includes data outside the video signal [4], by placing an additional carrier between the colour and sound carriers. This is an example of the third category, which also includes such systems as that proposed by Dinsel [5], involving an additional carrier, modulated by a 16 Quadrature Amplitude Modulation (QAM), which is subsequently modulated by the sound carrier. This technique enables a typical throughput of between 128 and 196kBit/s.

Summarising these general findings suggests that the maximum achievable data rate is bound to approximately 200 kBit/s. To achieve higher rates means that the second of the above alternatives must be considered, where data is inserted within the active video signal. In adopting this strategy, one must always be mindful that such methods inevitably encroach upon the sensitive issue of compatibility. Early research in this area [6, 7] used a correlation decoder for demodulating the data signal, which was modulated with a subjective optimised carrier at very low amplitudes. Another novel approach was proposed by Ruppel [8], who employed QAM of the picture carrier and obtained a data rate of 500kBit/s.

The technique discussed in this paper also belongs to this second category and is based upon a QAM of the colour sub-carrier [9]. In [10, 11, 12] during the development of the European PALplus widescreen standard, a variant of this arrangement was proposed for modulating additional widescreen information. In practice however, the proposed method was purely analogue-based and never implemented as part of the standard.

Manuscript received June 17, 1998

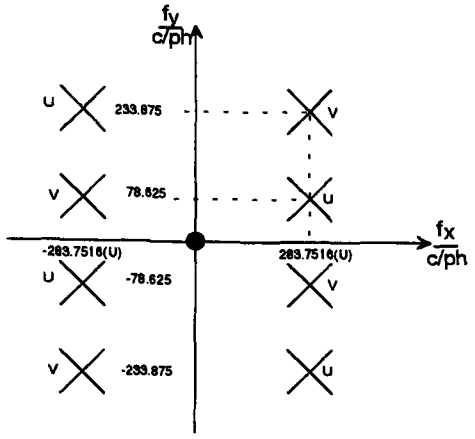

Figure 1: Colour carrier positions for U and V components

II. Overview

A. Principles

In contrast to the NTSC-system, where the two colour difference signals I and Q are quadrature modulated, PAL alternates the phase of the V-component carrier between 90 and 270 degrees from line to line, where the U-component is fixed to the 0 degree carrier phase. **Figure 1** shows the location for the two modulated colour components in the horizontal / vertical frequency plot of the PAL television signal. The switching leads to a spectral offset of the two colour components in the three dimensional frequency domain, with the V-carrier modulated on its 90-degree phase and the U-carrier on its 0-degree. Hence, both frequencies can be additionally modulated by using the respective orthogonal components and provide two sub-channels which are suitable for further digital transmission. For realisation, the carrier phase of the "digital U-component", D_U, must turn between 0 and 180 degrees from line to line during the carrier phase of D_V is fixed to 90 degrees. **Figure 2a)** displays this more graphically for the given colour and data vector F and D in two consecutive lines n and n+1. Their addition forms the output vector S, which undergoes the usual further processing before transmission. In the receiver, at the PAL line delay, the vector sum of two neighboured lines is derived so that the U and D_V signals are obtained from the in-phase and quadrature components respectively and also in the same way V and D_U from the colour vector difference (**Figure 2b)**). This perfect possibility of separation is only valid if the neighboured lines have identical content, which is not what happens in reality so that crosstalk distortions will occur.

The block diagram in **Figure 3** provides an insight into the conceptual implementation of the aforementioned technique. The colour signals, U and V, are processed as usual with the subtle difference that a vertical lowpass, $H_U(f_y)$ and $H_V(f_y)$ component is added in each signal path (see next section). The data stream is initially split into two channels which operate at half the original data rate before subsequently form filtering. This filter together with the ensuing up-sampling and vertical interpolation is part of the two dimensional form filtering technique detailed in Section III. Following modulation as alluded to above, the resulting data vector is added to the colour and multiplexed with the luminance. At the decoder, after luminance / chrominance separation, the colour data signal is processed by the PAL line delay, which splits it into components whose carrier phase respectively alternates and remains fixed (V, D_U and U, D_V respectively). Finally the demodulation provides the reconstruction of each signal. The post filters are necessary to suppress higher order frequency parts from the demodulation and for the data signal parts, to suppress the single sideband components from the colour signal. At the end, the two data channels are combined to rebuild the original data stream.

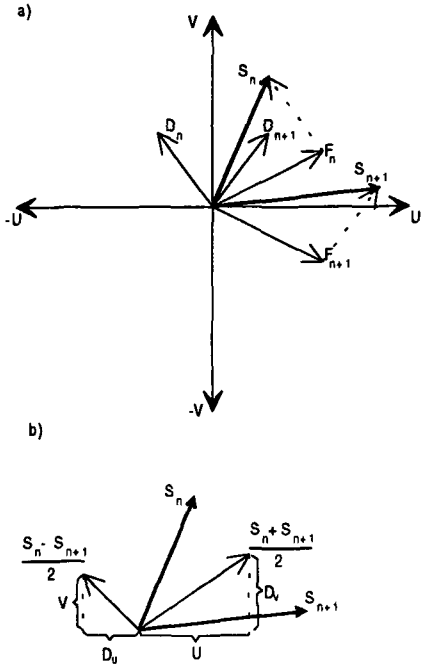

Figure 2: a) Colour and data vector addition at the encoder and b) demodulation at the receiver

B. Cross talk distortions

The highest priority must be given to the issue of compatibility with standard TV-sets, which is the consistency of an implemented data stream with the ordinary decoded video signal. The previously mentioned crosstalk effects are the major error source for degrading the subjective quality of the compatible video signal.

Two specific forms of crosstalk distortion will be considered. Firstly, *intra-carrier crosstalk*, where D_U

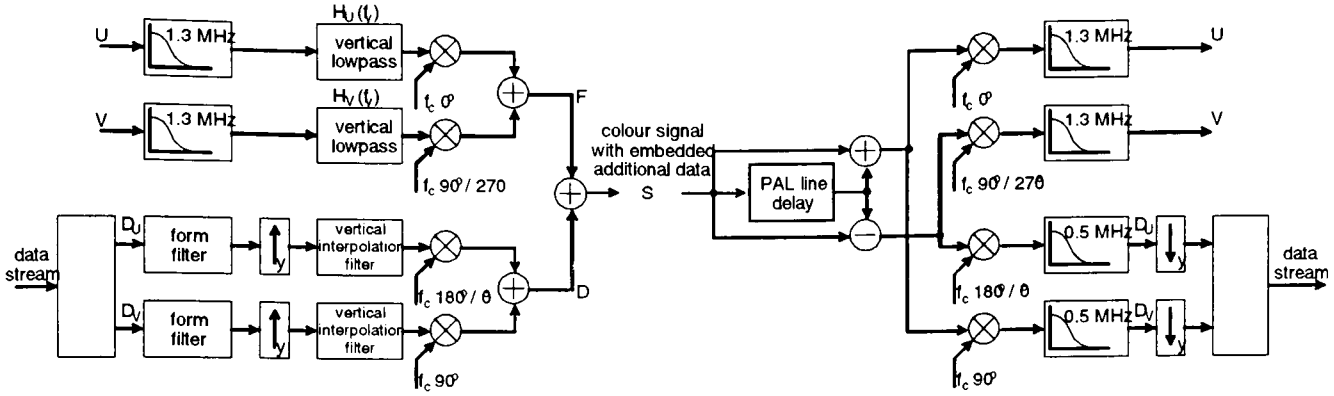

Figure 3: Block diagram of the encoder-decoder structure

and D_V crossover and appear as their quadrature parts, which are of course the colour signals, and secondly *inter-carrier crosstalk*, where the two digital components are demodulated at the wrong carrier frequency. In both cases, the resulting distortions will appear as visible colour noise, which directly impinges upon the perceived picture quality.

The cause of intra-carrier crosstalk distortion is the non-symmetrical interference of the side-bands around the colour carrier, so that perfect demodulation of the in-phase and quadrature components is limited. This happens either because of the overall frequency response during transmission or the data signals exceed their maximum bandwidth range. Employing an equalisation filter, as in the well-known peaking technique for the NTSC system [13], will reduce this first particular effect. The maximum data channel bandwidth is given from the PAL standard. It derivatives B,G,H and I defines a colour carrier frequency of 4.433 MHz together with an overall video bandwidth of 5 and 5.5 MHz for B,G,H and I respectively. This implies that for colour frequencies higher then approximately 0.5 MHz (1 MHz) the modulation becomes single side band and therefore a limitation of the bandwidth where additional quadrature modulation is possible. The design, however, has to guarantee that the bandwidth of the additional data streams does not exceed 0.5 MHz.

The inter-carrier crosstalk distortion compromises the compatibility aspect in a very critical manner. The data signal combination D_U / D_V is uncorrelated, so their spectra are uniform within the three dimensional video frequencies, f_x, f_y, f_t,. The consequence of this is a total spectral overlap between the colour and data signals, and further visible colour noise. Filters must be included to define definite locations for each component and thus attenuate these effects. The U / V separation of the PAL line delay at the receiver also has to be considered, because its poor separation limits the possibility of a perfect overall separation.

Another source of cross distortion is the converse scenario of the above discussion, where the colour is crossing over and affects the data channels. These errors are not so critical, because the issue of compatibility is not influenced and the subsequent disturbances impinge only upon the digital data stream, which is inherently more robust. Two different sources for these distortions can be distinguished. Firstly, the colour signals cross over and secondly inter-carrier crosstalk between the two data channels.

The colour signal crosstalk arises from high vertical frequency components in the picture contents. The probability of those components is generally less in a natural scene however, a vertical filter with a cut-off frequency of at least one half of the vertical Nyquist frequency has still to be included in order to attenuate this effect and thus reduce the error rates. As well documented in the D2MAC TV [14] transmission system, such filtering does not compromise subjective quality, so the same vertical colour pre-filter is suggested in this application.

The inter crosstalk between data channels is limited due to the aforementioned spectral forming. In formalising the development of the proposed solution, the encoder-decoder implementation for the data stream is directly equivalent to the transmultiplexer structure proposed by Verterli [15]. By selecting a special set of filter responses, all aliasing, amplitude and phase errors can be eliminated and perfect separation achieved. This however excludes the possibility of using the PAL line delay for data channel separation, so an additional filter set must be included in the configuration.

III. Encoder Design and Subjective Performance

The encoder design discussed in this paper concentrates primarily on a number of different possible spectral forming filters for the data signals, to avoid inter-carrier cross-colour noise distortion. Their role is most crucial in the context of compatibility and subjective performance.

A. Theoretical analysis

An understanding of the three dimensional spectral position is provided in **Figure 4.** The locations of the modulated colour signals U and V, are given with their carrier position at the centre. The spectra of the embedded data signals are in theory uniformly distributed along the three axes of the 3-D frequency plot, since each data value is uncorrelated both with respect to adjacent line and frame samples. To constrain these spectra to specific locations so avoiding the aforementioned crosstalk effects, form filtering must be applied. Horizontal forming is performed using the traditional filter included to avoid intersymbol interference and ensures that the bandwidth is limited to 0.5 MHz. In addition, either vertical or temporal filtering is necessary to provide non-overlapping frequency regions for the data spectra. Due to the fact that for the colour signal separation at the decoder a vertical filter, the PAL line delay, is used, also for the data channel vertical forming filters are essential.

The vertical filters providing these spectral locations for each data component have to be lowpass. Analysing the distortions raising from crossing over into the colour channels, the data signals passing through mentioned vertical lowpass before subsequently processed by the PAL line delay, which is a sine-shaped high pass response for D_V. Similar argument can be applied to D_U, so the crosstalk attenuation response is the same in both cases and can be readily computed from the relationship:

$$C_A(f_y) = H_D(f_y)\ H_P(f_y) \qquad (1)$$

where $H_P(f_y)$ is the sine-shaped PAL line delay separation, and $H_D(f_y)$ the vertical low pass forming filter for the data signal at the encoder.

Quantifying the aforementioned cross-distortions is very difficult since they only interfere in the colour channel. Their appearance is blocky colour noise which is unusual in comparison with normal noise degradation's and therefore is perceptually very annoying. To provide a quantitative measure, the noise power accruing from the crosstalk data signals is evaluated so both the signal to noise ratio within each colour channel (SNR_U and SNR_V), together with the display signal to noise ratio (DSNR) can be derived. This latter measure is similar to the model published in [16].

Assuming the data signal U_D has a uniform probability distribution function with zero mean over a range from $-\alpha$ to α, the noise power can be computed directly from the variance σ^2. Depending on the number of symbol levels per data channel, which will be for example N=2

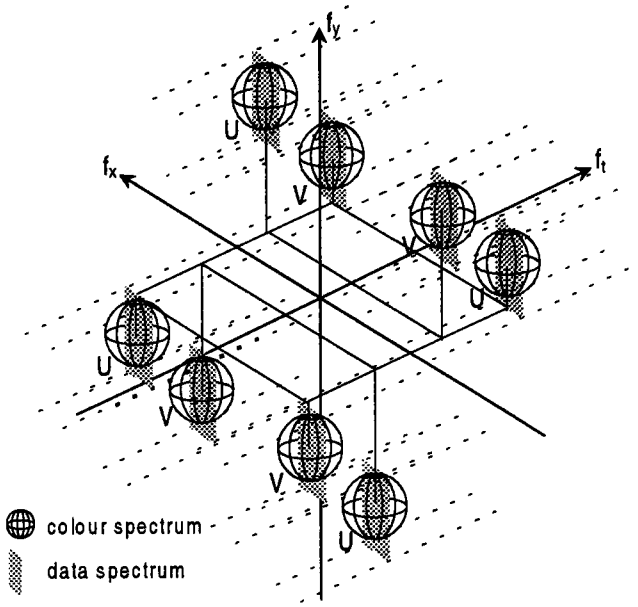

Figure 4: Three dimensional spectrum perspective

for 4 QAM, N=4 for 16 QAM [1] and so on, the following relationship can be used:

$$\sigma^2 = \frac{\alpha^2}{3}\frac{N+1}{N-1}\ ; \quad N \geq 2 \qquad (2)$$

Assuming the conditions of a noise-free transmission, which means ideal filter characteristics for both luminance and chrominance splitting, as well as chroma demodulation at the receiver, so that only the colour difference signals are effected by cross colour noise distortions. The noise power in each colour channel introduced from the data signal is then given as:

$$P_N = \int_0^{fsx}\int_0^{fsy} \sigma^2 \left|H_F(f_x)\right|^2 \left|C_A(f_y)\right|^2 df_x df_y \qquad (3)$$

where $C_A(f_y)$ is the crosstalk attenuation response introduced in Eq. 1 and $H_F(f_x)$ the horizontal forming filter. f_{sx} and f_{sy} are the horizontal and vertical sampling frequency, respectively. If no vertical forming filter is used in the encoder, so that $C_A(f_y) = H_P(f_y)$, Eq. 3 is simplified to

$$P_R = \frac{\sigma^2}{2}\int_0^{fsx} |H_F(f_x)|^2\, df_x \qquad (4)$$

In evaluating the noise performance, the eye weighting function has to be taken into account. In this case however, the noise bandwidth is less than 0.5MHz where the eye's perception has nearly no degradation [17]. The same situation is assumed for the luminance/chrominance separation and also for the

[1] The noise power is evaluated separately for each channel.

colour post filters, so that only $C_A(f_y)$ and $H_F(f_x)$ have to be considered.

From Eq. 3 the signal to noise ratio (SNR) is given as

$$\left.\frac{SNR}{[dB]}\right|_{U,V} = 10\log\frac{P_{U,V}}{P_N} \tag{5}$$

The maximum peak-to-peak signals for U and V are different and are [18]:

$$U=0.612V_{p\text{-}p}$$

$$V=0.861V_{p\text{-}p}$$

So the inter carrier crosstalk can be qualified:

$$SNR|_U = 10\log\frac{0.375V^2}{P_N} \tag{6}$$

$$SNR|_V = 10\log\frac{0.741V^2}{P_N} \tag{7}$$

From this objective SNR measure, a more subjectively oriented method is derived, whose basis is a modification of the DSNR definition in [16]. This technique takes cognisance of the fact that the crosstalk noise encroaches upon the principle of constant luminance, which implies an additional crosstalk into the luminance component, because of the non-linearity of the picture tube, a phenomena known as the gamma law.

Eq. 3 quantifies the distortion within each colour signal, U′ and V′. To assess the visibility at the display, the expression for signal plus noise at the output of the decoder matrix must be derived. With R′-Y′=1.14V′ and B′-Y′=2.03U′ the three distorted primary colour signals are given as:

$$R'+n_R = R'+1.14\sqrt{P_N}$$

$$G'+n_G = G'+0.96\sqrt{P_N}$$

$$B'+n_B = B'+2.03\sqrt{P_N}$$

where $R'=R^{1/\gamma}$, $G'=G^{1/\gamma}$, $B'=B^{1/\gamma}$ are the pre-gamma corrected colour signals and n_R, n_G, n_B the respective cross colour noise distortions. The displayed luminance Y_D at the output of the display tube can be obtained by separately weighting the three primary colour signals and adding each term after applying the gamma law [16].

$$Y_D = 0.3(R'+1.14\sqrt{P_N})^\gamma + 0.59(G'+0.96\sqrt{P_N})^\gamma + 0.11(B'+2.03\sqrt{P_N})^\gamma \tag{8}$$

Using the relationship $(1+a)^\gamma \approx 1+\gamma a$, for $a \ll 1$ Eq. 8 can be written as

$$Y_D = 0.3R+\gamma\frac{0.342R\sqrt{P_N}}{R'}+0.59G+\gamma\frac{0.566G\sqrt{P_N}}{G'}+0.11B+\gamma\frac{0.22B\sqrt{P_N}}{B'} \tag{9}$$

and letting $\delta = 1-\frac{1}{\gamma}$ and adding signal terms in voltage and noise terms in power [16]

$$Y_D = 0.3R+0.59G+0.11B+\gamma\sqrt{P_N}\sqrt{((0.342R^\delta)^2+(0.566G^\delta)^2+(0.22B^\delta)^2)}$$

The DSNR is then given by

$$DSNR = 20\log\frac{Y}{\gamma\sqrt{P_N}\sqrt{((0.342R^\delta)^2+(0.566G^\delta)^2+(0.22B^\delta)^2)}} \tag{10}$$

which can be computed for a given P_N and γ, where P_N is direct related to both α, the data signal amplitude and the number of symbol levels N. For increasing N, Eq. 1 shows that σ^2 moves to a threshold of 1/3 for $\alpha=1$, so a 16-QAM or 64-QAM, N=4 or N= 8 respectively, will balance the DSNR gain with complexity.

B. Filter Optimisation

Two methods will be discussed for the implementation of the vertical spectral forming filter, namely vertical partial response coding and a vertical interpolation technique.

Partial response coding performs a spectral forming by introducing more than two symbols and therefore an energy concentration within a smaller bandwidth. If Duo-Binary coding is considered for instance, the data spectrum becomes cosine shaped, which reduces the crosstalk effects, the cross talk attenuation of $C_A(f_y)$ is however insufficient. Higher order partial response codes will increase this attenuation and the overall subjective performance, but also the number of symbol levels, which decreases the transmission robustness.

The other spectral forming technique involves transmitting data only every n^{th} line, where n is the interpolation factor. This has the effect of reducing the bandwidth of the data signal by 1/n. An interpolation filter interpolates the omitted lines and performs the vertical spectral forming. To preserve the data rate a higher order QAM technique is suggested which gives 1/n, 2/n or 3/n for a 4-, 16- or 64-QAM respectively of the original data rate. At the decoder, to ensure optimal reconstruction of the data signals, the overall vertical filter chain during transmission must maintain the original data samples. This prerequisite is fulfilled provided every n^{th} sample of the overall filter's impulse

response is zero in the aforementioned cases. A specially designed interpolation filter family has therefore to be applied at the encoder, exhibiting these properties. and then exclude the other vertical filters of the chain, which is the PAL line delay, if this will used for separation of the data channels. Otherwise the PAL line delay must be considered only for the compatibility issue and for the decoding process additional filters must be applied.

The frequency response of any filter where only the n^{th} coefficient is non-zero has the property of providing an attenuation of more than 6dB at 1/n of the Nyquist frequency. Excluding the frequency response of the PAL line delay which is cosine shaped, such attenuation is limited and nearly independent from the filter design. This confines any crosstalk improvement within the filter design process, so that only minor changes are possible by varying for example, filter complexity.

A combination of the interpolation technique together with the duobinary coding will provide a possible solution of this lemma. A duobinary coded signal spectrum is cosine shaped, so it has a zero at the Nyquist frequency. Up-sampling by a factor of n moves this null point to 1/n of the new Nyquist frequency and thus introduces a notch at the aforementioned critical location. The pyrrhic effect however, is that this is only possible with two symbol levels per data channel leading to a lower data rate, otherwise, due to the combination, to much symbol levels occur.

IV. Discussion of Results

The technique presented in this paper is based upon modulating the active video part of a PAL signal. To be compatible with the PALplus standard, only 432 of the total 576 active PAL lines are available, which forms the kernel 16:9 widescreen signal. The remaining 144 lines are reserved for the transmission of the so-called vertical helper signal. The ensuing discussion and results relate to the 432 line core signal. The helper components remain unaffected, also for a pure PAL signal.

For the initial simulations the horizontal form filter, avoiding inter-symbol interference, is chosen with a roll off slope of 0.5. The overall data channel bandwidth is, as given in II.B.:

$$f_{Bdata} = 5\text{MHz} - 4.433\ \text{MHz} = 0.567\ \text{MHz}$$

so that the bit duration might not exceed

$$T_{Bit} = \frac{1}{2 f_{Bdata}} 1.5 = 1.323 \mu s$$

With an active line length of 52µs, this results in a maximum of 39 symbols per line and per additional data channel. For simplification of the simulation and to avoid the worst case, 36 symbols are used, so for both channels 72 symbols per line are available and every line contains an integer number of bytes. The overall data rate provided can be derived as follows:

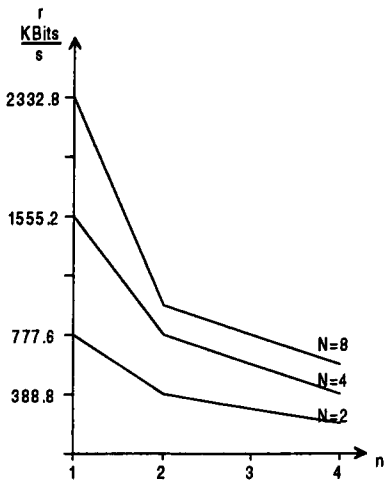

Figure 5: Achievable data rates versus interpolation factor.

$$r = 72 \frac{symbols}{line} 432 \frac{line}{frame} 25 \frac{frame}{s} ldN \frac{Bits}{symbols} \frac{1}{n}$$
$$= 777.6 \frac{KBits}{s} \frac{ldN}{n}$$

where N is the number of symbol levels per channel and n the interpolation factor (**Figure 5**).

The roll-off filter design is straight forward and implemented as usual separated in a pre- and post filter at the encoder and decoder, respectively. Considering the vertical forming filter, not much flexibility in designing this filter is given, neither for the partial response coding, where the vertical filter are fixed due to the chosen order, nor for the interpolation technique as alluded in the previous section. The most important parameters, which having an impact to the overall efficiency, that is data rate and subjective quality, are the amplitude of the data signal, α, the number of symbol levels, N, and the interpolation factor n. With Eq. 1 and Eq. 2 the power of the intercarrier crosstalk can be derived within each colour channel and an objective quality is given using Eq. 10.

Example	N	n	r KBits/s	α=0.15 P_N	α=0.15 $SNRI_U$	α=0.15 $SNRI_V$	α=0.075 P_N	α=0.075 $SNRI_U$	α=0.075 $SNRI_V$
P1	2	1	777.6	$3.574\ 10^{-4}$	30.21 dB	33.17 dB	$0.934\ 10^{-4}$	33.17 dB	39.19 dB
P2	2	1	777.6	$1.768\ 10^{-4}$	33.22 dB	36.17 dB	$0.447\ 10^{-4}$	39.24 dB	42.20 dB
I1	2	2	388.8	$3.015\ 10^{-4}$	30.94 dB	33.91 dB	$0.753\ 10^{-4}$	36.97 dB	39.93 dB
	4	2	777.6	$1.675\ 10^{-4}$	33.50 dB	36.46 dB	$0.419\ 10^{-4}$	39.52 dB	42.48 dB
I4	2	3	259.2	$0.705\ 10^{-4}$	37.26 dB	40.22 dB	$0.176\ 10^{-4}$	43.28 dB	46.24 dB
	4	3	518.4	$0.392\ 10^{-4}$	39.82 dB	42.77 dB	$0.098\ 10^{-4}$	45.83 dB	48.79 dB
P1/I1	2	2	388.8	$0.628\ 10^{-4}$	37.76 dB	40.72 dB	$0.157\ 10^{-4}$	43.78 dB	46.73 dB
P1/I4	2	3	259,2	$0.160\ 10^{-4}$	43.69 dB	46.65 dB	$0.040\ 10^{-4}$	49.71 dB	52.67 dB

Table 1: Comparison of different crosstalk noise

Three different design methods together with their parameters are compared in **Table 1**. Px refers to partial response coding, Ix to interpolation and Px/Ix to the combination of both methods. I1 and I4 are designed as alluded in Sec. IIIB. with an amplification of the interpolation factor, n, to keep the data signal power independent from the interpolation factor. The corresponding filter responses $H_D(f_y)$ and $C_A(f_y)$ are given from with **Figure 7**. Is obvious that with an increasing cross talk attenuation the achieving data rate decreases. Giving the priority to the subjective picture quality the values from example I4, P1/I1 and P1/I4 produce the best compromise, where the 16 QAM version of I4 provides a superb bit rate efficiency. The data amplitude, α, should be within the limits of 0.075 and 0.15 in relation to the normalised video range. A value of 0.15 causes an overshoot of 20% of the resulting video signal (**Figure 6**), which is a little bit less than for saturated yellow and therefore acceptable. Further α should not be below 0.075, because of an increasing data error rate in noisy transmission channels.

Table 2 shows the DSNR of an EBU colour bar for the examples given in **Table 1**. It gives a very good impression of what distortions are definite visible within the possible signal parts of a video signal. Surely, the degradation's are more visible in dark uniform areas than in bright parts. The DSNR varies within a range of approximately 20 dB depending on the form filtering. For values greater than 35dB, almost no visible distortions are perceived by non expert viewers.

The previous discussion relates only to the issue of compatibility, which as alluded earlier is of paramount importance and parameter settings are consequently chosen to reflect this. Also of interest however are the properties of the data channels, is respect of their achievable data rate and also the Bit Error Rate (BER). The data rates have already been discussed, the BER is direct dependent upon the data signal amplitude α, and the numbers of signal levels, N. **Figure 9** and **Figure 10** show the measured eye patterns and corresponding signal space for 2 and 4 signal levels per data channel, respectively. The asymmetric shape of the symbol positions is caused by arithmetic rounding being used in the signal processing. Despite this, the example reveals that perfect data reconstitution is certainly possible. This ideal situation inevitably deteriorates when white Gaussian noise is added during transmission. The noise degrades the symbol positions within the signal space, so they become less and less defined and the openness of the eye narrows, leading to an increased probability of bit errors with the number of symbol levels. **Figure 8** compares the examples for signal to noise ratios within the range 30dB to 40 dB for the 16 QAM case. The 4 QAM together with the duo-binary coding technique provides a BER greater than 10^{-5} within these tests.

Another source of bit errors are introduced from high vertical colour frequencies, which cross over into the data channel. Due to the probability occurrence of those frequencies the resulting errors appear as burst errors. The previous mentioned vertical filter in the colour signal paths will prevent these effects.

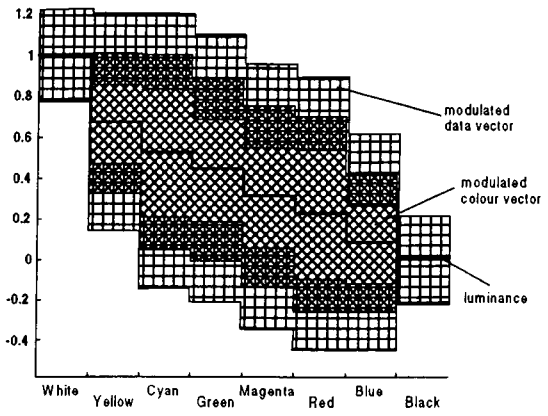

Figure 6: EBU colour bar added with the modulated data signal

Example							
P1 α=0.15	30.7587 dB	29.0814 dB	27.7221 dB	26.8687 dB	26.5172 dB	25.3461 dB	20.3343 dB
P1 α=0.0.75	36.5868 dB	34.9095 dB	33.5502 dB	32.6968 dB	32.3453 dB	31.1742 dB	26.1624 dB
P2 α=0.15	33.8154 dB	32.1381 dB	30.7789 dB	29.9254 dB	29.5739 dB	28.4028 dB	23.3910 dB
P2 α=0.0.75	39.7872 dB	38.1099 dB	36.7506 dB	35.8971 dB	35.5457 dB	34.3746 dB	29.3627 dB
I1 α=0.15	31.4974 dB	29.8201 dB	28.4608 dB	27.6074 dB	27.2559 dB	26.0848 dB	21.0729 dB
I1 α=0.0.75	37.5223 dB	35.8450 dB	34.4857 dB	33.6323 dB	33.2808 dB	32.1097 dB	27.0979 dB
I1 α=0.15	34.0501 dB	32.3728 dB	31.0135 dB	30.1601 dB	29.8086 dB	28.6375 dB	23.6257 dB
I1 α=0.0.75	40.0681 dB	38.3908 dB	37.0315 dB	36.1781 dB	35.8266 dB	34.6555 dB	29.6437 dB
I4 α=0.15	37.8084 dB	36.1311 dB	34.7718 dB	33.9183 dB	33.5669 dB	32.3958 dB	27.3839 dB
I4 α=0.0.75	43.8351 dB	42.1578 dB	40.7986 dB	39.9451 dB	39.5936 dB	38.4225 dB	33.4107 dB
I4 α=0.15	40.3574 dB	38.6801 dB	37.3208 dB	36.4674 dB	36.1159 dB	34.9448 dB	29.9330 dB
I4 α=0.0.75	46.3780 dB	44.7007 dB	43.3414 dB	42.4880 dB	42.1365 dB	40.9654 dB	35.9536 dB
P1/I1 α=0.15	38.3106 dB	36.6334 dB	35.2741 dB	34.4206 dB	34.0692 dB	32.8980 dB	27.8862 dB
P1/I1 α=0.0.75	44.3312 dB	42.6540 dB	41.2947 dB	40.4412 dB	40.0898 dB	38.9186 dB	33.9068 dB
P1/I4 α=0.15	44.2490 dB	42.5717 dB	41.2125 dB	40.3590 dB	40.0076 dB	38.8364 dB	33.8246 dB
P1/I4 α=0.0.75	50.2696 dB	48.5923 dB	47.2331 dB	46.3796 dB	46.0282 dB	44.8570 dB	39.8452 dB

Table 2: DSNR of an EBU Colour bar for various examples

V. Conclusions

The paper introduces a novel modulation possibility which enables embedded digital subchannels within a standard video signal. The technique uses the active video part, so that crosstalk distortions occur. These degradation of compatibility has been fully analyzed and qualified. The concept of a more dimensional form filtering is proposed to suppress these effect, which, however, balance the data rate efficiency. Looking at noisy transmission channels, the proposed system provides acceptable bit error rates for signal to noise ratios better than 30 dB.

The subjective quality of the standard video signal, data rate and also the noise robustness are the major properties, which compromises each other. The best solution is found for the example P1/I1 with the priority on subjective quality. Shifting the focus a bit more to the data rate efficiency, the 16 QAM example of I4 is the best.

As mentioned earlier, only the center signal is used for additional modulation, which is ¾ of the overall picture space. To improve bit rate efficiency the consistency of the proposed modulation, or a modification of it, with the PALplus helper is currently under development.

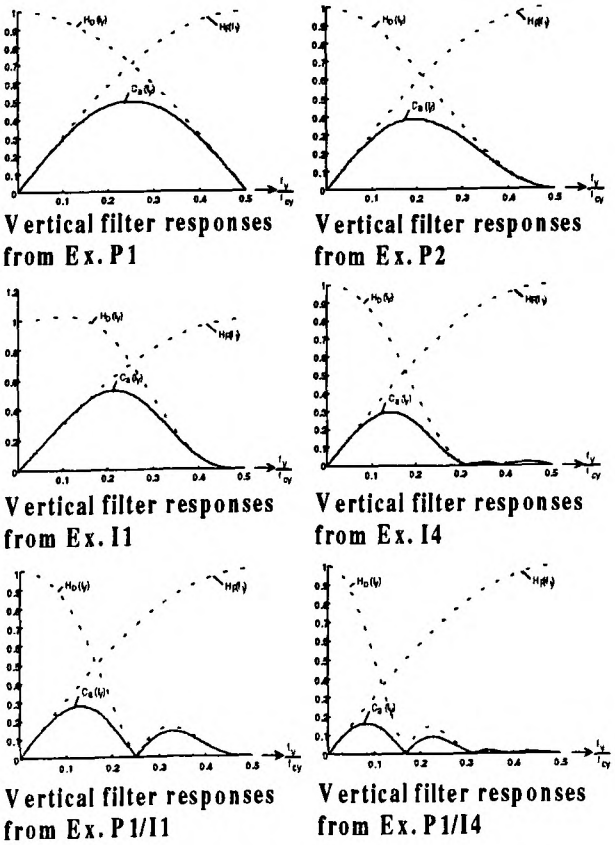

Vertical filter responses from Ex. P1 | Vertical filter responses from Ex. P2

Vertical filter responses from Ex. I1 | Vertical filter responses from Ex. I4

Vertical filter responses from Ex. P1/I1 | Vertical filter responses from Ex. P1/I4

Figure 7: Filter responses for various examples

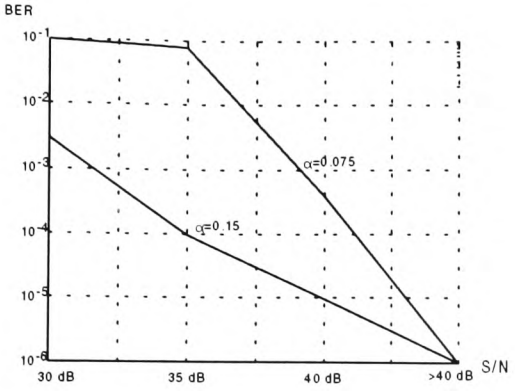

Figure 8: Measured bit error rate (BER) for the 16 QAM approach

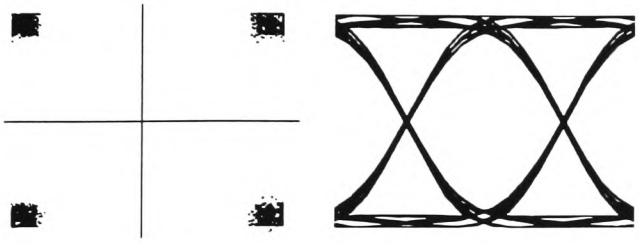

Figure 9: Eye pattern and signal space for 4 QAM

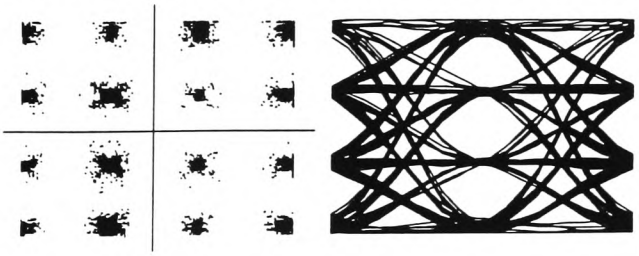

Figure 10: Eye pattern and signal space for 16 QAM

VI. Reference

[1] M. A. Isnaradi, *Exploring and Exploiting Subchannels in the NTSC Spectrum*, SMPTE Journal, July 1988, pp.526-532

[2] T. Fukinuki and Y. Hirano, *Extended Definition TV Fully Compatible with Existing Standards*, IEEE Trans. on Communications, Vol. 32, No.3

[3] Finger, A; Hiller, H; Goetting, O; Schoenthier, J; *A new digital add on data transmission within analogue Television channels, German;* Proceedings of the 17. FKTG Annual Conference; pp. 476-485; 1996

[4] NAB'95 Engineering Conference Proceedings

[5] Dinsel,S; *TV-Datacast A compatible digital data system for analogue TV networks*; Proceedings of the 17. FKTG Annual Conference; pp. 496; 1996

[6] Szepanski,W; Transmission of non othogonal additional signals in TV channels, (German)

[7] Stoetera,A; Synthesis and detection of additional signals in TV channels, (German)

[8] Ruppel,W; *Compatible transmission of additional digital signals with conventional TV systems, (German);* Frequenz, Vol. 48, No.5-6, pp.133-138, 1994

[9] Schmidt,G; Buchwald,W.P.; Dooley,L.S; A Comparative Review of Modulation Techniques for integrating digital components within a PALplus signal; Digest of technical papers, ICCE'96, pp. 12-13

[10] Plantholt, M.; German Patent DE 3841073 A1;1988

[11] Riemann, U.; Plantholt, M.; European Patent EP 0521028 B1; 1991

[12] Kraus, U.;Riemann, U.; Plantholt, M.; European Patent EP 0542812 B1; 1991

[13] Schönfelder, H.;*Picture Communication, (German)* ; Springer-Verlag; 1983

[14] *Handbook for the D2-MAC/Packet - Transmissionsystem, (German)*;Institut fuer Rundfunktechnik, Muenchen; 1988

[15] Vetterli, M.; *Perfect transmultiplexers*, Proc. IEEE Int. Conf, Acoust. Speech and Signal Proc.; pp.2567-2570;1986

[16] Selvan,B; Green R.J; Objective noise evaluation of component video signals using an electric colour video simulator, IEEE Transaction on Broadcasting, Vol. 39, No.3, pp. 327-330,1993

[17] CCIR Rec. 567-3; *Transmission performance of television circuits designed for use in international connections*; Annex II to Part C

[18] Windram, M.D.; Tonge, G.; Morcom, R.; *Mac - A Television system for high quality satellite broadcasting*; IBA Experimental & Development Report 118/82; 1982

VII. Bibliographies

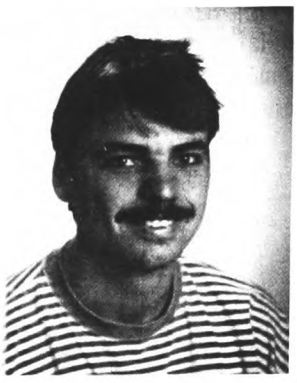

Gunnar Schmidt (M'93) was born in Braunschweig, Germany in 1966. He received his Dipl-Ing. degree in Electronics and Communication Technology in 1990 from the Fachhochschule Braunschweig/Wolfenbuettel, Germany. From 1990 to 1997 he worked with the video

signal processing group in the Department of Communication Technology at the Fachhochschule Braunschweig / Wolfenbuettel. He is a registered research student in the Department of Electronics and Information Technology at the University of Glamorgan, Wales, studying for his Ph.D. degree. Since 1997 he is been employed with Robert Bosch GmbH, Advanced Development Multimedia Systems.

His main research interests are in the fields of digital signal processing, related to the area of data communication

Laurence S. Dooley (M'81-SM'92) was born in Cwmbran, Wales in 1959. He received his B.Sc. (Hons), M.Sc. and Ph.D. degrees in Electrical and Electronic Engineering from the University College of Wales, Swansea in 1981, 1983 and 1987 respectively. He worked as an Industrial Consultant, principally in the area of digital sound systems for Marine and Bridge Simulators before joining the School of Electronics at the University of Glamorgan, in 1986, where he is currently a Senior Lecturer. In 1989 he was a Visiting Scholar in the Department of Electrical Engineering at the University of Sydney, Australia.

His main research interests are in the fields of digital signal processing, HDTV, multimedia and video technology. He is a Senior member of the IEEE, a Chartered Engineer (C.Eng.) and corporate member of the British Computer Society.

Prof. Dr. Wolf-Peter Buchwald was born in 1954. He studied Communication Technology at the Technical University of Braunschweig, Germany, where he received his Ph.D. degree in 1986. In 1989 he was appointed Professor in Communication Technology and Digital TV techniques at the Fachhochschule Braunschweig/ Wolfenbuettel, Germany. He has provided a number of course for industry in the general area of digital video technology.

His main research interests are in the fields of digital signal processing, in particular relating to CCD sensors and digital video signal processing.